

The Effects of Glucose Deprivation and Ketone Supplementation on the Growth and Function of Neural Stem and Neuronal Precursor Cells



David J. Lee BSc
Discipline of Anatomy
School of Medicine

A dissertation submitted to the University of Dublin
in candidature for the degree of
Doctor of Philosophy


Year Degree Awarded: 2023

Supervisor
Dr. Denis Barry

Declaration, Online Access, and the General Data Protection Regulation

I declare that this thesis has not been submitted as an exercise for a degree at this or any other university and it is entirely my own work.

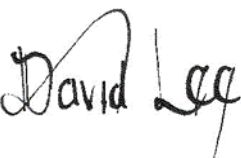
I agree to deposit this thesis in the University's open access institutional repository or allow the library to do so on my behalf, subject to Irish Copyright Legislation and Trinity College Library conditions of use and acknowledgement. I consent / do not consent to the examiner retaining a copy of the thesis beyond the examining period, should they so wish (EU GDPR May 2018).

Signed:  Date: 16/12/2022

Declaration and Statement of Plagiarism

I declare that this thesis has not been submitted as an exercise for a degree at this or any other university and it is entirely my own work.

I agree to deposit this thesis in the University's open access institutional repository or allow the library to do so on my behalf, subject to Irish Copyright Legislation and Trinity College Library conditions of use and acknowledgement.

Signed:  Date: 16/12/2022

Acknowledgements

Firstly, to my supervisor, Dr. Denis Barry, thank you for your guidance, support, advice, and confidence in me over the last five years. Your patience has no bounds and our many meetings discussing the different directions to take the experiments have provided invaluable insight into shaping this thesis. Thank you for being an amazing mentor, you have taught me so much and it's been a great privilege to be a student of yours.

To Dr. Mohammad Alherz, your brilliant mind, insight, and quick wit kept me laughing and smiling through some difficult days in the lab when there were consecutive days/weeks/months when our experiments failed to produce any meaningful or interesting data. I'll forever be grateful you came into my life and into the Discipline as not only did you give me fresh energy for the research, but you also helped me greatly in looking at our data and experiments with a different lens and light.

Claire Murphy, Mary Lynch, and Philomena McAteer, ever since I first stepped foot into the Discipline of Anatomy on that September day five years ago, the three of you have shown me nothing but kindness, consideration, and thoughtfulness. From helping me work the Oracle delivery system to dropping down my deliveries to the Lab when I'd be down in the microscopy suit, the three of you really helped me settle into the Discipline.

I reserve the last lines of my acknowledgements to my family. To my brother Rob and his partner Sinead and my nephew Oliver, thank you for always being there for me. Finally, to my father and mother Patrick (Pat) and Collette, it's almost indescribable to say how much I owe the both of you and the love I have for you. Thank you for always believing in me when sometimes I didn't believe in myself. You have always told me and shown me to never settle for anything less than what I want and the pair of you have always told me to reach for the stars and beyond. Thank you for always pushing me and sometimes pulling me through the hard times and for the invaluable love, care, and affection you've shown me throughout my life (and thanks for the loans when the PhD stipend would run low towards the end of the month).

Table of Contents

| | |
|---|--------------|
| Declaration, Online Access, and the General Data Protection Regulation..... | i |
| Declaration and Statement of Plagiarism | ii |
| Acknowledgements..... | iii |
| Table of Contents | iv |
| List of Figures | xi |
| List of Tables | xiv |
| Abbreviations..... | xvi |
| Abstract..... | xxi |
| Lay Abstract..... | xxiii |
| Value of Research..... | xxiv |
| Publications Resulting from this Work..... | xxv |
| Presentations Resulting from this Work..... | xxvi |
| Chapter 1 | 1 |
| 1. Introduction | 1 |
| 1.1 Glucose Deprivation, the Ketogenic Diet and Metabolism..... | 1 |
| 1.2 Ketone Metabolism | 2 |
| 1.3 Systemic Ketone Body Levels | 4 |
| 1.4 Glucose and Pyruvate Metabolism..... | 5 |
| 1.5 Glutamine Metabolism..... | 6 |
| 1.6 Ketone Bodies in Cancer Biology..... | 7 |
| 1.7 Glycolysis and Oxidative Phosphorylation..... | 8 |
| 1.8 The Warburg Effect..... | 11 |
| 1.9 Overview of CNS Development and Ketone Bodies in Brain Development | 14 |
| 1.10 Effects of Ketone bodies During Neonatal Development and Early Lactation | 18 |
| 1.11 Sustained Effects of a Gestational KD in Adulthood..... | 19 |
| 1.12 Overview of Cell Metabolism Phenotypes: Comparing Developing Brain Cells, Adult Brain Cells, and Cancer Cells | 20 |

| | |
|---|-----------|
| 1.13 Metabolism of Ketone Bodies During Brain Development and in Cancer | 23 |
| 1.14 Role of the Ketone Diet in Disease Prevention and Health Maintenance | 26 |
| 1.15 The β -Hydroxybutyrate Paradox..... | 28 |
| 1.16 Neuroectodermal NE-4C cells and Neuroblastoma SH-SY5Y cells | 28 |
| 1.17 The Role of the Culture Medium | 29 |
| 1.18 Overall Aims and Hypothesis of the Project..... | 30 |
| Chapter 2 Materials & Methods | 32 |
| 2.1 Materials | 32 |
| 2.2 Experimental Overview | 32 |
| 2.3 Databases and Search Strategy | 32 |
| 2.4 Article Selection..... | 32 |
| 2.5 Cell Lines..... | 33 |
| 2.6 NE-4C and SH-SY5Y Cell Culture, Subculturing, and Media Change | 33 |
| 2.7 Aseptic Technique | 34 |
| 2.8 Cell Seeding, Counting, and Plating..... | 34 |
| 2.9 Preparation of β OHB media..... | 35 |
| 2.10 Proliferation Experiments | 36 |
| 2.11 Differentiation Experiments..... | 38 |
| 2.12 Assays | 41 |
| 2.13 Immunocytochemistry | 43 |
| 2.13.1 Proliferation Experiments | 43 |
| 2.13.2 Differentiation Experiments..... | 43 |
| 2.13.3 Assays | 44 |
| 2.14 Imaging and Analysis | 45 |
| 2.14.1 Randomisation of Fields | 45 |
| 2.14.2 DAPI Count | 46 |
| 2.14.3 A Novel Method for Measuring Cell Density..... | 50 |

| | |
|---|-----------|
| 2.14.4 Protein Expression..... | 53 |
| 2.15 Statistical Analysis | 54 |
| Chapter 3 The Effects of Ketone Body Supplementation on Cell Growth <i>In Vitro</i>: | |
| A Systematic Review | 55 |
| 3.1 Introduction..... | 55 |
| 3.1.2 Aims..... | 56 |
| 3.1.3 Hypothesis..... | 56 |
| 3.2 Methods..... | 57 |
| 3.2.1 Database and Search Strategy | 57 |
| 3.2.2 Article Selection..... | 57 |
| 3.3 Results..... | 58 |
| 3.3.1 Positive effect results | 58 |
| 3.3.2 Negative Effect Results..... | 67 |
| 3.3.2 No Effect Results | 75 |
| 3.3.3 Proposed Mechanism of Action for Positive Ketone Effect..... | 79 |
| 3.3.4 Proposed Mechanism of Action for Negative Ketone Effect | 80 |
| 3.3.5 Proposed Mechanism for No Effect Ketone Studies | 80 |
| 3.3.6 Relationship with the Medium..... | 81 |
| 3.3.7 Relationship with the Cell Type | 82 |
| 3.3.8 The Relationship between the Ketones and the Concentration | 86 |
| 3.3.9 Relationship with Other Media Components..... | 88 |
| 3.4 Discussion | 88 |
| 3.5 Conclusion | 92 |
| Chapter 4 The Impact of Glucose, Glucose Deprivation & Ketone Supplementation | |
| on Brain Cell Growth | 93 |
| 4.1 Introduction..... | 93 |
| 4.1.2 Aims | 95 |

| | |
|---|-----|
| 4.1.3 Hypothesis | 95 |
| 4.2 Methods | 96 |
| 4.2.1 Cell lines and General Culture Conditions | 96 |
| 4.2.2 Experimental Design for Chapter 4 | 96 |
| 4.2.3 Experiments undertaken | 98 |
| 4.2.3.1 Cell Viability..... | 98 |
| 4.2.3.2 Immunocytochemistry | 98 |
| 4.2.3.3 Imaging and Analysis | 98 |
| 4.3 Results | 100 |
| 4.3.1 SH-SY5Y Cell Density, Morphology, and Viability | 100 |
| 4.3.2 SH-SY5Y Proliferation in Glucose and Glucose Deficient Conditions Over 120 hr | 103 |
| 4.3.3 SH-SY5Y Cytotoxicity & Viability | 105 |
| 4.3.4 MTT Assay | 106 |
| 4.3.5 SH-SY5Y Differentiation | 107 |
| 4.3.6 SH-SY5Y Cell Density in Glucose, Glucose Deficient Media, and Ketone Supplementation Following RA Differentiation..... | 108 |
| 4.3.7 SH-SY5Y Proliferation Rates Following RA Differentiation | 110 |
| 4.3.8 SH-SY5Y Differentiation Rates following RA treatment | 111 |
| 4.3.9 Proliferation of NE-4C cells in Regular RG, GF and β OHB Treatment Conditions across 168 hrs..... | 112 |
| 4.3.10 NE-4C Cell Density in the RG and GF Groups over 168 hr | 114 |
| 4.3.11 NE-4C Cell Density for All Treatment Groups across 168 hr..... | 115 |
| 4.4 Discussion..... | 116 |
| 4.4.1 β OHB Supplementation Does Not Rescue Cell Growth in a Glucose Deprived Environment..... | 117 |
| 4.4.2 β OHB Impacts SH –SY5Y Toxicity and Viability..... | 118 |
| 4.4.3 Cell Density Decreases Following RA Differentiation | 119 |

| | |
|---|-----|
| 4.4.4 Proliferation Rates are Slowed by β OHB Following RA Differentiation..... | 119 |
| 4.4.5 Differentiation is not Affected by β OHB Following RA Treatment | 119 |
| 4.4.6 NE-4C Cells Show Enhance Growth and Survival in Glucose Media Compared to Glucose-Free Media | 120 |
| 4.4.7 NE-4C Cells Can Both Survive and Proliferate in Varying Concentrations Of β OHB Over 168 Hr | 120 |
| 4.5 Conclusion..... | 121 |
| Chapter 5 The Impact of Nutrient Deprivation and Ketone Supplementation on the Differentiation and Metabolic Health of Neural Stem and Neuronal Precursor Cells | 122 |
| 5.1 Introduction..... | 122 |
| 5.2 Experimental aims | 123 |
| 5.2.2 Hypothesis..... | 123 |
| 5.3 Methods..... | 124 |
| 5.3.1 Cell Lines and General Culture Conditions..... | 124 |
| 5.3.2 Experimental Design..... | 124 |
| 5.3.3 Experiments Undertaken..... | 125 |
| 5.3.3.1 Cell Viability..... | 125 |
| 5.3.3.2 Immunocytochemistry | 125 |
| 5.3.3.3 Imaging and Analysis | 125 |
| 5.4.1 The Effects of Glucose Deprivation on Differentiating NE-4C Density, Phenotype, Morphology and Metabolic Viability | 126 |
| 5.4.2 The Impact of Substrate Deprivation and β OHB Supplementation on Differentiated NE-4C Viability, Density, and Morphology at 5 DIV..... | 130 |
| 5.4.3 The Impact of Substrate Deprivation and β OHB Supplementation on Differentiated NE-4C Viability, Density, and Morphology at 10 DIV..... | 134 |
| 5.4.4 The Impact of Substrate Deprivation and β OHB Supplementation on Differentiated NE-4C Viability, Density, and Morphology at 15 DIV..... | 139 |

| | |
|--|------------|
| 5.4.5 The Effects of Glucose Deprivation on Differentiating SH-SY5Y Density, Phenotype, Morphology and Metabolic Viability | 143 |
| 5.4.6 The Impact of Substrate Deprivation and β OHB Supplementation on Differentiated SH-SY5Y Viability and Density and Morphology at 5 DIV | 145 |
| 5.4.7 The Impact of Substrate Deprivation and β OHB Supplementation on Differentiated SH-SY5Y Viability and Density and Morphology at 10 DIV | 150 |
| 5.4.8 The Impact of Substrates Deprivation on Differentiated SH-SY5Y Viability and Density and Morphology at 15 DIV | 154 |
| 5.5 Discussion..... | 158 |
| 5.5.1 Glucose and Nutrient Deprivation is Detrimental to Cell Differentiation..... | 158 |
| 5.5.2 Ketone Supplementation May Rescue the Effects of Nutrient Deprivation When Cells are Undergoing OXPHOS | 160 |
| 5.6 Conclusion | 163 |
| Chapter 6 General Discussion & Future Directions | 164 |
| 6.1 General Discussion | 164 |
| 6.1.1 Study Overview | 164 |
| 6.1.2 A Systematic Review of the Effects of Ketone Body Supplementation on Cells <i>In Vitro</i> | 166 |
| 6.1.3 The Impact of Glucose, Glucose Deprivation and Ketone Body Supplementation on Cell Growth..... | 167 |
| 6.1.4 Ketone Supplementation May Rescue the Impact of Nutrient Deprivation When Cells are Undergoing OXPHOS | 168 |
| 6.2 Future Directions | 170 |
| Chapter 7 Appendices | 171 |
| Cell Lines..... | 171 |
| Cell Culture Reagents | 171 |
| Cell Assays..... | 172 |
| General Laboratory Chemicals | 172 |
| General Laboratory Products | 173 |

Immunocytochemistry..... 173
Chapter 8 Bibliography xxvii
References..... xxvii

List of Figures

| | |
|---|-----|
| Figure 1.1 The pathway of ketogenesis and ketolysis | 2 |
| Figure 1.2 Glycolysis pathway | 9 |
| Figure 1.3 A summary diagram of OXPHOS..... | 10 |
| Figure 1.4 Warburg Effect..... | 13 |
| Figure 1.5 Formation of neural tube..... | 14 |
| Figure 1.6 Cell generation in the developing CNS..... | 15 |
| Figure 1.7 Metabolic Changes in NSCs.. .. | 21 |
| Figure 1.8 Ketone Bodies Synthesis..... | 24 |
| Figure 2.1 Diagram representing the haemocytometer grid and an example of how cells were counted..... | 35 |
| Figure 2.2 Six well plate experimental design for the initial proliferation assay | 36 |
| Figure 2.3 96 well plate experimental design for the proliferation assay investigating the effect of media composition on the response to β OHB..... | 37 |
| Figure 2.4 Six well plate experimental design for the initial differentiation assay | 38 |
| Figure 2.5 96 well plate experimental design for the differentiation assay investigating the effect of media composition on the response to β OHB..... | 40 |
| Figure 2.6 96 well plate mitochondrial cytotoxicity assay experimental design..... | 41 |
| Figure 2.7 Diagram representing the fields of view (FOV) taken for the proliferation experiments (A) and the differentiation, β DH1 and mitochondrial cytotoxicity (B). | 45 |
| Figure 2.8 Overview of ImageJ DAPI cell count. | 46 |
| Figure 2.9 Excel spreadsheet of how counts were entered..... | 47 |
| Figure 2.10 N number overview | 47 |
| Figure 2.11 Overview of N numbers | 48 |
| Figure 2.12 Overview of how the correct image parameters were measured to get cells per mm^2 | 49 |
| Figure 2.13 How the mean, SD and SEM were calculated. | 50 |
| Figure 2.14 A schematic of the process underlying the cell density quantification in whole-well images..... | 52 |
| Figure 3.1 Overview schematic of the selection process of the papers included in the systematic review | 58 |
| Figure 3.2 Schematic diagram outlining how ketone bodies can positively or negatively impact cell lines..... | 81 |
| Figure 4.1 Cell density at 48 and 120 hr in RG and GF..... | 100 |

| | |
|--|-----|
| Figure 4.2 Cell density at 48 and 120 hr in RG, GF, 1 mM β OHB, 5 mM β OHB, 10 mM β OHB and 50 mM β OHB.. | 101 |
| Figure 4.3 Actin expression at 48 hrs and 120 hrs in RG, GF, 1 mM β OHB, 5 mM β OHB, 10 mM β OHB and 50 mM β OHB. | 102 |
| Figure 4.4 Cell proliferation at 48, 72, 96 and 120 hr, in RG and GF..... | 103 |
| Figure 4.5 Cell proliferation at 48, 72, 96 and 120 hr, in RG, GF, 1 mM β OHB, 5 mM β OHB, 10 mM β OHB and 50 mM β OHB..... | 104 |
| Figure 4.6 Cell cytotoxicity at 72 and 144 hr in RG, GF, 1 mM β OHB, 5 mM β OHB, 10 mM β OHB and 50 mM β OHB. | 105 |
| Figure 4.7 Cell cytotoxicity at 72 and 144 hr in RG, GF, 1 mM β OHB, 5 mM β OHB, 10 mM β OHB and 50 mM β OHB. | 106 |
| Figure 4.8 Cell viability at 96 hr in RG, LG GF, 1 mM β OHB, 5 mM β OHB, 10 mM β OHB, 25 mM β OHB and 50 mM β OHB. | 107 |
| Figure 4.9 Bright-field images of SH-SY5Y cell culture groups, RG, GF and 10 mM β OHB, at 72 hr, 120 hr, and 168 hr of RA treatment. | 108 |
| Figure 4.10 Cell density at 72, 120 and 168 hr (post RA differentiation) in RG, GF, and 10 mM β OHB following RA differentiation. | 109 |
| Figure 4.11 Cell proliferation at 72 and 120 hr, in RG and GF and 10 mM β OHB..... | 110 |
| Figure 4.12 Cell differentiation at 72 and 120 hr, in RG and GF and 10 mM β OHB. | 111 |
| Figure 4.13 High magnification representative images of NE-4C cells cultured in RG, GF, 1 mM β OHB, 5 mM β OHB, 10 mM β OHB and 50 mm β OHB at 168 hr. | 112 |
| Figure 4.14 A –AD Brightfield representative images of NE-4C cells cultured in RG, GF, 1 mM β OHB, 5 mM β OHB, 10 mM β OHB and 50 mM β OHB at 48 hr, 72 hr, 96 hr, 120 hr and 168 hr. | 113 |
| Figure 4.15 Cell density at 48, 72, 96, 120 and 168 hr in RG and GF conditions..... | 114 |
| Figure 4.16 Cell density at 48, 72, 96, 120 and 168 hr in GF, 1 mM, 5 mM, 10 mM and 50 mM β OHB | 115 |
| Figure 5.1 Growth and viability of NE-4C cells in RG, LG, and GF condition at 5, 10 and 15 DIV. | 129 |
| Figure 5.2 Growth and viability of NE-4C cells in GF, GF-Pyr, GF-Lglut, GF-Pyr-Lglut at 5 DIV. | 131 |
| Figure 5.3 Growth and viability of NE-4C cells in GF, GF-Pyr, GF-Lglut, GF-Pyr-Lglut conditions at 5 DIV compared to 10 mM β OHB supplemented conditions..... | 133 |

| | |
|--|-----|
| Figure 5.4 Growth and viability of NE-4C cells in GF, GF-Pyr, GF-Lglut, GF-Pyr-Lglut at 10 DIV..... | 135 |
| Figure 5.5 Growth and viability of NE-4C cells in GF, GF-Pyr, GF-Lglut, GF-Pyr-Lglut conditions at 10 DIV compared to 10 mM β OHB supplemented conditions..... | 138 |
| Figure 5.6 Growth and viability of NE-4C cells in GF, GF-Pyr, GF-Lglut, GF-Pyr-Lglut at 15 DIV..... | 141 |
| Figure 5.7 Growth and viability of NE-4C cells in GF, GF-Pyr, GF-Lglut, GF-Pyr-Lglut conditions at 15 DIV compared to 10 mM β OHB supplemented conditions..... | 142 |
| Figure 5.8 Growth and viability of SH-SY5Y cells in RG, LF and GF condition at 5, 10 and 15 DIV..... | 145 |
| Figure 5.9 Growth and viability of SH-SY5Y cells in GF, GF-Pyr, GF-Lglut, GF-Pyr-Lglut at 5 DIV..... | 148 |
| Figure 5.10 Growth and viability of SH-SY5Y cells in GF, GF-Pyr, GF-Lglut, GF-Pyr-Lglut supplemented with 10 mM β OHB at 5 DIV..... | 149 |
| Figure 5.11 Growth and viability of SH-SY5Y cells in GF, GF-Pyr, GF-Lglut, GF-Pyr-Lglut at 10 DIV..... | 152 |
| Figure 5.12 Growth and viability of SH-SY5Y cells in GF, GF-Pyr, GF-Lglut, GF-Pyr-Lglut supplemented with 10 mM β OHB at 10 DIV..... | 153 |
| Figure 5.13 Growth and viability of SH-SY5Y cells in GF, GF-Pyr, GF-Lglut, GF-Pyr-Lglut at 15 DIV..... | 156 |
| Figure 5.14 Growth and viability of SH-SY5Y cells in GF, GF-Pyr, GF-Lglut, GF-Pyr-Lglut supplemented with 10 mM β OHB at 15 DIV..... | 157 |
| Figure 6.1 An overview of the findings from each chapter..... | 165 |

List of Tables

| | |
|--|-----|
| Table 1.1 Expression of brain MCT 1 and 2 during development and adulthood..... | 3 |
| Table 1.2 Overview of ketone levels in the blood | 5 |
| Table 1.3 Overview of ketone body function in CNS cell types during development | 16 |
| Table 1.4 Ketone body overview in CNS cell types during postnatal and adult life..... | 17 |
| Table 1.5 Overview of the three Sussman et al., 2013b 2013a and 2015 papers | 20 |
| Table 1.6 Overview of the use of ketones and their use in health maintenance | 27 |
| Table 1.7 A comparison of the metabolite concentrations in plasma and in culture | 30 |
| Table 2.1 List of media concentrations for the proliferation assay..... | 36 |
| Table 2.2 A summary of the utilised media groups and their corresponding compositions | 37 |
| Table 2.3 List of media concentrations for the differentiation assay..... | 39 |
| Table 2.4 Timeline for the initial differentiation assay..... | 39 |
| Table 2.5 List of media concentrations for the differentiation assay..... | 40 |
| Table 2.6 List of media concentrations for the initial MTT assay..... | 42 |
| Table 2.7 List of media concentrations for the MTT assay investigating the impact of media composition on the response to ketone bodies..... | 42 |
| Table 2.8 A summary of the image-based experiments used | 53 |
| Table 3.1 Positive ketone studies..... | 62 |
| Table 3.2 Positive Ketone studies media formulations..... | 66 |
| Table 3.3 Negative Ketone Studies | 71 |
| Table 3.4 Negative ketone studies media formulations | 74 |
| Table 3.5 No effect ketone studies..... | 77 |
| Table 3.6 No effect media formulations | 78 |
| Table 3.7 Cells relationship with the media..... | 85 |
| Table 4.1 A summary of the media groups in each SH-SY5Y experiment..... | 97 |
| Table 4.2 A summary of the media groups in each NE-4C experiment | 97 |
| Table 4.3 A summary of the image-based assays | 99 |
| Table 5.1 A summary of the media groups in each experiment. | 124 |
| Table 5.2 A list of the image-based assays | 125 |
| Table 7.1 Cell lines used..... | 171 |
| Table 7.2 Cell Culture Reagents | 171 |
| Table 7.3 Cell Assays | 172 |
| Table 7.4 General Laboratory Chemicals | 172 |

| | |
|--|-----|
| Table 7.5 General Laboratory Products..... | 173 |
| Table 7.6 Immunocytochemistry Reagents | 173 |
| Table 7.7 Cell culture media reagents | 174 |
| Table 7.8 Proposed mechanisms for positive ketone effect on cell lines..... | 179 |
| Table 7.9 Proposed mechanisms for negative ketone effect on cell lines..... | 183 |
| Table 7.10 Proposed mechanisms for no ketone effect on cell lines..... | 184 |
| Table 7.11 Relationship with the medium..... | 190 |
| Table 7.12 Relationship with the ketone | 193 |
| Table 7.13 Recorded ketone concentrations for the positive studies | 194 |
| Table 7.14 Recorded ketone concentrations for the negative effect studies | 195 |
| Table 7.15 Recorded ketone concentrations for the no effect ketone studies | 196 |
| Table 7.16 Combination Therapy | 198 |

Abbreviations

| | |
|----------------------|--|
| 1,3 BPG | 1,3 – Bisphosphoglycerate |
| 3-PG | 3 – Phosphoglycerate |
| 6-OHDA | 6-Hydroxydopamine |
| α -KG | Alpha-Ketoglutarate |
| A β | Amyloid – Beta |
| A β AD | Amyloid – Beta Binding Alcohol Dehydrogenase |
| AACS | Acetoacetyl-CoA synthetase |
| AcAc | Acetoacetate |
| ADP | Adenosine Diphosphate |
| ANOVA | Analysis of Variance |
| ATP | Adenosine Triphosphate |
| β -III tubulin | Beta – III – Tubulin |
| B | Bovine |
| BBB | Blood Brain Barrier |
| BDNF | Brain Derived Neurotrophic Factor |
| β OHB | β -Hydroxybutyrate |
| β DH1 | β -Hydroxybutyrate Dehydrogenase 1 |
| BrdU | Bromodeoxyuridine |
| CAC | Citric Acid Cycle |
| CNS | Central Nervous System |
| DAPI | 4', 6-diamidino-2-phenylindole |
| DIV | Days <i>In Vitro</i> |
| DKA | Diabetic Ketoacidosis |
| DMEM | Dulbecco's Modified Eagle Medium |
| DMSO | Dimethyl Sulfoxide |
| DNA | Deoxyribonucleic Acid |
| E13.5/E17.5 | Embryonic Day 13.5/17.5 |
| ETC | Electron Transport Chain |
| ERR γ | Oestrogen Related Receptor Gamma |
| FADH | Flavin Adenine Dinucleotide |
| FBS | Foetal Bovine Serum |

| | |
|----------------|---|
| FCS | Foetal Calf Serum |
| FDG | Fluorodeoxyglucose |
| FDG-PET | Fluorodeoxyglucose Positron Emission Tomography |
| FOV | Field of View |
| F6P | Fructose 6 Phosphate |
| F1-6BP | Fructose 1,6-Bisphosphate |
| FST | Forced Swim Test |
| GA3P | Glyceraldehyde 3-Phosphate |
| GAPDH | Glyceraldehyde 3-Phosphate Dehydrogenase |
| G6P | Glucose 6 Phosphate |
| GF | Glucose Free |
| GF-Lglut | Glucose Free without L-glutamine |
| GF-Pyr | Glucose Free without pyruvate |
| GF-Pyr/-Lglut | Glucose Free without pyruvate and L-Glutamine |
| GLS | Glutaminase |
| GLUT | Glucose Transporter |
| GLUT1/3 | Glucose Transporter 1/3 |
| GP | Guinea Pig |
| GTP | Guanosine Triphosphate |
| GSH | Glutathione |
| H ⁺ | Proton |
| HBSS | Hanks Balanced Salt Solution |
| HCl | Hydrochloric Acid |
| HDAC | Histone Deacetylase |
| HIF1 | Hypoxia Inducible Factor 1 |
| HK1/2 | Hexokinase 1 / 2 |
| HMGCL | 3-Hydroxy-3-Methylglutaryl CoA Lyase |
| HMG-CoA | 3-hydroxy-3-methylglutaryl coenzyme A |
| HMGCS2 | 3-hydroxy-3-methylglutaryl-CoA synthase 2 |
| Hr | Hours |
| IgG | Immunoglobulin G |
| IL | Interleukin |

| | |
|-----------------|--|
| IHC | Immunohistochemistry |
| KD | Ketogenic Diet |
| LCN-2 | Lipocalin-2 |
| LDH | Lactate Dehydrogenase |
| LDHA | Lactate Dehydrogenase A |
| L-G | L-glutamine |
| LG | Low Glucose |
| LPS | Lipopolysaccharide |
| M | Mouse |
| MAPK/ERK | Mitogen Activated Protein Kinase |
| MEM α | Minimum Essential Media alpha |
| MeSH | Medical Subject Headings |
| MAT | Methyl Acetoacetyl-CoA Thiolase |
| MCT | Monocarboxylate Transporter |
| mESC | Mouse Embryonic Stem Cells |
| ml | Millilitre |
| mm ² | Millimetre |
| mM | Millimolar |
| MMS | Monomethyl Succinate |
| MPP+ | 1-methyl-4-phenylpyridinium |
| mRNA | Messenger Ribonucleic Acid |
| MRI | Magnetic Resonance Imaging |
| MTT | 3-(4,5-dimethylthiazol-2-yl)-2,5 diphenyltetrazolium bromide |
| mTOR | Mammalian Target of Rapamycin |
| NADH | Nicotinamide Adenine Dinucleotide |
| NADPH | Nicotinamide Adenine Dinucleotide Phosphate |
| NB | Neuroblastoma |
| NGS | Normal Goat Serum |
| NeuN | Neuronal Nuclei |
| NMDA | N-methyl-D-Aspartate |
| NSC | Neural Stem Cells |
| OFT | Open Field Test |

| | |
|------------------|--|
| OXCT1 | 3-oxoacid CoA-transferase 1 |
| OPT | Optical Projection Tomography |
| OXPHOS | Oxidative Phosphorylation |
| P21.5/P90.5 | Postnatal Day 21.5/90.5 |
| PBS | Phosphate Buffered Saline |
| PBS-T | 0.05% Triton X-100 in 1X PBS |
| PEP | Phosphoenolpyruvate |
| PDH | Pyruvate Dehydrogenase |
| PDK | Pyruvate Dehydrogenase Kinase |
| PFA | Paraformaldehyde |
| PFK-1 | Phosphofructokinase |
| PGC - 1 α | Pparg coactivator 1 alpha |
| PGI | Phosphoglucoisomerase |
| PGK | Phosphoglycerate Kinase |
| PGM | Phosphoglycerate Mutase |
| PKM1/2 | Pyruvate Kinase Isoform 1/2 |
| PK | Pyruvate Kinase |
| PNS | Peripheral Nervous System |
| PS | Penicillin Streptomycin |
| P-S | Phosphatidylserine |
| PPAR α | Proliferator-activated receptor alpha |
| PPP | Pentose Phosphate Pathway |
| Q cycle | Ubiquinone Cycle |
| R | Rat |
| RA | Retinoic Acid |
| RG | Regular Glucose |
| RM | Regular Media |
| ROS | Reactive Oxygen Species |
| RPMI | Roswell Park Memorial Institute Medium |
| RT | Room Temperature |
| SC | Suggested Control |
| SD | Standard Diet |

| | |
|---------------|----------------------------------|
| SCOT | Succinyl CoA-Oxoacid Transferase |
| SEM | Standard Error of the Mean |
| SN | Substantia nigra |
| SP | Sodium Pyruvate |
| TBI | Traumatic Brain Injury |
| TCA | Tricarboxylic Acid |
| TGF- β | Transforming Growth Factor Beta |
| TNF- α | Tumour Necrosis Factor alpha |
| μm | Micron |
| WB | Western Blot |

Abstract

The cellular and phenotypic effects that carbohydrate restriction have on brain development are unclear. Ketone bodies become a primary energy source in periods of prolonged glucose deprivation, due to dieting, strenuous exercise, starvation and fasting. Moreover, recent studies have highlighted how the ketone bodies β -hydroxybutyrate (β OHB) and Acetoacetate (AcAc) are vital metabolic and signalling mediators in the mature and developing brain even when glucose is in abundance. The goals of this study are to elucidate the effects of glucose deprivation and ketone body supplementation on the growth, development, and health of rapidly dividing neural stem and neural precursor cells. Neuroblastoma (NB) derived SH-SY5Y cells and neuroepithelial cell derived NE-4C cells are characterised by a high proliferative capacity and glucose demand as a hallmark of their growth and metabolism. However, the impact of glucose deprivation and ketone body supplementation on SH-SY5Y and NE-4C cell growth, lineage and metabolic health are unclear due to conflicting reports in the literature and complexities underlying the Warburg effect.

Firstly, a systematic review of literature researching the impact of ketone bodies, glucose and other media formulations *in vitro* was undertaken to determine if they exert a positive or negative effect on cell growth. The species of cell line, type of cell line, experimental duration, concentration, and media formulations used in each study were assessed. It was determined that over half of the studies that used ketone bodies on cell growth *in vitro* produced a positive result. The most used ketone body was β OHB and the experimental concentration ranges were between 5 and 10 mM. The systematic review also showed that human derived neuronal cells were the most frequently utilized species and type of cell line. There were inconsistent data gathered with respect to media formulations used in each study. Most studies did not outline whether glucose, pyruvate or glutamine were included in their culturing media.

Based on data generated from the systematic review and the inconsistencies in reported data in outlining the specific culture formulations, we investigated the impact of ketone bodies and glucose deprivation, and pyruvate and glutamine deprivation on neural stem and neural precursor cell growth.

Ketone supplementation did not reveal an effect on cell growth and health in culture formulations deprived of glucose but containing glutamine and pyruvate.

Given the potentially confounding effects of other substrates in media formulations, the next set of experiments aimed to clarify the metabolic roles of culture substrates on the growth and health of NE-4C neuroepithelial cells and SH-SY5Y human NB cells in the presence and absence of β OHB. SH-SY5Y and NE-4C cells survived and appeared morphologically healthy in media deprived of all anaplerotic inputs and supplemented with ketone bodies; however, their growth patterns and metabolic activities were reduced. Pyruvate appeared to mask the effects of ketone supplementation, most likely due to competition at the monocarboxylate transporters, which shuttles β OHB into cells, but is also involved in lactate, an end-product of glycolysis, efflux. Experimental analysis enabled the development of standard media control culture conditions for use in future experiments, in which β OHB appeared most available for metabolism. This standard media culture condition consisted of low glucose, supplemented with β OHB in the absence of pyruvate and glutamine.

This study next aimed to reveal the metabolic roles of glucose, pyruvate and glutamine on the lineage potentials and metabolic health of differentiating NE-4C and SH-SY5Y cells in the presence and absence of β OHB as their metabolic profile shifts from aerobic glycolysis to oxidative phosphorylation (OXPHOS). Glucose and substrate deprivation is detrimental to NE-4C and SH-SY5Y cell metabolic health and phenotype during differentiation. Supplementation with β OHB over 5 and 10 days *in vitro* (DIV) failed to rescue cell growth in both lines; however, cells were partially rescued at 15DIV, indicating a shift from glycolytic metabolism to OXPHOS.

From the data gathered in the systematic review and experiments undertaken in the present study, the role of culture metabolic substrates in experimental paradigms appears to be critical when understanding how cells tolerate and grow in media supplemented with β OHB and deprived of glucose. Pyruvate appears to play a key role in brain cell metabolism in the absence of glucose in culture, which impacts their capacity to metabolise ketone bodies.

These data contribute to research underlying the role of ketone body metabolism on neural stem and neural progenitor growth *in vitro* and may have implications for our understanding of the roles of ketone body metabolism on brain growth and function.

Lay Abstract

Prolonged starvation and fasting can have degenerative consequences on brain function which if left without energy may be irreversible. Brain development is a complicated process which necessitates a balance between different energy sources to mediate cell growth and function across the central nervous system. The goals of this study were to understand the mechanisms underlying energy deprivation at key stages of neural development and to understand if these could be rescued by alternate fuel source supplementation.

Ketone bodies are produced in the liver and are used primarily as a metabolic source of energy when carbohydrate concentration is low. Experiments conducted on cells using ketone bodies have shown conflicting results, with some experiments showing ketones to have anti-inflammatory and neuroprotective effects, whilst other studies have shown them to be detrimental to cell growth and health. To this end, the first chapter of this thesis looks at the existing literature on the impact of ketone body supplementation on cell growth *in vitro*. Following on from the findings of this systematic review we initially used two cell lines (immortalized stem cells), the SH-SY5Y NB cell line, which is a childhood cancerous cell line derived from the adrenal glands and the NE-4C neuroepithelial cell line which is derived from the cerebral vesicles of 9-day old mouse embryos. The SH-SY5Y cell line was the most used cell line in this type of research and described ketone bodies as having both positive and negative impacts on cell growth. Therefore, to further understand the impact of carbohydrate reduction and ketone supplementation, we examined the role of the culturing media in which the cells were grown to determine if there are alternative sources of energy which may be confounding in the reported results. These experiments showed that culture media components are critical to the outcome of experiments testing the roles of ketone supplementation and carbohydrate deprivation. Removing these additional substrates is fundamental to establishing experimental conditions suitable for ketone and glucose related metabolic research on brain development.

We showed that ketones may be used as an alternate fuel source under very tightly controlled experimental conditions when studying brain cell development. Glucose is fundamental to the normal maturation of the brain and much care must be taken when removing or supplementing neural stem and neural progenitor cells with alternative fuel sources. Taken together our data sheds light on dietary influences on in utero brain development and how metabolic requirements may vary across a brain cells life cycle.

Value of Research

These findings have general applicability to *in vitro* models of β OHB metabolism and explain the wide variety of findings in the literature according to their respective methodologies. Proposed in this study is a general paradigm which presents the capacity to metabolise ketone bodies not as a purely intrinsic property of the cells in question, but as a dynamic function of an interplay between the extrinsic elements and the cell's own metabolic phenotype. Thus, the results of previous and future *in vitro* investigations into the proliferative and differentiative effects of ketone bodies, given the widely varied methodologies will partially be pre-determined by the choice of the culture conditions. It is therefore important for any *in vitro* study of the metabolic effects of ketones to consider the contributions of their culture conditions and supplements as suggested by others and as practically shown in this study. We suggest a standard control which may be used with the aim of contributing to replicable findings with respect to research underlying glucose deprivation and ketone body metabolism and its therapeutic applications.

Publications Resulting from this Work

1. Mohammad Alherz, **David Lee**, Amnah Alshangiti, Darren Roddy, Gerard O'Keeffe, Robin White, Denis Barry. (2021). *The Growth Response to Beta-Hydroxybutyrate in SH-SY5Y Neuroblastoma Cells is Suppressed by Glucose and Pyruvate Supplementation. Neurochemical Research.* PMID: 33389384
2. Denis Barry, Sarah Ellul, Lindsey Watters, **David Lee**, Robert Haluska Jr, Robin White. (2018). *The Ketogenic Diet in Disease and Development. International Journal of Developmental Neuroscience.* PMID: 29689338

Presentations Resulting from this Work

1. **David Lee**, Dr. Denis Barry (12th International Cancer Conference Autumn Meeting 2022). *The Effects of Ketone Body Supplementation on the Growth of SH-SY5Y Neuroblastoma Cells*. October 13th – October 14th. Poster Presentation.
2. **David Lee**, Dr. Mohammad Alherz, Dr. Denis Barry. (Federation of European Neuroscience Societies Summer Meeting 2022). *Investigating the Effects of Ketone Body Supplementation on the Growth and Development of Cortical Neural Stem Cell*. July 9th – July 13th. Poster Presentation.
3. **David Lee**, Mohammad Alherz, Gerard O’Keeffe, Denis Barry. (Anatomical Society Winter Meeting 2021). *The Effects of Ketone Body Supplementation on the Growth of SH-SY5Y Neuroblastoma Cell*. 6th – 8th January. Poster Presentation
4. Dr. Denis Barry, **David Lee**, Dr. Robin White. (British Neuroscience Association Summer Meeting 2019) *The Effects of a Ketogenic Diet During Pregnancy on the Developing Mouse Brain*. 14th – 17th April. Poster Presentation.
5. Andrew Hynes, Aisling Bracken, **David Lee**, Dr. Jennifer England, Dr. Mohammad Alherz, Dr. Robin White, Dr. Denis Barry. (British Neuroscience Association Summer Meeting 2019). *Investigating the Effects of Ketone Supplementation on Neuroepithelial and Neuronal Cell Growth, Lineage, and Health*. 14th – 17th April. Poster Presentation.
6. Lindsey Watters, **David Lee**, Dr. Robin E. White, Dr. Denis Barry. (Anatomical Society Winter Meeting 2017). *Examining the Cellular and Lineage Significance of Ketone Supplementation on CNS Neural Precursors During Development*. 18th – 20th December. Poster Presentation.

Chapter 1

Introduction

1. Introduction

1.1 Glucose Deprivation, the Ketogenic Diet and Metabolism

Glucose metabolism is the process whereby simple sugars from carbohydrates are converted into glucose, which travels through the blood to the cells. In the cytosol of the cell, glycolytic metabolism converts glucose to pyruvate, generating energy in the form of adenosine triphosphate (ATP) and nicotinamide adenine dinucleotide (NADH) in the process. Glucose is the body's primary energy source, and the brain is the main consumer of glucose. Its metabolism is very tightly controlled to maintain homeostasis and to avoid the pathophysiological consequences of fuel deprivation. Glucose cannot be replaced as the brain's primary energy source, but it can be supplemented in times of strenuous physical activity, starvation and in carbohydrate restrictive diets. Ketone bodies generated from the β -oxidation of fatty acids and released from the liver represent the body's alternative energy source during prolonged glucose deprivation when glycogen stores are exhausted. This is characterized by rapid increases in blood brain barrier (BBB) transporter levels (such as monocarboxylate transporters (MCTs)) and elevated blood ketone levels. Ketone bodies not only serve as a source of energy via oxidative phosphorylation pathways (OXPHOS) but also promote increased resistance to oxidative and inflammatory stress, with a decrease in anabolic insulin-dependent energy expenditure (Kolb et al., 2021).

The ketogenic diet (KD) is a high fat, moderate protein and low carbohydrate diet that aims to induce a state of glucose starvation resulting in a shift towards ketone body metabolism. It was originally observed that high concentrations of ketone bodies in the blood (ketonemia) reduced the frequency of seizures in epilepsy (Wilder, 1921), and the KD was subsequently developed as a treatment for intractable epilepsy, its potential therapeutic role has been highlighted in a range of disorders including obesity, diabetes, fatty liver disease, neurological disease, and cancer (Puchalska and Crawford, 2017). As such, it is becoming increasingly popular due to its perceived benefits in disease and well-being (Barry et al., 2018a).

The three ketone bodies in circulation in the human body are β -Hydroxybutyrate (β OHB), acetoacetate (AcAc) and acetone, with acetone being the least abundant (Laffel, 1999). The metabolic shift is achieved by an increase in plasma ketone bodies synthesized by the liver as a by-product of the β -oxidation of fatty acids in hepatic mitochondria (Cotter et al., 2013). These are transported into circulation and cells by the MCTs (Tildon et al., 1994).

Subsequently, ketolysis takes place in the extrahepatic mitochondria of various tissues with the conversion of the ketones β OHB and AcAc into acetyl-coenzyme A (acetyl-CoA) for incorporation into the tricarboxylic acid (TCA) cycle (Cotter et al., 2013). The result is the generation of ATP via OXPHOS (Figure 1.1).

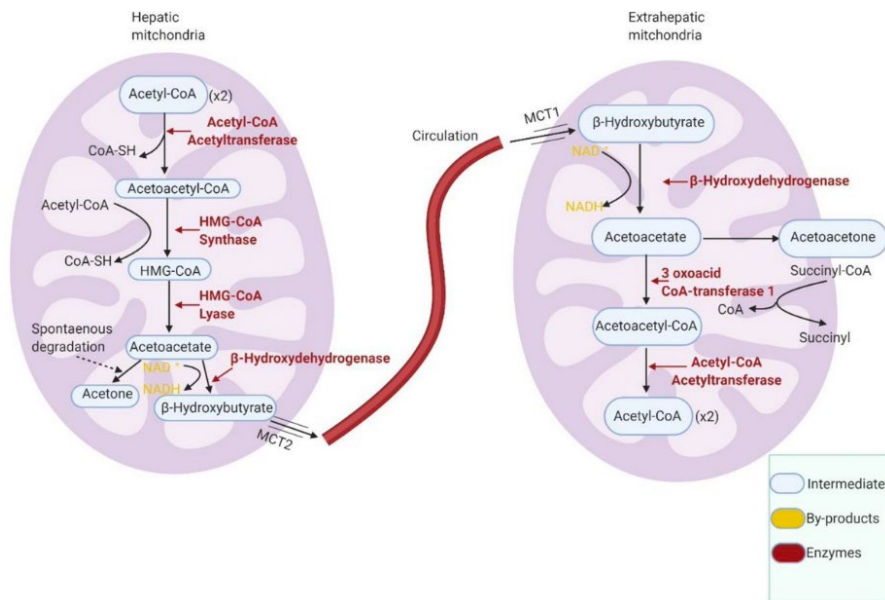


Figure 1.1 The pathway of ketogenesis and ketolysis (created with BioRender.com).

1.2 Ketone Metabolism

Fatty acyl-CoA is transported into liver mitochondria and degraded to acetyl-CoA before being converted to aceto-acetyl-CoA by acetyl-CoA acetyltransferase (Laffel, 1999). Acetoacetyl-CoA is then sequentially converted to 3-hydroxy-3-methylglutaryl coenzyme A (HMG-CoA) and AcAc by HMG-CoA synthase and HMG-CoA lyase respectively (Laffel, 1999). AcAc undergoes spontaneous decarboxylation to form acetone, or reduction to form β OHB which is catalysed by β -hydroxybutyrate dehydrogenase (β DH1) (Newman and Verdin, 2014). β OHB and AcAc are transported out of the hepatic tissue, enter systemic circulation and travel to extrahepatic organs such as the brain (Puchalska and Crawford, 2017). MCTs are responsible for the active transport of ketone bodies across biological membranes such as the BBB due to their hydrophobic nature (Barry et al., 2018; Melo et al., 2006). The expression levels of these MCTs have also been demonstrated to change throughout development and in response to the cell's energy requirements (Hawkins et al., 1986; Leino et al., 2001; Pierre et al., 2000). In rats, the levels of MCT expression indicates the ability of the central nervous system (CNS) to metabolise ketone bodies (Vannucci and Simpson, 2003) (see Table 1.1).

| Age/ Condition | MCT Expression | MCT phenotype / Region / Methodology | Authors |
|------------------|---|--|-----------------------------|
| Embryonic | Cortex : MCT1 ↓ from E16 to P3 then ↑, MCT2 ↑ from P0 to P5 then ↓ Hypothalamus : MCT1 ↑ from E18 to E19 then ↓ until P4, MCT2 ↑ from E17 to E 19 then ↓ | Rat / MCT1 and MCT2 expressed in radial glial cells and neurons prenatally and in astrocytes postnatally with higher expression of MCT2; IHC | Baud, et al., 2003 |
| Postnatal | MCT1 expression constant from P7 to P37, MCT2 peak expression at P7 then ↓ to P35 | Rat cortex, hippocampus, cerebellum, thalamus; WB and IHC | Vannucci and Simpson, 2003 |
| | MCT2 ↑ at P35 compared to adult | Rat cortex; WB | Prins and Giza, 2006 |
| | MCT2 ↑ from P1 to P21 compared to adulthood, MCT4 ↑ from P0 to P14 | Rat astrocytes; IHC | Rafiki, et al., 2003 |
| | MCT1 and MCT2 ↑ in newborn compared to adult | MCT1 in neurons and astrocytes of newborn rats, MCT2 in newborn rat neurons; mRNA | Mac and Nałęcz, 2003 |
| Adult | MCT2 | Adult rat cerebellum Purkinje cells, brainstem sensory fibres and cortex synapses; IHC | Pierre, et al., 2002 |
| | MCT1 and MCT2 | Rat cortex astrocytes in glia limitans and white matter tracts; IHC | Hanu, et al., 2000 |
| | MCT1, MCT2 and MCT4 | MCT1 and MCT4 primarily expressed in rat astrocytes. MCT2 expressed in neurons | Pellerin, et al., 2005 |
| | MCT2 | Rat hypothalamic neurons; mRNA | Cortes-Campos, et al., 2013 |

Table 1.1 Expression of brain MCT 1 and 2 during development and adulthood. MCT, monocarboxylate transporter, IHC, Immunohistochemistry, mRNA, messenger RNA; WB, western blot (Adapted from Barry et al., 2018).

Once inside extrahepatic organs, ketolysis occurs which is the energy yielding stage of ketone metabolism. The first step involves β OHB being oxidised to AcAc by β DH1, following which AcAc gains a CoA moiety forming acetoacetyl-CoA which is catalysed by SCOT (succinyl CoA-oxoacid transferase) (Laffel, 1999). Acetoacetyl-CoA is cleaved by MAT (methylacetoacetyl-CoA thiolase) forming two molecules of acetyl-CoA which feed into the TCA cycle via condensation with oxaloacetate and contribute to ATP production through OXPHOS (Barry et al., 2018a).

The metabolism of ketone bodies has an important homeostatic role in supplying energy to the brain during periods of carbohydrate restriction, where glycolysis is limited. Certain ketone bodies have a non-oxidative fate and contribute to biosynthesis of fatty acids, sterols, and cerebral proteins in the developing CNS of human embryos and neonates (Patel et al., 1975). Astrocytes are able to undergo ketogenesis (whereas neurons cannot) providing energy from ketone bodies to neighbouring neurons (Foll and Levin, 2016). With this, neurons can switch between carbohydrate/lactate oxidation to ketone bodies in a process called “G to K switch” (Mattson et al., 2018). This switch was observed in mice that were

placed on either a ketone diet/intermittent fasting containing diet which showed the brain utilizing ketone bodies (Mattson et al., 2018). Ketone bodies and their effect on neurogenesis is still uncertain, but there is evidence supporting its role in improving synaptic plasticity, learning and spatial memory (Hernandez et al., 2018, Murray et al., 2016). The expression of brain derived neurotrophic factor (BDNF) has been shown to be increased by β OHB and thus promoted cellular resistance, however prolonged exposure to ketones has been shown to stimulate hypothalamic neuropeptides and glucose homeostasis dysregulation (Carneiro et al., 2016, Sleiman et al., 2016). The interplaying role of ketone metabolism has been indicated in primary mouse embryonic neurons and in adipocytes as Acetoacetyl-CoA synthetase (AACS – an enzyme that converts AcAc to acetoacetyl-CoA) knockdown decreased differentiation of each cell type (Hasegawa et al., 2012a, Hasegawa et al., 2012b).

Serving as an alternative energy source to glucose, β OHB is released by the liver during periods of nutrient deprivation (Grabacka et al., 2016). The presence of ketone bodies in the bloodstream is induced pathologically in diabetic ketoacidosis (DKA) (Stojanovic and Ihle, 2011) or physiologically through fasting and carbohydrate-restricted dietary regimens including the KD described above (Paoli et al., 2013).

Such dietary restrictions are frequently purported as a potential cancer therapy in NB and other neoplasms (Morscher et al., 2015, Aminzadeh-Gohari et al., 2017, Weber et al., 2018). This stems from the observation that increased glucose uptake is a key characteristic of cancer, which also forms the biologic basis of 18 Fluorodeoxyglucose positron emission tomography (FDG-PET) scans for detecting the spread of the disease (Jadvar, 2016).

1.3 Systemic Ketone Body Levels

Blood samples taken from the umbilical cord of a new-born has shown that blood ketone levels range between 0.2 - 0.4 mM. Blood ketone body levels then peak 48 hr after birth and range between 0.8 - 1 mM (Persson and Gentz, 1966). In adults, normal levels of blood ketone bodies are between 0.1 to 0.25 mM (Wildenhoff et al., 1974). β OHB levels in non-pregnant and pregnant women (at 16 to 22 weeks gestation) following 84 hr of fasting rose from 0.2 - 0.5 mM to 4 - 4.5 mM. In the same study, blood samples taken from the amniotic fluid of pregnant women showed levels of β OHB were between 3.5 – 4 mM (Rudolf and Sherwin, 1983) (Table 1.2).

During ketosis, when carbohydrates are unavailable, ketone levels in the blood may rise to 7 mM from the postprandial level of 1 mM (Hall et al., 1984) (Table 1.2). If the release of free fatty acids from adipose tissue exceeds the capacity of tissues to metabolize them, such as during insulin deficiency of type 1 diabetes, β OHB levels may reach 25 mM which can be fatal (Cahill and Veech, 2003) (Table 1.2).

| Ketone | Levels | Timeframe | Model | Authors |
|---|--|---|--------------|---|
| βOHB | 25 mM (Blood sample) | Diabetic ketoacidosis | Humans | (Cahill and Veech, 2003) |
| βOHB | 0.2 – 0.4 mM (Blood sample) | 13 and 26 months old (C57Bl/6 Mice) 8 weeks old (CD1 mice) | Mice | (Roberts et al., 2018, Sussman et al., 2015) |
| βOHB | 0.7 – 0.8 mM | 9 weeks | Wistar rats | (Si et al., 2017) |
| βOHB | From 0.2 – 0.5 mM to 4 - 4.5 mM (Blood sample) | Adulthood- following 84 hours of fasting | Humans | (Rudolf and Sherwin, 1983). |
| βOHB | From 0.2 – 0.5 mM to 4 - 4.5 mM (Blood sample) | 16 – 22 weeks pregnant – following 84 hours of fasting | Humans | (Rudolf and Sherwin, 1983). |
| βOHB | 3.5 – 4 mM (amniotic fluid) | Taken from the amniotic fluid of 16 – 22 weeks pregnant – following 84 hours of fasting | Humans | (Rudolf and Sherwin, 1983). |
| βOHB / AcAc | 7 mM (from the post prandial (after a meal) level of 1 mM (Blood sample) | 48 – 72 hours after fasting | Humans | (Hall et al., 1984) |
| βOHB / AcAc/ Acetone | 0.2 – 0.4 mM (Blood sample) | Taken from the umbilical cord – directly after birth | Humans | (Persson and Gentz, 1966) |
| βOHB / AcAc / Acetone | 0.8 – 1.0 mM (Blood sample) | 48 hr after birth | Humans | (Persson and Gentz, 1966) |
| βOHB / AcAc / Acetone | 0.1 - 0.25 mM (Blood sample) | Adulthood | Humans | (Wildenhoff et al., 1974) |

Table 1.2 Overview of ketone levels in the blood

1.4 Glucose and Pyruvate Metabolism

Glucose is an essential source of cellular carbon and is a critical fuel source that is employed in a specific set of metabolic pathways. Glucose is brought into the cell via glucose transporters through facilitated diffusion. Hexokinase (HK) phosphorylates glucose which then becomes glucose-6-phosphate (G6P) and through further additional steps in glycolysis eventually becomes pyruvate. Alternatively pyruvate can be transferred to the mitochondrial matrix where it can be further broken down through oxidation to acetyl-CoA or through carboxylation to oxaloacetate or malate in the Krebs cycle and used for further energy production (Tatapudy et al., 2017). Pyruvate dehydrogenase (PDH) catalyzes pyruvate oxidation, the activity of PDH is modulated by acetyl-CoA, NADH and through the phosphorylation of pyruvate dehydrogenase kinase (PDK). The by-product of glucose and fatty acid oxidation, acetyl-CoA, contributes carbon atoms to the citric acid cycle (CAC), which is then oxidized to produce ATP or guanosine triphosphate (GTP) and NADH₂. As the intermediates from the CAC are used to produce amino and nucleic acids, they must be constantly removed from the cycle and must be reproduced via an anaplerosis reaction.

NADH₂, flavin adenine dinucleotide (FADH), and succinate from the CAC donate electrons to the electron transport chain (ETC) for OXPHOS in the mitochondrial inner membrane.

Embryonic stem cells differentiating into neural stem cells (NSC) is followed with an increase in glycolysis and a decrease in mitochondrial OXPHOS indicating that glycolytic regulation is critical in NSC growth (Birket et al., 2011). Glycolysis in NSC appears to be critical as it supplies the necessary amino and nucleic acids required for differentiation and growth. Even though glycolysis only produces 2 ATP per molecule of glucose, it produces more ATP through this method than through mitochondrial OXPHOS (Guppy et al., 1993). With this, mature NSC have messenger ribonucleic acids (mRNAs) and proteins which are necessary for glucose metabolism, this includes GLUT1 and GLUT3 (Maurer et al., 2006).

The information available regarding how metabolism is reorganized when neurons undergo differentiation is still quite vague. In a study using NSCs, a reduction in hexokinase (HK2) and lactate dehydrogenase (LDH) expression with PK gene splicing switching from PKM2 (pyruvate kinase isoform 2) to PKM1 (pyruvate kinase isoform 1) describes the shift from glycolytic metabolism to neuronal OXPHOS. The protein levels of c-MYC and N-MYC (transcriptional activators of HK2 and LDHA) are significantly reduced. This reduction in HK2 and LDHA during neuronal differentiation leads to apoptosis, which signifies that stopping glycolytic metabolism is necessary for neuronal survival (Agostini et al., 2016). In a study investigating the impact of high levels of glucose on the differentiation of C17.2 mouse NSC it was found that oxidative stress and endoplasmic reticulum stress mediate the inhibitory effect of high glucose on NSC differentiation (Chen et al., 2018). In a set of experiments investigating HRD1 on neuronal differentiation, endoplasmic reticulum stress was found to inhibit dendrite outgrowth (Kawada et al., 2014) In a separate study, mouse embryonic stem cells (mESC) differentiating into neurons at 14 DIV was inhibited by high concentrations of glucose also (Yang et al., 2016).

1.5 Glutamine Metabolism

The blood plasma concentration of glutamine is around 0.57 mM (Bergström et al., 1974). It's an essential source of energy which also provides the nitrogen needed for the synthesis of nucleotides and supports non-essential amino acid pools. The metabolism of glutamine provides a source of carbon that facilitates the cells ability to use glucose derived carbon and TCA cycle intermediates as biosynthetic precursors (DeBerardinis et al., 2007). Glutamine is converted into glutamate by the enzyme glutaminase (GLS) where it either gives away the amide nitrogen to biosynthetic pathways or is released as ammonia. In the

cell, glutamate is the most widely available amino acid and is generated by a mitochondrion – associated GLS. Glutamate is further broken down (through further deamination) by the enzyme glutamate dehydrogenase which produces α – ketoglutarate (α -KG), an intermediate of the TCA cycle and a substrate for dioxygenases which can modify deoxyribonucleic acid (DNA) and proteins (Hensley et al., 2013). Furthermore, glutamate is a precursor of glutathione (GSH), a major endogenous antioxidant that can prevent damage to critical cellular elements by reactive oxygen species (ROS) such as free radicals and peroxides. Using the aspartate – malate shuttle, glutamine increases the nicotinamide adenine dinucleotide phosphate (NADPH/NADP (+)) ratio, which reduces actions of oxidative stress on the cell (Son et al., 2013). Thus, the metabolism of glutamine can assist in the control of redox balance through the biosynthesis of GSH and/or NADPH production (Matés et al., 2002). To add to this, glutamine modulates mammalian target of rapamycin (mTOR) activity, translation and autophagy to co-ordinate cell growth and proliferation (Nicklin et al., 2009). GLS is expressed in adult NSCs and includes glutamine in the cellular GSH pool, this is critical for sustaining redox homeostasis (Yeo et al., 2013). MYC is the most recognized regulator of glutaminolysis (Gao et al., 2009). How glutamine metabolism functionally controls NSCs (since MYC is an important factor in regulating stem cell metabolism) still needs to be fully characterized. With this, recent studies have provided evidence on how critical glutamine metabolism is in stem cell redox homeostasis, proliferation, protein and nucleic acid metabolism and epigenetic modifications.

1.6 Ketone Bodies in Cancer Biology

Links between cancer and ketone bodies are quickly emerging but research in both animal and human studies have produced conflicting results. As the metabolism and production of energy from ketone bodies can be influenced by other metabolic substrates, there is a premise to pursuing biological links between cancer and ketone bodies due to the potential of specific patient centred nutritional therapies. Cancer cells undergo metabolic reprogramming in order to sustain accelerated proliferation and growth (DeNicola and Cantley, 2015, Pavlova and Thompson, 2016). Carbon from glucose is fed through lipogenesis, the pentose phosphate pathway (PPP) and through mainly glycolysis (Grabacka et al., 2016, Shukla et al., 2014, Yoshii et al., 2015). Cancer cells acclimate to decreased levels of glucose through its unique ability to utilize alternative energy sources such as pyruvate, glutamine, and aspartate (Jaworski et al., 2016, Sullivan et al., 2015). For example, if cancer cells are exposed to limited levels of pyruvate, then the cell can transform

glutamine into acetyl-CoA through carboxylation which ensures both its energetic and anabolic needs (Yang et al., 2014). Cancer cells can also use acetate as an energy source (Comerford et al., 2014, Jaworski et al., 2016, Mashimo et al., 2014, Wright and Simone, 2016, Yoshii et al., 2015). Acetate is a derivative from lipogenesis and this process is a key component to cancer cell proliferation and increased levels of acetate is associated with increased tumour sizes and decreased patient lifespans (Comerford et al., 2014, Mashimo et al., 2014, Yoshii et al., 2015). Healthy cells can switch their energy source from glycolysis to ketogenesis during periods of glucose deprivation. This ability to switch varies among cancer cells but implanted brain tumours in *in vivo* studies oxidized [2,4-¹³C₂]-βOHB to a similar degree as surrounding brain tissue (De Feyter et al., 2016).

1.7 Glycolysis and Oxidative Phosphorylation

Glycolysis is an anaerobic process, while the TCA cycle and OXPHOS are aerobic (Vander Heiden et al., 2009). However, cells have means of producing ATP even under periods of reduced oxygen supply. This is known as lactic acid fermentation, which is the process of transforming the glycolytic product, pyruvate, into lactate. This occurs in most organisms when oxygen is not present and therefore cannot undergo respiration (Shyh-Chang et al., 2013). LDH is the enzyme that catalyses the reduction of pyruvate to lactate with the oxidation of NADH into NAD⁺. By regenerating NAD⁺ it allows glycolysis to continue to run and generate ATP.

Brain cell metabolism switches from glucose hungry glycolysis to oxidative maturation as cells cease dividing and acquire mature functional phenotypes. Carbohydrate metabolism involves the breakdown of glucose to produce ATP. Through glycolysis, the TCA cycle and OXPHOS, one molecule of glucose can be oxidized completely to carbon dioxide and produce ATP. In glycolysis, glucose enters the cell via GLUTs and as previously mentioned glucose is then converted to G6P by HK. Phosphoglucose isomerase (PGI) then converts G6P into fructose 6-phosphate (F6P). Phosphofructokinase (PFK-1) catalyses the conversion of F6P to fructose 1,6-bisphosphate (F1-6BP). F1-6BP is then catalysed to glyceraldehyde 3-phosphate (GA3P) by aldolase. GA3P is then converted to 1,3-bisphosphoglycerate (1,3 BPG) by glyceraldehyde 3-phosphate dehydrogenase (GAPDH) (Alves et al., 2020). 1,3 BPG is catalysed to 3-phosphoglycerate (3-PG) by phosphoglycerate kinase (PGK). Phosphoglycerate mutase (PGM) converts 3-PG to 2-phosphoglycerate. This is then converted to phosphoenolpyruvate (PEP) by enolase. PK then converts PEP to two molecules of pyruvate. Pyruvate is then oxidized to acetyl-CoA in the mitochondrial matrix

by PDH, producing NADH and acetyl-coA will then enter the TCA cycle (Alves et al., 2020) (Fig. 1.2).

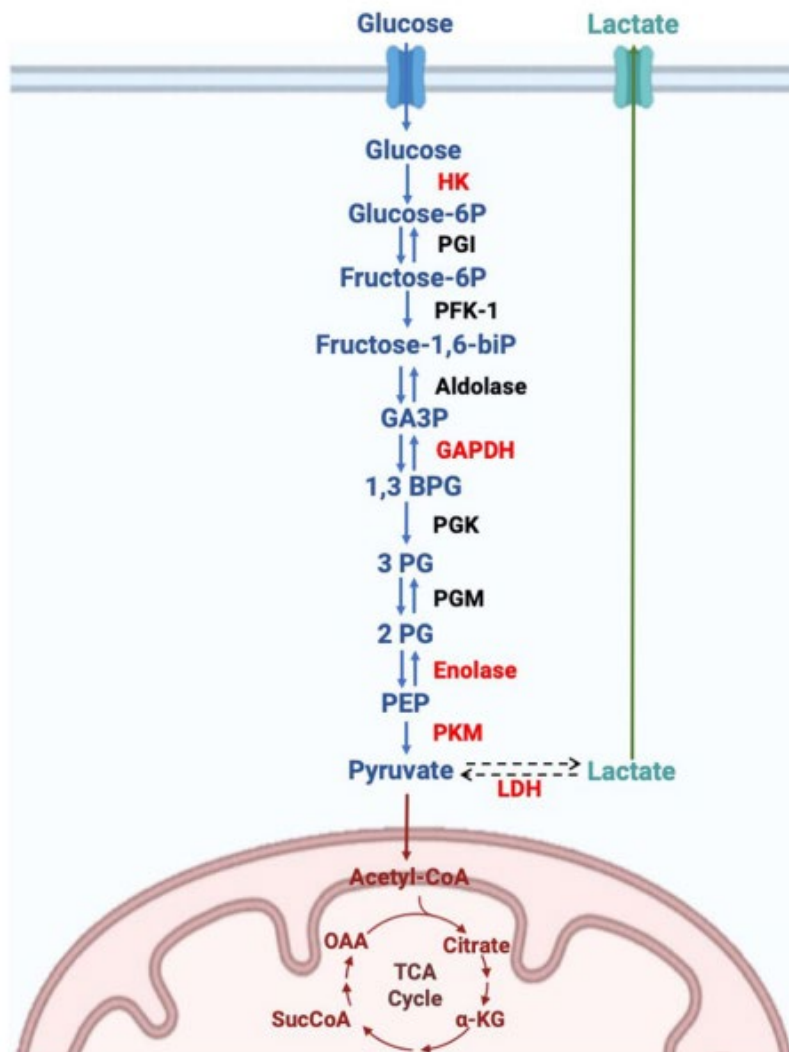


Figure 1.2 Glycolysis pathway, adapted from Alves et al., 2020

OXPHOS occurs at the site of mitochondrial ETC in the inner mitochondrial membrane and the ETC consists of five protein complexes embedded within it. The TCA in the mitochondrial matrix supplies NADH and FADH₂ to the ETC which donates electrons to the ETC via complex I and II. This transfer of electrons from complex I to the ubiquinone cycle (Q cycle) results a total of four protons (H⁺) being pumped across the inner membrane into the intermembrane space. Electrons from either complex I (donates two electrons at a time) or complex II (donates two electrons one at a time) are donated to ubiquinone which is reduced to ubiquinol (Nolfi-Donagan et al., 2020).

Complex III oxidizes ubiquinol which allows one electron at a time to pass through cytochrome c. Two H⁺ are pumped into the intermembrane space for every electron

transferred to cytochrome c which results in a total of four H^+ being brought into the intermembrane space for every pair of electrons that move through the cycle. Cytochrome c transports electrons to the complex IV where oxygen acts a terminal electron acceptor and is reduced into water. This reduction requires four electrons and causes four H^+ to be pumped into the intermembrane space. However, two H^+ are consumed in the process which results in a net total of two H^+ being pumped into the intermembrane space at complex IV (Nolfi-Donagan et al., 2020). The net movement of protons from the mitochondrial matrix to the intermembrane space creates a proton motive force (this is the proton concentration combined with the electrochemical proton gradient called the mitochondrial membrane potential). This proton motive force is critical in the process of energy storage and production during OXPHOS since it couples electron transport (from complexes I – IV) and oxygen consumption to the activity of complex V (ATP synthase). Complex V is a multi-protein complex consisting of an extra-membranous (F_1) and transmembrane (F_0) complexes and produces ATP through a rotational motor mechanism. The transfer of protons through F_0 from the intermembrane space is coupled to the rotation that results in the addition of phosphate to adenosine diphosphate (ADP) to form ATP at sites in F_1 (Nolfi-Donagan et al., 2020) (Fig. 1.3).

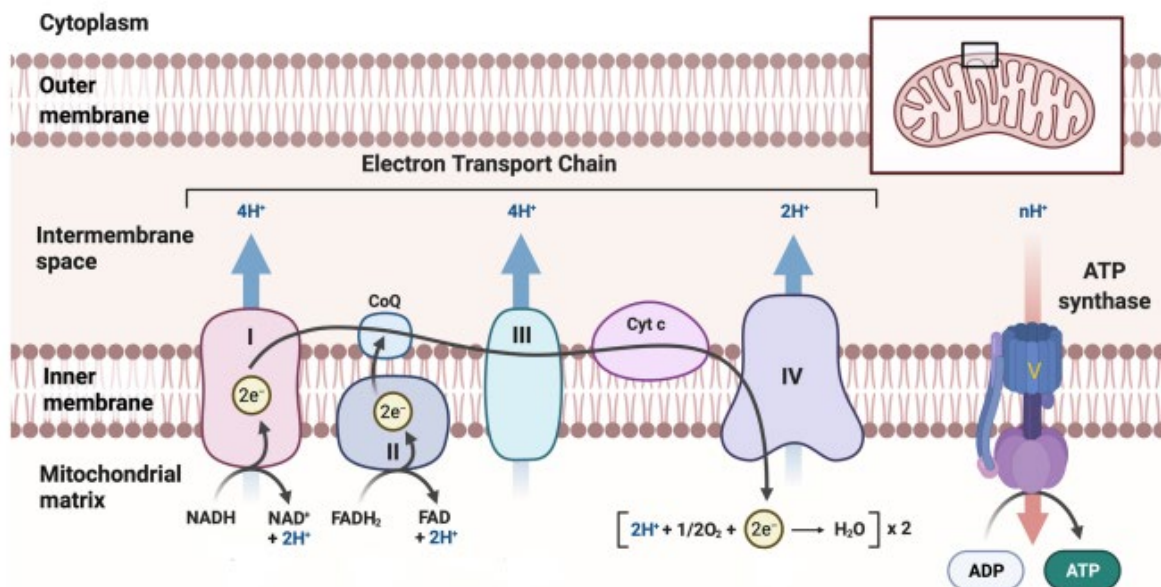


Figure 1.3 A summary diagram of OXPHOS, adapted From Wu et al., 2022

Under various conditions, such as in neural development and cancer, the pathways can be modified and exploited to meet the specific energy demands of the cell. Metabolism in adult neuronal cells involves the full oxidation of glucose to produce between 36-38 ATP molecules. During the catabolism process, intermediate metabolites of these pathways are

also used to synthesize nucleotides, amino acids, and lipids for generation of daughter cells via mitosis (Marie and Shinjo, 2011). Therefore, glucose can be used for both ATP synthesis or diverted into synthetic pathways, such as using acetyl-CoA for fatty acids, glycolytic intermediates for amino acids and ribose for nucleotides (Marie and Shinjo, 2011). The process of proliferation requires high flux through these synthetic pathways in order to generate the required building blocks for new cells. Conversely, differentiated adult neuronal cells have fewer anabolic demands and instead require larger amounts of energy to fuel other processes such as cellular homeostasis and specialized functions such as synaptic transmission (Folmes et al., 2012). Therefore, when cells have lower requirements of anabolic precursors, they preferentially catabolize glucose fully through the TCA cycle and OXPHOS to produce the maximum amount of ATP (Folmes et al., 2012).

1.8 The Warburg Effect

Almost all cancer cells use anaerobic glycolysis to produce energy, using a phenomenon called the “Warburg effect” where glycolytic pyruvate is changed into lactate in the cytosol of the cell. The Warburg effect in cancer cell metabolism stems from the critical role that glycolysis and lactic acid fermentation play in providing ATP and in compensating for lower dependence on OXPHOS and restricted mitochondrial respiration (De Feyter et al., 2016, Grabacka et al., 2016, Kang et al., 2015, Poff et al., 2014, Shukla et al., 2014).

The reliance on excessive glycolysis in neoplastic cells even in the presence of oxygen, coupled with the efflux of lactate was described by Otto Warburg as a hallmark of cancer almost a century ago (Warburg, 1925a). For every molecule of glucose, glycolysis produces only 2 molecules of ATP compared with 36 produced during OXPHOS (Devic, 2016), and Warburg’s effect is thus perceived by some to be a compensatory mechanism for defective mitochondrial function (Seyfried, 2015). Despite its seemingly inefficient nature however, it is observed in cancer even with normally functioning mitochondria and is thought to be beneficial in rapidly supporting the biosynthetic requirements of uncontrolled proliferation (Liberti and Locasale, 2016). This metabolic profile has been cited as the potential barrier to ketone metabolism (Seyfried *et al.*, 2014) and studies have observed that the lactate efflux associated with this phenomenon correlates with the suppressive effect of ketones on tumor proliferation (Whitaker-Menezes et al., 2011).

It has been seen that cancer cells have insufficient mitochondrial mRNA and poor oxidative machinery, and this has been theorized to be the reason for their glycolytic metabolic

phenotype (Bartmann et al., 2018). Additionally, when tumour cells grow, they can far exceed their blood supply and therefore end up living in hypoxic environments. Based on these two factors, cancer cells are believed to operate under the Warburg effect, being highly energetic but gaining most of their energy from running glycolysis independently (Bartmann et al., 2018).

These differences from normal cells are the target of the dietary therapeutic proposals, as glucose deprivation achieved through ketosis would be expected to preferentially starve cancer cells reducing their growth and survival (Kansara and Berridge, 2004), while healthy cells can readily adapt their metabolism to use ketone bodies such as β OHB to meet their energy demands (Weber et al., 2018). This would cause cancer cells to starve of energy, while normal cells could survive through metabolic adaptation (Weber et al., 2018). Utilizing this method of cancer therapy would be preferred, as methods of chemotherapy and radiation do not spare normal cells (Weber et al., 2018).

In this regard, several studies have observed that a reduction in glucose availability as seen in dietary restriction (Longo and Fontana, 2010, O'Flanagan et al., 2017), or pathologically in hypoglycemia, leads to preferential damage of cancer cells (Kansara and Berridge, 2004). The mechanisms of the high glycolytic process have also been targeted, such as the upregulated glucose transporter1 (GLUT1) enabling increased glucose uptake (Zambrano et al., 2019), as well as the MCTs which allow the resultant lactate efflux (Pérez-Escuredo et al., 2016a, Payen et al., 2020). Inhibitors of these have shown promising results but with the distinct disadvantages of substantial off-target effects (Park et al., 2018), as well as resistance occurring with upregulation of other transporter subtypes (Quanz et al., 2018).

The metabolic phenotype of NSCs is glycolytic (Locasale and Cantley, 2011). NSCs initially exist in a state of hypoxia due to the absence of a developed vascular system to deliver oxygen to their local environment (Jády et al., 2016). To accomplish this, NSCs generate ATP in an anaerobic fashion and subsequently use glycolysis followed by lactic acid fermentation. Additionally, NSCs also utilize glycolysis even when the environment becomes normoxic (Jády et al., 2016). This process appears paradoxical, such that it would be predicted that if oxygen became available to NSCs, metabolism would shift to OXPHOS. However, this is not the case, as these cells use the Warburg effect which has been previously described (Fig. 1.4).

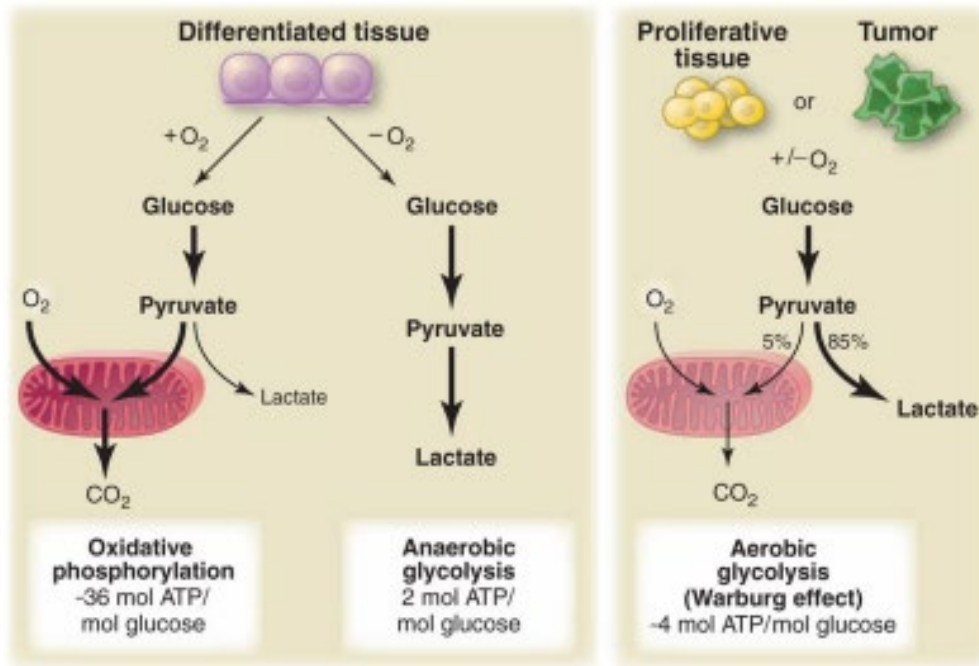


Figure 1.4 Warburg Effect. Schematic showing the metabolic differences between differentiated tissue, proliferative tissue, and tumours (adapted from (Vander Heiden et al., 2009)).

‘Two compartment tumour metabolism models’, otherwise known as the ‘Reverse Warburg effect model’ state that cancer cells can produce β OHB in adjacent fibroblasts, fulfilling the tumour cells energy requirements (Bonuccelli et al., 2010, Martinez-Outschoorn et al., 2012a). Hepatocellular carcinoma that originates from the liver shifts from ketogenesis to ketone oxidation and is consistent with the increased activity of β DH1 and SCOT enzymes in two hepatoma cell lines (Zhang et al., 1989). Hepatoma cells express both β DH1 and OXCT1 and oxidize ketones but only when they’re starved of serum (Huang et al., 2016). Alternatively, tumour cell ketogenesis has also been proposed. Changes in ketogenic gene expression are noticed during the transformation of colonic epithelium into metastatic colon cancer, this type of cell normally expresses HMGCS2 and a recent study proposed that this gene may be a marker for a poor prognosis in colorectal and squamous cell carcinomas (Camarero et al., 2006, Chen et al., 2017). β OHB production by melanoma and glioblastoma cells by the peroxisome proliferator-activated receptor alpha (PPAR α) agonist fenofibrate was associated with decreased cell proliferation (Grabacka et al., 2016). What’s evident is that further research is needed to understand the impact of HMGCS2/SCOT expression, ketogenesis and ketone oxidation in cancer cells.

1.9 Overview of CNS Development and Ketone Bodies in Brain Development

During embryonic development, the CNS is one of the first systems to begin to form and the last to be completed (Volpe, 2000). In humans, neurogenesis (the process by which neurons are generated from NSCs) happens mainly prenatally and has a larger gestation period where in mice this occurs prenatally and postnatally, thus, this is a critical period for nervous system development (Jones and Rolph, 1985).

Neurulation, the folding process in vertebrate embryos, which includes the transformation of the neural plate into the neural tube, is the first step in nervous system formation and occurs at the end of the third week of gestation in humans (Stiles and Jernigan, 2010). The neural plate which extends the rostral – caudal axis of the embryo is the beginning of where all CNS and peripheral nervous system (PNS) structures will form (Volpe, 2000). Nervous system development first begins in the dorsal region of the embryo. Signals from the notochord (around day 18) induces the lateral regions of the neural plate to fold inwards and forms the neural tube when both sides fuse, with the anterior and posterior ends of the tube fully closing at day 24 and day 26 respectively (Fig 1.5) (Volpe, 2000).

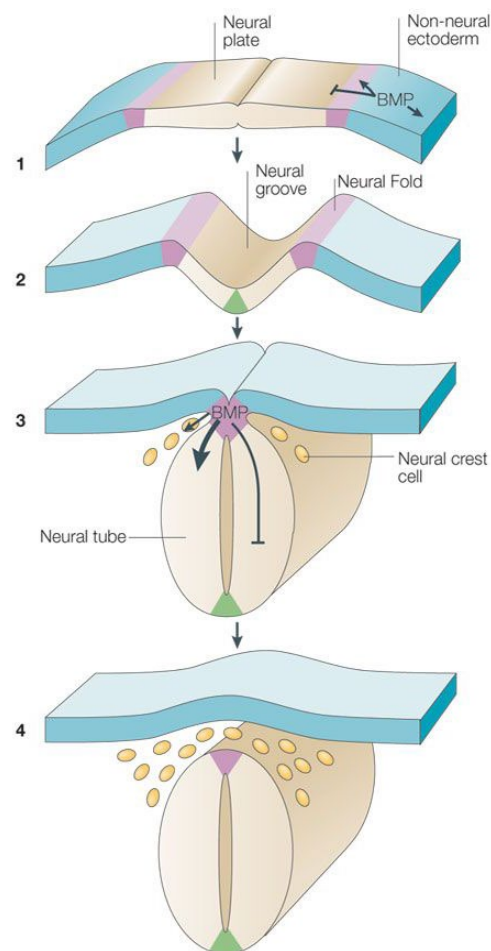


Figure 1.5 Formation of neural tube. Adapted from Liu and Niswander, 2005

The neural tube and ectoderm consist of neuroepithelial stem cells, which give rise to all nervous system cell lineages; these include radial glial cells, neurons, astrocytes, and oligodendrocytes (Fig 1.6).

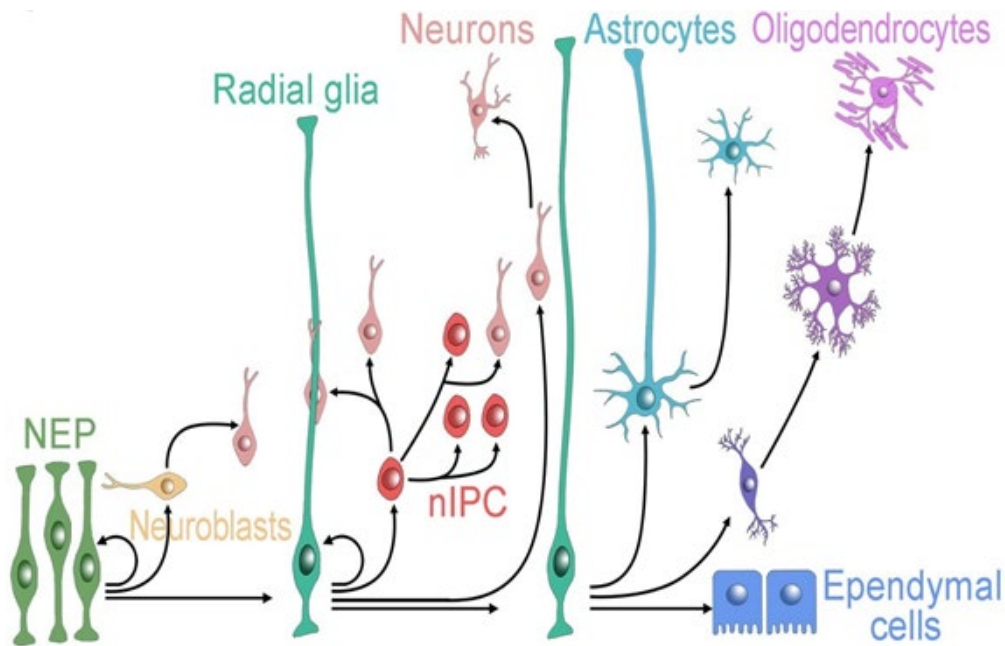


Figure 1.6 Cell generation in the developing CNS Adapted from Barry et al., 2014

At day 28, the primary vesicles (the prosencephalon, mesencephalon and rhombencephalon) are formed and by day 49, these vesicles will have differentiated into their secondary vesicles (Stiles and Jernigan, 2010). The prosencephalon will give rise to the telencephalon and diencephalon, the mesencephalon will not differentiate, and the rhombencephalon will differentiate into the metencephalon and myelencephalon. From these vesicles, the brain will fully differentiate into its compartments. Myelination is one the last stages of cellular maturation during CNS development and ketone bodies play a key role in the formation of myelin and the coating of neural processes, as ketone body uptake and metabolism coincides with myelination (Jones and Rolph, 1985). Myelin is principally comprised of cholesterol, triglycerides and phospholipids and ketone bodies act as a substrate to produce these biomolecules (Jones and Rolph, 1985). The placenta allows for the exchange of metabolites between the mother and developing offspring and the gestational diet has a significant impact on the development of the offspring in utero. In maternal ketosis, ketone bodies can effectively cross the placenta to the embryo acting as an alternative to glucose for ATP production. It is used as a substrate for amino acid and lipid biosynthesis by feeding into the PPP (Nehlig, 2004, Nehlig and Pereira de Vasconcelos, 1993).

Neurons, astrocytes, oligodendrocytes, and microglia all have the ability to metabolize ketone bodies, yet preference for ketone body use as an energy or lipid source varies (Table 1.3 and Table 1.4).

| Ketone | Stage / Cell Type / Region / Model | Observations | Author(s) |
|--------------------------|--|---|----------------------------|
| AcAc | In vitro embryonic cortical astrocytes and neurons (M) | More efficient fatty acid and cholesterol production than glucose | Lopes-Cardozo et al., 1986 |
| βOHB | In vitro embryonic forebrain neurons and perinatal astrocytes, (M) NE-4C cells | NE-4C cells utilized ketone in mitochondrial oxidation. No change in ketone induced O ₂ consumption between cell types | Jády et al., 2016 |
| βOHB/AcAc | In vivo embryonic oligodendrocytes and brain homogenates (R) | More efficient production of fatty acids and cholesterol than glucose | Koper et al., 1981 |
| βOHB/AcAc | In vitro postnatal cortical oligodendrocytes (R) | More efficient ketone body oxidation and synthesis of lipids than glucose | Sykes et al., 1986 |
| βOHB/AcAc | In vitro embryonic cortical oligodendrocytes, neurons and astrocytes (R) | Ketone body oxidation seven to nine times greater than glucose oxidation | Edmond et al., 1987 |
| βOHB/AcAc/Acetone | In vitro embryonic brain astrocytes, and neurons (R) and oligodendrocytes (B) | Ketone enzyme activity in all cell types, greatest in astrocytes | Chechik et al., 1987 |
| βOHB/AcAc/Acetone | In vivo embryonic brain oligodendrocytes, astrocytes and neurons (R) | Ketone bodies are the precursors for fatty acids synthesis. Hypo/hyperketonemia did not significantly alter lipid production | Poduslo and Miller, 1991 |
| βOHB/AcAc/Acetone | In vitro embryonic hippocampal neurons (R) and HT22 cell line | βOHB and AA protect HT22 and hippocampal neurons against glutamate- neurotoxicity. AA decreased glutamate-ROS | Noh et al., 2006 |

Table 1.3 Overview of ketone body function in CNS cell types during development; R (Rat), M (Mouse), B (Bovine) (Adapted from Barry et al., 2018)

Neurons and astrocytes favour glucose utilization in the PPP and these use ketone bodies nine times more effectively than glucose as a substrate for respiration (Edmond et al., 1987). The developing brain of some animals such as mice and rats show a preference for ketone utilization during gestation and the neonatal stage of development where ATP production (up to 70%) is due to the oxidation of ketone bodies (Hawkins et al., 1986, Hawkins et al., 1971b).

| Ketone | Stage / Cell Type / Region / Model | Observations | Author(s) |
|------------------|--|--|---------------------------------|
| AcAc | In vivo and in adult hippocampal neurons, R | Protect against glutamate neurotoxicity | (Massieu et al., 2003) |
| βOHB | In vivo postnatal and adult brain homogenates, R | Rate of ketone fatty acid production higher during development than in adult | (Lopes-Cardozo and Klein, 1984) |
| βOHB | In vitro adult hippocampal slices, GP | Post – synaptic field potentials decreased with ketone when compared to glucose | (Arakawa et al., 1991) |
| βOHB | C6 glioblastoma cells and in vitro postnatal cerebellar astrocytes, M | Ketone increases mitochondrial metabolism. C6 cells release glutamate in the presence of ketone | (Eloqayli et al., 2011) |
| βOHB | In vitro adult hippocampal neurons, R | Protect SN neurons from MPP toxicity and hippocampal neurons from Aβ | (Kashiwaya et al., 2000) |
| βOHB | In vitro postnatal cerebellar glutamatergic neurons, M | Altered glutamate – glutamate homeostasis. Ketone reduces glutamate release | (Lund et al., 2009) |
| βOHB | In vitro postnatal hippocampal slices, R | Protect against chronic hypoglycemia, oxygen – glucose deprivation and NMDA excitotoxicity, but not synaptic transmission | (Samoilova et al., 2010) |
| βOHB | In vitro adult hippocampal neurons, M, and u87ng, u251mg, lnt-229, t98g and a172 glioma lines | Ketone protected hippocampal neurons from glucose deprivation, not glioma lines | (Maurer et al., 2011) |
| βOHB | In vivo adult cortical and hippocampal neurons and in vitro cortical neurons, R | Protection from hypoglycemia – induced ROS and cell death | (Julio-Amilpas et al., 2015) |
| βOHB | In vitro adult forebrain neurons and astrocytes, in vitro hippocampal mixed cultures and slices, M | Ketone inhibition of glycolysis in astrocytes. Increase in mitochondrial pyruvate metabolism. | (Valdebenito et al., 2016) |
| βOHB | In vitro adult cortical slices, GP | βOHB metabolism occurs mainly in neurons and can decrease available glutamine. Ketone can not compensate for glucose in hypoglycemia | (Achanta et al., 2017) |
| βOHB | In vitro adult hippocampal neurons, R | Protect mitochondrial function and hypoxia mediated cell death | (Masuda et al., 2005) |
| βOHB/AcAc | In vivo and in adult hippocampal slices and cells, R | Unaltered ligand gated ion channels mediated excitatory or inhibitory neurotransmission | (Thio et al., 2000) |
| βOHB/AcAc | In vitro postnatal GABAergic SN neurons, R, M | Ketone depress signaling by opening K _{ATP} channels | (Ma et al., 2007) |
| KD | In vivo adult hippocampus, M | Inhibition of caspase-3 mediated apoptosis | (Noh et al., 2003) |
| KD | In vivo adult hippocampus, R | Elevate glutathione peroxidase to protect against oxidative stress | (Ziegler et al., 2003) |

Table 1.4 Ketone body overview in CNS cell types during postnatal and adult life. R, Rat; GP, Guinea Pig; M, Mouse; SN, substantia nigra; MPP 1, 1 methyl phenylpyridinium; Aβ, amyloid beta; NMDA, N- methyl-D-aspartate; ROS, reactive oxygen species (Adapted from Barry et al., 2018).

(Sussman et al., 2013b) investigated the effects of a gestational KD on embryonic CD1 mice development. Female mice were fed either the KD or a standard diet (SD) 30 days prior to as well as during pregnancy. Images of the embryonic brains were taken at embryonic day 13.5 (E13.5) using optical projection tomography (OPT) and E17.5 using magnetic resonance imaging (MRI). The size of the embryos and their brains were then compared. Specific organ-based analysis (volume analysis) on the embryos revealed that at E13.5 the average KD embryo size was larger than the SD fed embryo. The study found that at E13.5, the embryos exposed to the KD were significantly larger than SD fed embryos. Yet at E17.5 these trends were reversed with KD embryos being smaller compared to the SD embryo. Using the same organ-based analysis – the KD brain at E13.5 occupied a smaller percentage

of the embryo volume when compared to the SD embryo but at E17.5 the KD brain occupied a larger percentage volume.

Using a different and more detailed imaging analysis method called deformation-based analysis; more localized anatomical changes were detected. At E13.5, this analysis revealed that when compared to the SD embryo, the KD embryo had a relative decreased volume in the cervical spinal cord and cerebral thalamus region with no increase seen in any brain region at this time point. Using the same deformation-based analysis at E17.5, the study claims the KD at this time point had an increase in several brain regions such as hypothalamus, thalamus, pons and midbrain and the cervical spine. A deeper investigation in the KD at both time points found that the midbrain and pons were smaller in relative volume at E13.5 but larger in volume at E17.5. Furthermore, the hypothalamus was smaller in relative volume at E13.5 and the thalamus were enlarged at E17.5. However, though the results show changes in brain volume at these different time points and experiments it is worth noting that different imaging analysis methods were used in each experiment, and this could have influenced the results. However, in humans, there is a limited consensus on how the KD during pregnancy may affect the normal patterning of the developing brain and any related consequences for brain compartment formation and function in life are unclear. Research investigating how ketone bodies impact neuronal and glial origin, differentiation and migration during development will clarify how the diet impacts normal grey and white matter compartment formation.

1.10 Effects of Ketone bodies During Neonatal Development and Early Lactation

Levels of β OHB and AcAc are high in neonatal rat pups during suckling (Nehlig, 2004). Maternal milk is mainly ketotic and experiments have demonstrated that when neonatal rats are suckling, they are in a nutritionally active state of ketosis due to the high fat percentage of the milk (Melo et al., 2006, Nehlig, 2004). During the suckling period, enzymes that break down ketone bodies are highly active and this rate of activity decreases gradually as weaning begins (Nehlig and Pereira de Vasconcelos, 1993). The BBB permeability of ketone bodies reaches a peak during the suckling period in rat brains, further demonstrating the new-borns necessity for ketone bodies during development (Erecinska et al., 2004). This early ketone preference is also seen in humans, where ketone bodies levels in the blood peak 48 hr after birth, and steadily decline as the baby matures and starts to preferentially metabolise glucose (Barry et al., 2018b). A second study by (Sussman et al., 2013a) investigated the effect of a

gestational KD on physiological growth and brain structure in the CD1 neonatal mouse compared to the previous study, which focused solely on the embryo. Female mice were fed either a KD or SD before and during gestation. Images were taken at early and later postnatal days using MRI with a 3D Diffusion Tensor Imaging sequence.

Analysis of overall brain volume between SD and KD mice pups between these timeframes found no statistical difference between groups at either point. However, in specific regions of the animal's brains, differences were observed. At the earlier postnatal days, the KD brain had an insignificantly smaller cortex compared to the SD brain. Using this same method at the later timepoint, greater regions of the cortex displayed a reduction in volume. This reduction at the later timepoint was also observed in the corpus callosum, fimbria, lateral ventricles, and hippocampus of the KD brain when compared to the SD brain. The hypothalamus, olfactory bulb and the medulla were increased relatively in size in the KD brain when compared to the SD brain. However, there has been no research conducted in humans to show this (Table 1.5).

1.11 Sustained Effects of a Gestational KD in Adulthood

The brain morphology of CD1 mice were assessed at postnatal day 21.5 (P21.5) and P90.5 following exposure to a KD or SD in utero using MRI (Sussman et al., 2015). These were then fed a SD in postnatal life. After imaging at P21.5, the mice went through a series of neurobehavioral assays such as the forced swim test (FST) and the open field test (OFT) at 8 weeks old which assessed anxiety in the control SD and experimental KD adult offspring (see Table 1.5 for a comparison of all three Sussman et al papers).

Adult rat's fed the KD were found to be less anxious and depressed when compared to the SD control group, this was determined using the FST. Overall, whole brain volume did not differ significantly with either diet regime at weaning (P21.5) or in adulthood (P90.5) independent of gender. Some brain structures differed in volume relative to total brain volume in the average KD brain, when compared with SD brain at both weaning and adulthood. The average KD brain had a bilateral increase in relative volume in the frontal cortex, cerebellum, and primary somatosensory cortex. A bilateral decrease in relative volume in the hippocampus, striatum, motor cortex and auditory cortex was also observed. The thalamus and dentate gyrus had a mix of larger and smaller regions in the KD brain.

| Paper | (Sussman et al., 2013b) | (Sussman et al., 2013a) | (Sussman et al., 2015) |
|---------------------------------------|--|--|---|
| Animal Model | CD1 mouse | CD1 mouse | CD1 mouse |
| Time points investigated | Embryonic stages (E13.5 & 17.5) | Neonatal stages P11.5 & P21.5 | Adult mice (P21.5 and P90) |
| Imaging Method | OPT at E13.5 and MRI at E17.5 | MRI with 3D Diffusion Tensor Imaging | MRI |
| Assessment of brain morphology | Volume Analysis & Deformation based analysis (DBA) | Volume Analysis & Voxel Wise Analysis (VWA) | Volume Analysis & Image registration (IR) |
| Findings: Volume Analysis | E13.5: KD embryos larger than SD embryos E17.5: KD smaller than SD embryos | No statistical difference between SD and KD brains at P11.5 and P21.5 | Brain volume did not differ significantly at P21.5 or P90 irrespective of gender |
| Findings: DBA/ VWA / IR | E13.5: KD embryo had a decreased volume in cervical spinal cord & cerebral thalamus when compared to SD embryo E17.5: KD embryo had an increased volume in the hypothalamus, thalamus, pons and midbrain when compared to the SD embryo | P11.5: KD brain had an insignificantly smaller cortex compared to the SD brain P21.5: The corpus callosum, fimbria, lateral ventricles and hippocampus of the KD brain when compared to the SD brain were smaller. The hypothalamus, olfactory bulb and the medulla were increased relatively in size in the KD brain when compared to the SD brain. | P21 (post weaning): No Difference between SD or KD mice P90: The average KD brain had a bilateral increase in relative volume in frontal cortex, cerebellum and primary somatosensory cortex when compared to the SD group . A bilateral decrease in relative volume in the hippocampus, striatum, motor cortex and auditory cortex was observed when compared to the SD group |

Table 1.5 Overview of the three Sussman et al., 2013b 2013a and 2015 papers

1.12 Overview of Cell Metabolism Phenotypes: Comparing Developing Brain Cells, Adult Brain Cells, and Cancer Cells

The two cells type under investigation in this study are the NB SH-SY5Y cell line and the NSC NE-4C cell line. Highly proliferative cells such as NB are glycolytic and have high requirements for NADPH and ATP, carbon, nitrogen and hydrogen in order to support biosynthesis (Folmes et al., 2012). If there was complete consumption of the available fuel substrates, which occurs in OXPHOS, anabolic requirements would not be met. Therefore, cells undergoing rapid proliferation instead mediate partial breakdown of glucose through glycolysis, generating some ATP for energy, while also shunting intermediates through the PPP (Folmes et al., 2012). The PPP runs alongside glycolysis to generate NADPH, pentose

(5-carbon sugars) and ribose-5-phosphate (Shyh-Chang et al., 2013). This provides a compromise between the catabolic generation of ATP and the anabolic biosynthesis.

As development proceeds, NSC will differentiate resulting in a shift in their metabolic phenotype to OXPHOS (Jády et al., 2016). The exact mechanism of the metabolic phenotype shift is unclear. However, noticeable changes in the intracellular expression of genes are evident (Jády et al., 2016) (Fig. 1.7).

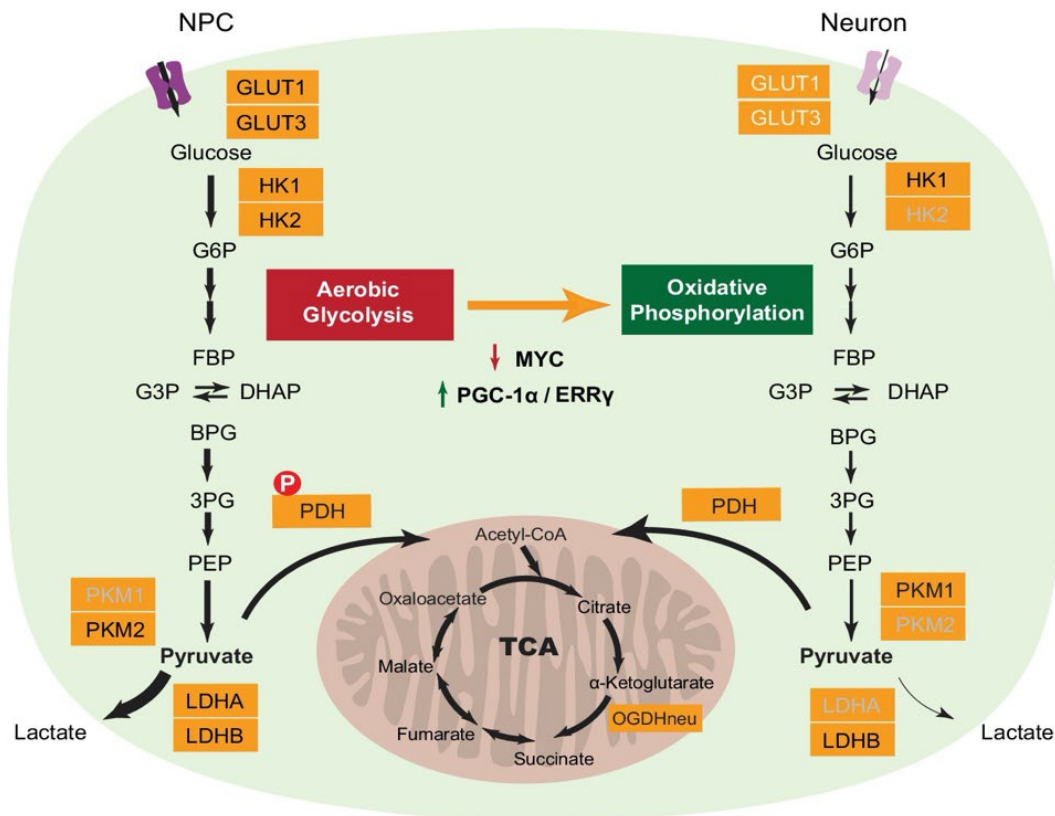


Figure 1.7 Metabolic Changes in NSCs. A schematic depicting the transcriptional modifications that coincide with the metabolic changes seen in neural stem cells. Comparing the pathways utilized by NSCs during aerobic glycolysis (RED) to oxidative phosphorylation (GREEN). Enzymes dimmed in the respective pathways indicate downregulation. Additionally, the black arrows are weighted to show amounts of substrates leaving or entering certain pathways. This figure was taken from (Zheng et al., 2016).

During brain development, NSCs are rapidly dividing, there are high levels of both GLUT1 and GLUT3 receptor transcription which results in high glycolytic flux (Shyh-Chang et al., 2013). Upon differentiation the expression of GLUT3 is reduced, leaving the low affinity GLUT1 responsible for transporting the glucose into the cell. This results in a lower rate of glucose getting into the cell, which is characteristic of non-proliferating cells that utilize OXPHOS (Shyh-Chang et al., 2013). In addition, under hypoxic conditions levels of hypoxia inducible factor 1 (HIF1) increases, promoting the upregulation of glycolytic genes (Zheng

et al., 2016) . One of the main changes seen is the loss of HK2 and LDH expression. This combined with a switch in PK splicing from PKM1 to PKM2, marks the transition from aerobic glycolysis to OXPHOS in NSCs. Upon neural differentiation, metabolic regulators such as Pparg coactivator 1 alpha (PGC-1 α), and oestrogen related receptor gamma (ERR γ) increase significantly to sustain the transcription of metabolic and mitochondrial respiratory complex genes (Zheng et al., 2016). This increase is coupled to an increase of mitochondrial biomass to facilitate OXPHOS that will be the main source of ATP (Zheng et al., 2016). Cancer cells also utilize aerobic glycolysis to generate energy. Tumour cells show elevated rates of glucose uptake for biosynthetic pathways, but reduced rates of OXPHOS (Marie and Shinjo, 2011). Metabolism is a key cellular process affected through the transition from normal to cancer cells (Marie and Shinjo, 2011). To maximize their ability to synthesize membrane substrates, nucleic acids and proteins for increased proliferation, cancer cells need both large amounts of ATP, as well as biosynthetic compounds. Therefore, they generate ATP through glycolysis, lactic acid fermentation and replenishment of NAD⁺ as well as shunting glucose intermediates into anabolic pathways. PDH links glycolysis and the TCA (Marie and Shinjo, 2011). However, its activity is blocked by pyruvate dehydrogenase kinase 1 (PDK1), which is induced by hypoxic conditions (Marie and Shinjo, 2011). This results in more anaerobic glycolysis, inhibiting the TCA cycle substrate and promoting the formation of lactate. In anaerobic conditions, lactate can be exported via MCT4, allowing cells to maintain normal pH (Marie and Shinjo, 2011). Oxygenated cells can remove lactate by using MCT1 and convert the lactate back to pyruvate using lactate dehydrogenase B (LDHB) for further oxidation (Marie and Shinjo, 2011).

A further characteristic that both NSCs and cancer cells share is the need for the availability of cellular material to support their rapid proliferation (Marie and Shinjo, 2011). The generation of these substrates cannot be undertaken with large amounts of ATP, but rather are obtained via the use of glucose and glutamine (Marie and Shinjo, 2011). Glutamine is a key component for cancer growth (Lu et al., 2010). It's role in malignant transformation and altered metabolism remains unclear, although evidence suggests that the conversion of glutamine to glutamate is critical for rapidly dividing cells. Through this conversion, nitrogen is released and can be used for the generation of purines and pyrimidines needed for division (Lu et al., 2010). Through further processing from glutamate to α -KG, glutamine can ultimately enter the TCA cycle which may support cancer growth (Lu et al., 2010).

In rapidly dividing cells, such as NSC and cancer cells, the predominant metabolic phenotype is aerobic glycolysis. Proliferating cells require heightened biosynthesis in order to generate and incorporate nutrients into their growing biomass (including nucleotides, amino acids and lipids). Under normal oxygen supply it would be assumed that cells would oxidize glucose completely, completing the process from glycolysis, through the TCA and ending with OXPHOS, to optimize the net ATP production. However, in proliferating cells such as NSCs and cancer cells, instead of shunting pyruvate into the mitochondria to start the TCA, it is instead transformed into lactate in order to continuously drive glycolysis (Vander Heiden et al., 2009), producing two ATP molecules. This is inefficient, and continuous glycolysis is only utilized in conditions of low oxygen, yet NSCs and cancer cells utilize glycolysis in the presence of sufficient oxygen supply (Vander Heiden et al., 2009). Here, glucose is shunted to make macromolecular precursors such as acetyl-CoA for fatty acids, ribose for nucleotides and intermediates of glycolysis for amino acids. In undifferentiated cells there are lower levels of OXPHOS, yet oxygen consumption is still important. ATP synthesis appears to be decoupled from oxygen consumption, where ATP is produced by glycolysis while oxygen consumption is used to maintain redox potential for lipid synthesis from citrate and amino acid synthesis from oxaloacetate and α -KG (Vander Heiden et al., 2009).

1.13 Metabolism of Ketone Bodies During Brain Development and in Cancer

Starvation occurs in nature and organisms have adapted means to survive periods of food scarcity. This occurs as a series of changes at the physiological and biochemical levels and are there to maintain energy homeostasis (Rojas-Morales et al., 2016). Initially, when the blood glucose levels drop, the liver will generate more glucose from breakdown of glycogen stores through a process called gluconeogenesis. However, when blood glucose levels drop further, the liver starts to synthesize ketone bodies which can then be used as metabolic fuels in other tissues. When the body reaches ketosis, the ketone bodies are predominantly produced by the liver. Through analysis of ketone body levels in the blood and urine it was observed that levels can get as high as 3 mM during short-term fasting, up to 6 mM during long-term fasting and are about 2 mM when adhering to the KD (Bartmann et al., 2018).

Ketone bodies, predominantly β OHB and AcAc, play a role in energy homeostasis in most living organisms. As previously discussed, these molecules can sustain energetic requirements when cells are experiencing periods of starvation (Rojas-Morales et al., 2016).

The synthesis of ketone bodies, known as ketogenesis, occurs within the mitochondrial matrix (Figure 1.8).

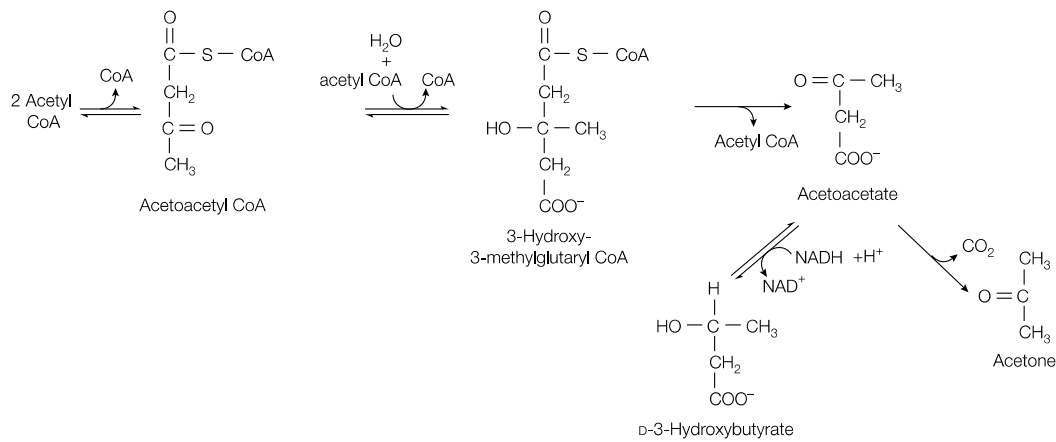


Figure 1.8 Ketone Bodies Synthesis. This schematic shows the production of β OHB and AcAc from molecules of acetyl Co.

It starts with condensation of acetyl CoA into the ketone body AcAc via the enzyme HMGCS2 and 3-hydroxy-3-methylglutaryl CoA lyase (HMGCL). Then via β DH1, AcAc can be converted to β OHB. From here, the ketone bodies are exported into the bloodstream and travel to various tissues to be utilized as energy intermediates. In these tissues, the β OHB is exported into the mitochondria and converted back to AcAc and then to acetyl CoA using the enzymes β DH1, SCOT and mitochondrial thiolase. Finally, acetyl-CoA can enter the TCA cycle to produce reducing equivalents that through OXPHOS produce ATP.

For cells to utilize ketone bodies they must be transported into the cell by MCTs, which have multiple isoforms, MCT2 having a high affinity for β OHB and MCT1 and MCT4 having a high affinity for lactate (Bartmann et al., 2018). Once inside the cell, the mitochondria break down the ketone bodies to acetyl-CoA which then enters the TCA cycle and can be metabolized to generate high energy intermediates that feed into the ETC and generate energy. This is important, such that in order to metabolize and utilize ketones for energy, cells must have both functioning mitochondria and a microenvironment that contains readily available glucose (Bartmann et al., 2018).

Ketone bodies are not only produced during periods of starvation, but also during prolonged exercise, the neonatal period, uncontrolled diabetes, or following a low-carbohydrate, high-fat KD (Rojas-Morales et al., 2016). In general, research has found that the neonatal cerebral metabolic rate is lower than that of the adult brain, however the level

of ATP is quite similar (Brekke et al., 2015). The low cerebral metabolic rate of glucose in neonatal brains is predicted to be the cause of the ability of the developing brain to survive prolonged periods of hypoxia, which in adults would be lethal (Brekke et al., 2015). It is well known that under normal conditions, glucose is the essential sole fuel for the adult brain. However, it has been described that in the neonatal brain other energy sources are utilized including ketone bodies (Schönfeld and Reiser, 2013). Up to 60% of the brain energy requirement can be matched by ketone bodies (Schönfeld and Reiser, 2013).

As described previously, NSC are predominantly glycolytic in their metabolism. This is used to drive the synthesis of biomaterials to promote cell sustainability and growth. However, it has been found that NSC also utilizes beta-oxidation for energy production (Maffezzini et al., 2020). During development the brain undergoes metabolic switches in fuel utilization (Prins, 2008). In utero, the brain relies on glucose for energy, followed by lactate shortly after birth. Then upon the suckling period, where nutrients come from breast milk which is made predominantly of fat, energy is obtained primarily from ketones and glucose. Finally, after weaning, the body once again switches metabolic machinery back to a primary reliance on glucose. These changes in metabolism are mediated by changes in cerebral transport systems and availability of metabolic enzymes (Prins, 2008). It has been found that towards the end of gestation the brain starts to express the ketone metabolizing enzymes in greater quantities (Prins, 2008). Additionally, MCTs are being upregulated and inserted into membranes to facilitate transport of ketones, pyruvate, and lactate into the brain (Prins, 2008). At peak ketone utilization, research has shown that the rate of ketone metabolism can be 6-times higher than that seen in the adult brain (Prins, 2008). It was found that in the foetus two enzymes important for ketone body production, HMGCS2 and β DH1 are upregulated (Puchalska and Crawford, 2017). However, HMGCS2 is methylated in the foetus, and this is reversed after birth (Puchalska and Crawford, 2017). As well, β DH1 exhibits a developmental expression pattern, whereby it increases from birth to weaning (Puchalska and Crawford, 2017). Similarly, β DH1 expression can be induced by the KD (Puchalska and Crawford, 2017).

Similarly, it has been said that cancer cells display a unique metabolic phenotype that has been characterized as aerobic glycolysis. This characteristic makes cancer cells susceptible, such that their reliance on excess glucose for survival makes them poor adaptors to changes in the environment (Poff et al., 2014). Unlike other cells, which adapt their metabolic profiles depending on the available substrates, cancer cells show minimal ability to adapt

(Poff et al., 2014). Experiments conducted have decreased the glucose availability to cancer cells and saw inhibition of metastatic cancer progression (Poff et al., 2014). However, it is also seen that by increasing ketone bodies this can also inhibit the metastatic spread of cancer progression. In NB, supplementation with β OHB and AcAc decreased the viability of the cells and increased apoptosis (Poff et al., 2014). This showed that although ketone bodies can be used by other tissues, cancer cells cannot effectively oxidize them to generate energy (Poff et al., 2014). From this the researchers investigated the mitochondrial pathology to determine why cancer cells cannot metabolize ketone bodies. The tumours had decreased mitochondrial number, abnormal structural morphology, abnormal fusion-fission, mutations and abnormal mitochondrial enzyme numbers and function (Poff et al., 2014). Subsequently, the cancer cells have impaired respiratory capacity and instead must rely on substrate-level phosphorylation to survive (Poff et al., 2014). Additionally, because ketone bodies must be metabolized via the mitochondria, and cancer cells have impaired mitochondrial function, the oxidation of ketone bodies is not an efficient source of energy for survival (Poff et al., 2014).

It was also found that many cancers do not express the SCOT enzyme (Poff et al., 2014). SCOT is necessary for ketone body utilization within the mitochondria and therefore without it, cancer cells experience a deficiency in ketone metabolism (Poff et al., 2014).

1.14 Role of the Ketone Diet in Disease Prevention and Health Maintenance

After its initial development as a treatment for intractable epilepsy (Nei et al., 2014, van der Louw et al., 2017, Wilder, 1921), the KD is currently used to help treat a spectrum of immune and brain related disorders. These include mitochondrial dysfunction (Frey et al., 2017, Stafstrom and Rho, 2012), movement disorders (Tieu et al., 2003), Alzheimer's Disease (AD) (Smith et al., 2005), cancer (Jaworski et al., 2016) obesity and diabetes (Yancy et al., 2005, Yancy et al., 2004) inflammation and oxidative stress (Youm et al., 2015) and traumatic brain injury (TBI) (Prins and Matsumoto, 2014). The KD has been found to reduce the volume of tumours in animal models of gliomas and prostate cancer (Zhou et al., 2007, Freedland et al., 2008). *In vivo* evidence in rats suggested the KD protects against brain trauma (Prins, 2008). (Murphy et al., 2004) showed that the KD may cause behavioural changes similar to the effects of antidepressants (Table 1.6).

In addition, GLUT1 deficiency, a childhood disorder which prevents glucose passing through the BBB and is caused by a mutation in the SLC2A1 gene, may be treated by the KD (De Vivo et al., 1991, Klepper, 2008, Klepper and Voit, 2002). Furthermore, alternating

hemiplegia which develops during childhood and causes paralysis on one side of the body by mutations in the ATP1A3 gene, is successfully controlled with the KD and flunarizine (a calcium antagonist), supplementation (Ulate-Campos et al., 2014) or a modified Atkin’s diet (Roubergue et al., 2015). Moreover, advances in understanding the specific nutritional requirements of the KD required for controlling seizures has made it the primary intervention to adequately limit and control infantile spasms, Dravet syndrome and other forms of epilepsy. As the BBB is more permeable in neonates the diet is considered more effective in new-borns and neonates when compared to adults (Saunders et al., 2012).

In healthy adults, the KD is considered safe due to the excess levels of ketone bodies being excreted in urine (Jaworski et al., 2016). However, long-term treatment of the KD has resulted in side effects such as stunted growth, kidney stones and bone fractures (Groesbeck et al., 2006). With correct nutritional supplementation and close monitoring, these side-effects may be controlled and after more than five years in ketosis accompanied with vitamin supplementation, no negative effects on body composition, bone mineral content, and bone mineral density were reported in three adults with GLUT1 deficiency syndrome, which is not consistent in studies of long term ketosis in children (Bertoli et al., 2014).

| Ketone | Disorder | Observation | Model | Author |
|---------------|--|--|--|---|
| βOHB | Mitochondrial dysfunction | Restored complex I activity and stability (a key component of mitochondrial metabolism) following glucose deprivation | SH-SY5Y cell | (Frey et al., 2017, Stafstrom and Rho, 2012) |
| βOHB | Parkinson’s Disease (PD) | Rescues mitochondrial respiration and partially protects dopaminergic neurons from neurodegeneration | C57Bl/6 (mice) | (Tieu et al., 2003) |
| βOHB | Alzheimer’s Disease | Partially protects hippocampal neurons from Aβ-42 protein | C56Bl/6 | (Smith et al., 2005) |
| βOHB | Inflammation & oxidative stress | Blocks NLRP3 inflammasome mediated inflammatory disease | NLRP3 knockout C57Bl/6 mice | (Youm et al., 2015) |
| βOHB | Traumatic brain injury (TBI) | Suckling rats, who rely upon ketone bodies in addition to glucose as necessary metabolic substrates recover metabolically and behaviourally faster than adults following TBI | Wistar | (Prins and Matsumoto, 2014) |
| KD | Cancer | The ketogenic diet is neuroprotective and lowers brain glucose uptake, even in the presence of glucose | SH-SY5Y cells | (Jaworski et al., 2016) |
| KD | Obesity & Diabetes | Greater weight loss in obese patients and improved glycaemic control in diabetic patients | Humans | (Yancy et al., 2005, Yancy et al., 2004) |
| KD | Tumour reduction | Reduced tumour growth in gliomas and prostate cancer | C57Bl/6 mice (Brain tumour) SCID mice (prostate tumour) | (Zhou et al., 2007, Freedland et al., 2008) |
| KD | Brain trauma | Cerebral tissue preservation | Sprague Dawley rats | Prins, 2008 |
| KD | Depression | Rats less like to exhibit behavioural despair | Wistar rats | (Murphy et al., 2004) |
| KD | Glucose transporter 1 (GLUT1) deficiency | Reduces seizure onsets | Humans (children) | (De Vivo et al., 1991, Klepper, 2008, Klepper and Voit, 2002) |
| KD | Alternating hemiplegia of childhood | Reduction in moments of temporary paralysis with added treatment of flunarizine | Humans (children) | (Ulate-Campos et al., 2014) |

Table 1.6 Overview of the use of ketones and their use in health maintenance

1.15 The β -Hydroxybutyrate Paradox

A non-pharmacological approach to treating cancer may also represent an effective way of circumventing the above issues of drug intervention; however, studies describing the impact of dietary alterations on NB growth and survival have been equivocal largely due to the lack of a mechanistic understanding behind the spectrum of findings. In particular, the “ β OHB paradox” describes the conflicting observations of the effect of ketone bodies on cancer growth and progression (Rodrigues et al., 2017). On the one hand, several studies have shown an inhibitory, anti-proliferative effect (Skinner et al., 2009, Poff et al., 2014, Shukla et al., 2014, Martuscello et al., 2016b) whereas others have demonstrated contradictory data, that ketone bodies promote the growth and survival of cancer cells (Bonuccelli et al., 2010, Martinez-Outschoorn et al., 2011b, Whitaker-Menezes et al., 2011). Other studies have shown that β OHB has no impact on the proliferation rate (Bartmann et al., 2018).

1.16 Neuroectodermal NE-4C cells and Neuroblastoma SH-SY5Y cells

The NE-4C NSC line originates from the ventral brain vesicles of nine-day old p53 deficient mouse embryos (Schlett et al., 1997, Livingstone et al., 1992). NE-4C cells have a high proliferative capacity and will cease proliferation and differentiate into neurons and glia if cultured in an environment with *all-trans* retinoic acid (Herberth et al., 2002, Jelitai et al., 2002, Schlett and Madarasz, 1997). In environments that promote neuronal differentiation, NE-4C cells form a mature neuronal phenotype, displaying morphological markers such as NeuN and β -III tubulin and other biochemical and electrophysiological properties of mature neurons (Jelitai et al., 2004, Jelitai et al., 2002). Critically, NSCs rely heavily on glycolytic metabolism before making a switch to OXPHOS when they differentiate into a mature neuronal phenotype (Fawal and Davy, 2018)

The use of SH-SY5Y NB cells in this study, given their mutual neoplastic and neuronal origin and their use in both fields may help to bridge some of the observations in cancer and development. Importantly, a key parallel in the metabolism of both cancer and developing brain cells is their high proliferation rates and reliance on aerobic glycolysis (DeBerardinis et al., 2008b). NB originates from sympathoadrenal progenitor cells derived from the neural crest and the lesions form predominantly in the adrenal cortex and paraspinal ganglia, presenting anywhere from the neck to the pelvis (Brodeur, 2003).

NB are the most common extracranial solid tumors in children and the most common cancer diagnosed during the first year of life (Ries LAG, 1999), and are responsible for a disproportionately high percentage of cancer related pediatric deaths (Young et al., 1986).

The prognosis can be extremely varied between the highest rate of spontaneous differentiation and regression amongst cancers (Carlsen, 1990), and in other cases as an aggressive, highly metastatic and treatment-resistant tumor (Davidoff, 2012).

1.17 The Role of the Culture Medium

The discrepancies highlighted above on the response to ketones between studies of diverse methodologies come with a background of an increasingly scrutinized role of experimental culture conditions and medium compositions in influencing outcomes (Cantor et al., 2017), especially in the context of cancer metabolism (Ackermann and Tardito, 2019). The choice between the two most used types of media, Dulbecco's Modified Eagle Medium (DMEM) and Roswell Park Memorial Institute Medium (RPMI) for instance (McKee and Komarova, 2017), is known to alter the metabolome of various cell lines (Wu et al., 2009, Huang et al., 2015). Further, the choice of at least 20 formulations of DMEM as advertised by a single supplier (Thermo Fisher Scientific, Rockford, IL, USA), formulated with or without pyruvate, plays a determining role when assessing the *in vitro* cytotoxicity of various chemicals (Babich et al., 2009).

A systematic review of the literature on the SH-SY5Y NB cell line in Parkinson's disease has identified the use of at least 8 different media formulations which are further distinguished by the addition of various supplements (Xicoy et al., 2017). Moreover, studies reporting the use of DMEM for example commonly do not specify whether the utilized formulation includes or excludes specific supplements (Babich et al., 2009), perhaps with an expectation that the components of culture media act in isolation (Yao and Asayama, 2017). These factors have been cited as a contributor to irreproducibility and a low translation rate into clinical success (Begley and Ellis, 2012), especially in the area of cancer research (Hutchinson and Kirk, 2011). In the study of the derivational state of ketosis (Paoli et al., 2015), these variations of methodology and the unstandardized presence of other major metabolic substrates may be particularly relevant. As such, we speculate that these wide-ranging outcomes are at least partly mediated by the chosen culture conditions, in particular, the presence of other fuels and metabolites such as pyruvate and glutamine which are commonly supplemented at supraphysiological concentrations when compared to human plasma as further detailed in Table 1.7 below (Ackermann and Tardito, 2019).

| Metabolite | Human Plasma (mM) | DMEM (mM) |
|-------------------|--------------------------|------------------|
| Glucose | 4.5– 5.3 | 25 |
| L-Glutamine | 0.4 – 0.7 | 2-4 |
| Pyruvate | 0.009 – 0.059 | 1-2 |

Table 1.7 A comparison of the metabolite concentrations in plasma and in culture

1.18 Overall Aims and Hypothesis of the Project

Considering the existing ambiguous literature underlying the potential effects of ketone bodies on cell growth *in vitro*, a systematic review of the literature was undertaken to evaluate and summarize the findings of all relevant individual studies related to ketone supplementation on cell line growth. Based on this data, we then investigated the effects of glucose deprivation on the growth and viability of SH-SY5Y NB cells and NE-4C neuroepithelial cells, and then further investigated its effect on the proliferation and morphology of SH-SY5Y cells. We then aimed to see if various concentrations of ketones have any rescuing effect on glucose deprived cells. We further examined whether the proliferative responses are affected by the medium compositions or incubation periods, with the aim of contributing to a standardised protocol which adequately recognises the extracellular environment as a primary determinant of experimental outcome and characterises the possible interactions of metabolic substrates with the β OHB variable. This may then provide a framework for understanding some of the determinants of variation in response to ketosis *in vitro* and point towards potential mechanisms of action. Finally, to further understand the roles of glucose, pyruvate, and glutamine during this metabolic transition on cell development, we investigated the health and phenotypes of differentiating neural stem and neuronal precursor cells in various conditions of substrate deprivation and β OHB supplementation over time. The aims and hypotheses in this study were arrived at in a stepwise consequential manner, such that the results of one investigation informed the basis of the succeeding aims:

1.18.1 Aims

1.18.1.1 To identify, evaluate, and summarize the findings of all relevant individual studies related to ketone supplementation on cell line growth.

1.18.1.2 To investigate the impact of glucose deprivation on NE-4C and SH-SY5Y cell growth and viability.

1.18.1.3 To investigate the impact of different concentrations of β OHB on NE-4C and SH-SY5Y and cell growth.

1.18.1.4 To investigate whether ketone supplementation can rescue the effects of glucose deprivation on cells.

1.18.1.5 To investigate the role of other culture substrates including pyruvate and glutamine on the effects of ketone body supplementation.

1.18.1.6 To search and test for the optimal conditions in the culture medium composition for a maximal response to the ketone.

1.18.1.7 To investigate the impact of glucose deprivation on NE-4C and SH-SY5Y differentiation.

1.18.1.8 To investigate the role of pyruvate and glutamine in the differentiation of NE-4C and SH-SY5Y cells.

1.18.1.9 To investigate whether ketone body supplementation can rescue the effects of glucose and substrate deprivation on NE-4C and SH-SY5Y cell differentiation.

1.18.2 Hypotheses

1.18.2.1 We hypothesise that maternal starvation, calorie restriction, prolonged exercise or carbohydrate-oriented diets that remove glucose may have detrimental effects on foetal neural stem and neuronal precursor cell growth and health.

1.18.2.2 We hypothesise that ketone bodies, the brains alternative metabolic fuel source, may influence the health and lineage of neural stem and neural precursor cells during development, which may have functional consequences in the adult brain.

Chapter 2

Materials & Methods

2.1 Materials

A list of the materials used in the experiments for these studies can be found in Chapter 7 of the Appendices in Supplementary Tables 7.1 to 7.7.

2.2 Experimental Overview

An initial systematic review of the existing literature that investigated the impact of ketone bodies on cell growth and health *in vitro* was conducted. From the data gathered in this systematic review, the ketone body β OHB was chosen as the ketone body to be investigated and a series of experiments investigating the impact of β OHB on SH-SY5Y and NE-4C cell density, and SH-SY5Y viability and differentiation using concentrations of 1 mM to 50 mM were investigated. We next began to systematically remove anaplerotic growth substrates including glucose, pyruvate and glutamine from the culturing media and then supplemented the growth media with 10 mM β OHB to see if this would have a positive impact on cell growth, health, and metabolism. Then we repeated this substrate removal and β OHB supplementation and investigated its impact of neuronal differentiation. The data produced from these experiments were tabulated using Microsoft Excel and then graphed and statistically analysed using Graphpad Prism version 9.5.

2.3 Databases and Search Strategy

A search strategy for a systemic review of the literature was designed using the relevant keywords to identify and examine the *in vitro* effects of exogenous ketone body supplementation in cell line models of ketosis (Exact terms in the Supplementary file S1 of the Appendices in Chapter 7). Articles were identified by searching Medline, Web of Science and EMBASE, on the 16th of June 2020. Controlled vocabulary terms (i.e., Medical Subject Headings [MeSH]) were used in the search to reach further results. No date restrictions were applied.

2.4 Article Selection

The initial search yielded a total of 2282 articles, the titles, and abstracts of which were imported into the Covidence® platform. Following the removal of 783 duplicates, 1499 abstracts were independently screened for possible inclusion by two reviewers. A total of 1160 studies were deemed irrelevant at this stage, leaving 338 articles for full-text screening against the inclusion and exclusion criteria (Supplementary file 1). In summary, 63 articles published between 1974 and 2020 were identified on full-text screening to report on the effects of exogenous ketones on various cell lines *in vitro* and were included in this review.

The following parameters from each of the included studies were extracted towards the final quantitative and qualitative syntheses: Cell line, cell origin, tissue type, the utilised ketone bodies and along with their concentration and duration, the investigated effects, as well the culture media formulations and the presence or absence of substrates such as glucose, pyruvate, and glutamine.

2.5 Cell Lines

The mouse NE-4C neuroectodermal cell line and the human SH-SY5Y NB cell line were obtained from ATCC and the European Collection of Authenticated Cell lines. The first set of experiments undertaken used both SH-SY5Y and NE-4C cells.

2.6 NE-4C and SH-SY5Y Cell Culture, Subculturing, and Media Change

The NE-4C and SH-SY5Y NB cell line beginning at passage 1 and passage 14 was used for all experiments. All the following steps were performed under sterile conditions using the appropriate aseptic techniques described below. Cells were grown and maintained in an incubator (inCu safe, MCO-5AC) at 37°C in 5% CO₂. Frozen NE-4C and SH-SY5Y cells were recovered from the -80°C freezer in a sterile laminar flow hood (Telstar Bio IIA Class II cabinet: Note, all cell culture experiments were conducted in the sterile laminar flow hood).

Cells were transferred to a sterile T75 flask containing 10 ml of regular media (RM) (the formulation of RM can be found in Table 2.1). RM is the basic growth medium which cells are cultured and maintained in daily before they are transferred and seeded into cell culture plates for experimentation. The flask was stored in an incubator overnight with the cap slightly unscrewed (to allow proper gaseous exchange). The following day, the RM was replaced to ensure removal of dead cells and the remaining freezing agent dimethyl sulfoxide (DMSO). The media in the flask was changed every two days and thereafter ensuring 8 ml of old RM was removed before replacing with 8 ml of new RM.

Cell viability and confluence (the percentage of the surface of a culture flask that is covered by adherent cells) was checked daily using a light microscope (VWR inverted light microscope). Cells were allowed reach a confluence of approximately 70% before being sub-cultured. For subculturing, the media was aspirated off and the T75 flask was washed with 2 ml of sterile Hanks balanced salt solution (HBSS) (this solution maintains pH and osmotic balance as well as provides cells with water and essential inorganic ions). 3 ml of trypsin (trypsin is produced from trypsinogen, secreted by exocrine cells of pancreas, it is

used to dissociate the adherent cells from the flask) was added to the flask and incubated for 5 min. Following agitation of the trypsinized cells, the contents of the flask were transferred to a 15 ml Falcon tube and flask was washed with 5 ml HBSS, which was also added to the Falcon tube. The contents of the Falcon tube were centrifuged for 3 min at 550 g (Sigma, 2-16PK, workbench Centrifuge). The supernatant was discarded, and the pellet was resuspended in 1 ml RM before being split equally into two new T75 flasks, adding new RM to make a final volume of 10 ml per flask.

2.7 Aseptic Technique

To ensure no fungal or microbial infection occurred to the NE-4C and SH-SY5Y cell lines, 70% ethanol was used as the sterilization agent. 100% ethanol (Sigma Aldrich) was diluted down to 70% ethanol using sterile distilled water. Nitrile free gloves were always worn during every experiment and before contact was made with any materials or reagents to be used in the cell culture experiments, hands were sprayed with 70% ethanol. When conducting cell culture experiments in the laminar flow hood all materials, solutions and reagents that were to be used for the experiment were sprayed with 70% ethanol before being placed in the hood. Before hands were placed in the sterile laminar flow hood, they were sprayed with 70% ethanol. When every experiment was finished, all materials would be removed from the laminar flow hood, the waste container would be removed and emptied, the waste container would be cleaned with 70% ethanol before being placed back in the laminar flow hood.

The entire surface of the laminar flow hood would then be cleaned with 70% ethanol. The hood would then be turned off and its protective cover pulled down. The built in ultraviolet (UV) ray would then be turned on for 30 mins to further sterilize the laminar flow hood.

2.8 Cell Seeding, Counting, and Plating

Experimental seeding was carried out when the confluency of both cell lines reached approximately 70%. Trypsin (3 ml) was used in this process to detach the adherent cells and allow a proportion to be sub-cultured in fresh medium. For the experiments, a 1 ml suspension of centrifuged cells in glucose free media was created. Following this, a sample was taken from the suspension to quantify the total number of cells. A haemocytometer and trypan blue were used for cell counting with the average cell count adjusted to account for both factors. Under a light microscope, the number of cells in each of the four (4x4) grids were counted (with cells touching the line not counted). The numbers from the four grids were averaged and multiplied by two to account for the dilution with trypan blue. This

number is then multiplied by 10^4 (to account for the haemocytometer dilution). For example, to calculate how much of the cell solution to put in each well of a six well plate – cross multiply the number multiplied by 10^4 and divide this by 1000 μl with the cell's density wanted divided by X. X will be the amount of cell solution needed per well. To ensure that there are enough cells for the desired plating volume, multiply x by the number of wells (Fig 2.1).

$$A(79) + B(103) + C(142) + D(200) = 524$$

$$524 \div 4 = 131$$

$$131 \times 2 = 262$$

$$262 \times 10^4 = 2,620,000 \text{ cells}$$

$$\frac{2,620,000}{1,000} = \frac{50,000}{X}$$

$$2,620,000x = 50,000,000$$

$$x = \frac{50,000,000}{2,620,000}$$

$$x = 19.08$$

$$x = 19.08 \mu\text{l of cell solution per well}$$

$$19.08 \mu\text{l} \times 6 \text{ wells} = 114.48 \mu\text{l of cell solution needed}$$

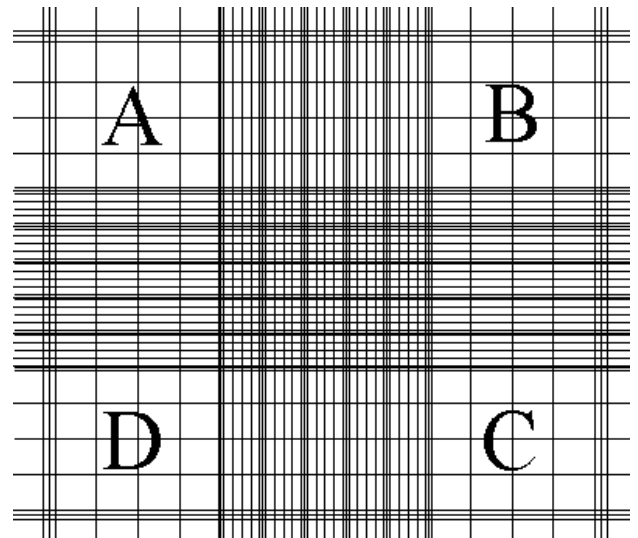


Figure 2.1 Diagram representing the haemocytometer grid and an example of how cells were counted.

2.9 Preparation of βOHB media

The treatment media of varying concentrations of βOHB was freshly made on the day of use. 10 ml of 100 mM βOHB stock was made dissolving by dissolving 126 mg of (R)-(-)-3-Hydroxybutyric acid sodium salt (Sigma) into 10 ml of glucose free - Dulbecco's modified eagle media (GF-DMEM) and vortexed before being sterile filtered. A sterile syringe (Norm-Ject), a sterile 0.22 μm syringe filter (Ultracruz) and a sterile needle (Sterican) was sprayed with ethanol and placed into the laminar flow hood. The needle was taken out of its packaging and attached to the syringe. The 10 ml 100 mM βOHB was taken up by the syringe, the needle was removed and discarded safely, and the sterile filter was then placed on the syringe and the 10 ml 100 mM βOHB stock was pressed through the filter into a 50 ml Falcon tube.

2.10 Proliferation Experiments

The NE-4C and SH-SY5Y cell lines were used to investigate the effect of ketone supplementation on cell growth over a 120-hr and 168-hr period. SH-SY5Y and NE-4C cells were plated at a density of 5×10^4 and 2×10^4 cells per well in six different media groups in poly-L-lysine coated six well plates. The media groups included, regular glucose (5 mM) (RG), glucose free (GF), 1 mM, 5 mM, 10 mM, and 50 mM concentrations of β OHB and proliferation was investigated over a period of 48, 72, 96 and 120 hr for SH-SY5Y cells and up to 168 hr for NE-4C cells. The media specifications are described in Table 2.1 below and see Fig. 2.2 for the six well plate design. See Supplementary Table 7.7 in the Appendices for the function of each of the reagents used in each media.

| Media group | Composition: (Baseline of DMEM/GF DMEM, 10% Foetal Bovine Serum (FBS), 1% Penicillin Streptomycin (PS) and 1% L-glutamine (LG)), +/- Sodium pyruvate (SP), +/- β OHB |
|-------------------|--|
| RM | 8.8 ml DMEM, 1 ml FBS, 100 μ l PS, 100 μ l LG |
| GF | 8.8 ml GF DMEM, 1 ml FBS, 100 μ l PS, 100 μ l SP |
| 1 mM β OHB | 8.7 ml GF DMEM, 1 ml FBS, 100 μ l PS, 100 μ l SP, 100 μ l 100 mM β OHB solution |
| 5 mM β OHB | 8.3 ml GF DMEM, 1 ml FBS, 100 μ l PS, 100 μ l SP, 500 μ l, 100 mM β OHB solution |
| 10 mM β OHB | 7.8 ml GF DMEM, 1 ml FBS, 100 μ l PS, 100 μ l SP, 1 ml 100 mM β OHB solution |
| 50 mM β OHB | 3.8 ml GF DMEM 1 ml FBS, 100 μ l PS, 100 μ l SP, 5 ml 100 mM β OHB solution |

Table 2.1 List of media concentrations for the proliferation assay

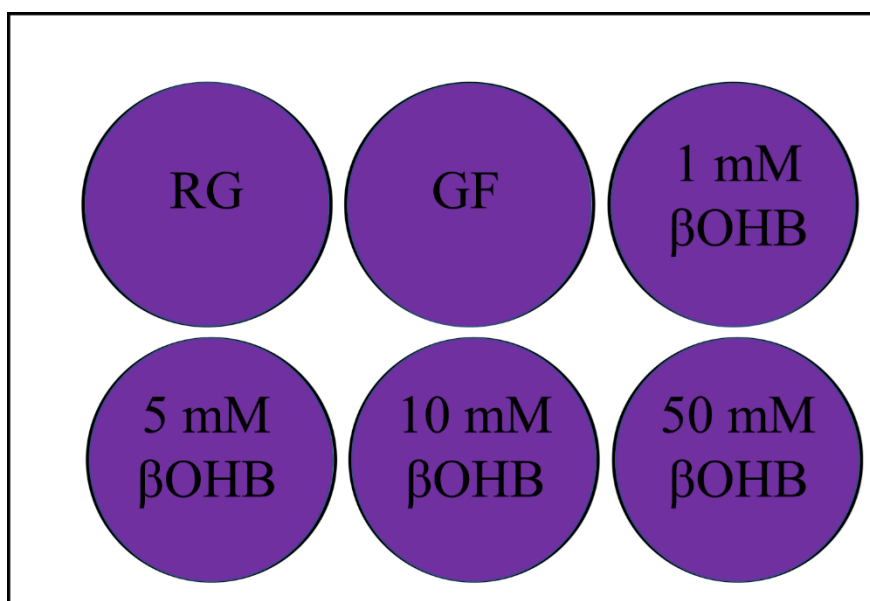


Figure 2.2 Six well plate experimental design for the initial proliferation assay

A subsequent set of experiments using the same timelines outlined above probed the effect of media composition on the response to ketone bodies employed the RG, low glucose (1 mM) (LG), GF groups, followed by the removal of pyruvate (GF-Pyr), L-glutamine (GF-Lglut) or both (GF-Pyr/Lglut), resulting in six medium groups of sequentially deprived fuel sources, paralleled with another six 10 mM β OHB-containing equivalents, as shown in Table 2.2. Cells were seeded in poly-L-lysine coated 96 well plates at a density of 5×10^3 or 2×10^3 cells per well for the SH-SY5Y and NE-4C cells (Fig 2.3).

| Medium group | Composition: (Baseline of DMEM and 10% FBS) +/- β OHB (10 mM) |
|--------------|---|
| RG | Glucose (5 mM), Sodium Pyruvate (1 mM), L-Glutamine (2 mM) |
| LG | Glucose (1 mM), Sodium Pyruvate (1 mM), L-Glutamine (2 mM) |
| GF | Sodium Pyruvate (1 mM), L-Glutamine (2 mM) |
| GF-Pyr | L-Glutamine (2 mM) |
| GF-Lglut | Sodium Pyruvate (1 mM) |
| GF-Pyr-Lglut | - |

Table 2.2 A summary of the utilised media groups and their corresponding compositions

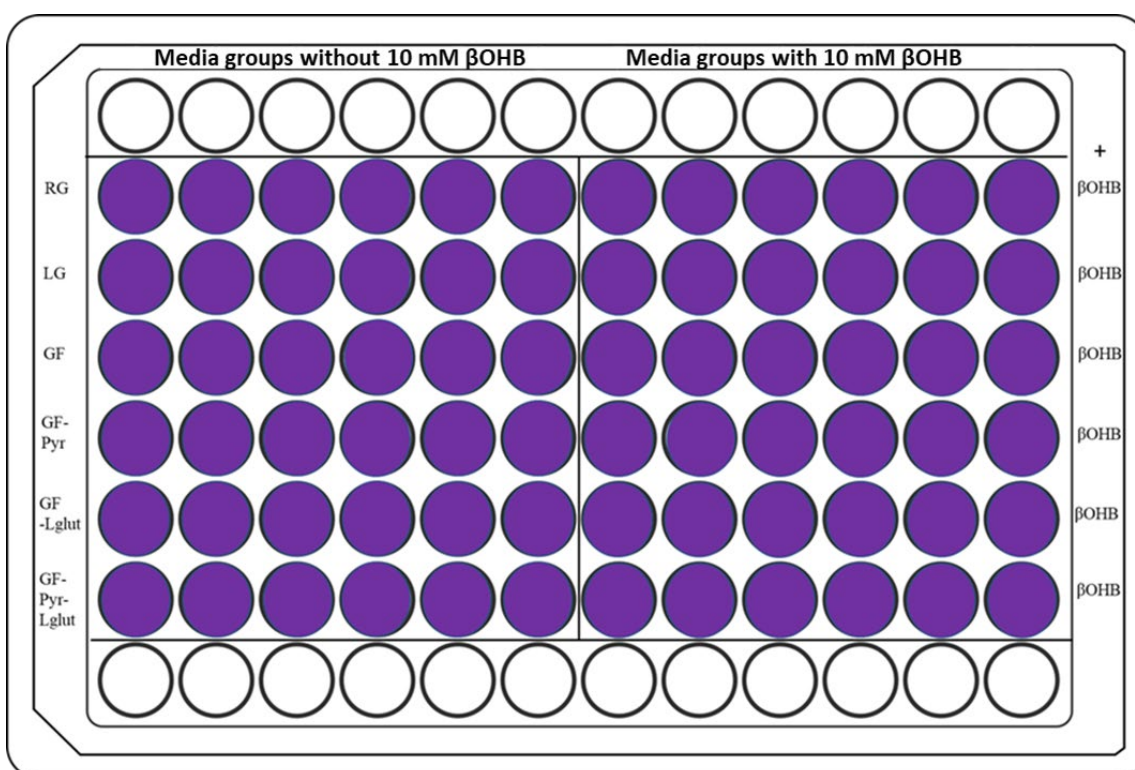


Figure 2.3 96 well plate experimental design for the proliferation assay investigating the effect of media composition on the response to β OHB

2.11 Differentiation Experiments

Only the SH-SY5Y cell line was initially used to investigate the impact of ketone supplementation on cell maturation growth and over a 168-hr period. The cells were plated at a density of 5×10^4 cells per well in three different media groups in six well plates. In each six well plate there were two RG groups, two GF groups and two 10 mM β OHB groups (Fig 2.4) (Table 2.3).

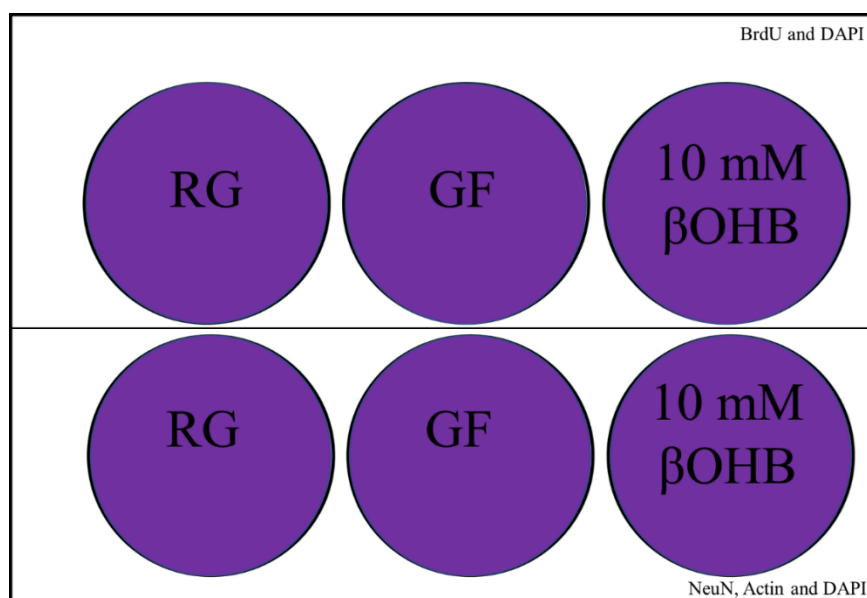


Figure 2.4 Six well plate experimental design for the initial differentiation assay

The differentiation media conditions differed from the growth media by a difference in FBS concentration (1% FBS for differentiation media compared to 10% for growth media) and the addition of 10 μ M retinoic acid (RA) diluted in DMEM and GF DMEM (Table 2.4). RA is a low-molecular-weight lipophilic metabolite of vitamin A or retinol and is the most potent natural retinoid able to influence biological processes, such as neuronal differentiation (Napoli, 1996, Fisher and Voorhees, 1996). RA acts by binding to retinoic receptors (RAR) α , β , γ , which form heterodimers with retinoid X receptors (RXR- α , β , γ). Treatment of SH-SY5Y cells in media containing RA results in the differentiation and maturation of SH-SY5Y and NE-4C cells. Cells were cultured for four days to ensure the cells were ketotic and the medium was changed every two days by replacing 1 ml of medium with 1 ml of fresh medium. Differentiation was investigated over a period of 72, 120 and 168 hr post differentiation. After four days, all the medium in each well was replaced with the appropriate differentiation medium containing RA (Table 2.3 for timeline). No other concentrations of RA were experimented with, as this concentration was successful in differentiating SH-SY5Y cells.

| Media group | Standard | Differentiation: Composition (Baseline: DMEM, 1% FBS and 1% RA) |
|--------------------|---|---|
| RG | 8.8 ml DMEM, 1 ml FBS, 100 µl PS, 100 µl LG, | 100 µl FBS, 100 µl PS, 100 µl LG (200 mM), 10 µM RA in DMEM |
| GF | 8.8 ml GF DMEM, 1 ml FBS, 100 µl PS, 100 µl SP | 100 µl FBS, 100 µl PS, 100 µl SP (200 mM), 10 µM RA in GF DMEM |
| 10 mM βOHB | 8.3 ml GF DMEM, 1 ml FBS, 100 µl PS, 100 µl SP, 500 µl 100 mM βOHB ketone stock | 100 µl FBS, 100 µl PS, 100 µl SP (200 mM), 10 mM βOHB 10 µM RA in GF DMEM |

Table 2.3 List of media concentrations for the differentiation assay

| Time | Action Taken |
|-------------|--|
| R0 | Recovered frozen SH-SY5Y cells into T75 flask of RM |
| R1 | Changed medium in T75 flask |
| | |
| R4 | T75 now confluent enough to be plated |
| R6/ P0 | Cells plated from T75 into 3x 6 well plates, each containing 2x RG, 2X GF and 10 mM βOHB |
| P3 | Changed medium in 6 well plates |
| P4/D0/ O hr | Switched to RA medium |
| 72 hr | Fixed one plate (72 hr time point) |
| 120 hr | Fixed one plate (120 hr time point) and changed medium in final plate |
| 168 hr | Fixed final plate (168 hr time point) |

Table 2.4 Timeline for the initial differentiation assay

A subsequent set of experiments using different timelines investigated the impact of media composition on the response to ketone bodies using the same groups as in the proliferation studies, these groups were RG, LG, GF, GF-Pyr, GF-Lglut and GF-Pyr/-Lglut (Table 2.6). These groups were subsequently supplemented with 10 mM BOHB. SH-SY5Y Cells were seeded in poly-L-lysine coated 96 well plates at a density of 5×10^3 cells whereas NE-4C cells were seeded at a density of 2×10^3 cells per well. All cells were grown in RG conditions for four days prior to being differentiated in 10 µM RA in their respective media groups for 5, 10 and 15 DIV (Fig 2.5).

| Media group | Composition: (Baseline of GF DMEM, 10% Foetal Bovine Serum (FBS), 1% Penicillin Streptomycin (PS) and 1% L-glutamine) +/- β OHB |
|--------------|---|
| RG | 5 mM Glucose, 1 mM Sodium Pyruvate, 2 mM L-glutamine, 0.01 M RA |
| LG | 1 mM Glucose, 1 mM Sodium Pyruvate, 2 mM L-glutamine, 0.01 M RA |
| GF | 1 mM Sodium pyruvate, 2 mM L-glutamine, 0.01 M RA |
| GF-Pyr | 2 mM L-glutamine, 0.01 M RA |
| GF-Lglut | 1 mM Sodium Pyruvate, 0.01 M RA |
| GF-Pyr-Lglut | - 0.01 M RA |

Table 2.5 List of media concentrations for the differentiation assay

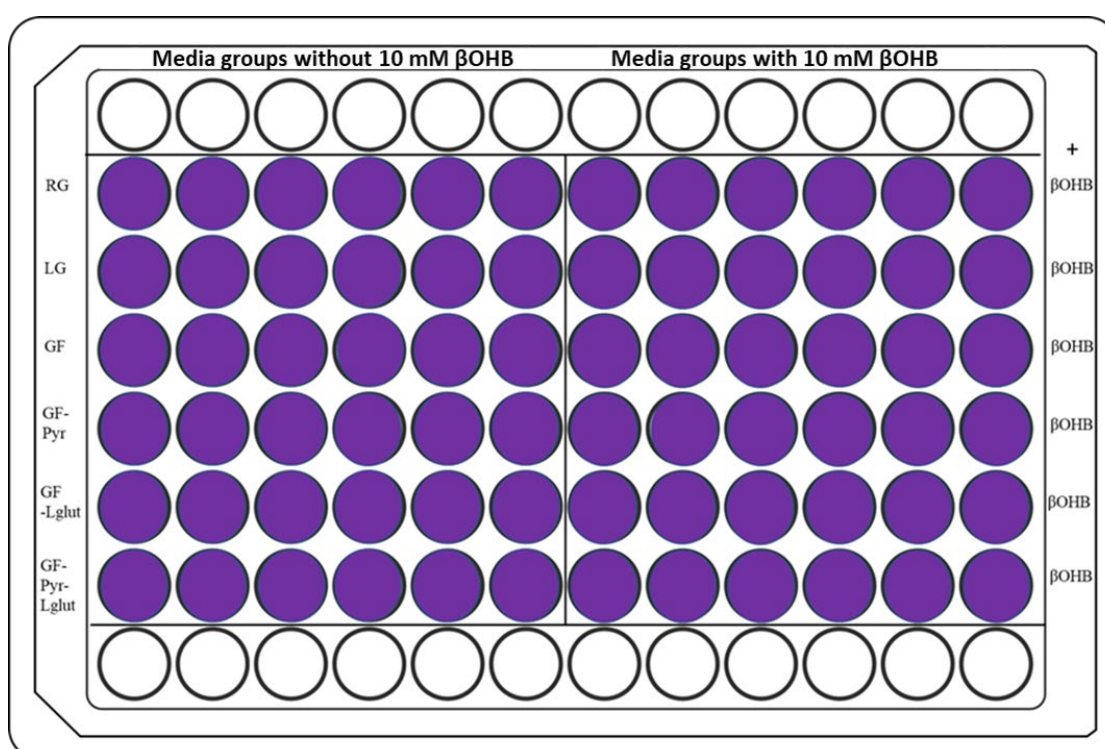


Figure 2.5 96 well plate experimental design for the differentiation assay investigating the effect of media composition on the response to β OHB

2.12 Assays

2.12.1 Apoptosis and Necrosis Assay

SH-SY5Y cells were used to assess cells undergoing apoptosis and necrosis in β OHB supplemented and substrate deprived environments at 96 hr and were seeded into a poly-L-lysine coated 96 well plate at (area well = 907.46 mm²) at a density of 5×10^3 cells per well (refer to Fig. 2.3 for plate design).

2.12.2 Mitochondrial Cytotoxicity Assay

SH – SY5Y cells were used to assess mitochondrial cytotoxicity and were seeded into a poly-L-lysine coated 96 well plate at a density of 5×10^3 cells per well. 200 μ l of media was added to each well, the timeframe investigated was 72 hr and 144 hr (Fig 2.6).

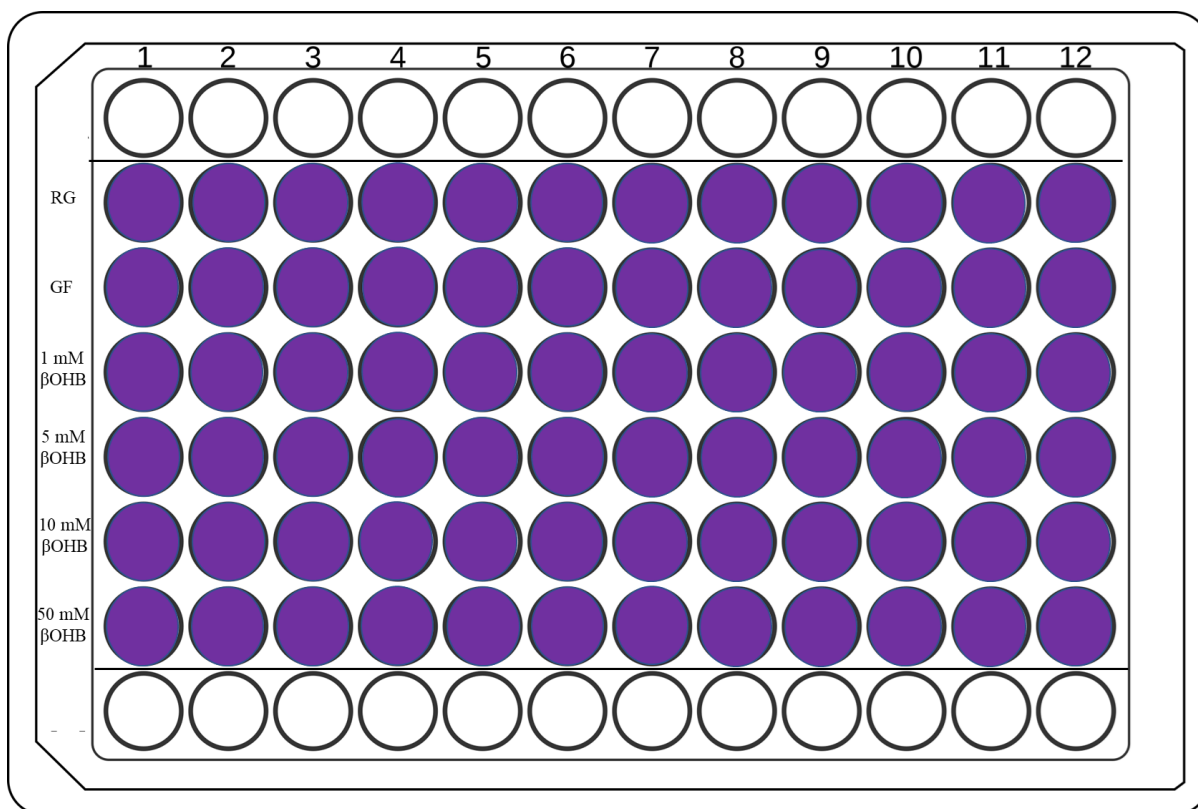


Figure 2.6 96 well plate mitochondrial cytotoxicity assay experimental design

2.12.3 Viability

Thiazolyl Blue Tetrazolium Bromide (MTT) (ThermoFisher, ROI) assays were performed as an indicator of metabolic activity and cell viability in media conditions set out in Table 2.6 and 2.7 (refer to Fig. 2.6 and Fig. 2.3 for plate designs). MTT was added to cells in each well at a concentration of 0.5 mg/ml in the culture medium and incubated for 4 hr. The culture medium was removed, and the cells were lysed in DMSO and repeatedly aspirated to solubilise the precipitated formazan crystals. Colorimetric absorbance was measured at a wavelength of 562 nm using an Epoch microplate reader. The timelines for these assays varied, with viability being investigated at 96 hr for the experiments investigating the impact of varying concentrations of ketone supplementation and when investigating differentiation, it was over 5, 10 and 15 DIV.

| Medium Type | Composition |
|-------------------|---|
| RG | 8.8 ml DMEM, 1 ml FBS, 100 μ l PS 100 μ l LG |
| LG | 8.791 ml GF DMEM, 1 ml FBS, 100 μ l PS, 100 μ l LG, 9 μ l glucose solution |
| GF | 8.8 ml GF DMEM, 1 ml FBS, 100 μ l PS, 100 μ l SP |
| 1 mM β OHB | 8.7 ml GF DMEM, 1 ml FBS, 100 μ l PS, 100 μ l SP, 100 μ l 100 mM β OHB solution |
| 5 mM β OHB | 8.3 ml GF DMEM, 1 ml FBS, 100 μ l PS, 100 μ l SP, 500 μ l 100 mM β OHB solution |
| 10 mM β OHB | 7.8 ml GF DMEM, 1 ml FBS, 100 μ l PS, 100 μ l SP, 1 ml 100 mM β OHB solution |
| 25 mM β OHB | 6.3 ml GF DMEM, 1 ml FBS, 100 μ l PS, 100 μ l SP, 2.5 ml 100 mM β OHB solution |
| 50 mM β OHB | 3.8 ml GF DMEM, 1 ml FBS, 100 μ l PS, 100 μ l SP, 5 ml 100 mM β OHB solution |

Table 2.6 List of media concentrations for the initial MTT assay

| Media group | Composition: (Baseline of GF DMEM, 10% Foetal Bovine Serum (FBS), 1% Penicillin Streptomycin (PS) and 1% L-glutamine) +/- β OHB |
|--------------|---|
| RG | 5 mM Glucose, 1 mM Sodium Pyruvate, 2 mM L-glutamine, 0.01 M RA |
| LG | 1 mM Glucose, 1 mM Sodium Pyruvate, 2 mM L-glutamine, 0.01 M RA |
| GF | 1 mM Sodium pyruvate, 2 mM L-glutamine, 0.01 M RA |
| GF-Pyr | 2 mM L-glutamine, 0.01 M RA |
| GF-Lglut | 1 mM Sodium Pyruvate, 0.01 M RA |
| GF-Pyr-Lglut | - 0.01 M RA |

Table 2.7 List of media concentrations for the MTT assay investigating the impact of media composition on the response to ketone bodies.

2.13 Immunocytochemistry

Cultures were fixed in 4% paraformaldehyde (4% PFA) in Phosphate-Buffered Saline (PBS) for 15 min at room temperature (RT).

2.13.1 Proliferation Experiments

To allow BrdU staining to occur, SH-SY5Y cells were pulsed (for a 4-hr period at 37°C to allow its full incorporation into the cells) with a BrdU solution (made from BrdU and sterile glucose free media at 1: 30 μ l dilution) (Figure 2.2). The cells were then fixed with 4% PFA. A 2N hydrochloric acid (HCl) solution was used for antigen retrieval. The cells were treated with 2N HCl for 45 mins before being immunolabelled with the primary antibody. The cells were washed with 1X PBS three times, at 5 mins per turn. A blocking solution was applied for 1 hr, which consisted of 5% normal goat serum (NGS) in 0.05% Triton X-100 in 1X PBS (PBS-T). The primary antibody, a mouse anti – BrdU IgG was diluted in blocking solution and 50 μ l was applied to the cells and incubated overnight. The secondary antibody, a goat anti – mouse IgG, and DAPI were diluted in a blocking solution and were both applied simultaneously at RT for 1 hr. The cells were washed for a final time in 1X PBS before being imaged.

2.13.2 Differentiation Experiments

In the set of differentiation plates that used RG, GF, and 10 mM β OHB, at each time-point, all the cells from the bottom three wells of the 6-well plate were dual-labelled for NeuN and β -Actin (Fig 2.4). The cells were treated with blocking solution for 1 hr, which consisted of 5 % NGS in 0.05% PBS-T and then incubated at 4°C overnight in anti-NeuN primary antibody in 0.05% PBS-T. The following day, the cells were washed with 1X PBS to remove the primary antibody and treated with a FITC anti-mouse secondary antibody and DAPI and Actin (Thermofisher) (2 drops per ml) in 0.05% PBS-T for 1 hr at RT. The cells were washed a final time before being imaged.

In the same set of differentiation plates (Fig 2.4), for each time-point, all the cells in the top three wells of the 6-well plate were pulsed with BrdU and fixed with 4% PFA 6-8 hr later. The fixed cells were washed with 1X PBS and treated with blocking solution for 1 hr at RT. The cells were incubated at 4°C overnight in anti-BrdU primary antibody in 0.05% PBS-T. The following day, the primary antibody was removed, and the cover slips were washed with 1X PBS three times for 5 mins. An anti-mouse FITC secondary antibody and DAPI in 0.05% PBS-T were added to the cells for 1 hr at RT. The cells were again washed with 1X PBS before imaging took place.

When investigating the effect of media composition on the response to ketone bodies cultures during differentiation (Fig 2.5), cells were fixed 4% PFA in PBS for 15 min at RT. To assess cells undergoing differentiation, cells were incubated with 5% NGS in 0.05% PBS-T for 1 hr and were then stained with anti-beta-III-tubulin (β -III tubulin) (1:500) primary antibody overnight at 4°C in 0.05% PBS-T. To assess cell density and cell size, cells were permeabilized and stained with DAPI (1:5000) and actin (2 drops per ml) in 0.05% PBS-T in 1X PBS for 1 hr at RT. Following this, cells underwent 3 x 5-minute 1X PBS washes.

2.13.3 Assays

To assess cells undergoing apoptosis and necrosis, the media was removed from each well, and each well was washed with PBS twice for 5 mins. 40 μ l of staining solution was added to each well and the plate was incubated at RT for 15 mins, protected from light. The staining solution comprised of FITC Annexin V, Ethidium Homodimer III and 1X Annexin binding buffer. Following incubation, the cells were washed twice with 1X binding buffer and maintained in 200 μ l of binding buffer at 5°C. 100 μ l of PFA was added to each well and the plate was incubated at RT for 15 min. 50 μ l DAPI solution (1:5000) was added to each well and the plate was incubated at RT for 1 hr, protected from light. The DAPI solution was removed, and each well was washed with PBS for 10 mins and maintained in PBS at 5°C.

To assess mitochondrial cytotoxicity in SH-SY5Y cells, three different stains were used, the Mitohealth stain, Image – iT Dead and Hoescht. Membrane potential is a central feature of healthy mitochondria, and membrane depolarization is a good indicator of mitochondrial dysfunction, which is increasingly implicated in drug toxicity. This assay uses Invitrogen MitoTracker Orange as an indicator of mitochondrial function because its accumulation in the mitochondria of live cells is proportional to the mitochondrial membrane potential. Hoechst 33342 is used as a segmentation tool to identify cells; a viability stain, such as the Invitrogen Image-iT DEAD Green Viability Stain, is easily incorporated to further multiplex the assay. These three dyes have sufficient retention of fluorescence signal intensity upon formaldehyde fixation and detergent permeabilization to be useful in fixed endpoint assays, as well as applications involving immunocytochemistry for specific protein detection. Under sterile conditions, the old media was removed and 125 μ l of fresh media and 50 μ l of staining solution was added. The cells were incubated at 37°C in 5% CO₂ for 30 mins. Following incubation, the media was removed and 100 μ l of the counterstain (consisting of 1 μ l

Hoechst per 2 ml of 4% PFA). The 96 well plate was incubated for 15 mins at RT. Following the counterstain, the wells were washed with 1X PBS and kept in 1X PBS until imaging.

2.14 Imaging and Analysis

For the proliferation and differentiation experiments, there were three / five fields of view (FOV) imaged depending on the experiment. To get overall cell count and the percentage of BrdU expression for the proliferation experiments pre differentiation five FOVs were imaged per well. Two images were taken per FOV for the proliferation experiments (BrdU and DAPI) (Fig 2.7). To get overall cell count for the percentage BrdU, β -III tubulin and NeuN expression post differentiation 3 FOVs were imaged per well. There were three FOV's taken also for the apoptosis and necrosis and the mitochondrial cytotoxicity assay. Between two (BrdU and DAPI) and three (Actin, β -III tubulin, DAPI and NeuN) images were taken per FOV for these experiments. These cells were imaged using an Olympus IX81 motorized epifluorescent microscope and the imaging software CellSens (version 2.8). Brightfield images were acquired using the same microscope. ImageJ was subsequently used for processing and analysis.

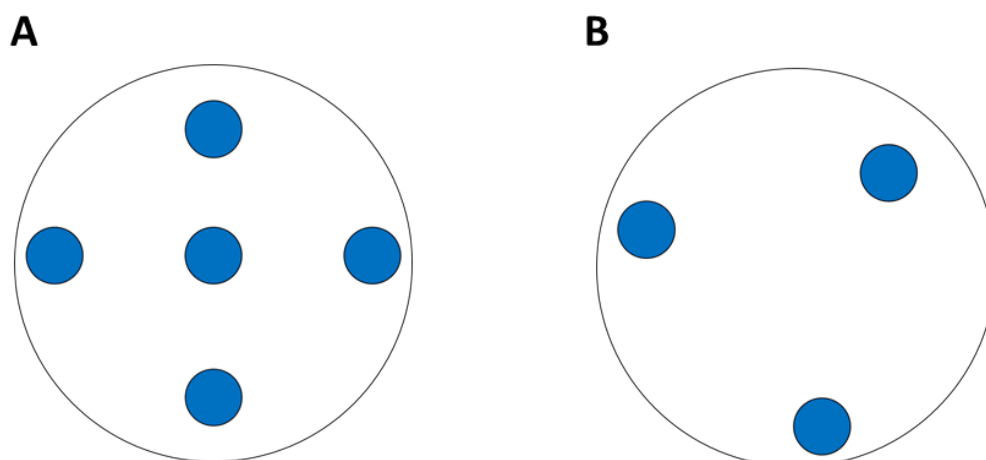


Figure 2.7 Diagram representing the fields of view (FOV) taken for the proliferation experiments (A) and the differentiation, β DH1 and mitochondrial cytotoxicity (B).

2.14.1 Randomisation of Fields

To remove bias from imaging, the imaging software on the computer was set to a level where once an image was taken, the fluorescence light would turn off showing no staining or image on the computer screen. The FOV would then be changed by using the stage controller on the microscope to move to a different FOV as outlined in the diagram above. Once the objective lens was in one of the FOVs, the “Live button” on the computer software would be turned on so that the florescent bulb would turn back on.

2.14.2 DAPI Count

The total number of cells per FOV was counted using the software programme ImageJ analysis. Every cell in the field of view was counted as follows – A DAPI image would be opened in ImageJ. The brightness and contrast would be adjusted to see every cell clearly defined. The image would be turned black and white, and the threshold of the image would be adjusted to the boundaries around each cell would be defined. Then clicking “OK” would give a table of the number of cells, total area, average surface area and %Area covered by the cells (see Fig 2.8).

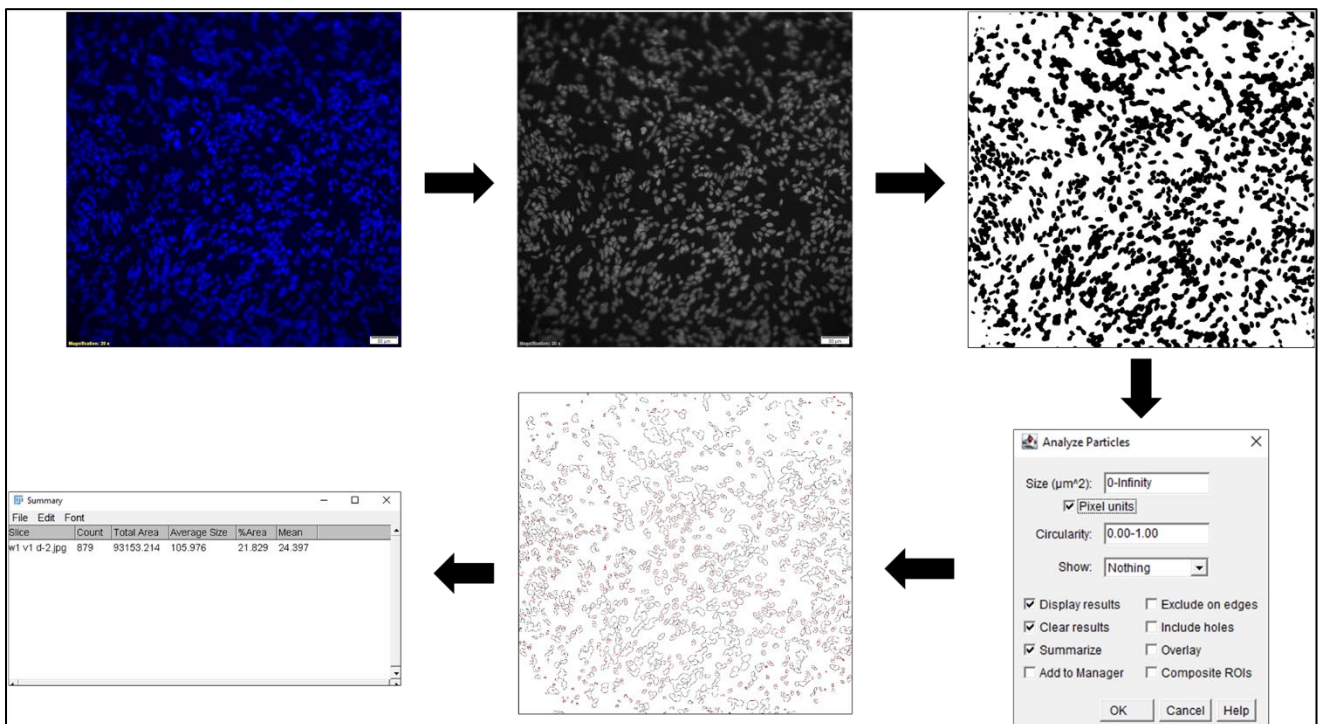


Figure 2.8 Overview of ImageJ DAPI cell count.

The image used in this example is from N1, 72 hr (Day 3) from the GF group of cell proliferation over 168 hr post differentiation. However, at times, this method may not work, and cells will have to be manually counted using a manual clicking counting tool from the software. This number is then entered into a excel spreadsheet of raw data which is featured below. The standard deviation (SDs) of every count from each well is then performed (Fig 2.9).

| REGULAR MEDIUM | | | | | | | | GF | | | | | | | | 10 mM BHB | | | | | | | | | | |
|----------------|----------|-------|---------|----------|------------|-------------|-----|---------|-----------|----------|-------|---------|------|------------|--------|-----------|---------|-----------|----------|-------|---------|----------|------------|----------|-----|---------|
| TIME | COVERSLI | IMAGE | BrdU | DAPI | Percentage | SD DEV | SEM | Outlier | TIME | COVERSLI | IMAGE | BrdU | DAPI | Percentage | SD DEV | SEM | Outlier | TIME | COVERSLI | IMAGE | BrdU | DAPI | Percentage | SD DEV | SEM | Outlier |
| 72 hours | CS 1 | | 1 | 505 | | | | | 72 hours | CS 1 | | 1 | 0 | 97 | | | | 72 hours | CS 1 | | 1 | 220 | | | | |
| | | | 2 | 295 | | | | | | | | 2 | 0 | 113 | | | | | | | 2 | 80 | | | | |
| | | | 3 | 701 | | | | | | | | 3 | 0 | 95 | | | | | | | 3 | 174 | | | | |
| | | | average | 500.3333 | | 203.040259 | | | | | | average | | 101.6667 | | 9.865766 | | | | | average | 161 | | 75.34587 | | |
| 72 hours | CS 2 | | 1 | 226 | | | | | 72 hours | CS 2 | | 1 | 127 | | | | | 72 hours | CS 2 | | 1 | 69 | | | | |
| | | | 2 | 775 | | | | | | | | 2 | 132 | | | | | | | | 2 | 78 | | | | |
| | | | 3 | 780 | | | | | | | | 3 | 83 | | | | | | | | 3 | 194 | | | | |
| | | | average | 593.6667 | | 318.4184877 | | | | | | average | | 114 | | 36.96294 | | | | | average | 113.6667 | | 69.71609 | | |
| 120 hours | CS 1 | | 1 | 578 | | | | | 120 hours | CS 1 | | 1 | 0 | 36 | | | | 120 hours | CS 1 | | 1 | 135 | | | | |
| | | | 2 | 517 | | | | | | | | 2 | 0 | 8 | | | | | | | 2 | 58 | | | | |
| | | | 3 | 687 | | | | | | | | 3 | 0 | 19 | | | | | | | 3 | 150 | | | | |
| | | | average | 594 | | 86.12200648 | | | | | | average | | 21 | | 14.10674 | | | | | average | 114.3333 | | 49.35923 | | |
| 120 hours | CS 2 | | 1 | 338 | | | | | 120 hours | CS 2 | | 1 | 16 | | | | | 120 hours | CS 2 | | 1 | 245 | | | | |
| | | | 2 | 155 | | | | | | | | 2 | 29 | | | | | | | | 2 | 122 | | | | |
| | | | 3 | 138 | | | | | | | | 3 | 57 | | | | | | | | 3 | 197 | | | | |
| | | | average | 210.3333 | | 110.8888332 | | | | | | average | | 34 | | 20.95233 | | | | | average | 188 | | 61.99193 | | |
| 168 hours | CS 1 | | 1 | 492 | | | | | 168 hours | CS 1 | | 1 | 0 | 215 | | | | 168 hours | CS 1 | | 1 | 10 | | | | |
| | | | 2 | 504 | | | | | | | | 2 | 0 | 114 | | | | | | | 2 | 244 | | | | |
| | | | 3 | 385 | | | | | | | | 3 | 0 | 103 | | | | | | | 3 | 168 | | | | |
| | | | average | 460.3333 | | 65.51590138 | | | | | | average | | 144 | | 61.7333 | | | | | average | 140.6667 | | 119.3706 | | |
| 168 hours | CS 2 | | 1 | 607 | | | | | 168 hours | CS 2 | | 1 | 0 | 30 | | | | 168 hours | CS 2 | | 1 | 193 | | | | |
| | | | 2 | 609 | | | | | | | | 2 | 0 | 165 | | | | | | | 2 | 192 | | | | |
| | | | 3 | 692 | | | | | | | | 3 | 0 | 186 | | | | | | | 3 | 176 | | | | |
| | | | average | 636 | | 48.50773134 | | | | | | average | | 127 | | 84.65814 | | | | | average | 187 | | 9.539392 | | |

Figure 2.9 Excel spreadsheet of how counts were entered.

The counts and standard deviations from each well for each N number are then averaged and the averaged values for each well are grouped together. This is repeated for all N numbers (Fig 2.10). The N numbers are then put on an overview page together (Fig 2.11).

| | | RM | | | NG | | | 10 mM BHB | |
|--------|----|-------------|----------|---|-------------|----------|---|-------------|----------|
| N1 | | | | | | | | | |
| TIME | CS | AVERAGE | ST DEV | | AVERAGE | ST DEV | | AVERAGE | ST DEV |
| 72 hr | 1 | 500.3333333 | 203.0402 | 1 | 101.6666667 | 9.865766 | 1 | 161 | 75.34587 |
| | 2 | 593.6666667 | 318.4185 | 2 | 114 | 26.96294 | 2 | 113.6666667 | 69.71609 |
| avg | | 547 | 260.7294 | | 107.8333333 | 18.41435 | | 137.3333333 | 72.53098 |
| st dev | | | | | | | | | |
| 120 hr | 1 | 594 | 86.12201 | 1 | 21 | 14.10674 | 1 | 114.3333333 | 49.35923 |
| | 2 | 210.3333333 | 110.8888 | 2 | 34 | 20.95233 | 2 | 188 | 61.99193 |
| avg | | 402.1666667 | 98.50542 | | 27.5 | 17.52953 | | 151.1666667 | 55.67558 |
| st dev | | | | | | | | | |
| 168 hr | 1 | 460.3333333 | 65.5159 | 1 | 144 | 61.7333 | 1 | 140.6666667 | 119.3706 |
| | 2 | 636 | 48.50773 | 2 | 127 | 84.65814 | 2 | 187 | 9.539392 |
| avg | | 548.1666667 | 57.01182 | | 135.5 | 73.19572 | | 163.8333333 | 64.45498 |
| st dev | | | | | | | | | |

Figure 2.10 N number overview

| RM | | | | | NG | | | | | 10 mM βHB | | | | |
|--------|----|----------|----------|----------------------------|-------------|---------|----------|----------------------------|-------------|-----------|----------|----------------------------|-------------|--|
| TIME | CS | AVERAGE | ST DEV | Nuclei per mm ² | STDEV | AVERAGE | ST DEV | Nuclei per mm ² | STDEV | AVERAGE | ST DEV | Nuclei per mm ² | STDEV | |
| 72 hr | 1 | 500.3333 | 203.0402 | 2146.453152 | | 1 | 101.6667 | 9.865766 | 436.1547045 | 1 | 161 | 75.34587 | 690.6974501 | |
| | 2 | 593.6667 | 318.4185 | 2546.957471 | | 2 | 114 | 26.96294 | 489.0652752 | 2 | 113.6667 | 69.71609 | 487.6352598 | |
| avg | | 547 | 260.7294 | 2346.655312 | 283.1286091 | | 107.8333 | 18.41435 | 462.6098999 | | 137.3333 | 72.53098 | 589.166355 | |
| st dev | | | | | | | | | | | | | 143.5867 | |
| 120 hr | 1 | 594 | 86.12201 | 2548.287487 | | 1 | 21 | 14.10674 | 90.09097175 | 1 | 114.3333 | 49.35923 | 490.4952907 | |
| | 2 | 210.3333 | 110.8888 | 902.339733 | | 2 | 34 | 20.95233 | 145.8615733 | 2 | 188 | 61.99193 | 806.5286995 | |
| avg | | 402.1667 | 98.50542 | 1725.31361 | 1163.860818 | | 27.5 | 17.52953 | 117.9762725 | | 151.1667 | 55.67558 | 648.5119951 | |
| st dev | | | | | | | | | | | | | 223.4694 | |
| 168 hr | 1 | 460.3333 | 65.5159 | 1974.851301 | | 1 | 144 | 61.7333 | 617.7666634 | 1 | 140.6667 | 119.3706 | 603.4665092 | |
| | 2 | 636 | 48.50773 | 2728.46943 | | 2 | 127 | 84.65814 | 544.8358768 | 2 | 187 | 9.539392 | 802.2386532 | |
| avg | | 548.1667 | 57.01182 | 2351.660366 | 532.8884893 | | 135.5 | 73.19572 | 581.3012701 | | 163.8333 | 64.45498 | 702.8525812 | |
| st dev | | | | | | | | | | | | | 140.5531 | |
| RM | | | | | NG | | | | | 10 mM βHB | | | | |
| TIME | CS | AVERAGE | ST DEV | Nuclei per mm ² | STDEV | AVERAGE | ST DEV | Nuclei per mm ² | STDEV | AVERAGE | ST DEV | Nuclei per mm ² | STDEV | |
| 72 hr | 1 | 943 | 40 | 4045.513636 | | 1 | 210.6667 | 67.71509 | 903.7697484 | 1 | 415.3333 | 115.2837 | 1781.799219 | |
| | 2 | 504.6667 | 248.3593 | 2165.043353 | | 2 | 150 | 79.79348 | 643.5069411 | 2 | 231 | 55.43465 | 991.0006893 | |
| avg | | 723.8333 | 144.1796 | 3105.278495 | 1329.693289 | | 180.3333 | 73.75429 | 773.6383447 | | 323.1667 | 85.35918 | 1386.399954 | |
| st dev | | | | | | | | | | | | | 559.179 | |
| 120 hr | 1 | 272.6667 | 132.7604 | 1169.752617 | | 1 | 79.33333 | 8.144528 | 340.3436711 | 1 | 152 | 48.38388 | 652.0870336 | |
| | 2 | 252.6667 | 61.65495 | 1083.951692 | | 2 | 116.6667 | 40.06661 | 500.5053986 | 2 | 192.6667 | 9.814955 | 826.5489154 | |
| avg | | 262.6667 | 97.20769 | 1126.852155 | 60.67041624 | | 98 | 24.10557 | 420.4245348 | | 172.3333 | 29.09942 | 739.3179745 | |
| st dev | | | | | | | | | | | | | 123.3632 | |
| 168 hr | 1 | 286 | 95.44108 | 1226.953234 | | 1 | 7.333333 | 2.309401 | 31.46033934 | 1 | 147.6667 | 42.35957 | 633.4968331 | |
| | 2 | 215.6667 | 60.61628 | 925.9199797 | | 2 | 97.33333 | 86.3269 | 417.564504 | 2 | 310.6667 | 165.4126 | 1332.774376 | |
| avg | | 250.8333 | 78.02868 | 1076.086607 | 213.3576304 | | 52.33333 | 44.31815 | 224.5124217 | | 229.1667 | 103.8861 | 983.1356044 | |
| st dev | | | | | | | | | | | | | 494.4639 | |
| RM | | | | | NG | | | | | 10 mM βHB | | | | |
| TIME | CS | AVERAGE | ST DEV | Nuclei per mm ² | STDEV | AVERAGE | ST DEV | Nuclei per mm ² | STDEV | AVERAGE | ST DEV | Nuclei per mm ² | STDEV | |
| 72 hr | 1 | 588.6667 | 17.09776 | 2525.40724 | | 1 | 152.3333 | 46.97162 | 653.5170491 | 1 | 132 | 24.57641 | 566.2861082 | |
| | 2 | 581.3333 | 239.7443 | 2493.946901 | | 2 | 252 | 141.3117 | 1081.091661 | 2 | 86.66667 | 37.44774 | 371.8040104 | |
| avg | | 585 | 128.421 | 2509.67707 | 22.24581929 | | 202.1667 | 94.14167 | 867.304355 | | 109.3333 | 31.01208 | 469.0450593 | |
| st dev | | | | | | | | | | | | | 137.5196 | |
| 120 hr | 1 | 205 | 54.06478 | 879.4594862 | | 1 | 77.66667 | 63.1295 | 333.1935939 | 1 | 177 | 73.99324 | 759.3381905 | |
| | 2 | 156.3333 | 50.06329 | 670.6772342 | | 2 | 69.66667 | 5.686241 | 298.8732338 | 2 | 206 | 135.0444 | 883.7495324 | |
| avg | | 180.6667 | 52.06403 | 775.0683602 | 147.6313462 | | 73.66667 | 34.40787 | 316.0334088 | | 191.5 | 104.5188 | 821.5438615 | |
| st dev | | | | | | | | | | | | | 87.9721 | |
| 168 hr | 1 | 121 | 114.9043 | 519.0955991 | | 1 | 55.33333 | 38.99145 | 237.3825605 | 1 | 309.3333 | 54.12332 | 1327.054314 | |
| | 2 | 211.6667 | 21.45538 | 908.0597946 | | 2 | 98.33333 | 52.69092 | 421.8545503 | 2 | 227 | 122.1925 | 973.8405042 | |
| avg | | 166.3333 | 68.17984 | 713.5776969 | 275.0392203 | | 76.83333 | 45.84119 | 329.6185554 | | 268.1667 | 88.15789 | 1150.447409 | |
| st dev | | | | | | | | | | | | | 249.7599 | |

Figure 2.11 Overview of N numbers

Though the DAPI cell count per image gives a proper representation of that field, it fails to give a proper calculation as to how many cells there are in each well. Thus, the number of cells per mm² must be calculated. Every image was taken at 20X (50 μm) which equals 1600 x 1200 pixels. This needs to be converted into micrometres. The length of the 50 μm scale bar is measured and gives the length and width in micrometres (557.49 x 418.2 μm = 2333097) (Fig 2.12). To get an overall representation of how many cells per mm² this number needs to be multiplied x10⁻⁶ (to convert micrometres to mm²) 233097x 10⁻⁶ = 0.2333097. This number is entered into the excel spreadsheet and divided into the average number of cells to get the overall average number of cells per field of view per mm².

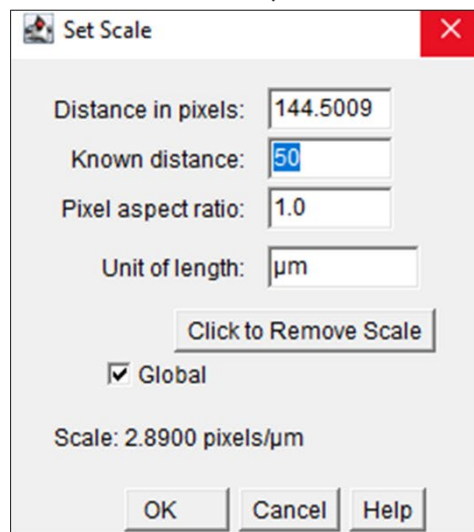
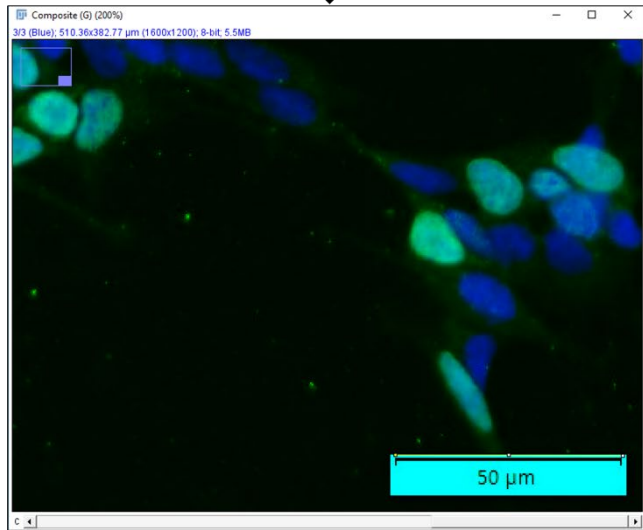
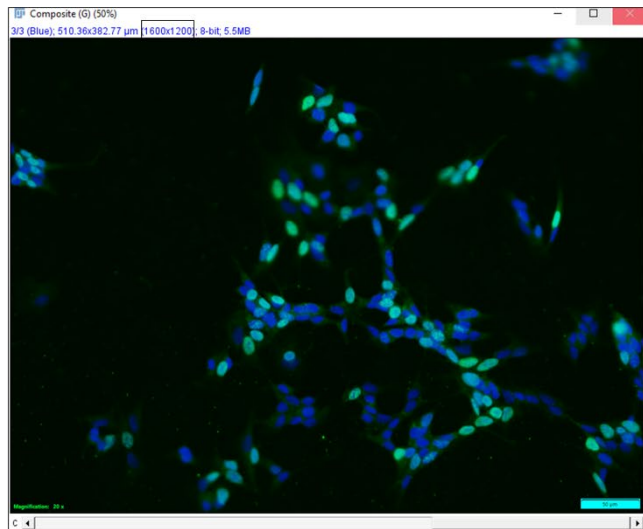


Figure 2.12 Overview of how the correct image parameters were measured to get cells per mm^2

Following on from this, the averages from each of the N numbers from each group are aligned and the average number calculated from this is taken as the mean and the SDs from these numbers are averaged and are then converted to the standard error of the mean (SEM) (Fig 2.13).

| | | RM | | | NG | | | 10 mM β HB | | | | |
|------------|----|--------------------|-----------------|-----------------|----|--------------------|-----------------|------------------|----|--------------------|-----------------|-----------------|
| 72hr | | | | | | | | | | | | |
| TIME | CS | AVERAGE | ST DEV | SEM | CS | AVERAGE | ST DEV | SEM | CS | AVERAGE | ST DEV | SEM |
| N1 | 1 | 2146.453152 | | | 1 | 436.1547045 | | | 1 | 690.6974501 | | |
| | 2 | 2546.857471 | | | 2 | 489.0652752 | | | 2 | 487.6352598 | | |
| N2 | 1 | 4045.513636 | | | 1 | 903.7697484 | | | 1 | 1781.799219 | | |
| | 2 | 2165.043353 | | | 2 | 643.5069411 | | | 2 | 991.0006893 | | |
| N3 | 1 | 2525.40724 | | | 1 | 653.5170491 | | | 1 | 566.2861082 | | |
| | 2 | 2493.946901 | | | 2 | 1081.091661 | | | 2 | 371.8040104 | | |
| AVG | | 2653.870292 | 705.2128 | 407.1548 | | 701.1842299 | 247.469 | 142.8763 | | 814.8704561 | 518.9561 | 299.6194 |
| 120hr | | | | | | | | | | | | |
| TIME | CS | AVERAGE | ST DEV | SEM | CS | AVERAGE | ST DEV | SEM | CS | AVERAGE | ST DEV | SEM |
| N1 | 1 | 2548.287487 | | | 1 | 90.09097175 | | | 1 | 490.4952907 | | |
| | 2 | 902.339733 | | | 2 | 145.8615733 | | | 2 | 806.5286995 | | |
| N2 | 1 | 1169.752617 | | | 1 | 340.3436711 | | | 1 | 652.0870336 | | |
| | 2 | 1083.951692 | | | 2 | 500.5053986 | | | 2 | 826.5489154 | | |
| N3 | 1 | 879.4594862 | | | 1 | 333.1935939 | | | 1 | 759.3381905 | | |
| | 2 | 670.6772342 | | | 2 | 298.8732238 | | | 2 | 883.7495324 | | |
| AVG | | 1209.078042 | 678.719 | 391.8586 | | 284.8114054 | 147.8982 | 85.38907 | | 736.4579437 | 143.4299 | 82.80929 |
| 168hr | | | | | | | | | | | | |
| TIME | CS | AVERAGE | ST DEV | SEM | CS | AVERAGE | ST DEV | SEM | CS | AVERAGE | ST DEV | SEM |
| N1 | 1 | 1974.851301 | | | 1 | 617.7666634 | | | 1 | 603.4665092 | | |
| | 2 | 2728.46943 | | | 2 | 544.8358768 | | | 2 | 802.2386532 | | |
| N2 | 1 | 1226.953234 | | | 1 | 31.46033934 | | | 1 | 633.4968331 | | |
| | 2 | 925.2199797 | | | 2 | 417.564504 | | | 2 | 1332.774376 | | |
| N3 | 1 | 519.0955991 | | | 1 | 237.3825605 | | | 1 | 1327.054314 | | |
| | 2 | 908.0597946 | | | 2 | 421.8545503 | | | 2 | 973.8405042 | | |
| AVG | | 1380.441557 | 820.5302 | 473.7333 | | 378.4774157 | 213.8562 | 123.47 | | 945.4785316 | 325.9525 | 188.1887 |

Figure 2.13 How the mean, SD and SEM were calculated.

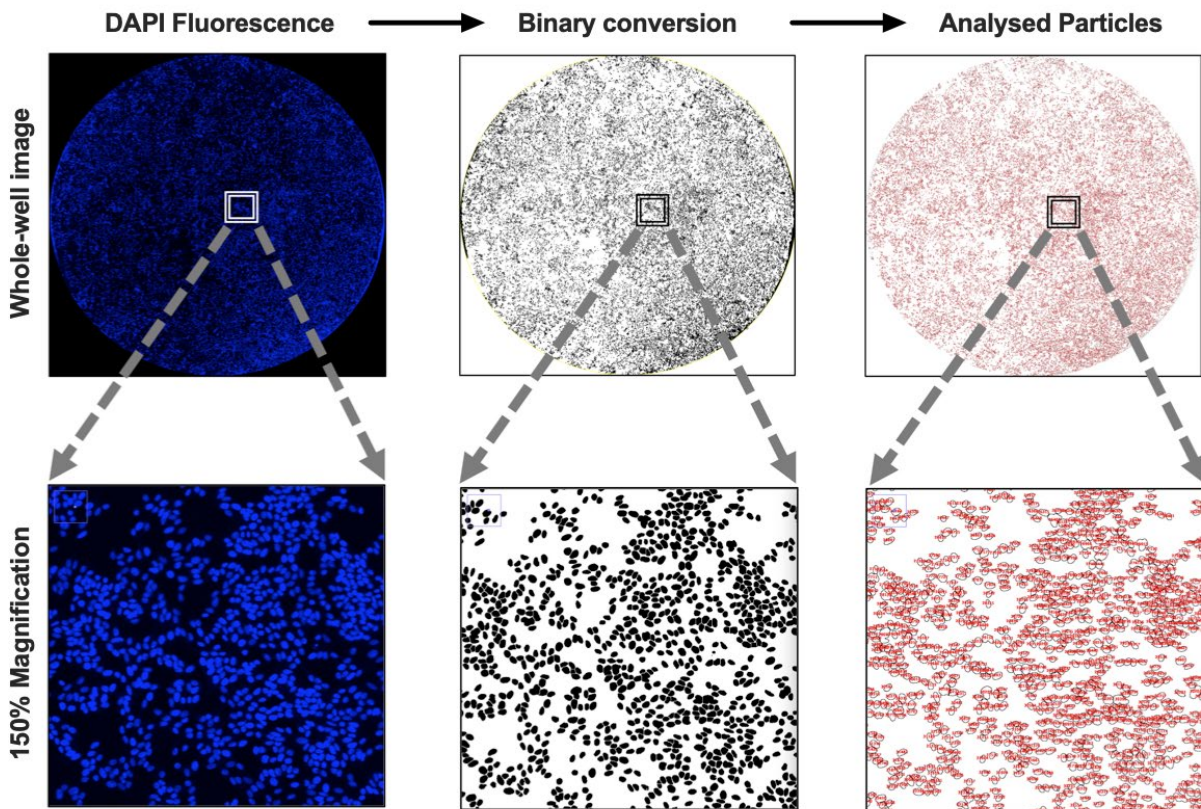
2.14.3 A Novel Method for Measuring Cell Density

For the image-based variables, three FOV imaged systematically for each well were deemed sufficient for the quantification of most parameters such as the process length, cell size, nuclear size, and the apoptosis/necrosis assay, as there was no cause to assume that these parameters might differ if images were taken elsewhere in the well. However, this approach posed several problems for the quantification of the cell density: 1) Cells appeared to aggregate where they become inconsistently dense in certain areas and sparse in other areas in a single well. 2) Depending on the experimental conditions, some fields of view contained hundreds of cells which had to be manually and inefficiently counted. 3) As such, this process was subject to substantial human error, particularly in images of high counts. 4) Later technical problems were observed such as the presence of pipette marks on the surface

of the well meant a complete absence of cells in some corners while a high density of cells was found in other areas. 5) The task of randomizing the fields of view was not straightforward or sufficient in addressing many of the problems.

Therefore, it was deemed that this approach was unlikely to be adequate in accurately characterizing the cell density. Instead, along with addressing some of the technical issues such as the pipette marks, a new method was developed to measure the cell density of the entire well in a manner that avoids image sampling and its associated issues. This was partly based on a method by (Guzmán *et al.*, 2014) for quantifying colony formation in 6-24 well plates stained with crystal violet, where image acquisition was relatively direct. However, due to the smaller wells and the fluorescent labelling, an image of high resolution, contrast and magnification had to be taken for each whole-well, with the surface coverage of DAPI labelled nuclei as the variable of interest. To that purpose, the Well Navigator tool within the CellSens microscopy software was used to calibrate the edges of the plate and demarcate circles around the wells of interest. The Multiple Image Alignment (MIA) function was used so that the motorized microscope can automatically capture 30-40 sequential images taken at 10x to be stitched into a single large image representing the entire well. One disadvantage for this method is the large image sizes of up to 0.5 Gigabytes, which required substantial storage and computer processing requirements to analyze.

To facilitate an automated, streamlined analysis which avoids human input, a macro code was written encompassing the necessary steps utilized in ImageJ for each stack of images. These steps involved blocking the background, converting the image into a binary mode, applying the Watershed function to distinguish the separate nuclei, and finally using the Analyze Particles function to obtain a measurement for the total area covered by the DAPI stained nuclei against the black background, which is expressed as a percentage of the surface of the whole well. This process is displayed in Fig 2.14 below.

A**B**

```

Density_Macro.ijm
1 for (s = 1; s <= nSlices(); s++){
2
3     setSlice(s);
4
5 setOption("BlackBackground", false);
6 run("Make Binary", "method=Default background=Default calculate");
7
8 run("Watershed", "stack");
9 run("Specify...", "width=10300 height=10300 x=5150 y=5150 oval constrain centered");
10 run("Analyze Particles...", "size=100-Infinity pixel show=Outlines clear summarize stack");
11
12

```

Figure 2.14 A schematic of the process underlying the cell density quantification in whole-well images.

2.14.4 Protein Expression

A region of interest was chosen at random (as described above) for the images acquired for the proliferation, differentiation and cytotoxicity experiments, the number of Actin, BrdU, β -III tubulin, Image - IT positive and NeuN cells were counted and the number of DAPI positive cells was also counted. The average per well was taken and merged (as described above). A description of image-based assays used in all experiments is detailed below (Table 2.8).

| Image-Based Assay | Method |
|--------------------------------|---|
| Apoptosis/Necrosis Assay | This was in accordance with manufacturer's protocol of the Apoptosis and Necrosis Quantification Kit (Biotium, UK). The staining solution comprised of FITC Annexin V (green fluorescence indicating apoptotic cells, Ethidium Homodimer III (red fluorescence indicating necrotic cells) and 1X Annexin binding buffer. The two parameters were quantified as a percentage of the total number of cells in an image. |
| Bromodeoxyuridine (BrdU) assay | BrdU as an indicator of proliferating cells was added to the cultured plates for 4 hr prior to fixation and labelling. Cells were washed in PBS and non-specific binding was prevented by incubation in normal goat serum for 40 min. Primary anti-BrdU antibody (Sigma, UK) was then added to the cells for 2 hr before incubating in the FITC secondary overnight at 4°C. Proliferative activity here was taken as the percentage of cells expressing green fluorescence. |
| Cell Density | Whole-well images were taken of the DAPI stained nuclei and density was measured as the percentage of the well covered by the nuclei. |
| Cell Differentiation | β III tubulin and NeuN as an indicator of differentiating cells was added to the culture plates. Cells were washed in PBS and non-specific binding was prevented by incubation in normal goat serum for 40 mins. Primary anti- β III tubulin (Sigma) and anti-NeuN (Millipore) was then added overnight before incubating with secondary for 2 hr at 4°C. Differentiation activity was taken as the percentage of cells expressing green fluorescence. |
| Cell Proliferation | As above for cell density in independent plates cultured over four timepoints: 48, 72, 96 and 120 hr to obtain a pattern of proliferation over time. |
| Cell Size | The total area covered by Actin fluorescence measured using the Analyse Particles function in ImageJ, divided by the number of cells in an Image, to obtain the average size. |
| Mitochondrial Cytotoxicity | The staining solution comprised of FITC Image-IT (green indicating mitochondrial cytotoxicity) and Hoescht (identifying the nuclei of each cell). The parameter was quantified as a percentage of the total number of cells in an image. |
| Nuclear Size | The average size of the DAPI stained nuclei in a field of view was measured with ImageJ's Analyse Particles function following binary conversion and watershedding to separate adjacent nuclei with a line. |
| Process Length | Neuronal processes of the Actin labelled cytoskeleton of cells were manually traced using ImageJ and the average length of processes in an image was obtained. |

Table 2.8 A summary of the image-based experiments used

2.15 Statistical Analysis

All data grouped using Microsoft excel and then imported into Graphpad Prism version 9.5 for statistical analysis and to generate graphs. All data were represented as mean \pm SEM. The assumption of normality was verified using QQ plots of the residual errors. Analysis was carried out using student t-tests, one-way analysis of variance (ANOVA) and two-way ANOVA with post-hoc bonferroni corrections where appropriate to determine whether there were any significant differences between the means of the groups. Statistical significance was set at $p < 0.05$.

Chapter 3

The Effects of Ketone Body Supplementation on Cell Growth *In Vitro*: A Systematic Review

3.1 Introduction

Ketone body metabolism is critical to fuel metabolism in the body. Traditionally viewed as sources of energy during restricted access to carbohydrates, recent studies have underlined the importance of ketone bodies as key metabolic and signalling mediators. In several studies, ketone bodies have exhibited protective roles against diseases such as cancer and cardiovascular and liver disease, opening avenues to potential therapeutic applications for ketone bodies in the future. However, controversies and discrepancies in ketone body metabolism and its impact on cellular growth, health and function exist in the current *in vitro* literature, with studies discussing beneficial effects of ketone body supplementation and others discussing negative or no effects.

Numerous studies have demonstrated the benefit of varying concentrations of AcAc and β OHB on different types of cell lines of varying species. Reports have shown β OHB to increase proliferation (Cheng et al., 2005), inhibit apoptosis and stabilize cell viability (Cheng et al., 2010) and decrease levels of ROS and inflammation (Xie et al., 2015). Yet there are numerous studies that outline the negative repercussions of ketone body supplementation on cell growth. Conflicting with the studies that have shown a positive impact of ketone bodies, studies have reported diminished cell growth and proliferation and have induced apoptosis in pancreatic cell lines (Shukla et al., 2014, McGee and Spector, 1974, Guh et al., 2003, Kadochi et al., 2017) and have increased levels of IL-6 and ROS also (Jain et al., 2003). In the studies where no effect was reported, β OHB enrichment failed to elicit a response on the butyrylation or acetylation level of histone H3 upon long term treatment (Mehdikhani et al., 2019).

The conflicting results highlighted above on the response to ketones bodies between studies come with a background of an increasingly scrutinized role of experimental culture conditions and medium formulations in influencing impacts on cell lines (Cantor et al., 2017), especially in the context of cancer metabolism (Ackermann and Tardito, 2019). Using different types of base media for culturing conditions such as DMEM and RPMI (McKee and Komarova, 2017), is known to alter the metabolism of various cell lines (Wu et al., 2009, Huang et al., 2015). Furthermore, the choice of at least 20 formulations of DMEM as advertised by a single supplier, Thermo Fisher Scientific, formulated with or without pyruvate, plays a determining role when assessing the *in vitro* cytotoxicity of various chemicals (Babich et al., 2009).

No comprehensive systematic review exists detailing the positive, negative or no effects that ketone bodies impose on cell lines. Furthermore, no comprehensive review exists examining at a descriptive level the exact media compositions and ketone bodies that exist in the growth medium of these experiments, including the concentrations and durations that the cells were cultured in these media for. In this systematic review, we provide a review of the reported effects of ketones on cell lines and summarize the proposed mechanisms of how ketones may exert these effects. We outline the concentration or concentration ranges where β OHB induces a positive and negative effect and no effect on cell lines and the cell lines where these effects have been observed most frequently. We further highlight possible confounders behind conflicting results through investigating the media formulations that cells were cultured in.

In this systematic review, we have outlined the studies that had a positive and a negative effect and no effect on cell lines. We also outline the different ketone bodies used in each study and their concentration and duration. We also described the cell lines that were used in the studies and the media formulations that these cells were cultured in and detail whether glucose, pyruvate and glutamine and any other substrate were included in the growth medium.

3.1.2 Aims

3.1.2.1 To provide a comprehensive review of the reported effects of ketones on cell lines.

3.1.2.2 To summarize the proposed mechanisms of how ketones positively, negatively, or equivocally impact cell lines.

3.1.2.3 To highlight possible confounders behind conflicting results.

3.1.3 Hypothesis

3.1.3.1 In this systematic review, there may be studies that outline a positive and negative effect and no effect of ketones on cell growth. Studies will include in full detail what was included in their culturing media including glucose, pyruvate, and glutamine yet there may be studies that will not specify this detail.

3.2 Methods

3.2.1 Database and Search Strategy

A search strategy for a systemic review of the literature was designed using the relevant keywords to identify and examine the *in vitro* effects of exogenous ketone body supplementation in cell line models of ketosis (Exact terms in the Supplementary file S1 in Chapter 8 of the Appendices). Articles were identified by searching Medline, Web of Science and EMBASE, on the 16th of June 2020. Controlled vocabulary terms (i.e., Medical Subject Headings [MeSH]) were used in the search to reach further results. No date restrictions were applied.

3.2.2 Article Selection

The initial search yielded a total of 2282 articles, the titles, and abstracts of which were imported into the Covidence® platform. Following the removal of 783 duplicates, 1499 abstracts were independently screened for possible inclusion by two reviewers. A total of 1160 studies were deemed irrelevant at this stage, leaving 338 articles for full-text screening against the inclusion and exclusion criteria (Supplementary file 1 in the Appendices of Chapter 7). In summary, 63 articles published between 1974 and 2020 were identified on full-text screening to report on the effects of exogenous ketones on various cell lines *in vitro* and were included in this review (Fig. 3.1). The following parameters from each of the included studies were extracted towards the final quantitative and qualitative syntheses: Cell line, cell origin, tissue type, the utilised ketone bodies and along with their concentration and duration, the investigated effects, as well the culture media formulations and the presence or absence of substrates such as glucose, pyruvate, and glutamine.

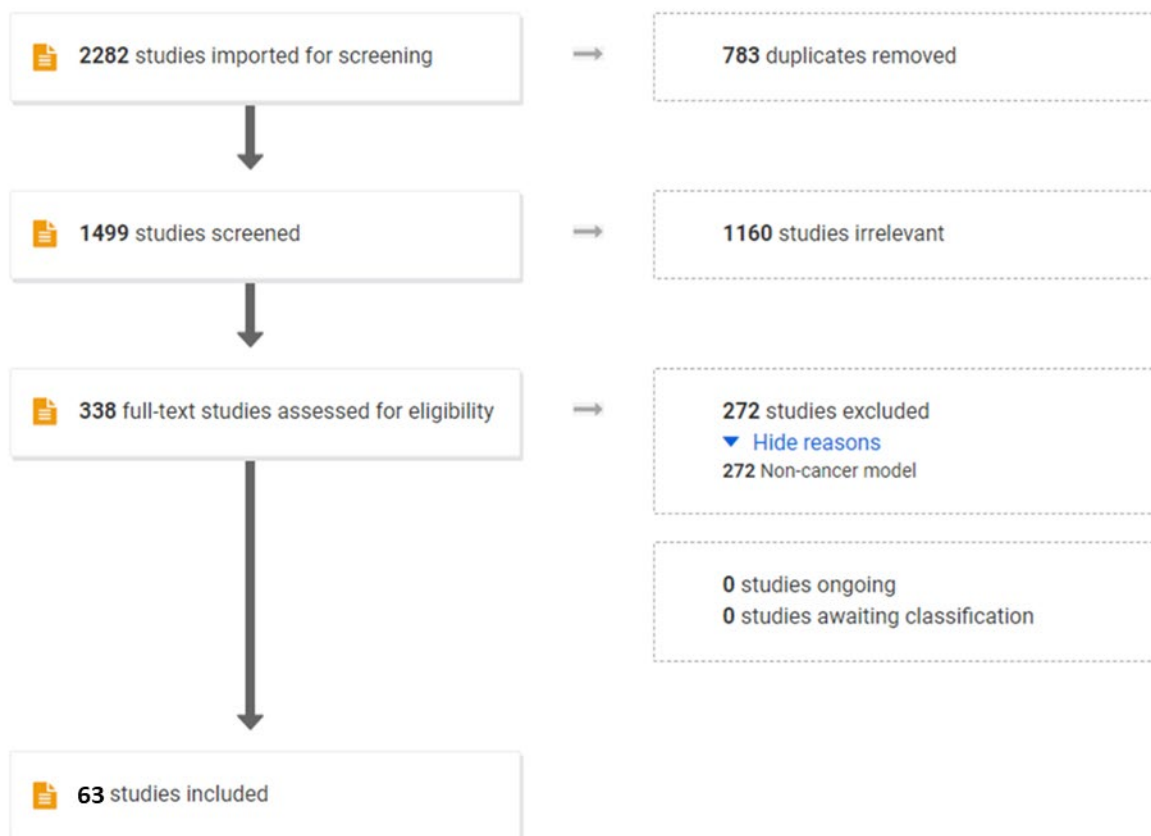


Figure 3.1 Overview schematic of the selection process of the papers included in the systematic review

3.3 Results

3.3.1 Positive effect results

In total, ketone bodies in 32 out of the 63 studies included in the systematic review were found to have positive effects on the cell lines they were cultured with (Cheng et al., 2013, Cheng et al., 2010, Cheng et al., 2007, Cheng et al., 2005, Durigon et al., 2018, Findlay et al., 2015b, Hasan et al., 2008, Imamura et al., 2006, Jiang et al., 2011, Kabiraj et al., 2012, Kweon et al., 2004, Lamichhane et al., 2017b, Li et al., 2020b, Liu et al., 2019a, Macdonald et al., 2008a, MacDonald et al., 2008b, Martinez-Outschoorn et al., 2012a, Martinez-Outschoorn et al., 2011b, Maurer et al., 2011a, McGee and Spector, 1974, Mikami et al., 2020, Patel et al., 1975, Shang et al., 2018, Tagawa et al., 2019, Vilà-Brau et al., 2011, Wang et al., 2017, Wang et al., 2016, Wang et al., 2019, Xie et al., 2015, Xu et al., 2011, Zhang et al., 2018b, Zhang and Xie, 2017). (Table 3.1)

Within these 32 studies, 52 cell lines were used which included 21 neuronal, three liver, seven skin, four kidney, three adrenal, three pancreatic, three breast, two fibroblast, one cartilage and one cervical cell line(s). Human cell lines were the most frequently used species of cell lines in these studies (14 studies), this was followed by rat cell lines (nine studies), mouse (five studies), human and mouse cell

lines (two studies), mouse and rat cell lines (one study) and human, rat and mouse cell lines (one study) (Table 3.1).

β OHB was the most investigated ketone body with 27 out of the 32 studies (84% of studies) reporting a positive effect. The other five studies investigated the impact of both AcAc and β OHB. AcAc or acetone was never studied individually in any of the investigations. The lowest concentration of β OHB that was used in a study was 0.0000011 mM (Wang et al., 2017). Some studies used varying concentrations of β OHB in ranges from 0, 0.5, 1, 2 and 4 mM (Xie et al., 2015) to ranges such as 0, 1, 10 and 25 mM and 0, 5, 10, 20, 40 and 80 mM β OHB (Li et al., 2020b, Shang et al., 2018). The concentration of β OHB that was used most frequently was 4 mM and 10 mM where four out of the 32 studies used each concentration. (Cheng et al., 2013, Cheng et al., 2010, Cheng et al., 2007, Martinez-Outschoorn et al., 2011a, Martinez-Outschoorn et al., 2012a, Mikami et al., 2020, Tagawa et al., 2019, Xu et al., 2011), this was followed by 5 mM β OHB which was used in two studies (Hasan et al., 2008, MacDonald et al., 2008b). The highest concentration of β OHB that was used was 87 mM and this was used in one study (McGee and Spector, 1974). The lowest and highest concentration used for the AcAc & β OHB studies were 0.5 mM and 22 mM (Abdelwahab et al., 2012, Jiang et al., 2011, Patel et al., 1981) (Table 3.1).

The shortest duration that β OHB was administered for in the positive studies was for 30 mins (McGee and Spector, 1974) and the longest it was administered was over 504 hr (21 days) (Durigon et al., 2018) (Table 3.2).

For the base medium, 20 out of the 32 studies used DMEM, 6 studies used DMEM/F-12 Hams mixture, two studies used RPMI 1640 medium, two studies used both RPMI 1640 Medium and Krebs ringer bicarbonate buffer, one study used Bicarbonate buffer and one study used both Minimum Essential Media alpha ($MEM\alpha$) media and RPMI 1640 media. 100% of the studies used some form serum (either FBS or foetal calf serum (FCS)) in their media (Table 3.2).

28 out of 32 studies applied antibiotics to their growth medium where three studies didn't specify if they used them or not and one study did not include antibiotics in their growth medium. Seventeen studies did not specify if they used glucose in their medium, where thirteen studies did use glucose in their experiments, two studies did not include glucose in their medium. Of the studies that specified their glucose concentration, the concentration ranges included 1 mM, 5 mM, 25 mM glucose (Durigon et al., 2018, Lamichhane et al., 2017b, Maurer et al., 2011a) (Table 3.2)

27 studies did not specify if they included pyruvate in their medium and one study did not include pyruvate in their growth medium. Four studies did include pyruvate in their growth medium and the concentrations used included 1 mM and 5 mM pyruvate (Durigon et al., 2018, Hasan et al., 2008, Macdonald et al., 2008a, MacDonald et al., 2008b).

26 studies did not specify if they included glutamine in their growth medium and of the six studies that did include glutamine in their culturing media, the glutamine concentrations included 2, 4, and 10 mM (Findlay et al., 2015a, Hasan et al., 2008, Macdonald et al., 2008a, Maurer et al., 2011a, Patel et al., 1975, Wang et al., 2019) (Table 3.2).

| Study ID | Ketone Effect | Cell line/s | Origin of cell/s | No of cell lines | Tissue type/s | Ketone | Ketone Concentration |
|-----------------|---------------|---|---|------------------|---|----------------------|---|
| Maurer 2011 | Positive | T98G/U87MG/NIH-3T3/A172/LNT229/U251MG | T98G/U87MG/A172/LNT-229/U251MG: Human NIH-3T3: Murine | 6 | 5 Neuronal & 1 Fibroblast | AcAc and β OHB | 5 mM for both |
| Cheng 2013 | Positive | PC12 | Rat | 1 | Adrenal | β OHB | 4 mM |
| Xie 2015 | Positive | PC12 | Rat | 1 | Adrenal | β OHB | 0 mM, 0.5 mM, 1 mM, 2 mM, 4 mM |
| Cheng 2010 | Positive | PC12 | Rat | 1 | Adrenal | β OHB | 4 mM |
| Durigon 2018 | Positive | HeLa/Human embryonic kidney cells | Human | 2 | Cervical/ Kidney | β OHB | 0.3 mM |
| Cheng 2005 | Positive | L929cells/umbilical vein endothelial cells/chondrocytes | L929: Mouse Endothelial: Human Chondrocytes: Rabbit | 3 | Fibroblast/Skin/ Articular Cartilage | β OHB | 0.1 mM - 2.17 mM (originally 0.005-0.10 g/L) |
| Jiang 2011 | Positive | LEF2 cells/RK3E cell | Rat | 2 | Kidney | AcAc and β OHB | AcAc: 21.74 mM, β OHB: 54.35 mM |
| Tagawa 2019 | Positive | Hepal c1c7 cells/HepG2 cells | Hepal c1c7: Mouse/ HepG2: Human | 2 | Liver | β OHB | 10 mM |
| Wang 2019 | Positive | HEP3B cell/Huh-7 cells | Human | 2 | Liver | β OHB | 5 mM, 10 mM, and 20 mM |
| Mikami 2020 | Positive | HepG2 cells/HLE cells | Human | 2 | Liver | β OHB | 10 mM |
| Vil  -Brau 2011 | Positive | HepG2/ HEK293 | Human | 2 | Liver/ Kidney | AcAc and β OHB | AcAc: 1mM and 10mM β OHB: 2mM and 20mM |
| Wang 2016 | Positive | HT22 | Mouse | 1 | Neuronal | β OHB | 2, 4, 8, 10 mM for impact of β OHB on cell viability alone. 4 mM and 8 mM for subsequent experiments. |
| Patel 1981 | Positive | C6/CI1300 (N2a) | C6: Rat/CI1300(N2a): Mouse | 2 | Neuronal | AcAc and β OHB | AcAc: 0.5mM, β OHB: 2.5mM |
| Lamichhane 2017 | Positive | SH-SY5Y | Human | 1 | Neuronal | β OHB | 8mM, 10mM |
| Xu 2011 | Positive | BV-2 | Mouse | 1 | Neuronal | β OHB | 4 mM |
| Kweon 2004 | Positive | MN9D/MN9X cells | Mouse | 2 | Neuronal | β OHB | 0, 4 and 8 mM |
| Li 2020 | Positive | SH-SY5Y | Human | 1 | Neuronal | β OHB | 0, 5, 10, 20, 40 or 80 mM |
| Cheng 2007 | Positive | PC12 | Rat | 1 | Neuronal | β OHB | 4 mM |
| Imamura 2006 | Positive | SH-SY5Y | Human | 1 | Neuronal | β OHB | 8 mM |
| Zhang 2018 | Positive | SH-SY5Y | Human | 1 | Neuronal | β OHB | 2 mM |
| Zhang 2017 | Positive | U251 | Human | 1 | Neuronal | β OHB | 1 mM |
| Findlay 2015 | Positive | SH-SY5Y | Human | 1 | Neuronal | β OHB | 0.0005 mM, 0.001 mM, 0.01 mM |
| Shang 2018 | Positive | C6 Glioma | Rat | 1 | Neuronal | β OHB | 0, 1, 10 and 25 mM |
| Kabiraj 2012 | Positive | SH-SY5Y | Human | 1 | Neuronal | β OHB | 0.1 mM |
| Liu 2018 | Positive | N1E-115/NIH-3T3 | Mouse | 2 | Neuronal/Skin | β OHB | 0.0005 mM, 0.001 mM, 0.005 mM, 0.01 mM |
| Hasan 2008 | Positive | INS-1832/13 cells | Rat | 1 | Pancreatic | β OHB | 5 mM |
| Macdonald 2008 | Positive | INS-1832/13 cells | Rat | 1 | Pancreatic | β OHB | 5 mM |

| | | | | | | | |
|-------------------------|----------|--------------------------|-------|---|---------------------|----------------------|--|
| MacDonald 2008 | Positive | INS-1832/13 cells | Rat | 1 | Pancreatic | AcAc and β OHB | AcAc: 10 mM, β OHB: 5 mM for insulin release studies. β OHB: 2mM, 4 mM, 6 mM, 8 mM, and 10 mM in combination with different concentrations of MMS. This β OHB concentration combination with MMS was repeated for lactate. AcAc and β OHB were 5 mM for inhibiting the MCT for insulin release studies |
| Wang 2017 | Positive | A549/A375 | Human | 2 | Skin | β OHB | 0.0000011 mM |
| McGee 1974 | Positive | Ehrlich tumour cells | Mouse | 1 | Skin | β OHB | 86.96 mM |
| Martinez-Otschoorn 2011 | Positive | hTERT-BJ1/MCF7 | Human | 2 | Skin/Breast | β OHB | 10 mM |
| Martinez-Otschoorn 2012 | Positive | hTERT-BJ-1/MCF7MDA-MB231 | Human | 3 | Skin/Breast /Breast | β OHB | 10 mM |

Table 3.1 Positive ketone studies

| Study ID | Duration of β OHB administration (hr) | Medium type | Serum (FBS/FCS) | Antibiotics | Glucose | Glucose concentration (mM) | Pyruvate | Pyruvate concentration (mM) | Glutamine | Glutamine concentration (mM) | Other media components? |
|--------------|--|--|-----------------|-------------|---------------|---|---------------|-----------------------------|---------------|------------------------------|--|
| Maurer 2011 | 24 hrs, 48 hrs, 84 hrs, 144 hrs | DMEM | Yes | Yes | Yes | Depending on the experiment; 0 mM, 1 mM, 2 mM, 5 mM, 10 mM or 25 mM | No | No | Yes | 2mM | Rotenone and 3-bromopyruvate were used in one experiment to investigate influence of ketones on cell sensitivity to cell death triggers. |
| Cheng 2013 | 2 hrs | DMEM | Yes | Yes | Not specified | Not specified | Not specified | Not specified | Not specified | Not specified | Culture media supplemented with horse serum then cells were treated with different concentrations of H2O2 |
| Xie 2015 | 24 hrs | RPMI 1640 medium | Yes | Yes | Not specified | Not specified | Not specified | Not specified | Not specified | Not specified | Not specified |
| Cheng 2010 | 4 hrs | DMEM | Yes | Yes | Not specified | Not specified | Not specified | Not specified | Not specified | Not specified | Heat inactivated horse serum |
| Durigon 2018 | 48 hrs / 96 hrs / 144 hrs / 188 hrs / 504 hrs (media changed every 48 hrs) | DMEM | Yes | Yes | Yes | 5 mM | Yes | 1 mM | Yes | Specified but not given | Not specified |
| Cheng 2005 | 72 hrs (L929 cells), 96 hrs (HUVECs), 120 hrs (Rabbit chondrocytes) | DMEM | Yes | Yes | Not specified | Not specified | Not specified | Not specified | Not specified | Not specified | Not specified |
| Jiang 2011 | Viability Assay - 24 hrs, ATP level measurement - 6 hrs after having been in culture medium for 24 hrs | DMEM/F12 medium | Yes | Yes | Yes | 2 mM | Not specified | Not specified | Not specified | Not specified | Not specified |
| Tagawa 2019 | 3 hrs or 6 hrs (mRNA and Protein Expression and SIRT1 activity) or 24 hrs (Cell Viability Assay) | Hepa1c1c7 - Minimum essential medium alpha (MEM α) HepG2 cells - RPMI 1640 medium | Yes | Yes | Not specified | Not specified | Not specified | Not specified | Not specified | Not specified | Not specified |
| Wang 2019 | Trypan Blue Cell Viability Assay (Cell | DMEM | Yes | Yes | Not specified | Not specified | Not specified | Not specified | Yes | 2 mM | Non-essential amino acids (0.1 mM) |

| | | | | | | | | | | | |
|-----------------|---|---|-----|---------------|---------------|-------------------|---------------|---------------|---------------|---------------|--|
| | Number) - 144 hrs MTT Cell Viability Assay - 3 hrs Proliferation - 48 hrs Wound Healing Migration Assay - 24 hrs | | | | | | | | | | |
| Mikami 2020 | 24 hrs, 48 hrs, 72 hrs | DMEM | Yes | Yes | Not specified | Not specified | Not specified | Not specified | Not specified | Not specified | Not specified |
| Vil  -Brau 2011 | 5 hrs | DMEM | Yes | Yes | Not specified | Not specified | Not specified | Not specified | Not specified | Not specified | Not specified |
| Wang 2016 | 12 hrs | DMEM | Yes | Yes | Not specified | Not specified | Not specified | Not specified | Not specified | Not specified | Not specified |
| Patel 1981 | 96 hrs or 144 hrs for both cell lines | DMEM | Yes | Yes | Yes | 5 mM | Not specified | Not specified | Yes | 2mM | Cells routinely subcultured with 0.5% trypsin in phosphate-buffered saline containing 0.5mM ethylene glycol bis( -aminoethylether)-N, N, N', N'-tetra acetic acid (EGTA) |
| Lamichhane 2017 | 24 hrs | DMEM | Yes | Yes | Yes | 1 mM, 5 mM, 25 mM | Not specified | Not specified | Not specified | Not specified | Not specified |
| Xu 2011 | Preincubation for 2 hrs with a further incubation of 24 hrs | DMEM | Yes | Yes | Not specified | Not specified | Not specified | Not specified | Not specified | Not specified | LPS |
| Kweon 2004 | Preincubated for 24 hrs then incubated for a further 72 hrs | DMEM | Yes | Not specified | No | No | Not specified | Not specified | Not specified | Not specified | 1 mM NaBu was used to differentiate the cells |
| Li 2020 | 24 hrs | A 1:1 vol/vol mixture of DMEM and DMEM/F12 medium | Yes | No | Not specified | Not specified | Not specified | Not specified | Not specified | Not specified | Trans Retinoic acid was used to differentiate the cells. |
| Cheng 2007 | 24 hrs | DMEM | Yes | Yes | Not specified | Not specified | Not specified | Not specified | Not specified | Not specified | 7% horse serum |
| Imamura 2006 | 1 hr | DMEM/F12 medium | Yes | Yes | Not specified | Not specified | Not specified | Not specified | Not specified | Not specified | Not specified |
| Zhang 2018 | 3 hrs | DMEM/F12 medium | Yes | Yes | Not specified | Not specified | Not specified | Not specified | Not specified | Not specified | Not specified |

| | | | | | | | | | | | |
|----------------|--|---|-----|---------------|---------------|---|---------------|---------------|---------------|----------------|---|
| Zhang 2017 | 3 hrs | DMEM | Yes | Yes | Yes | Not specified | Not specified | Not specified | Not specified | Not specified | Not specified |
| Findlay 2015 | 48 hrs | DMEM/F12 medium | Yes | Yes | Yes | 2.5 mM | Not specified | Not specified | Yes | 4 mM | Not specified |
| Shang 2018 | Depending on the experiment; 2 hrs, 15rs or 24 hrs | DMEM | Yes | Yes | Yes | "High glucose" is all that's described | Not specified | Not specified | Not specified | Not specified | Not specified |
| Kabiraj 2012 | 144 hrs | 1:1 mixture of DMEM and Ham's F12 medium | Yes | Yes | Not specified | Not specified | Not specified | Not specified | Not specified | Not specified | Not specified |
| Liu 2018 | 120 hrs | DMEM | Yes | Yes | No | No | Not specified | Not specified | Not specified | Not specified | Not specified |
| Hasan 2008 | 1 hr | RPMI 1640 medium | Yes | Yes | Yes | 11 mM | Yes | 1 mM | Yes | 10 mM | 50 µM B-mercaptoethanol, 10 mM Sodium HEPES buffer |
| Macdonald 2008 | 1 hr | RPMI 1640 tissue culture medium / Krebs ringer bicarbonate buffer | Yes | Yes | Yes | Cells maintained in a glucose concentration of 11.1 mM but 22 hrs before the insulin release experiment the concentration was reduced in 5 mM and 2 hrs before the experiment the concentration was reduced again to 3 mM | Yes | 1 mM | Yes | 2 mM and 10 mM | The Krebs Ringer Bicarbonate buffer contained 15 mM sodium HEPES and 15 mM NaHCO3 |
| MacDonald 2008 | 1 hr | RPMI 1640 medium, two hr before the experiments began, the medium was replaced with Krebs-Ringer bicarbonate buffer | Yes | Yes | Yes | 11.1 mM, one day before the experiment was to begin the glucose concentration was reduced to 5 mM, the concentration was further decreased when the Krebs Ringer solution was added in 2 hr before the experiment to 3 mM | Yes | 1 mM and 5 mM | Not specified | Not specified | 50 µM B mercaptoethanol, 10 mM sodium HEPES - Given with the INS-1 medium 15 mM HEPES and 15 mM NaHCO3 - Given in the Krebs-Ringer solution |
| Wang 2017 | 24 hrs | DMEM | Yes | Not specified | Yes | Glucose Deprived DMEM was used (5.5mM) | Not specified | Not specified | Not specified | Not specified | Cells were cultured in either CAF or fibroblast conditioned media and also non-conditioned media for |

| | | | | | | | | | | | |
|--------------------------|---------|--------------------|-----|---------------|---------------|---------------|---------------|---------------|---------------|---------------|--|
| | | | | | | | | | | | controls in experiment 1. |
| McGee 1974 | 0.5 hrs | Bicarbonate Buffer | Yes | Not specified | Yes | 11mM | Not specified | Not specified | Not specified | Not specified | The Bovine Serum Albumin was added after it had been "defatted" and fatty acids were subsequently added. Bicarbonate buffer was also used. |
| Martinez-Outschoorn 2011 | 48 hrs | DMEM | Yes | Yes | Not specified | Not specified | Not specified | Not specified | Not specified | Not specified | No (outside of drugs investigated) |
| Martinez-Outschoorn 2012 | 48 hrs | DMEM | Yes | Yes | Not specified | Not specified | Not specified | Not specified | Not specified | Not specified | Not specified |

Table 3.2 Positive Ketone studies media formulations.

3.3.2 Negative Effect Results

Out of the 63 studies from the systematic review, 22 studies reported negative effects from the supplementation and use of ketone bodies in the cell culture medium (D'Alessandro et al., 2011, Dardis et al., 2016, Guh et al., 2003, Huang et al., 2017, Jain et al., 2003, Jain et al., 2002, Jain et al., 1999, Ji et al., 2020, Kadochi et al., 2017, Kaya et al., 2018, Liu et al., 2019a, Luo et al., 2017, Magee et al., 1979, Meroni et al., 2018, Poff et al., 2014, Rains and Jain, 2011, Rodrigues et al., 2017, Shakery et al., 2018, Shukla et al., 2014, Skinner et al., 2009, Vallejo et al., 2020, Zhang et al., 2018a) (Table 3.3)

Overall, 53 cell lines were used in these studies. 14 of these cell lines were neuronal (D'Alessandro et al., 2011, Ji et al., 2020, Skinner et al., 2009, Vallejo et al., 2020), eight were breast (Huang et al., 2017, Kaya et al., 2018, Rodrigues et al., 2017), seven were nasal (Luo et al., 2017), five were pancreatic (Shukla et al., 2014, Zhang et al., 2018a), five were lymphatic (Jain et al., 2003, Jain et al., 2002, Jain et al., 1999, Rains and Jain, 2011), four were skin (Dardis et al., 2016, Kaya et al., 2018, Meroni et al., 2018, Skinner et al., 2009), three were colon (Kadochi et al., 2017, Liu et al., 2019a, Shakery et al., 2018), two were kidney (Guh et al., 2003, Liu et al., 2019a) and one cell line each were of a bone, cervical, fibroblast, lung and muscle cell line (Abdelwahab et al., 2012, Liu et al., 2019a, Shukla et al., 2014, Zhuang et al., 2014). Of the cell lines used in the negative studies, 16 out of the 22 negative (73%) ketone studies used human cell lines, four studies (18%) used only mouse cell lines and two studies (9%) used both human and mouse cell lines (Table 3.3).

The most investigated ketone body was β OHB with 12 out of the 22 studies (55%) reporting a negative effect, with the remaining 10 studies using both AcAc and β OHB (45%). No studies used solely AcAc or acetone (Table 3.3). For the studies that used solely β OHB, the lowest concentration used in their experiments was 0.1 mM β OHB which was used in a human kidney cell line (Guh et al., 2003). The highest concentration of β OHB used was 40 mM (Magee et al., 1979) The concentration ranges of β OHB used in these studies vary. These ranges include 0 mM, 1, mM, 5 mM, 10 mM, 20 mM, and 40 mM (Ji et al., 2020, Magee et al., 1979, Rodrigues et al., 2017). Some studies only used a single concentration in their experiments, of these studies, the two most prominent concentrations used were 5 mM and 10 mM β OHB (D'Alessandro et al., 2011, Dardis et al., 2016, Liu et al., 2019a, Poff et al., 2014). For the studies that used both AcAc and β OHB, the lowest concentration used their experiments was 0.005 mM β OHB (Jain et al., 1999), where the highest concentration for both ketone bodies used was 54 mM and 98 mM (Skinner et al., 2009). As the with studies that used only β OHB, the concentration ranges of the studies that used both AcAc and β OHB varies. These ranges include 0.005 mM, 0.01 mM, 0.02 mM (Skinner et al., 2009), 0.1 mM,

0.25 mM, 0.5 mM, 1 mM, 2.5 mM, and 5 mM (Shakery et al., 2018), 1, mM, 2.5 mM 5 mM, 10 mM and 20 mM (Vallejo et al., 2020, Luo et al., 2017). Out of the 10 studies using both AcAc and β OHB, there is no single individual concentration used but there is one range that was used more commonly in two studies that produced negative effects in the cell lines. These ranges were 0 – 3 mM (Jain et al., 2003, Jain et al., 2002) (Table 3.3).

Out of the 22 studies, seven of these studies used DMEM as their base growth medium (32%), five used RPMI 1640 medium (22%), three used DMEM/F12 medium (14%), one study used both DMEM and defined keratinocyte serum free medium, one used both DMEM and MCOY's media, one used DMEM & RPMI 1640 medium, one used Eagles Minimum Essential Medium (EMEM), one study used MCDB131 media, and one study did not specify the growth medium used (5% for each of the individual studies). 20 out of the 22 (91%) studies used either FBS or FCS in their growth media and two studies did not specify whether serum was included in their media (9%).

17 out of 22 (77%) studies declared they included antibiotics in their growth medium and the other five studies did not specify whether they were included or excluded. 10 out of the 22 studies included glucose in their growth medium, one study specifically excluded glucose and eleven studies did not specify as to whether glucose was included or excluded (Table 3.4). Of the studies that included glucose, the concentrations included 2.5 mM (Rodrigues et al., 2017), 3 mM (Guh et al., 2003), 7 mM (Rains and Jain, 2011) and 11 mM (Liu et al., 2019a). Two studies included two ranges of a normal glucose concentration (5 and 7 mM) and a high a glucose concentration (30 mM) (Jain et al., 2003, Jain et al., 2002). The highest glucose concentration used was 98 mM and this concentration was used in two studies (Shakery et al., 2018, Skinner et al., 2009).

Four out of the 22 studies noted that they included pyruvate in their growth medium, one study specifically excluded pyruvate and 17 did not specify whether it was included or excluded. Of the studies that declared they included pyruvate, the concentrations included 1 mM (Ji et al., 2020, Zhang et al., 2018a) and 2 mM (Meroni et al., 2018) (Table 3.4).

However, one of the studies that declared pyruvate was included in the growth medium did not specify its concentration (Luo et al., 2017). 10 out of the 22 studies included glutamine their growth medium. 12 of these studies did not specify as to whether it was included or excluded. Of the studies that included glutamine, the lowest concentration used was 0.109 mM (Liu et al., 2019a), the most common concentration was 2 mM (Dardis et al., 2016, Jain et al., 2003, Jain et al., 2002, Jain et al., 1999, Ji et al., 2020, Rains and Jain, 2011). The only concentration range described is between 2 and 7 mM (Magee et al., 1979) and one study that mentioned it included glutamine in its media did not mention its concentration (Luo et al., 2017) (Table 3.4).

| Study ID | Ketone Effect | Cell line/s | Origin of cell/s | No of cell lines | Tissue type/s | Ketone | Ketone Concentration |
|-------------------|---------------|--|--|------------------|--|---------------|---|
| Huang 2017 | Negative | MCF7/MDA-MB-157/MDA-MB-231/MDA-MB-361/MDA-MB-468/SKBR3 | Human | 6 | Breast | βOHB | 20 mM |
| Rodrigues 2017 | Negative | C-neu, HER2-induced mammary carcinoma cells | Mouse | 1 | Breast | βOHB | 0.5 mM, 5 mM, and 10 mM |
| Zhang 2018 | Negative | HeLa cells/PANC-1 cells | Human | 2 | Cervical /Pancreatic | βOHB | 5 mM, 10 mM |
| Kaya 2018 | Negative | MCF-7 cells/Human foreskin fibroblast cells (HFF) | Human | 2 | Breast/ Skin Fibroblasts | AcAc and βOHB | 10 mM and 20 mM |
| Shukla 2014 | Negative | Capan1/C2C12/3T3L1/S2-013/HPNE/RAPAN | Capan1/S2013/HPNE/RAPAN: Human C2C12/3T3L1: Mouse | 6 | Capan1/S2-013/HPNE/RAPAN: Pancreatic cancer C2C12: Muscle 3T3L1: Embryonic Fibroblast | AcAc and βOHB | 1 mM, 5 mM, 10 mM, 20 mM |
| Shakery 2018 | Negative | SW480 cells | Human | 1 | Colon | βOHB | Viability Assay - 0.1 mM, 0.25 mM, 0.5 mM, 1 mM, 2.5 mM, 5 mM); Oxygen Consumption/ Extracellular Acidification Rate/ Colony formation assay/ Scratch Assay - 0.25 mM |
| Kadochi 2017 | Negative | CT26 cells | Human | 1 | Colon | βOHB | 1 mM |
| Guh 2003 | Negative | HK-2 | Human | 1 | Kidney | βOHB | 0.1 - 10 mM |
| Liu 2019 | Negative | H1299/293T/U2OS/HCT116 | Human | 4 | Lung/ Kidney/ Bone/ Colon | βOHB | 10 mM |
| Magee 1979 | Negative | Raji cells | Human | 1 | Lymphatic | βOHB | 0 mM, 10 mM, 20 mM, 40 mM |
| Jain 2003 | Negative | U937 cells | Human | 1 | Lymphatic | AcAc and βOHB | 0 - 3 mM |
| Jain 2002 | Negative | U937 cells | Human | 1 | Lymphatic | AcAc and βOHB | 0 - 3 mM |
| Rains 2011 | Negative | U937 cells | Human | 1 | Lymphatic | AcAc and βOHB | 0 - 10 mM |
| Jain 1999 | Negative | U937 cells | Human | 1 | Lymphatic | AcAc and βOHB | Both AcAc and βOHB were used at concentrations of 0.005 mM, 0.01 mM and 0.02 mM |
| Luo 2017 | Negative | CNE1/CNE2/HONE1/HK1/5-8F/6-10B/NP69 | Human | 7 | Nasal | AcAc and βOHB | 0 mM, 2.5 mM, 5 mM, 10 mM |
| Vallejo 2020 | Negative | U87/SJGBM2/Glio3/Glio9/Glio14/Glio38/Glio40 | Human | 7 | Neuronal | AcAc and βOHB | 0 mM, 1 mM, 5 mM, 10 mM, 20mM |
| Ji 2020 | Negative | GSC line/NCH421k, Neural stem like cells (NSC) | NCH421k: Human/ NSC: Mouse | 2 | Neuronal | βOHB | 0 mM, 1 mM, 5 mM, or 10 mM |
| Poff 2014 | Negative | VM-M3/Fluc | Mouse | 1 | Neuronal | βOHB | 5 mM |
| D'Alessandro 2011 | Negative | tTA-40/wtSOD1/G93ASOD1 | Mouse | 3 | Neuronal | βOHB | 5 mM |

| | | | | | | | |
|--------------|----------|---|-------|---|----------------------------|----------------------|--|
| Skinner 2009 | Negative | SH-SY5Y/Human foreskin fibroblast (HFF) cells | Human | 2 | Neuronal/ Skin Fibroblasts | AcAc and β OHB | 54 mM or 98 mM for both β OHB and AcAc |
| Meroni 2018 | Negative | HMEC-1 | Human | 1 | Skin | AcAc and β OHB | Cell Viability: β OHB: 2 to 20 mM and AcAc: 0.5 to 5 mM. All further experiments were performed using 4 mM β OHB and 1mM AcAc |
| Dardis 2016 | Negative | B16 Cells | Mouse | 1 | Skin | β OHB | 10 mM |

Table 3.3 Negative Ketone Studies

| Study ID | Duration of β OHB administration (hr) | Medium type | Serum (FBS/FCS) | Antibiotics | Glucose | Glucose concentration (mM) | Pyruvate | Pyruvate concentration (mM) | Glutamine | Glutamine concentration (mM) | Other media components? |
|----------------|--|--|-----------------|---------------|---------------|---|---------------|---|---------------|---|---|
| Huang 2017 | 1 hr | DMEM/F12 medium | Yes | Yes | Not specified | Not specified | Yes | 1 mM | Yes | 2 mM | 1 mM non-essential amino acids |
| Rodrigues 2017 | 0 hrs and 24 hrs | DMEM | Yes | Yes | Not specified | Not specified | Not specified | N/A | Not specified | Not specified | Not specified |
| Zhang 2018 | 0 hrs, 12 hrs, 24 hrs, 48 hrs, 72 hrs and 96 hrs | DMEM or RPMI-1640 medium | Yes | Yes | Yes | For the cell number experiments, the concentration was 3 mM (Low glucose) | Not specified | Not specified | Not specified | Not specified | Not specified |
| Kaya 2018 | 24 hrs | DMEM | Yes | Yes | Yes | Controls: 4.5g/L, 1.125g/L, 0g/L Ketone Treated: 0g/L | Not specified | Not specified | Not specified | Not specified | Not specified |
| Shukla 2014 | 24 hrs to 72 hrs | DMEM | Yes | Yes | No | No | Not specified | Not specified | Not specified | | Not specified |
| Shakery 2018 | Depending on the experiment; 2 hrs, 36 hrs, 72 hrs and 14 days | DMEM | Yes | Yes | Not specified | Not specified | Not specified | Not specified | Yes | 1% L-glutamine | Not specified |
| Kadochi 2017 | 24 hrs | DMEM | Yes | Not specified | Yes | 450mg/dl, 100mg/dl, 0mg/dl | Not specified | Not specified | Not specified | Not specified | Not specified |
| Guh 2003 | 24 hrs and 48 hrs | DMEM/F12 medium | Yes | Yes | Yes | 11 mM | No | Not specified | Yes | L-glutamine, 5ug/mL | Insulin 5ug/mL, transferrin 5 ng/mL, sodium selenite 5 pg/mL, T35 ng/mL hydrocortisone, 5 pg/mL prostaglandin E1(PGE1), and 10 ng/mL epidermal growth factor. |
| Liu 2019 | 16 hrs and 24hrs | DMEM: H1299, 293T and U2OS MCOY: HCT116 | Yes | Not specified | Not specified | Not specified | Yes | Not specified but used as control for β OHB | Yes | Not specified but used as control for β OHB | Not specified |

| | | | | | | | | | | | |
|-------------------|--|---|---------------|---------------|---------------|----------------|---------------|---------------|---------------|--|---|
| Magee 1979 | Depending on the experiment 0 hrs, 24 hrs, 48 hrs, 72 hrs, 144 hrs | RPMI 1640 medium | Yes | Yes | Not specified | Not specified | Not specified | Not specified | Yes | 2 – 7 mM | 20 mM Hepes |
| Jain 2003 | 24 hrs | RPMI 1640 medium | Yes | Yes | Yes | 7 mM and 30 mM | Not specified | Not specified | Yes | 2 mM | 12 mM sodium bicarbonate, 12 mM HEPES |
| Jain 2002 | 24 hrs | RPMI 1640 medium | Yes | Yes | Yes | 5 mM 30 mM | Not specified | Not specified | Yes | 2 mM | 12 mM sodium carbonate, 12 mM HEPES, |
| Rains 2011 | 24 hrs | RPMI 1640 medium | Yes | Yes | Yes | 7 mM | Not specified | Not specified | Yes | 2 mM | 12 mM sodium carbonate 12 mM HEPES (buffer) |
| Jain 1999 | Depending on the experiment; 4 hrs or 72 hrs | RPMI 1640 medium | Yes | Yes | Not specified | Not specified | Not specified | Not specified | Yes | 2 mM | Not specified |
| Luo 2017 | 24 hrs | DMEM and Defined keratinocyte serum-free medium: | Yes | Not specified | Not specified | Not specified | Not specified | | Not specified | Not specified | Not specified |
| Vallejo 2020 | Depending on the experiment. 24 hrs, 72 hrs or 14 days | RPMI 1640 medium (U82 and SJGBM2) DMEM/F12 medium (all glia cultures) | Yes | Yes | Not specified | Not specified | Not specified | Not specified | Not specified | Not specified | Glia cultures only: 20 ng/ml each of human epidermal growth factor and human fibroblast growth factor, and 2% Gem21 NeuroPlex Serum-Free Supplement |
| Ji 2020 | 120 hrs, 144 hrs and 168 hrs | DMEM/F12 medium | Not specified | Not specified | Yes | 2.5 mM | Not specified | Not specified | Not specified | Not specified | epidermal growth factor (20ng/ml), basic fibroblast growth factor (20ng/ml) |
| Poff 2014 | Depending on the experiment - 24, 48, 72, 96, 120 and 144 hrs | Eagles' minimum essential medium | Yes | Yes | Yes | 3 mM or 25 mM | Yes | 2mM | Not specified | Not specified | Not specified |
| D'Alessandro 2011 | 24 hrs | DMEM | Yes | Yes | Not specified | Not specified | Yes | 1 mM | Not specified | No glutamine added when β OHB was in media | hygromycin B was added (0.2 mg/mL). 0.02 mM cystine was added to the BHB media also. |
| Skinner 2009 | 24 hrs | DMEM | Yes | Yes | Yes | Not specified | Not specified | Not specified | Not specified | Not specified | Not specified |
| Meroni 2018 | Depending on the experiment 2, 6, 14, 24 and 48 hrs. | MCDB131 medium | Yes | Yes | Not specified | Not specified | Not specified | Not specified | Yes | 2 mM | 10 ng/mL epidermal growth factor. 1g/mL hydrocortisone. 20 mM HEPES buffer. |

| | | | | | | | | | | | |
|-------------|--|---------------|---------------|---------------|---------------|---------------|---------------|---------------|---------------|---------------|---------------|
| Dardis 2016 | 0 hrs, 20 hrs 24 hrs, 48 hrs, 72 hrs, 96 hrs | Not specified | Not specified | Not specified | Not specified | Not specified | Not specified | Not specified | Not specified | Not specified | Not specified |
|-------------|--|---------------|---------------|---------------|---------------|---------------|---------------|---------------|---------------|---------------|---------------|

Table 3.4 Negative ketone studies media formulations

3.3.2 No Effect Results

Out of the 63 studies investigating the impact of ketone bodies on cell lines, nine of these studies reported no effect from the supplementation of ketone bodies in cell culture medium (Bennett et al., 2011, Briscoe et al., 1994, Cui et al., 2019, Denton and Howard, 1987, Du Yan et al., 2000, Eloqayli et al., 2011b, Mehdikhani et al., 2019, Otto et al., 2014, Tisdale, 1984).

Overall 17 cell lines were used, five of these were neuronal (Denton and Howard, 1987, Eloqayli et al., 2011b, Tisdale, 1984), five were colon (Otto et al., 2008), two were liver (Bennett et al., 2011, Briscoe et al., 1994), two were kidney (Cui et al., 2019, Du Yan et al., 2000), one was breast (Mehdikhani et al., 2019), one was cervical (Bennett et al., 2011) and one was gastric (Otto et al., 2014). Of the cell lines used in the no effect studies, three out of the nine no effect (33.33%) ketone studies used human cell lines, two studies used only rat cell lines, two studies used mouse and rat cell lines, one study used human and rat cell lines, and one study used a primate cell line (Table 3.5).

The most investigated ketone body was β OHB with seven out of the nine studies (77.78%) reporting no effect, with the remaining two studies using both AcAc and β OHB. No studies used solely AcAc or acetone. For the studies that used solely β OHB, the lowest concentration used in their experiments was 1 mM β OHB (Eloqayli et al., 2011b) and the highest individual concentration used was 20 mM (Denton and Howard, 1987). The β OHB ranges that were used varies considerably, however most of the ranges spanned from 2.5 mM, 5 mM, 10 mM, 20 mM, 30 mM, and 40 mM (Cui et al., 2019, Du Yan et al., 2000, Mehdikhani et al., 2019). In the studies that investigated the impact of both AcAc and β OHB, there was no study that investigated just one individual concentration. The concentration ranges span from 0.5 mM and 2.5 mM AcAc and β OHB (Tisdale, 1984) and 0.5 mM, 1 mM, 2 mM, 5 mM and 10 mM (Briscoe et al., 1994) (Table 3.5).

Out of the nine studies, five of the studies used DMEM (56%), two studies used RPMI1640 medium (22%), one study used EMEM (11%) and one used Krebs Henseleit Bicarbonate Buffer (11%). Eight studies out of nine stated they included some form of serum in their media formulations (89%), whereas only one study (11%) did not specify whether serum was included. Five of the studies (56%) stipulated that they included antibiotics in their growth medium and four studies (44%) did not clarify if they were included or not (Table 3.6).

Seven out of the nine studies included glucose in their culture medium (78%) and two studies did not specify whether it was included in their culture medium. Of the glucose concentrations used in the seven studies, the concentrations span between 1 and 10 mM. The lowest concentration used was 1 mM (Bennett et al., 2011). The highest concentration used was 22 mM (which was in the DMEM base medium) (Mehdikhani et al., 2019). One study used 3 mM (Eloqayli et al., 2011a), another used 5 mM (Tisdale, 1984) and another used 6 mM (Briscoe et al., 1994). There were only two studies that used varying concentrations, the concentration ranges span from 1 to 5.5 mM of glucose (Bennett et al., 2011, Otto et al., 2008) (Table 3.6).

Three of the nine studies included pyruvate in their culture medium (33%) and six studies did not explain as to whether pyruvate was included in the culture medium. The lowest concentration of pyruvate used was 0.2 mM (Briscoe et al., 1994) and the highest concentration used was 7.5 mM (Denton and Howard, 1987). The remaining concentration used was 3.5 mM (Bennett et al., 2011). Four of the studies included glutamine (44%) and five studies did not specify as to whether it was included in the medium. For the studies that included glutamine, the lowest concentration used was 0.75 mM (Briscoe et al., 1994), and the highest concentration was 2 mM (Bennett et al., 2011, Otto et al., 2008, Tisdale, 1984) (Table 3.6).

| Study ID | Ketone Effect | Cell line/s | Origin of cell/s | No of cell lines | Tissue type/s | Ketone | Ketone Concentration |
|-----------------|---------------|--|---|------------------|--|----------------------|---|
| Mehdikhani 2019 | No effect | MDA-MB231 cell line | Human | 1 | Breast | β OHB | 5 mM (long term study), 25 - 1000 mM (cytotoxicity), |
| Otto 2014 | No effect | CaCo/HCT-116/HT29/SW-620/WiDr/gastric carcinoma cell line 23132/87 | Human | 6 | CaCo, HCT-116, HT29, SW-620 and WiDr: Colon Cell line 23132/87: Gastric | β OHB | 4 mM |
| Bennett 2011 | No effect | HeLa/H4IIE | Hela: Human/H4IIE: Rat | 2 | Cervical/ Liver | β OHB | 3.5 mM |
| DuYan 2000 | No effect | ABAD-COS cells | Primate | 1 | Kidney | β OHB | Viability Assay and Energy Charge: 0 mM, 5 mM, 10 mM, and 20 mM. ABAD metabolism - 0 mM, 10 mM, 20 mM, 30 mM, 40 mM. NMR Spectroscopy – 10 mM |
| Cui 2019 | No effect | ccRCC cells | Human | 1 | Kidney | β OHB | 0 mM, 2.5 mM, 5 mM, 10 mM |
| Briscoe 1994 | No effect | AS -30D cells | Rat | 1 | Liver | AcAc, β OHB | AcAc (0.5 mM, 1mM, 2 mM, 5 mM, 10 mM), β OHB (10 mM) |
| Tisdale 1984 | No effect | C6/C1300 (N2a) | C6: Rat/ C1300 (N2a): Mouse | 2 | Neuronal | AcAc and β OHB | AcAc (0.5 mM) an β OHB (2.5 mM) |
| Eloqayli 2011 | No effect | Cerebellar astrocytes/C6 | Cerebellar astrocytes - Mouse C6 - Rat | 2 | Neuronal | β OHB | 1 mM |
| Denton 1987 | No effect | PC12 | Rat | 1 | Neuronal | β OHB | 20 mM |

Table 3.5 No effect ketone studies

| Study ID | Duration of β OHB administration (hr) | Medium type | Serum (FBS/FCS) | Antibiotics | Glucose | Glucose concentration (mM) | Pyruvate | Pyruvate concentration (mM) | Glutamine | Glutamine concentration (mM) | Other media components? |
|-----------------|---|------------------------------------|-----------------|---------------|---------------|---|---------------|-----------------------------|---------------|------------------------------|--|
| Mehdikhani 2019 | 720 hrs (30 days) | DMEM | Yes | Not specified | Yes | DMEM with 1 g/L glucose or DMEM with 250 mg/L glucose | Not specified | Not specified | Not specified | Not specified | N/A |
| Otto 2014 | 96 hrs (4 days) | RPMI 1640 medium | Yes | Yes | Yes | 2 or 5 mM | Not specified | Not specified | Yes | 2 mM | No |
| Bennett 2011 | 18 - 24 hrs | DMEM | Yes | Yes | Yes | 1 - 5.5 mM | Yes | 3.5 mM | Yes | 2 mM | Phenol red |
| DuYan 2000 | Depending on the experiment – 10 mins, 24 hrs, 48 hrs, 72 hrs, 96 hrs and 120 hrs and 192 hrs | DMEM | Yes | Not specified | Not specified | Not specified | Not specified | Not specified | Not specified | Not specified | None |
| Cui 2019 | 24 hrs - 144 hrs (1 - 6 days) | RPMI 1640 medium | Yes | Not specified | Not specified | Not specified | Not specified | Not specified | Not specified | Not specified | None |
| Briscoe 1994 | 1 hr | Krebs Henseleit bicarbonate buffer | Not specified | Not specified | Yes | 6 mM | Yes | 0.2 mM | Yes | 0.75 mM | 125 mM KCl, 2 mM K ₂ HPO ₄ , 1 mM MgCl ₂ , 0.4 mM ADP, 20 mM HEPES, 0.1 mM Malate |
| Tisdale 1984 | 96 hrs | Eagles' minimal essential medium | Yes | Yes | Yes | 5 mM | Not specified | Not specified | Yes | 2 mM | None |
| Eloqayli 2011 | 4 hrs | DMEM | Yes | Yes | Yes | 3 mM | Not specified | Not specified | Not specified | Not specified | No other media components are mentioned |
| Denton 1987 | 2 mins | DMEM | Yes | Not specified | Yes | 5.6 mM | Yes | 7 mM | Not specified | Not specified | None |

Table 3.6 No effect media formulations

3.3.3 Proposed Mechanism of Action for Positive Ketone Effect

There has been no detailed review of the proposed mechanisms of how ketone bodies directly produce positive and negative effects or no effects on cell lines, until now. Supplementary Table 7.8 and Fig. 3.2 outline the 32 studies that reported positive cellular effects regarding the addition of ketone bodies and their mechanism of action. One of the aims of this study was to categorize the mechanisms of actions of ketone bodies and how they produce their effects whether it was through extracellular, intracellular, or genetic mechanisms. Out of the 32 positive studies, 23 of these studies reported ketone bodies to produce their effect through intracellular mechanisms, five produced their effects through both intracellular and genetic mechanisms, two produced their effects through genetic mechanisms, one produced their effect through both extracellular and genetic mechanisms and only one study failed to outline the ketone bodies mechanism of action.

β OHBs positive impact on cell lines stems from regulating ROS levels (Cheng et al., 2013, Wang et al., 2017, Wang et al., 2016, Xie et al., 2015), inhibiting apoptosis, (Cheng et al., 2010, Wang et al., 2019, Mikami et al., 2020, Cheng et al., 2007, Kabiraj et al., 2012), increasing mitochondrial activity (Martinez-Outschoorn et al., 2011b), stimulating cell cycle progression through upregulation of intracellular calcium levels (Cheng et al., 2005) and suppressing endoplasmic reticulum stress (Tagawa et al., 2019). β OHB protects cells in a glucose deficient environment through ERK activation (Lamichhane et al., 2017a), inhibits microglial ROS and nitrogen monoxide production (Xu et al., 2011), reduces toxicity through increasing the cellular energy state (Kweon et al., 2004), improves viability through upregulation of TrkA (Li et al., 2020b), β OHB protects neurons via the anti-oxidation pathway (Findlay et al., 2015a), and upregulates FTO expression (Liu et al., 2019b). AcAc and β OHB reduce the expression of c-Myc which in turn reduced glucose transporters and glycolytic enzymes (Shukla et al., 2014), β OHB fuels mitochondrial metabolism and acts through epigenetic mechanisms to promote tumour growth (Shakery et al., 2018), β OHB attenuates p53 activity, which in turn allows the cells to proliferate more rapidly (Liu et al., 2019a). AcAc and β OHB cause oxidative stress to endothelial cells (Meroni et al., 2018), both AcAc and β OHB were found to impair glycolysis and cause histone polyacetylation (Dardis et al., 2016). AcAc was found to have phosphatidylserine (P-S) externalisation and monocyte action which in turn secreted proinflammatory cytokines and caused an immunological cascade event to occur (Jain et al., 1999). β OHB induced upregulation of IL-1 β and LCN2 genes promotes tumorigenesis (Huang et al., 2017) (Supplementary Table 7.8 and Figure 3.2).

3.3.4 Proposed Mechanism of Action for Negative Ketone Effect

Supplementary Table 7.9 outlines all the potential mechanisms mentioned in the studies where ketone bodies produced a negative effect on the cell lines, whereas Fig. 3.2 shows a general schematic of the mechanisms involved. 14 out of the 22 studies reported ketone bodies to produce their negative effects through intracellular mechanisms, four reported ketone bodies to produce their effects through intracellular and nuclear mechanisms, two studies reported that their mechanisms acted through intracellular and genetic mechanisms. One study reported that ketones acted through extracellular and intracellular mechanisms and one study reported that the negative effects the ketone produced was through genetic mechanisms.

Ketone bodies produced negative cellular effects through increasing oxidative stress (which subsequently reduced proliferation and induced apoptosis) (Ji et al., 2020), increased concentrations of AcAc and β OHB resulted in apoptosis (Skinner et al., 2009, Vallejo et al., 2020). AcAc can generate excess oxygen radicals – increasing the oxidative environment and damaging the cell (Rains and Jain, 2011). AcAc stimulated tumour necrosis factor alpha (TNF- α) and IL-6 whereas β OHB didn't and IL-6 was consequently found to stimulate ROS production (Jain et al., 2003, Jain et al., 2002), β OHB inhibited proliferation and impacted GSH homeostasis (Luo et al., 2017, D'Alessandro et al., 2011), both AcAc and β OHB changed the energy production pathway from glycolysis and lactate fermentation to OXPHOS which in turn increased oxidative stress and ROS production and damaged mitochondria causing apoptosis (Kadochi et al., 2017). β OHB induced growth inhibition of cells which was dependent on transforming growth factor beta (TGF- β), p21 and p27 protein expression in HK-2 cells and further inhibited mito-genesis (Guh et al., 2003) (Supplementary Table 7.9).

3.3.5 Proposed Mechanism for No Effect Ketone Studies

Supplementary Table 7.10 outlines all the potential mechanisms where ketone bodies showed no effect on the cell lines. Out of the nine studies, five showed their effects through intracellular mechanisms and the remaining four studies did not provide a mechanism. Out of the studies that provided mechanisms, the mechanisms included β OHB acting as a substrate for cellular energy charge as well as a source for increased production of neurotransmitters (Du Yan et al., 2000). β OHB caused an increase in lipid synthesis (Tisdale, 1984), and increases mitochondrial metabolism in glioblastoma cells (Eloqayli et al., 2011a).

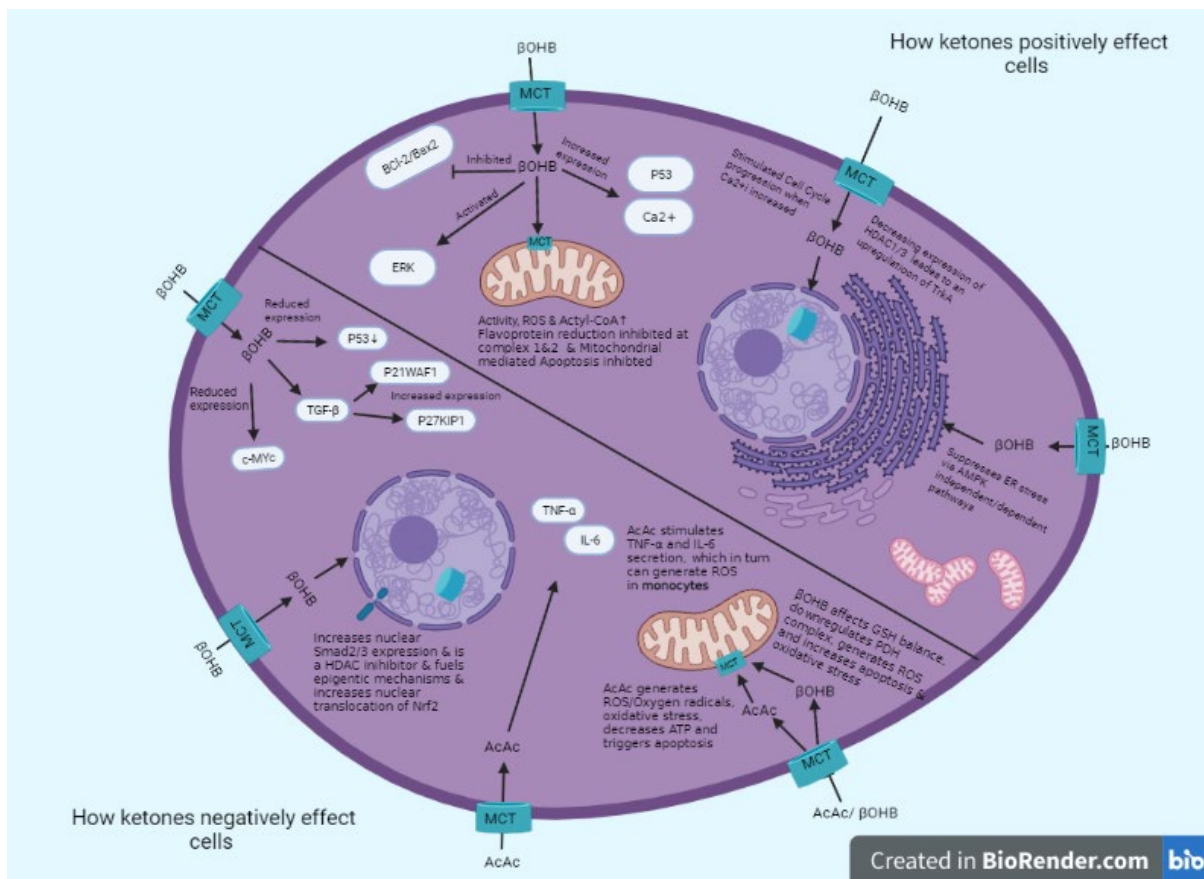


Figure 3.2 Schematic diagram outlining how ketone bodies can positively or negatively impact cell lines

3.3.6 Relationship with the Medium

To elucidate potential confounders between conflicting results we next wished to establish links with the parameters we extracted from the studies. To do this, we looked at the relationships with the media, with the cell type, with the ketone and whether it was combined with something else in the media.

When investigating the relationship between the cells and the media compositions (Supplementary Table 7.11), 100% of studies that showed a beneficial, negative, and no ketone effect included some sort of base media in their culture formulations. 100% of the studies that included serum in their growth media found a positive effect of ketones on cell growth, whereas in the studies where no effect or a negative effect was found, 89% and 91% included serum in their media and 11% and 9% of studies did not specify as to whether serum was included or not. 91% of studies that included antibiotics in their growth medium observed a positive effect of ketones on the cells compared to 78% of studies that observed no effect and 77% of studies that observed a negative effect. 41% of studies that found a

beneficial ketone effect on cells supplemented their media with glucose, compared with 6% of studies that did not supplement with glucose and 53% of studies that did not specify.

78% of studies that found no effect of ketones on the cell lines supplemented their growth media with glucose compared to 22% of these studies that did not specify whether it was included. 45% of studies that found a negative effect of ketones on cell growth supplemented glucose into the culture media, compared to 5% that did not and 50% of studies that did not specify. 84% of studies that found a beneficial effect of ketones of cell growth did not specify as to whether it was included in the growth media, compared to 3% that did not include it and 13% that supplemented it in the media. For the studies that found no effect of ketones on cell growth, 67% of studies did not specify whether pyruvate was included in the culture media, compared to 33% of studies that did include it in the media.

18% of the studies that found a negative ketone effect on cell growth included pyruvate in the media compared to 5% that did not and 77% of these studies did not specify whether pyruvate was included. 22% of the studies that found a beneficial ketone effect supplemented the growth media with glutamine compared to 78% that did not specify whether it was included. 44% of the studies that found ketones had no effect on cell growth included glutamine in their growth media compared to 56% that did not specify if it was included. For the studies that found a negative effect of ketones of cell growth, 45% included glutamine in the culture media and 55% of studies did not specify if they included it in the growth media (Supplementary Table 7.10).

3.3.7 Relationship with the Cell Type

When investigating the relationship with the cell type (Table 3.7), we found out of the 63 studies that included positive, no effect and negative ketone effects on cell growth that in total 122 cell lines had been used when combining all studies. 43% of these cell lines were used in the positive ketone effect studies, 14% of these cell lines were used in the no effect studies and 43% of these cell lines were used in the studies that found a negative effect using ketones on cell growth.

Out of the positive studies, four different species of cell lines were used, these included human, mouse, rat, and rabbit cell lines. Overall, 56% of the cell lines used in the positive studies were of a human origin, 21% of the cell lines were of a mouse and rat origin and 2% of the cell lines were of a rabbit origin. Of the human cell lines used in the positive studies, 41% of these cell lines were of a neuronal phenotype, 21% were of a liver phenotype, 14%

were of a skin phenotype, 10% were of a breast phenotype, 7% were of a kidney phenotype and 3% were of a cervical and fibroblast phenotype. Of the mouse cell lines used in the positive ketone studies, 55% of these cell lines were of a neuronal phenotype, 27% were of a skin phenotype and 9% were of a fibroblast and liver phenotype. For the rat cell lines used, 27% of the cell lines were of a neuronal, pancreatic, and adrenal phenotype, 18% of the studies were of a kidney phenotype. For the rabbit cell line used in the in the positive studies, the cell line used was of a cartilaginous phenotype (Table 3.7).

Out of the negative effect studies, two different species of cell lines were used which included human and mouse cell lines. In total, 83% of cell lines were of a human origin and 17% were of a mouse origin. For the human cell lines used in the studies that found a negative effect of ketones on cell growth, 20% of these cell lines were of a neuronal tissue type, 16% of these were of a nasal and breast tissue type, 11% of these were of a lymphatic and pancreatic tissue type, 7% were of a skin and colon tissue type, 5% were of a kidney tissue type and 2% of cell lines were of a lung, cervical and bone tissue type. For the mouse cell lines used, 56% of these were of a neuronal tissue type, and 11% of these cell lines were of a skin, breast, fibroblast, and muscle tissue type.

For the no effect studies, four different species of cell lines were used, these included human, mouse, rat, and primate cell lines. In total 53% of these cell lines were of a human origin, 12% were of a mouse origin, 29% were of a rat origin and 6% were of a primate origin. For the human cell lines found in the no effect studies, 56% of these cell lines were of a colon tissue type, and 11% of cell lines were of a kidney, breast gastric and cervical tissue type. For the mouse cell lines used in the no effect studies, both cell lines were of a neuronal tissue type. Of the rat cell lines used, 60% of these cell lines were of a neuronal tissue type and the remaining 40% were of a liver tissue type. The primate cell line that was used in the no effect studies was of a kidney tissue type (Table 3.7).

| Study ID | Cell line/s | Origin of cell/s | Number of cell lines used | Tissue type/s | Ketone Effect |
|--------------------------|--|--|---------------------------|--|---------------|
| Maurer 2011 | T98G/U87MG/NIH-3T3/A172/LNT-229/U251MG | T98G/U87MG/A172/LNT-229/U251MG: Human NIH-3T3: Murine | 6 | 5 Neuronal & 1 Fibroblast | Positive |
| Cheng 2013 | PC12 | Rat | 1 | Adrenal | Positive |
| Xie 2015 | PC12 | Rat | 1 | Adrenal | Positive |
| Cheng 2010 | PC12 | Rat | 1 | Adrenal | Positive |
| Durigon 2018 | HeLa/Human embryonic kidney cells | Human | 2 | Cervical/ Kidney | Positive |
| Cheng 2005 | L929 cells/umbilical vein endothelial cells/chondrocytes | L929: Mouse/Endothelial: Human/Chondrocytes: Rabbit | 3 | Fibroblast/Skin/Articular Cartilage | Positive |
| Jiang 2011 | LEF2 cells/RK3E cell | Rat | 2 | Kidney | Positive |
| Tagawa 2019 | Hepa1c1c7 cells/HepG2 cells | Hepa1c1c7: Mouse/ HepG2: Human | 2 | Liver | Positive |
| Wang 2019 | HEP3B cell/Huh-7 cells | Human | 2 | Liver | Positive |
| Mikami 2020 | HepG2 cells/HLE cells | Human | 2 | Liver | Positive |
| Vil  -Brau 2011 | HepG2/ HEK293 | Human | 2 | Liver/ Kidney | Positive |
| Wang 2016 | HT22 | Mouse | 1 | Neuronal | Positive |
| Patel 1981 | C6/CI1300 (N2a) | C6: Rat/CI1300(N2a): Mouse | 2 | Neuronal | Positive |
| Lamichhane 2017 | SH-SY5Y | Human, Mouse | 1 | Neuronal | Positive |
| Xu 2011 | BV-2 | Mouse | 1 | Neuronal | Positive |
| Kweon 2004 | MN9D/MN9X cells | Mouse | 2 | Neuronal | Positive |
| Li 2020 | SH-SY5Y | Human | 1 | Neuronal | Positive |
| Cheng 2007 | PC12 | Rat | 1 | Neuronal | Positive |
| Imamura 2006 | SH-SY5Y | Human | 1 | Neuronal | Positive |
| Zhang 2018 | SH-SY5Y | Human | 1 | Neuronal | Positive |
| Zhang 2017 | U251 | Human | 1 | Neuronal | Positive |
| Findlay 2015 | SH-SY5Y | Human | 1 | Neuronal | Positive |
| Shang 2018 | C6 Glioma | Rat | 1 | Neuronal | Positive |
| Kabiraj 2012 | SH-SY5Y | Human | 1 | Neuronal | Positive |
| Liu 2018 | N1E-115/NIH-3T3 | Mouse | 2 | Neuronal/Skin | Positive |
| Hasan 2008 | INS-1 832/13-derived cells | Rat | 1 | Pancreatic | Positive |
| Macdonald 2008 | INS-1832/13 cells | Rat | 1 | Pancreatic | Positive |
| MacDonald 2008 | INS-1 832/13 cells | Rat | 1 | Pancreatic | Positive |
| Wang 2017 | A549/A375 | Human | 2 | Skin | Positive |
| McGee 1974 | Ehrlich tumour cells | Mouse | 1 | Skin | Positive |
| Martinez-Outschoorn 2011 | hTERT-BJ1/MCF7 | Human | 2 | Skin/Breast | Positive |
| Martinez-Outschoorn 2012 | hTERT-BJ-1/MCF7/MDA-MB 231 | Human | 3 | Skin/Breast /Breast | Positive |
| Huang 2017 | MCF7/MDA-MB-157/MDA-MB-231/MDA-MB-361/MDA-MB-468/SKBR3 | Human | 6 | Breast | Negative |
| Rodrigues 2017 | C-neu, HER2-induced mammary carcinoma cells | Mouse | 1 | Breast | Negative |
| Zhang 2018 | HeLa cells/PANC-1 cells | Human | 2 | Cervical /Pancreatic | Negative |

| | | | | | |
|-------------------|--|---|---|--|-----------|
| Kaya 2018 | MCF-7 cells/Human foreskin fibroblast cells (HFF) | Human | 2 | Breast/ Skin Fibroblasts | Negative |
| Shukla 2014 | Capan1/C2C12/3T3L1/S2-013/HPNE/RAPAN | Capan1: Human/ C2C12: Mouse/ 3T3L1: Mouse/ S2-013: Human/ HPNE: Human/ RAPAN: Human | 6 | Capan1/S2-013/HPNE/RAPAN: Pancreatic C2C12: Muscle (myoblast) 3T3L1: embryonic fibroblast (preadipocyte) | Negative |
| Shakery 2018 | SW480 cells | Human | 1 | Colon | Negative |
| Kadochi 2017 | CT26 cells | Human | 1 | Colon | Negative |
| Guh 2003 | HK-2 | Human | 1 | Kidney | Negative |
| Liu 2019 | H1299/293T/U2OS/HCT116 | Human | 4 | Lung/ Kidney/ Bone/ Colon | Negative |
| Magee 1979 | Raji cells | Human | 1 | Lymphatic | Negative |
| Jain 2003 | U937 cells | Human | 1 | Lymphatic | Negative |
| Jain 2002 | U937 cells | Human | 1 | Lymphatic | Negative |
| Rains 2011 | U937 cells | Human | 1 | Lymphatic | Negative |
| Jain 1999 | U937 cells | Human | 1 | Lymphatic | Negative |
| Luo 2017 | CNE1/CNE2/HONE1/HK1/5-8F/6-10B/NP69 | Human | 7 | Nasal | Negative |
| Vallejo 2020 | U87/SJGBM2/Glio3/Glio9/Glio14/Glio38/Glio40 | Human | 7 | Neuronal | Negative |
| Ji 2020 | GSC line/NCH421k, Neural stem like cells (NSC) | NCH421k: Human/ NSC: Mouse | 2 | Neuronal | Negative |
| Poff 2014 | VM-M3/Fluc | Mouse | 1 | Neuronal | Negative |
| D'Alessandro 2011 | tTA-40/wtSOD1/G93ASOD1 | Mouse | 3 | Neuronal | Negative |
| Skinner 2009 | SH-SY5Y/Human foreskin fibroblast (HFF) cells | Human | 2 | Neuronal/ Skin Fibroblasts | Negative |
| Meroni 2018 | HMEC-1 | Human | 1 | Skin | Negative |
| Dardis 2016 | B16 Cells | Mouse | 1 | Skin | Negative |
| DuYan 2000 | ABAD-COS cells | Primate | 1 | Kidney | No Effect |
| Tisdale 1984 | C6/C1300 (N2a) | C6: Rat/C1300 (N2a): Mouse | 2 | Neuronal | No Effect |
| Cui 2019 | ccRCC cells | Human | 1 | Kidney | No Effect |
| Mehdikhani 2019 | MDA-MB231 cell line | Human | 1 | Breast | No Effect |
| Otto 2014 | CaCo/HCT-116/HT29/SW-620/WiDr/gastric carcinoma cell line 23132/87 | Human | 6 | CaCo, HCT-116, HT29, SW-620 and WiDr: Colon cell line 23132/87: Gastric | No Effect |
| Eloqayli 2011 | Cerebellar astrocytes/C6 | Cerebellar astrocytes - Mouse C6 - Rat | 2 | Neuronal | No Effect |
| Bennett 2011 | HeLa/H4IIE | HeLa: Human/H4IIE: Rat | 2 | Cervical/ Liver | No Effect |
| Briscoe 1994 | AS -30D cells | Rat | 1 | Liver | No Effect |
| Denton 1987 | PC12 | Rat | 1 | Neuronal | No Effect |

Table 3.7 Cells relationship with the media

3.3.8 The Relationship between the Ketones and the Concentration

β OHB was the most frequently used ketone out of the 63 studies (Supplementary Table 7.12). In the studies that outlined a beneficial effect of ketone bodies on cell growth, 84% of studies used β OHB. The remaining 16% of studies used a combination of both AcAc and β OHB. In the studies that found a negative impact of ketone bodies on the cell lines, 55% of these studies used β OHB and 45% of the studies used both AcAc and β OHB. Similarly in the studies that found ketone bodies had no effect on cell growth, 78% of studies used β OHB and 22% of studies used both AcAc and β OHB.

For the positive ketone studies that used only β OHB, there were 20 different concentrations and concentration ranges recorded (Supplementary Tables 7.12 & 7.13). The three most used concentrations that were observed to have a beneficial effect on cell growth were 4 mM, 5 mM, and 10 mM β OHB. 15% of studies cultured their cell lines in either 4 mM or 10 mM β OHB whereas 7% of studies cultured their cells in 5 mM β OHB. The remaining 17 concentrations and concentration ranges only had one study associated with one of these timepoints. These other concentrations included 1 mM, 2 mM, 8 mM, and 87 mM. Furthermore, there are varying concentration ranges used within some of these studies which include ranges from 0.0005 mM to 0.01 mM, 0.01 mM to 2.17 mM, 0.5 mM to 4 mM, 1 mM to 80 mM. For the positive studies that used both AcAc and β OHB in their experiments, the concentration ranges for AcAc include 0.5 mM, 1 mM, 5 mM, 10 mM, 21.74 mM, and the concentration ranges for β OHB include 2 mM, 2.5 mM, 5 mM, 6 mM, 8 mM, 20 mM and 54 mM (Supplementary Tables 7.12 & 7.13).

Similarly, within the positive ketone studies that used only β OHB, there were 18 specific timepoints recorded. The four most common timepoints were 1, 3, 24 and 28 hr (Supplementary Table 7.12). 19% of studies cultured cells in β OHB for a duration of 24 hr, 11% of studies cultured cells in β OHB for 1 hr and for 28 hr. 7% of these studies cultured cells in β OHB for a duration of 3 hr. The other 14 recorded timepoints and timeframes only had one study associated with each timepoint. These timepoints included, 0.5, 2, 3, 4, 6, 12, 48, 120 and 144 hr. For the five positive studies that used both AcAc and β OHB in their experiments, AcAc and β OHB were cultured in five different timepoints, these included 1 hr, 5 hr, 24 hr, 96 hr, and over a period of 24, 48, 84 and 144 hr (Supplementary Table 7.12).

Within the studies that found a negative effect of β OHB on cell growth, there were 10 different concentrations and concentration ranges recorded (Supplementary Tables 7.12 and 7.14). The two most common concentrations of β OHB that were found to negatively impact cell growth included 5 mM and 10 mM β OHB. 17 % of these studies cultured their cells in either 5 mM or 10 mM β OHB. The other concentrations recorded included 1 mM and 20 mM. Some of the studies used varying concentration ranges, one study used a range of 0 mM, 1 mM, 5 mM and 10 mM, another study used a range from 0.1 mM to 10 mM β OHB and one used a range included 10 mM, 20 mM and 40 mM, and another study used a range which included, 0.1 mM, 0.25 mM, 0.5 mM, and 1 mM. For the negative studies that used both AcAc and β OHB, the concentration ranges include 0.005 mM, 0.01 mM, 0.02 mM, 1 mM, 5 mM, 10 mM, 20 mM and 54 mM and 98 mM. for both ketone bodies (Supplementary Tables 7.12 and 7.14).

For the negative ketone studies that used solely β OHB, there were 10 different timepoints and durations recorded where cells were cultured in β OHB. 25% of these studies described culturing cells for a duration of 24 hr. The other nine remaining timeframes included 1 hr, from 12, 24, 48, 72, and 96 hr 120 and 144 hr, between 12 and 24 hr, for a duration of 20 hr, between 24 and 48 hr, and 168 hr (Supplementary Table 7.12). Within the negative ketone studies that used both AcAc and β OHB, five different timepoints were recorded where cells were cultured in both ketone bodies, these include from between 4 hr to 72 hr, for a duration of 24 hr, from 24 hr to 72 hr, from 2 hr up to 72 hr and from 24 hr up to 336 hr (Supplementary Table 7.12).

Within the no effect studies that used solely β OHB and found that it had no effect on cell growth, there were 7 different concentrations and concentration ranges used. The concentrations included 1 mM, 3.5 mM, 4 mM, and 20 mM β OHB (Table 3.12 & Table 3.15). The concentration ranges for one study included 0 mM, 2.5 mM, 5 mM, 10 mM, for another study, it was 0 mM, 5 mM, 10 mM and 20 mM, 30 mM, and 40 mM and for another study the range included 5 mM, 25 mM to 1000 mM β OHB. Then for the no effect studies that included both AcAc and β OHB, the concentration ranges for AcAc included 0.5 mM, 1 mM, 2 mM, 5 mM, and 10 mM and for β OHB the concentration ranges spanned from 2.5 mM to 10 mM (Supplementary Tables 7.12 and 7.15).

For the no effect studies that used only β OHB, there were seven different timepoints recorded. Cells were cultured in β OHB for a duration of 2 mins, 4 hr, between 18 and 24 hr, between 24 and 144 hr, for 96 hr, for 720 hr and one study cultured their cell line in β OHB for 10 mins and for 24, 48, 72, 96 and 120, 144 and 192 hr. For the two no effect studies that used both AcAc and β OHB, cells were cultured with both ketone bodies for 1 hr and 96 hr (Supplementary Tables 7.12 and 7.15).

3.3.9 Relationship with Other Media Components

For the studies that described a beneficial effect of ketones on cell growth, there were other substances that were in the culture media also (Supplementary Table 7.16). These other media components included monomethyl succinate (MMS), 10 mM rotenone, amyloid beta ($A\beta$), metformin, ERK inhibitors, GSK3 inhibitors, lipopolysaccharide, 6 hydroxydopamine (6-OHDA), verapamil, l leucine, cisplatin, tunicamycin, tamoxifen or arsenic trioxide.

For the studies that described no effect, there were also some other substances in the culture media with the ketone bodies. In some studies, the ketone was given with a radioactive isotope label, β OHB was given with the enzyme $A\beta$ peptide binding alcohol dehydrogenase (ABAD).

Within the studies that detailed a negative effect of ketones on cell growth, the ketone bodies were also administered with substances such as LPS, chromium niacinate (chromium III), N-acetylcysteine, nutlin and doxorubicin.

3.4 Discussion

To date, there has been no detailed review of the existing *in vitro* literature in systematically examining the impact of ketone bodies on cell growth and health. The purpose of this review was to provide a comprehensive and thorough review of the reported effects of ketones on cell lines and to summarize the proposed mechanisms of how ketones can impose a positive and negative effect or have no effect on cells and to highlight possible confounders behind conflicting results.

A total of 63 articles reporting either a beneficial, detrimental, or no effect of ketone bodies on cell growth were identified and summarized. 32 articles (51% of all studies) described a beneficial effect of ketones on cell growth and health, while 22 articles (35% of all studies) described a negative effect on cells and the remaining 9 articles (14% of all studies) described ketones that imposed no effect on the cell lines.

Notably in the studies that described a beneficial effect of ketones on cell growth, human cell lines were the most frequently used cell line (56% of positive ketone effect studies). Out of the seven different tissue types of cell lines, the most frequent type of cell line used within this species was a neuronal cell line (with 41% of all human cell lines used being a neuronal cell line) (Findlay et al., 2015a, Imamura et al., 2006, Kabiraj et al., 2012, Lamichhane et al., 2017b, Li et al., 2020b, Maurer et al., 2011a, Zhang et al., 2018a, Zhang et al., 2017). The ketone bodies used in these studies brought about positive effects to the cell by producing energy by catabolizing the reversible transfer of CoA from succinyl-CoA to AcAc and by increasing the availability of acetyl CoA to the TCA cycle (Maurer et al., 2011b, Findlay et al., 2015a), induced neuroprotection against glucose deficiency by mediating ERK activation (Lamichhane et al., 2017a), ameliorated A β induced down regulation of cell viability through lowering histone deacetylase (HDAC) 1 and HDAC 3 expression (Li et al., 2020b). Ketone bodies protected SH-SY5Y cells against rotenone exposure by inhibition of flavoprotein reduction at complex I and complex II by supplying cytosolic and mitochondrial free NADH (Imamura et al., 2006, Zhang et al., 2017, Kabiraj et al., 2012), and protected cells via the anti-oxidation pathway (Zhang et al., 2018b).

The concentration of β OHB used in these studies included 8 mM and 10 mM (Lamichhane et al., 2017b, Imamura et al., 2006), 5 mM, 10 mM, 20 mM, 40 mM and 80 mM (Li et al., 2020b), 1 mM (Zhang et al., 2017), 2 mM (Zhang et al., 2018a), 0.0005 mM, 0.001 mM and 0.01 mM (Findlay et al., 2015a) 5 mM (Maurer et al., 2011a) and 0.1 mM (Kabiraj et al., 2012). Four of these studies failed to specify as to whether or not they included glucose, pyruvate and glutamine (Imamura et al., 2006, Li et al., 2020b, Zhang et al., 2018a, Kabiraj et al., 2012), whereas two of these studies included both glucose and glutamine in their culture media but did not include pyruvate (Findlay et al., 2015a, Maurer et al., 2011a), the remaining two studies included glucose in their growth medium but did not specify whether or not pyruvate and glutamine were included in their growth medium (Lamichhane et al., 2017b, Zhang and Xie, 2017).

The next common species of cell line used in the studies that found a beneficial effect were mouse cell lines (21% of all positive ketone studies) and here the most frequently used types of cell lines were the neuronal cell lines (55% of all mouse lines were of a neuronal tissue type) (Kweon et al., 2004, Liu et al., 2019a, Patel et al., 1981, Wang et al., 2016, Xu et al., 2011). Ketone bodies caused a positive effect in neuronal cell growth and health in the mouse cell lines by protecting neurons against MPTP induced toxicity and by inhibiting microglial ROS and nitrogen monoxide production (Xu et al., 2011), β OHB caused a

significant reduction in rotenone induced toxicity by increasing the cells energy state (Kweon et al., 2004). β OHB upregulated a number of genes by increasing histone acetylation (Liu et al., 2019b) and increased autophagy in cancer cells and by repressing mTOR activation (Wang et al., 2017). β OHB increased the activity of CoA transferase in NB cells (Patel et al., 1981).

The concentrations for the ketones used included 0.0005 mM, 0.001 mM, and 0.01 mM (Liu et al., 2019b), 2 mM, 4 mM, 8 mM and 10 mM (Wang et al., 2016), 0.5 mM and 2.5 mM (Patel et al., 1981), 4 mM (Xu et al., 2011) and 4 and 8 mM (Kweon et al., 2004). Two of these studies did not include glucose in the culture media and did not specify whether pyruvate and glutamine were included in the media (Kweon et al., 2004, Liu et al., 2019b). Two of these studies did not specify whether glucose or pyruvate or glutamine were included in the media (Wang et al., 2016, Xu et al., 2011) and one study did include glucose and glutamine in their media (Patel et al., 1981).

Similarly, and contradicting and conflicting with the positive studies, out of the studies that found a negative effect of ketones on cell growth, human cell lines were the most frequently used species of cell lines (44% of all negative ketone studies) and out of the 11 different tissue types used from this species, the most commonly used tissue type was a neuronal cell line (with 20% of all human cell lines being a neuronal cell line) (Ji et al., 2020, Skinner et al., 2009, Vallejo et al., 2020).

In these studies, ketone bodies caused negative effects in the cell by inhibiting proliferation & glycolysis, promoting apoptosis through mitochondrial damage and increased ROS production (Ji et al., 2020). AcAc increased ROS levels, decreased ATP levels and triggered apoptosis (Vallejo et al., 2020), both AcAc and β OHB increased the rate of apoptosis through increased ROS production from ketone metabolism and NB cells inability to detoxify ROS (Skinner et al., 2009).

The concentration of β OHB used in these studies included ranges from 1 mM, 5 mM, 10 mM and 20 mM (Ji et al., 2020, Vallejo et al., 2020) and concentrations such as 54 mM and 98 mM for both AcAc and β OHB were used (Skinner et al., 2009). When looking at the media formulations of these three studies, two of these studies included glucose in their culture medium but failed to specify whether or not pyruvate and glutamine were included in their media (Ji et al., 2020, Skinner et al., 2009) and the remaining study did not specify as to whether glucose, pyruvate or glutamine were included in their growth medium (Vallejo et al., 2020).

The second most common species of cell lines used that found a negative effect of ketones on cell growth were of a mouse origin where (17% of all negative ketone studies) and the most frequently used cell line used was a neuronal cell line (56% of all mouse cell lines) (D'Alessandro et al., 2011, Ji et al., 2020, Poff et al., 2014).

β OHB exerted a negative influence in these studies through acting on GSH homeostasis regulation (D'Alessandro et al., 2011), decreased proliferation and viability in cells due to the a lack of necessary enzymes such as SCOT (Poff et al., 2014) and inhibited the proliferation of glia like stem cells (GSCs) through metabolic imbalance, which in turn caused oxidative stress and induced apoptosis (Ji et al., 2020). The concentrations of β OHB used in the studies include ranges of 1 mM, 5 mM, and 10 mM (D'Alessandro et al., 2011, Ji et al., 2020, Poff et al., 2014). Two of these studies supplemented their growth media with glucose and pyruvate (D'Alessandro et al., 2011, Poff et al., 2014) and one study supplemented their culture media with glucose but did not specify as to whether glucose or pyruvate were included in the culture media (Ji et al., 2020).

From this review it's evident that most of the studies detailed above have not provided sufficient information in relation to the growth media their cell lines were cultured in. If we look at the data from Supplementary Table 7.11, we can see that most studies do not specify whether they included, glucose, pyruvate, and glutamine in their culturing medium and their concentration. 53% of the studies that described a beneficial effect of ketones of cell growth did not specify as to whether glucose was included in the growth medium or not, 50% of studies that found a negative effect with ketones on cell growth also failed to specify whether glucose was included or not as did 22% of the studies that found an equivocal effect of ketones on cell growth.

84% of studies that found a beneficial effect of ketones of cell growth did not specify as to whether pyruvate was in the media. Similarly, 77% of these studies did not specify whether pyruvate was included in the negative studies. For the studies that found no effect of ketones on cell growth, 67% of studies did not specify whether pyruvate was included in the culture media. 78% of the studies that found a beneficial ketone effect did not specify whether glutamine was included. 55% of studies that found a negative effect of ketone on cell growth did not specify if they included it in the growth media and 56% of the studies that found ketones had an no effect on cell growth did not specify if it was included or not.

3.5 Conclusion

This systematic review showed that an understanding of growth medium constituents and concentrations are fundamental to the impact ketones may have on cell growth and health. For a more thorough understanding of what is occurring at the metabolic level and how cells are using each energy substrate, we would propose that any future study involving ketone bodies as an energy source that they provide the exact media formulations use to culture their cells in. This would include detailing exactly whether the energy substrates such as glucose, pyruvate and glutamine were included in the growth media and at exactly what concentration. This would allow greater transparency and understanding as to what fuels are being used at the metabolic level of the cell and importantly this would allow greater reproducibility and would allow investigators to accurately identify where ketone bodies produce either a beneficial or negative effect on cell lines.

From the data gathered from the literature above, undertaking experiments using both human and murine neuronal cell lines and investigating the impact of removing growth substrates such as glucose, pyruvate and glutamine and supplementing the culture media with β OHB could provide a deeper and greater insight into its role in cell metabolic health and growth.

Chapter 4

The Impact of Glucose, Glucose Deprivation & Ketone Supplementation on Brain Cell Growth

4.1 Introduction

From the systematic review of the existing *in vitro* literature in Chapter 3, various human and rodent and cell lines have outlined β OHB as the most frequently used ketone body in the studies that described either beneficial or detrimental effects to cell growth. From the systematic review, it was deduced that human and mouse cell lines are the most frequently used species for cell lines when investigating the impact of ketone bodies on cell growth. The most common type of cell type where β OHB exerted a beneficial impact was in a neuronal cell line and out of these neuronal cell lines, the SH-SY5Y cell line was the, most routinely used (Table 3.1 of Chapter 3). From the data gathered in Chapter 3, the SH-SY5Y human NB cell line and the NE-4C mouse NSC lines were chosen to use for investigating the effects of glucose deprivation and ketone supplementation on brain cell growth.

The SH-SY5Y cell line is a subclone of a bone marrow biopsy derived line of a SK-N-SH from paediatric NB. The NB cell is commonly used in neuronal development and signalling studies and in experimental models of NB (Xie et al., 2015). It originates from developing sympathoadrenal progenitor cells derived from the neural crest and lesions form predominantly in the adrenal cortex and paraspinal ganglia (Brodeur, 2003). NB is the most common extracranial solid tumour in children and the most commonly diagnosed cancer in the first year of life (Matthay et al., 2016). NB prognosis includes a highly aggressive and metastatic malignancy, or a unique propensity for spontaneous resolution and differentiation (Brodeur and Bagatell, 2014). The latter transformation into a benign subtype is cytologically distinguishable by longer neuronal processes among other features characterising a mature morphological appearance (Kwiatkowski et al., 1998).

NE-4C cells are cloned from the anterior brain vesicles of 9-day-old p53 deficient mouse embryos (Livingstone et al., 1992, Schlett et al., 1997). NE-4C cells continuously proliferate at a high rate and in environments favoring neural tissue type differentiation, they can differentiate into mature neurons displaying morphological, biochemical, and bioelectric characteristics (Jelitai et al., 2004, Jelitai et al., 2002).

If implanted into an embryonic brain, they will mature into neurons and integrate into the surrounding neural tissue, yet in a fully grown adult mouse brain, their ability to migrate is hampered and they only survived in regions where active neurogenesis was occurring (Demeter et al., 2004). Even though there was no mention of this cell line in the systematic review, NE-4C cells seemed an appropriate second cell line to use to investigate the impact of glucose deprivation and ketone supplementation on NSC growth due to their neoplastic origin and because it's a neuronal cell line that originated from a mouse.

From the systematic review, it's evident that β OHB has provided beneficial and positive effects to SH-SY5Y cells. β OHB protected the cells against glucose deficiency induced apoptosis through ERK activation (Lamichhane et al., 2017a), protected cells from rotenone induced exposure by supplying cytosolic and mitochondrial free NADH to complex I and complex II (Imamura et al., 2006), prevented BACE1 activity dependent deficit in glucose oxidation (Findlay et al., 2015a), protected cell against A β through the anti-oxidation pathway (Zhang et al., 2018b). β OHB also improved cell viability and prevented a reduction in TrkA expression induced by A β (Li et al., 2020b) and had a prophylactic effect against nitrosative-stress related apoptotic cell death in SH-SY5Y cells (Kabiraj et al., 2012). From the systematic review, the most frequently used concentrations of β OHB that provided a beneficial effect in all neuronal cell lines were 4 mM and 10 mM β OHB (Kabiraj et al., 2012, Kweon et al., 2004, Lamichhane et al., 2017b, Liu et al., 2019a). Conflictingly, the most common concentration of β OHB that was detrimental to neuronal health was 5 mM and 10 mM (D'Alessandro et al., 2011, Ji et al., 2020, Vallejo et al., 2020).

The use of SH-SY5Y and NE-4C cells in this study, given their mutual neoplastic and neuronal origin and their use in both fields and in a diverse set of experiments may help to bridge some of the observations in cancer and neuronal development. Importantly, a key parallel in the metabolism of both cancer and developing neuronal cells is their high proliferation rates and reliance on aerobic glycolysis. Using SH-SY5Y and NE-4C cells, this study attempts to shed light on the impact of varying concentrations of β OHB on NB and NSC growth *in vitro* and to determine the optimum ketone concentration to use for further investigations. We investigated the impact of glucose deprivation and ketone supplementation on cell differentiation, growth, mitochondrial cytotoxicity, proliferation, and viability.

In the present study, we investigated the impact of glucose, glucose deprivation and different concentrations of ketone supplementation on the growth the maturation of the NE-4C and the SH-SY5Y cell lines by measuring cell density, cell differentiation, mitochondrial cytotoxicity, proliferation, and viability as indicators of cell health and function.

4.1.2 Aims

- 4.1.2.1 To investigate the impact of glucose deprivation on SH-SY5Y and NE-4C cell growth over 120 and 168 hrs.
- 4.1.2.2 To investigate the impact of different concentrations of β OHB on SH-SY5Y and NE-4C cells over 120 and 168 hrs.
- 4.1.2.3 To investigate the impact of different concentrations of β OHB on SH-SY5Y mitochondrial cytotoxicity at 72 hrs and 144 hrs.
- 4.1.2.4 To investigate the viability of SH-SY5Y cells in glucose deprived conditions and in the presence of different concentrations of β OHB.
- 4.1.2.5 To investigate the growth of SH-SY5Y cell differentiation in the absence of glucose and in the presence of β OHB over 72, 120 and 168 hrs.

4.1.3 Hypothesis

4.1.3.1 As growing brain cells depend on glucose for growth and survival, the deprivation of this fuel source will be detrimental to cell proliferation, viability, and growth. As the existing literature is ambiguous in answering whether ketone bodies positively impact cell growth, testing different concentrations of β OHB on cell growth will provide us with a clearer insight into which concentration will produce these positive effects.

4.2 Methods

4.2.1 Cell lines and General Culture Conditions

The NE-4C mouse NSC and SH-SY5Y human NB cell lines were recovered and subcultured in the same manner as described in the general methods in Chapter 2. This allowed the necessary volume of cell solution to be calculated for SH-SY5Y and NE-4C cells to be cultured at density of 5×10^4 and 2×10^4 cells per well in the six well plate proliferation and differentiation experiments and at a density of 5×10^3 cells per well in the 96 well plate cell viability and mitochondrial cytotoxicity assays for the SH-SY5Y cells.

Cells were seeded in poly-L-lysine coated six well plates with six different media groups which included RG, GF, 1 mM, 5 mM, 10 mM, and 50 mM β OHB. These same media groups were used for the mitochondrial cytotoxicity assay and the viability assay (where LG was added). For the differentiation experiments cells were seeded in three different medium groups which included RG, GF, and 10 mM β OHB for the proliferation experiments. The compositions mentioned above are outlined in the general methods section of Chapter 2. All procedures were carried out in the same aseptic manner as described in previously with minimal exposure to light.

4.2.2 Experimental Design for Chapter 4

To assess the effects of glucose deprivation in the first experiments, SH-SY5Y cells were cultured in regular glucose RG and GF conditions over 48 and 120 hrs. The effects of ketone supplementation were initially investigated in the second set of experiments with RG and the addition of 1 mM, 5 mM, 10 mM, and 50 mM concentrations of β OHB to the GF over 48, 72, 96 and 120 hrs for SH-SY5Y cells. The subsequent third set of experiments used the same media groups as the second experiment when investigating mitochondrial cytotoxicity over 72 and 144 hrs. In the fourth experiment, cell viability was investigated using an MTT assay using the media groups RG, LG, GF, 1 mM, 5 mM, 10 mM, and 50 mM β OHB. In the final experiment, the impact of glucose deprivation and ketone supplementation on SH-SY5Y differentiation was investigated using the RG, GF, and 10 mM β OHB media groups at 72, 120 and 168 hrs (see Table 4.1 for a summary of the experimental media groups).

In the NE-4C cell, cells were grown in RG and GF conditions over 48 and 120 hrs in the first experiment. In the second experiment, the impact of ketone supplementation on cell density in a glucose deprived environment was investigated using GF, 1 mM, 5 mM, 10 mM, and 50 mM β OHB over 48, 72, 96, 120 and 168 hrs (Table 4.2).

| Experiment 1 | Experiment 2 | Experiment 3 | Experiment 4 | Experiment 5 |
|--------------|---------------------|---------------------|---------------------|---------------------|
| RG | RG | RG | RG | RG |
| GF | GF | GF | LG | GF |
| | + 1 mM β OHB | + 1 mM β OHB | GF | + 10 mM β OHB |
| | + 5 mM β OHB | + 5 mM β OHB | + 1 mM β OHB | |
| | + 10 mM β OHB | + 10 mM β OHB | + 5 mM β OHB | |
| | + 50 mM β OHB | + 50 mM β OHB | + 10 mM β OHB | |
| | | | + 50 mM β OHB | |

Table 4.1 A summary of the media groups in each SH-SY5Y experiment

| Experiment 1 | Experiment 2 |
|--------------|---------------------|
| RG | GF |
| GF | + 1 mM β OHB |
| | + 5 mM β OHB |
| | + 10 mM β OHB |
| | + 50 mM β OHB |

Table 4.2 A summary of the media groups in each NE-4C experiment

4.2.3 Experiments undertaken

4.2.3.1 Cell Viability

MTT assays were performed to assess cell viability for 96 hrs. MTT was added to cells at a concentration of 0.5 mg/mL in the culture medium and incubated for 3 hr and 30 minutes. The culture medium was removed, and the cells were lysed in DMSO. The plate was put on a plate rocker for 5 mins to ensure the precipitated formazan crystals were completely solubilized. Colorimetric absorbance was measured at a wavelength 562 nm using an Epoch microplate reader.

4.2.3.2 Immunocytochemistry

Cultures were fixed 4% PFA in PBS for 15 min at RT. To assess cells undergoing proliferation and differentiation, cells were incubated with 5% NGS blocking solution in 0.05% PBS-T for 1 hr and were stained with BrdU and NeuN overnight at 4°C. To assess cell density, cell size and nuclear size, cells were permeabilized and stained with DAPI (1:5000) and actin (2 drops per ml) along with the FITC secondary in 0.05% PBS-T for 1 hr at RT. Following this, cells underwent 3 x 5-min 1X PBS washes. After this incubation, cells were washed in 1X PBS.

To assess mitochondrial cytotoxicity, cells were stained with image-IT and Hoescht. A summary of the fluorescent imaging-based parameters and their method of quantification in this study is shown in Table 4.2 below.

4.2.3.3 Imaging and Analysis

Cells were imaged using an Olympus IX81 motorized epifluorescent microscope using CellSens Dimension software (version 2.8). ImageJ/Fiji was subsequently used for processing and analysis. Data is presented as the mean \pm the SEM. The assumption of normality was verified using QQ plots of the residual errors. Statistical analysis and graphs were generated using GraphPad prism version 9.5 (Graphpad Software, CA USA). Statistical differences in the data were analysed using one-way or two-way ANOVA as appropriate with a post hoc Bonferroni correction to reveal the differences between the groups. P-values ≤ 0.05 were considered statistically significant.

| Image-Based Assay | Method |
|----------------------------|--|
| BrdU Assay | BrdU as an indicator of proliferating cells was added to the cultured plates for 4 hr prior to fixation and labelling. Cells were washed in PBS and non-specific binding was prevented by incubation in normal goat serum for 40 min. Primary anti-BrdU antibody (Sigma,UK) was then added to the cells for 2 hr before incubating in the FITC secondary overnight at 4°C. Proliferative activity here was taken as the percentage of cells expressing green fluorescence. |
| Cell Density | Whole-well images were taken of the DAPI stained nuclei and density was measured as the percentage of the well covered by the nuclei (Detailed in section 3.6 below). |
| Cell Differentiation | NeuN as an indicator of differentiating cells was added to the culture plates. Cells were washed in PBS and non-specific binding was prevented by incubation in normal goat serum for 40 mins. Anti-NeuN was then added overnight before incubating with secondary for 2 hr at 4°C. Differentiation activity was taken as the percentage of cells expressing green fluorescence. Differentiation was investigated over 48, 72 and 168 hrs. |
| Cell Proliferation | As above for cell density in independent plates cultured over four timepoints: 48, 72, 96 and 120 hr to obtain a pattern of proliferation over time. |
| Mitochondrial Cytotoxicity | The staining solution comprised of FITC Image-IT (green indicating mitochondrial cytotoxicity) and Hoescht (identifying the nuclei of each cell). The parameter was quantified as a percentage of the total number of cells in an image. |

Table 4.3 A summary of the image-based assays

4.3 Results

4.3.1 SH-SY5Y Cell Density, Morphology, and Viability

Cell densities, morphology and viability between the RG and GF groups (Fig 4.1) and the β OHB conditions (Fig 4.2) over 120 hr were compared. Cells showed large cell bodies with multiple processes extending from the soma (Fig 4.3). An overall effect of time ($F=16.2$, $p=0.0038$) was observed for SH-SY5Y cell density between 48 hr and 120 hr. There was no significant growth medium effect or interaction effect between RG and GF. Within time, post hoc testing revealed that SH-SY5Y cell density was significantly higher at 120 hr ($t=4$, $p=0.0084$), yet there was no significant effect in the GF conditions between 48 hr and 120 hr (see Fig 4.1)

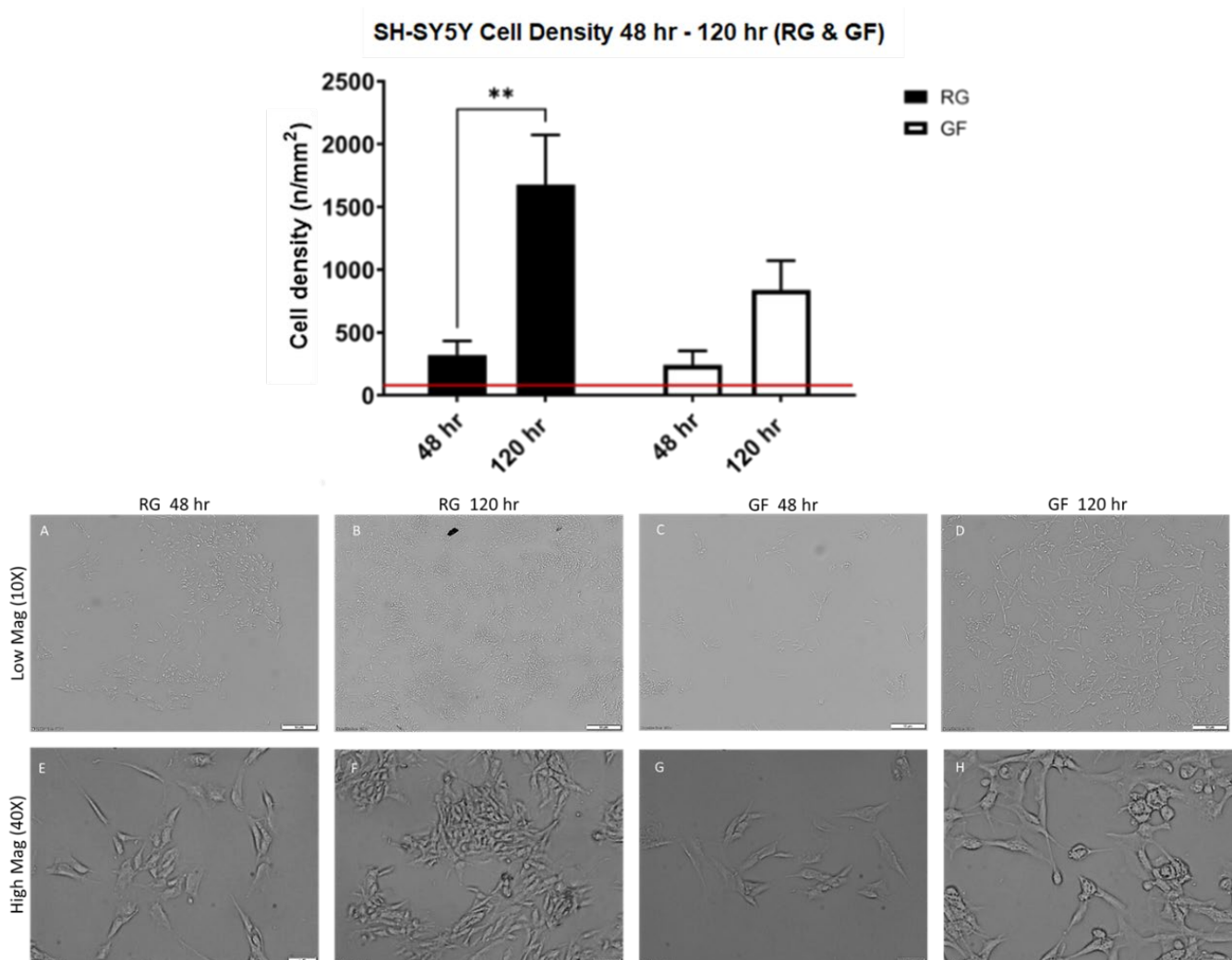


Figure 4.1 Cell density at 48 and 120 hr in RG and GF. Brightfield images of SH-SY5Y in RG and GF at low mag (10X) and high mag (40X). The red bar indicates cell density per mm² (52.08 cells per mm²). Scale bar in low mag images at 10 μ m. Scale bar in high mag images at 40 μ m Two – way anova with Bonferroni Multiple Comparisons test, Mean \pm SEM; **P < 0.01; N = 3

Cell density was assessed in the ketone supplemented groups at the same time-points and compared. An overall effect of time ($F=31.2$, $p<0.0001$) and growth medium ($F=2.8$, $p=0.037$) was observed for SH-SY5Y cell density. No significant interaction effect between time and growth medium was observed. Within media, post hoc testing revealed no significant effects between medium conditions at 48 hr. SH-SY5Y cell density was significantly less comparing 1 mM β OHB ($t=3.6$, $p=0.024$), 5 mM β OHB ($t=4.3$, $p=0.0033$) and 50 mM β OHB ($t=4.0$, $p=0.072$) media to the RG medium at 120 hr. Within time, SH-SY5Y cell density was significantly higher in RG conditions ($p=5.2$, $p=0.0002$) at 120 hr when compared to 48 hr.

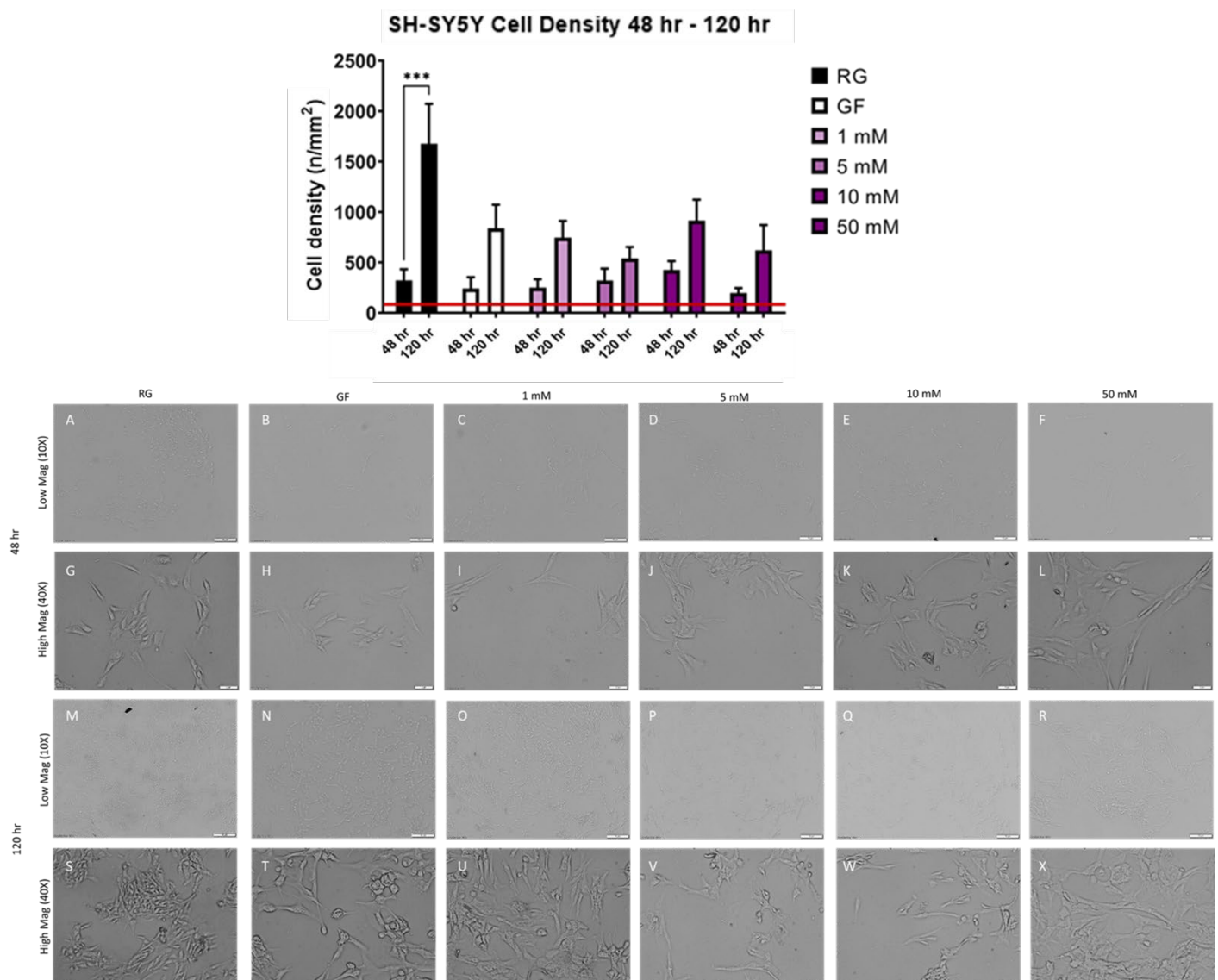


Figure 4.2 Cell density at 48 and 120 hr in RG, GF, 1 mM β OHB, 5 mM β OHB, 10 mM β OHB and 50 mM β OHB. Brightfield images of SH-SY5Y in RG and GF at low mag 10X and high mag 40X at 48 and 120 hr. The red bar indicates cell density per mm² (52.08 cells per mm²). Scale bar in low mag images at 10 μ m. Scale bar in high mag images at 40 μ m. Two – way anova with Bonferroni Multiple Comparisons test, Mean \pm SEM; * $P < 0.05$, ** $P < 0.01$; N = 3

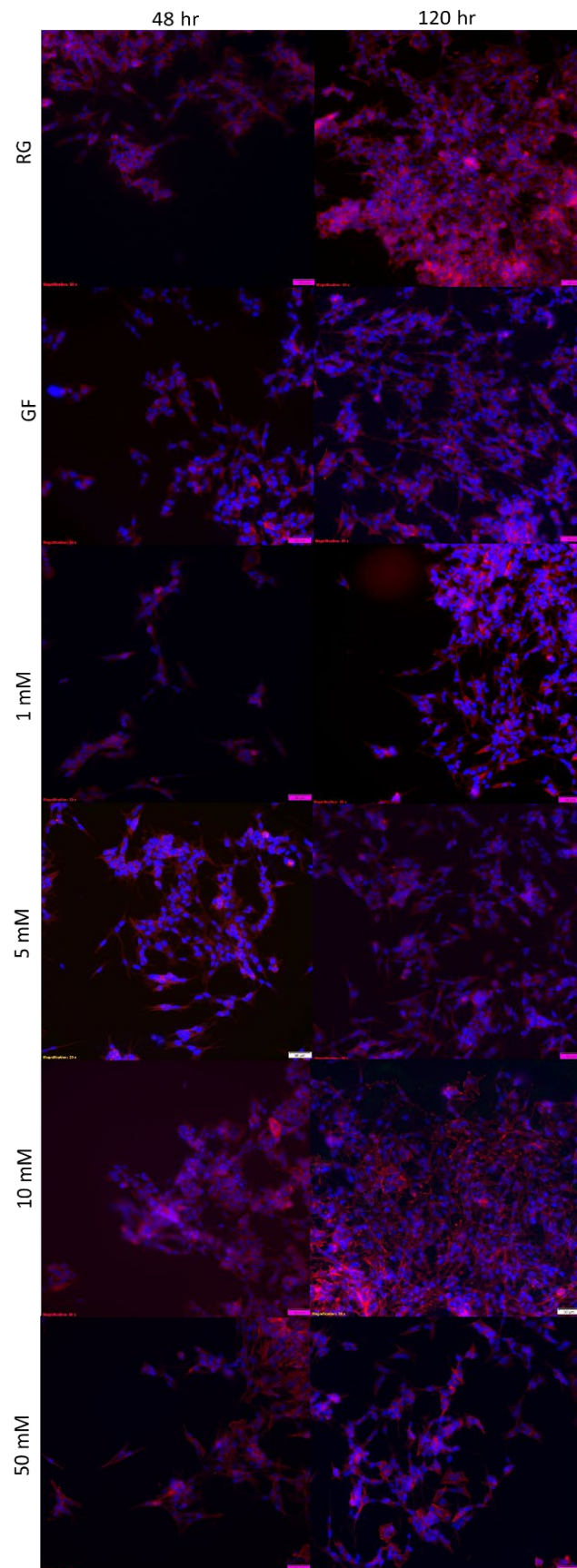


Figure 4.3 Actin expression at 48 hrs and 120 hrs in RG, GF, 1 mM β OHB, 5 mM β OHB, 10 mM β OHB and 50 mM β OHB. Red labelling shows actin staining (labelling the cytoskeleton) and blue staining shows DAPI labelling. Scale bar at 50 μ m.

4.3.2 SH-SY5Y Proliferation in Glucose and Glucose Deficient Conditions Over 120 hr

At 48 hr, 72 hr, 96 hr and 120 hr cell densities were measured to determine rates of proliferation in RG, GF and β OHB groups. No overall effect of time, growth medium and interaction was observed for BrdU expression between RG and GF conditions and in β OHB supplemented conditions between 48 hr and 120 hr (Fig 4.4 to Fig 4.5). No post hoc testing was performed.

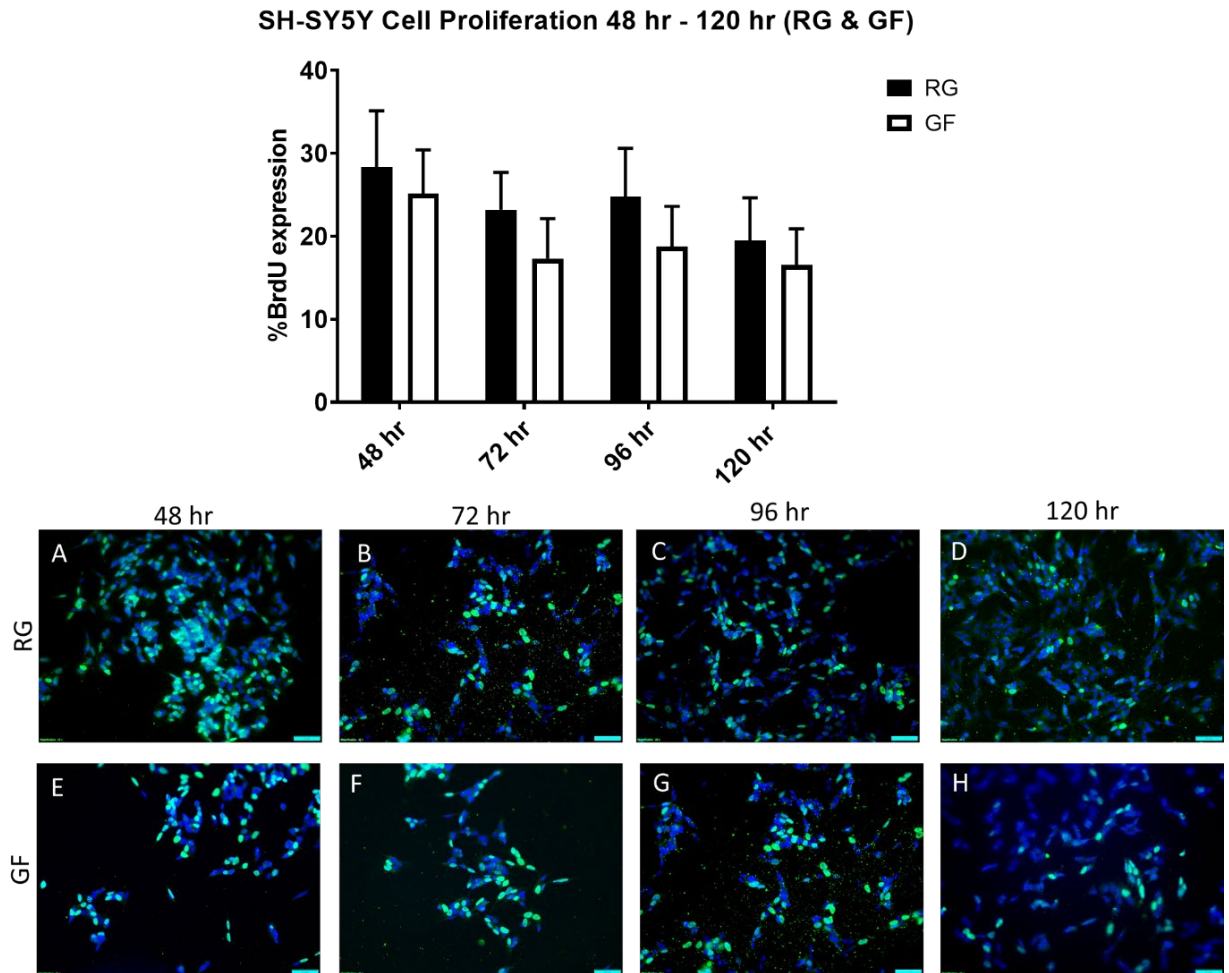


Figure 4.4 Cell proliferation at 48, 72, 96 and 120 hr, in RG and GF. Green labelling shows proliferating cells and blue staining indicates DAPI labelling. Scale 50 μ m. Two – way anova, Mean \pm SEM. N = 3

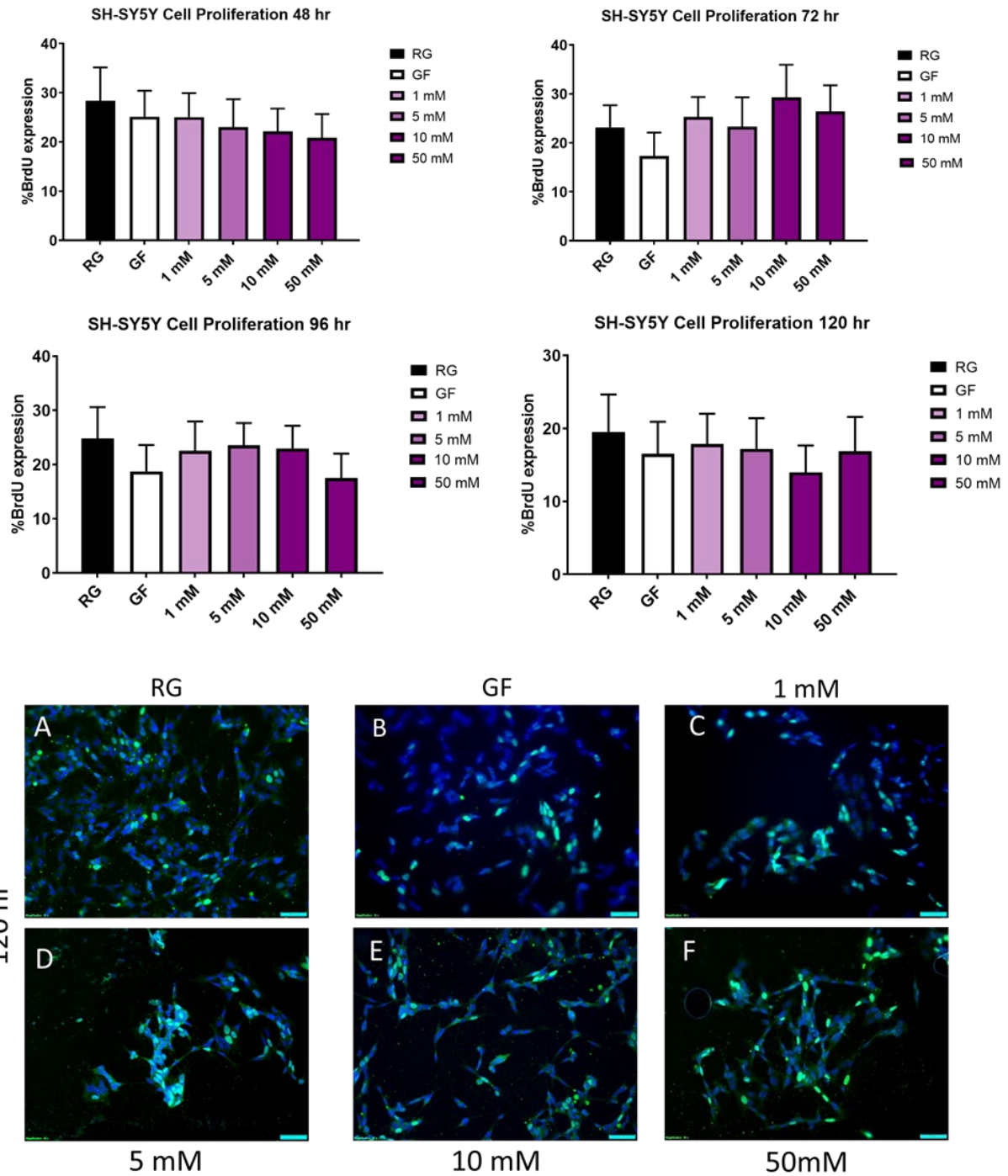


Figure 4.5 Cell proliferation at 48, 72, 96 and 120 hr, in RG, GF, 1 mM β OHB, 5 mM β OHB, 10 mM β OHB and 50 mM β OHB. Green labelling shows proliferating cells and blue staining indicates DAPI labelling. Scale 50 μ m. One-way Anova, Mean \pm SEM. N = 3.

4.3.3 SH–SY5Y Cytotoxicity & Viability

Between 72 hr and 144 hr mitochondrial cytotoxicity was investigated using RG, GF, 1 mM β OHB, 5 mM β OHB, 10 mM β OHB and 50 mM β OHB media at 72 hr and 144 hr. An overall effect of time ($F=24.3$, $p<0.0001$) and growth medium ($F=9.6$, $p<0.0001$) was observed for mitochondrial cytotoxicity in SH-SY5Y cells. No significant interaction effect between growth medium and time was observed.

Within media groups, post hoc testing revealed mitochondrial cytotoxicity was significantly higher comparing GF ($t=6.4$, $p<0.0001$), 1 mM β OHB ($t=4.0$, $p=0.0019$) and 50 mM β OHB ($t=5.8$, $p<0.0001$) to RG medium at 144 hr. Mitochondrial cytotoxicity was significantly less comparing 5 mM β OHB ($t=5.3$, $p<0.0001$) and 10 mM β OHB ($t=3.7$, $p=0.0049$) to GF medium at 144 hr. Mitochondrial cytotoxicity was significantly less comparing 5 mM β OHB ($t=4.8$, $p<0.0001$) and 10 mM β OHB ($t=3.2$, $p=0.0276$) to 50 mM β OHB at 144 hr (Fig. 4.6)

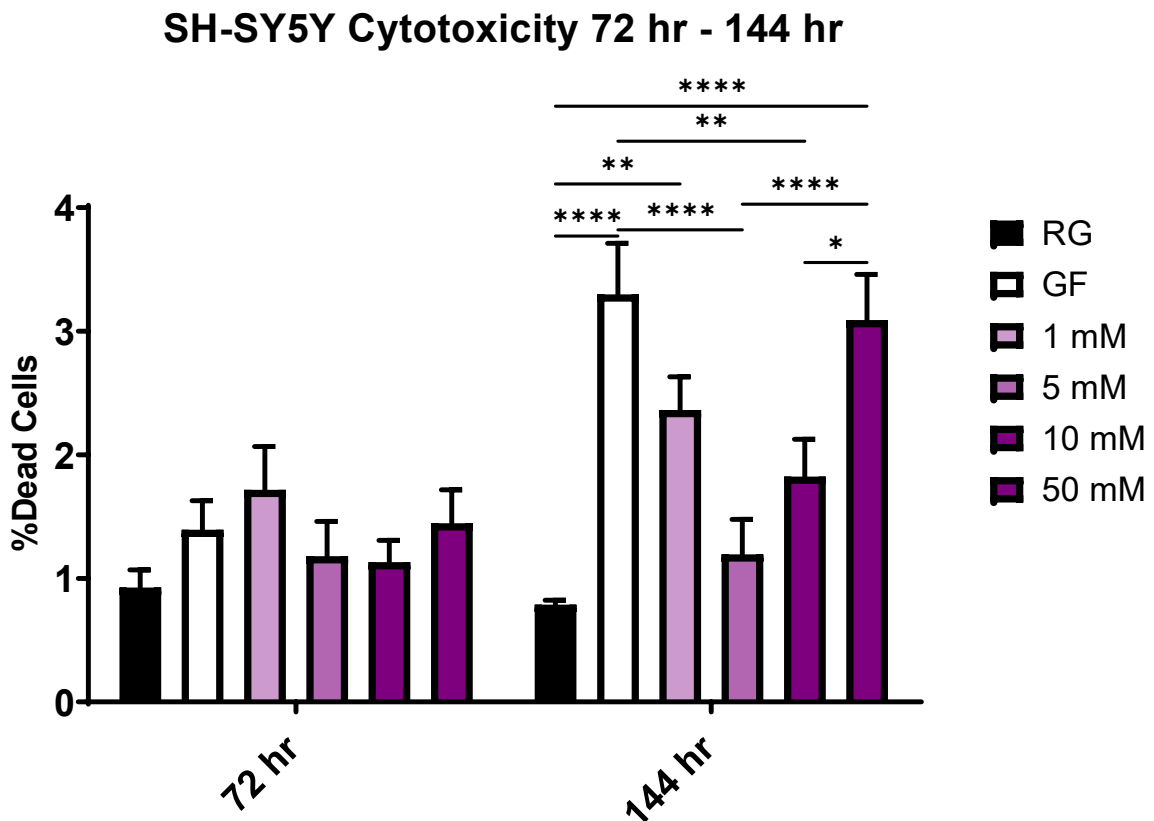


Figure 4.6 Cell cytotoxicity at 72 and 144 hr in RG, GF, 1 mM β OHB, 5 mM β OHB, 10 mM β OHB and 50 mM β OHB. Two – way anova with Bonferroni Multiple Comparisons test, Mean \pm SEM; * $P < 0.05$, ** $P < 0.01$ **** $P < 0.0001$. N = 3

Within time, post hoc testing revealed mitochondrial cytotoxicity was significantly higher in GF ($t=4.8$, $p<0.0001$) and 50 mM β OHB ($t=4.2$, $p=0.004$) at 144 hr when compared to their 48 hr media groups (Fig. 4.7).

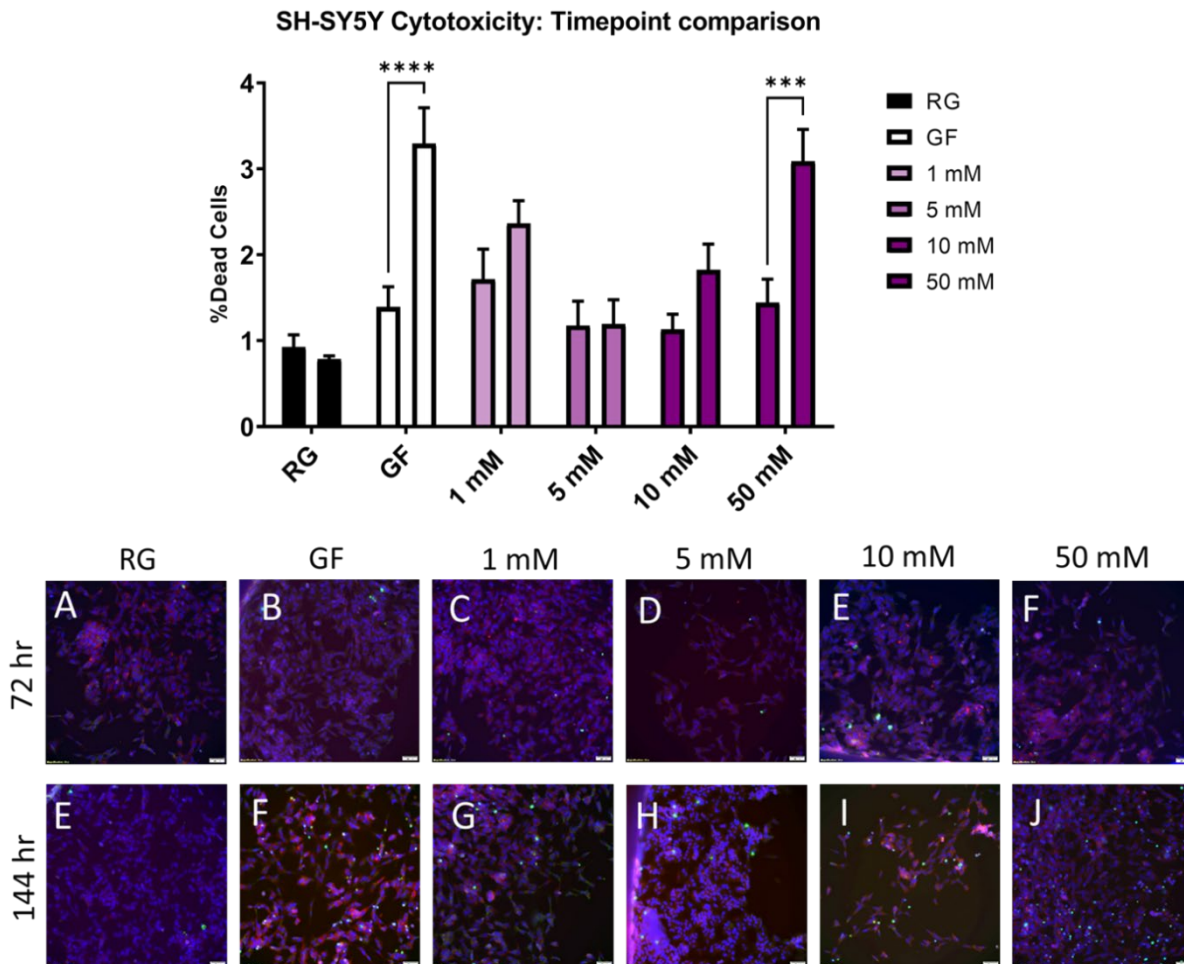


Figure 4.7 Cell cytotoxicity at 72 and 144 hr in RG, GF, 1 mM β OHB, 5 mM β OHB, 10 mM β OHB and 50 mM β OHB. Red staining indicates viable cells. Green staining indicates dead cells. Blue staining indicates DAPI labelling. Two – way anova with Bonferroni Multiple Comparisons test, Mean \pm SEM; *** $P<0.001$, **** $P<0.0001$. N = 3.

4.3.4 MTT Assay

SH-SY5Y cell viability was also assessed using the MTT assay to determine the cytotoxic effects of the β OHB concentrations during SH-SY5Y proliferation. An overall effect of growth medium ($F=13.9$, $p<0.0001$) was observed for SH-SY5Y cell viability at 96 hr. Within the growth media, post hoc testing revealed SH-SY5Y cell viability was significantly less comparing GF ($t=5.1$, $p=0.0031$), 1 mM β OHB ($t=5.5$, $p=0.0015$), 5 mM β OHB ($t=6.4$,

p= 0.0003), 10 mM β OHB (t=6.1, p = 0.0004), 25 mM β OHB (t=6.7, p = 0.0001) and 50 mM β OHB (t=7.0, p=<0.0001) to the RG medium at 96 hr.

Post hoc testing further revealed within the growth media that SH-SY5Y cell viability was significantly less comparing GF (t=3.8, p=0.0431), 1 mM β OHB (t=4.2, p=0.0194), 5 mM β OHB (t=5.1, p=0.0031), 10 mM β OHB (t=4.8, p=0.0052), 25 mM β OHB (t=5.5, p=0.0015) and 50 mM β OHB (t=5.7, p=0.0009) to the LG medium at 96 hr. No significant differences were observed between the GF and β OHB supplemented conditions (Fig. 4.8).

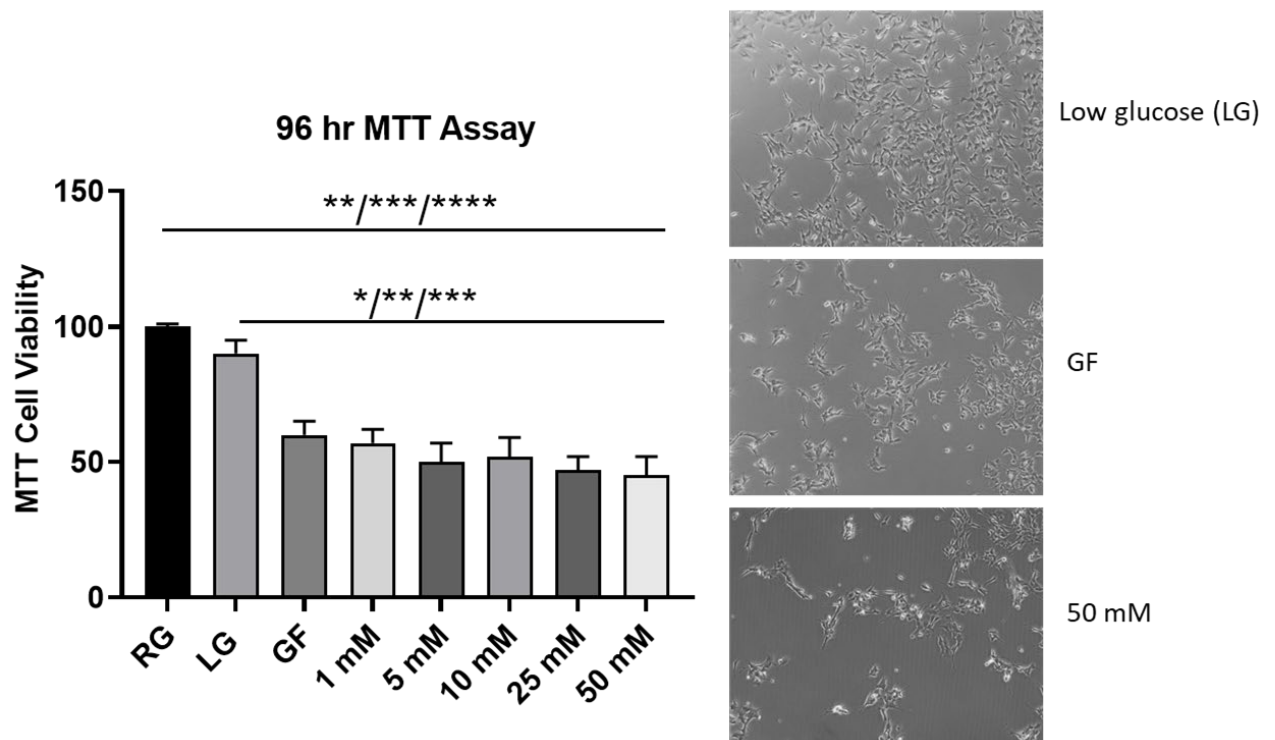


Figure 4.8 Cell viability at 96 hr in RG, LG GF, 1 mM β OHB, 5 mM β OHB, 10 mM β OHB, 25 mM β OHB and 50 mM β OHB. One-way anova with Bonferroni Multiple Comparisons test. Mean \pm SEM; * P < 0.05, **P<0.01, *** P<0.001, ****P<0.0001.

4.3.5 SH-SY5Y Differentiation

To examine cell viability, cultures were grown for 4 days prior to retinoic acid (RA) treatment and bright-field images were captured at 72 hr, 120 hr, and 168 hr post RA differentiation. In the RG, GF, and 10 mM β OHB treatment groups, the cells appeared to elongate and decrease in density with time, showing cell survival and differentiation (Fig 4.9).

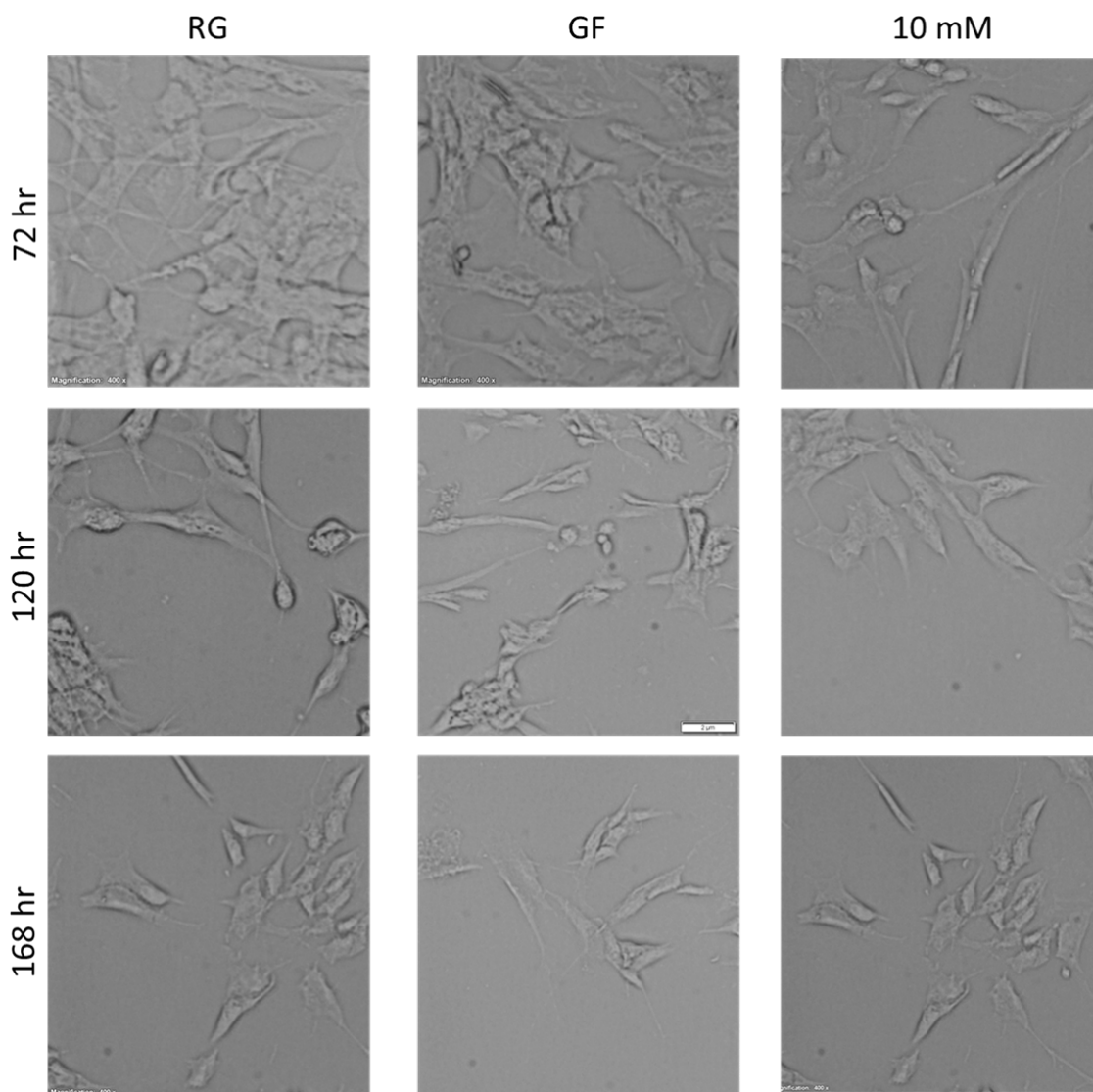


Figure 4.9 Bright-field images of SH-SY5Y cell culture groups, RG, GF, and 10 mM β OHB, at 72 hr, 120 hr, and 168 hr of RA treatment. Scale bar 50 μ m.

4.3.6 SH-SY5Y Cell Density in Glucose, Glucose Deficient Media, and Ketone Supplementation Following RA Differentiation

An overall effect of time ($F=6.2$, $p=0.0092$) and growth medium ($F=19.0$, $p=<0.0001$) was observed in SH-SY5Y cell density following the addition of RA differentiation media. No significant interaction effect between growth medium and time was observed. Post hoc testing time revealed significant differences comparing 72 hr and 120 hr and comparing 72 hr and 120 hr ($t=3.0$, $p=0.0212$ for both comparisons). Post-hoc testing within each media group and comparing time revealed that RG was significantly less comparing 120 hr and 168 hr ($t=3.9$, $p=0.0030$ for both comparisons) to RG conditions at 72 hr.

Post hoc testing within time comparing media conditions revealed SH-SY5Y cell density following differentiation was significantly less comparing GF ($t=5.3$, $p=0.0001$) and 10 mM β OHB ($t=5.0$, $p=0.0003$) to the RG medium at 72 hr (Fig. 4.10). At 120 hr and 168 hr no significant effects were observed between the different media groups.

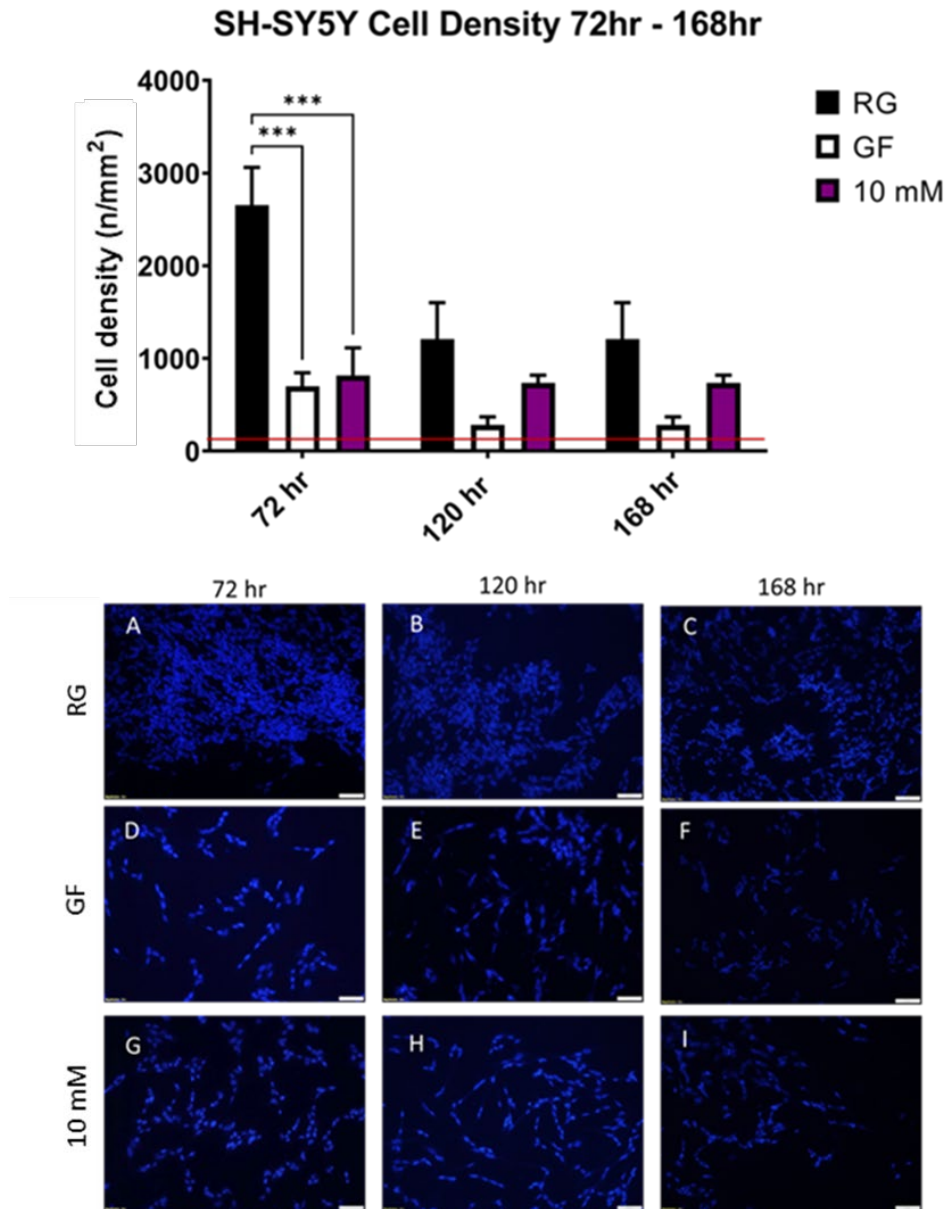


Figure 4.10 Cell density at 72, 120 and 168 hr (post RA differentiation) in RG, GF, and 10 mM β OHB following RA differentiation. Blue labelling indicates DAPI staining. Red bar indicates cell density per mm² (52.08 cells per mm²). Scale bar at 50 μ m. Two – way anova with Bonferroni Multiple Comparisons test, Mean \pm SEM; *** $P<0.001$; N = 3.

4.3.7 SH-SY5Y Proliferation Rates Following RA Differentiation

An overall effect of time ($F=10.2$, $p=0.0077$) and growth medium ($F=14.3$, $p=0.0007$) was observed in the levels of BrdU expressed in SH-SY5Y cells following differentiation. There was no significant interaction effect between time and growth medium. Post hoc testing within time revealed BrdU expression was significantly less comparing 10 mM β OHB ($t=3.2$, $p=0.0248$) at 168 hr to 10 mM at 72 hr. No significant effects were observed between RG and GF between 72 hr and 168 hr. Post hoc testing within time and comparing media conditions revealed BrdU expression levels were significantly less comparing GF ($t=4.5$, $p=0.002$) to the RG medium at 72 hr (Fig. 4.11). No significant difference was observed between 10 mM β OHB and RG medium. However, at 168 hr, there was a significantly lower BrdU expression when comparing both GF ($p=2.9$, $p=0.0408$) and 10 mM β OHB ($t=3.0$, $p=0.0319$) to RG medium (Fig. 4.11).

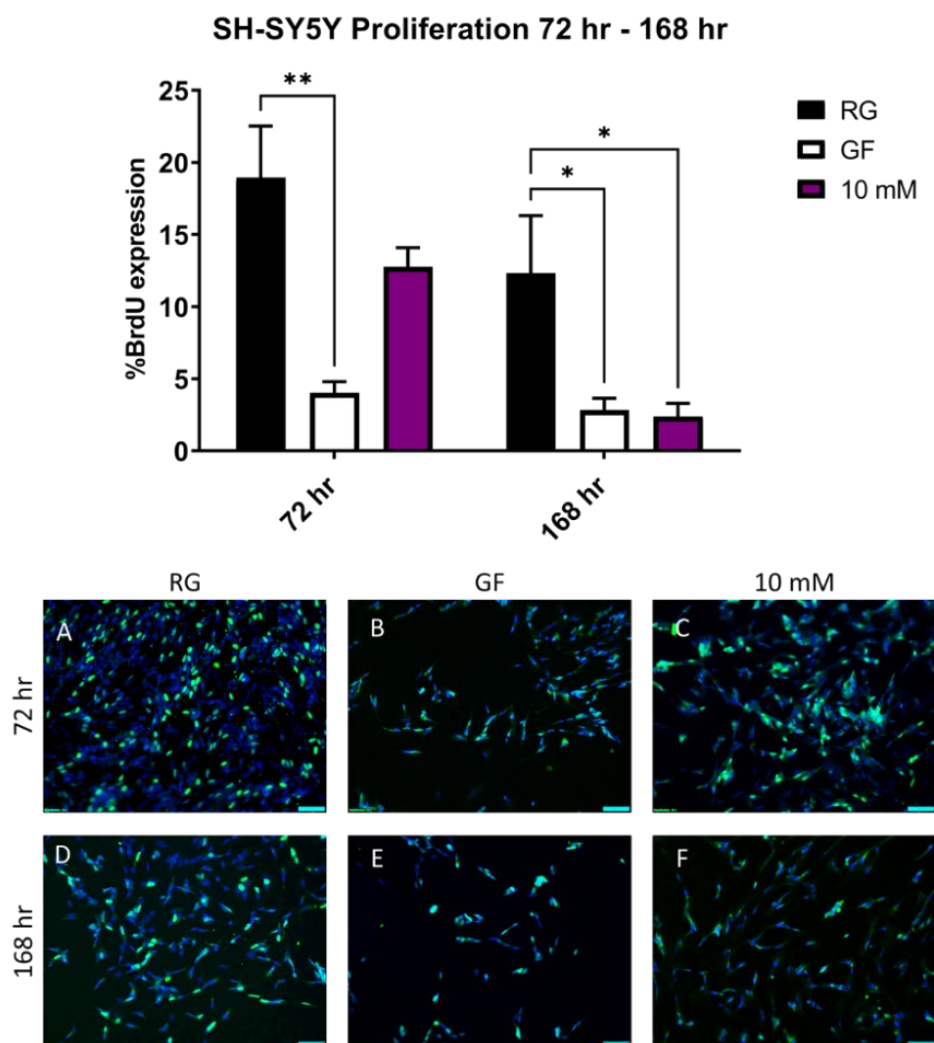


Figure 4.11 Cell proliferation at 72 and 120 hr, in RG and GF and 10 mM β OHB. Green labelling shows proliferating cells and blue staining indicates DAPI labelling. Scale bar at 50 μ m. Two – way anova with Bonferroni Multiple Comparisons test, Mean \pm SEM; * $P < 0.05$, ** $P < 0.01$. N = 3.

4.3.8 SH-SY5Y Differentiation Rates following RA treatment

An overall effect of growth medium ($F=8.9$, $p=0.0042$) was observed for the expression levels of NeuN in SH-SY5Y cells. There was no significant time effect or interaction effect between time and growth medium. Post hoc testing within time comparing media conditions revealed NeuN expression levels were significantly less comparing GF ($t=3.5$, $p=0.0144$) and 10 mM β OHB ($t=3.7$, $p=0.0203$) to the RG medium at 72 hr (Fig. 4.12). No significant differences were observed between the different growth media conditions at 168 hr.

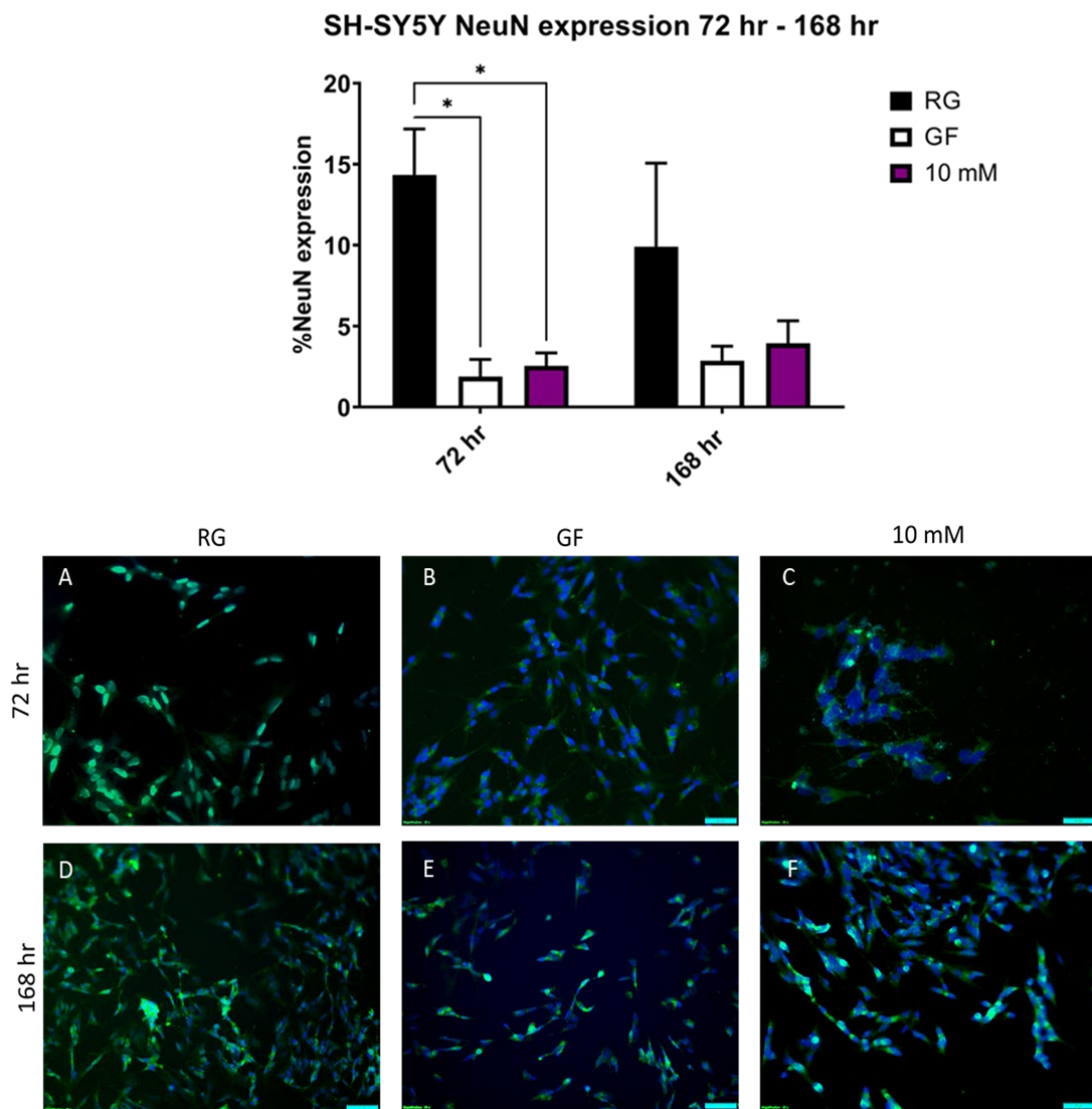


Figure 4.12 Cell differentiation at 72 and 120 hr, in RG and GF and 10 mM β OHB. Green labelling shows differentiating cells and blue staining indicates DAPI labelling. Scale bar at 50 μ m. Two – way anova with Bonferroni Multiple Comparisons test, Mean \pm SEM; * $P < 0.05$. N = 3

4.3.9 Proliferation of NE-4C cells in Regular RG, GF and β OHB Treatment Conditions across 168 hrs

Representative images of NE-4C cells in RG, GF, 1 mM, 5 mM, 10 mM, and 50 mM β OHB conditions were taken at 168 hr (Fig. 4.13).

Cells appeared most confluent in the RG group at 96 hr (Fig. 4.14C) and appeared least confluent in the GF group at 72 hr (Fig 4.14G). Out of the β OHB treatment groups, cells appeared most confluent in the 5 mM β OHB and 10 mM β OHB groups at 168 hr (Fig. 4.14T, Y), and least confluent in the 1 mM β OHB group at 48 hr (Fig. 4.14K).

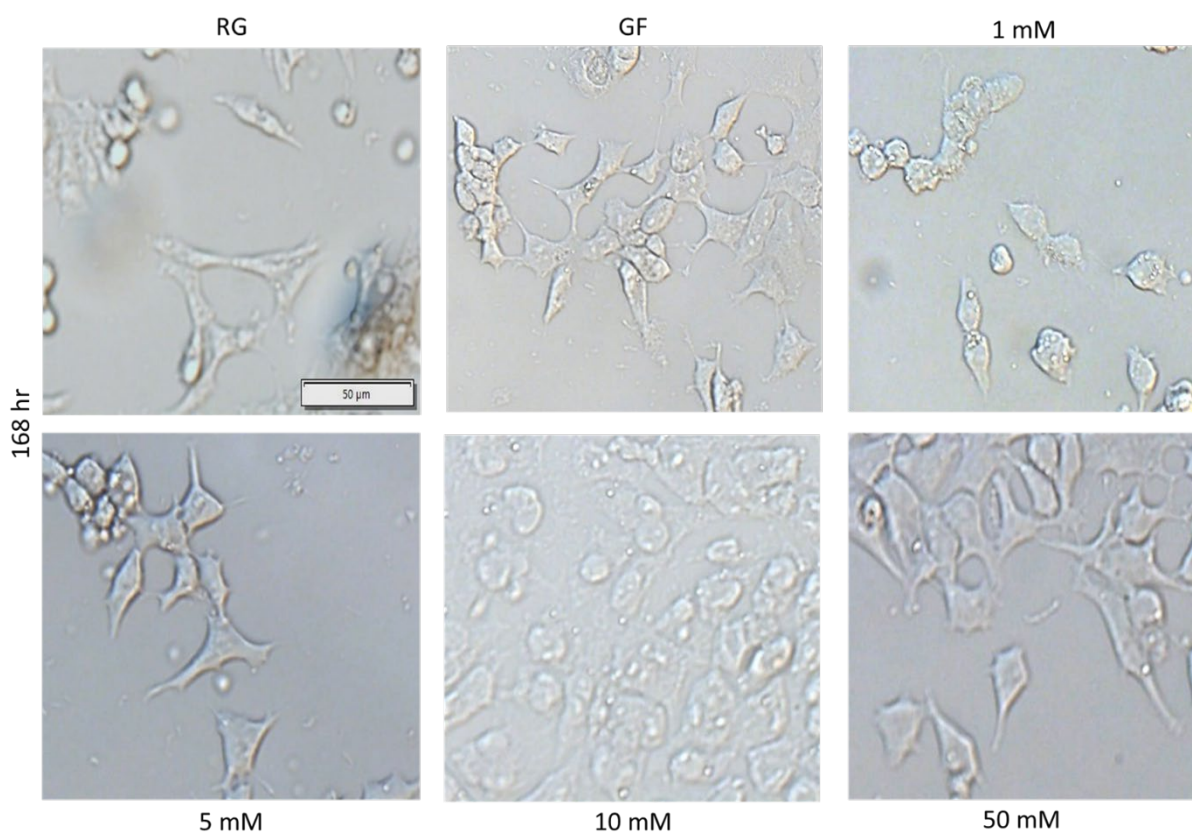


Figure 4.13 High magnification representative images of NE-4C cells cultured in RG, GF, 1 mM β OHB, 5 mM β OHB, 10 mM β OHB and 50 mm β OHB at 168 hr. Scale bar at 50 μ m.

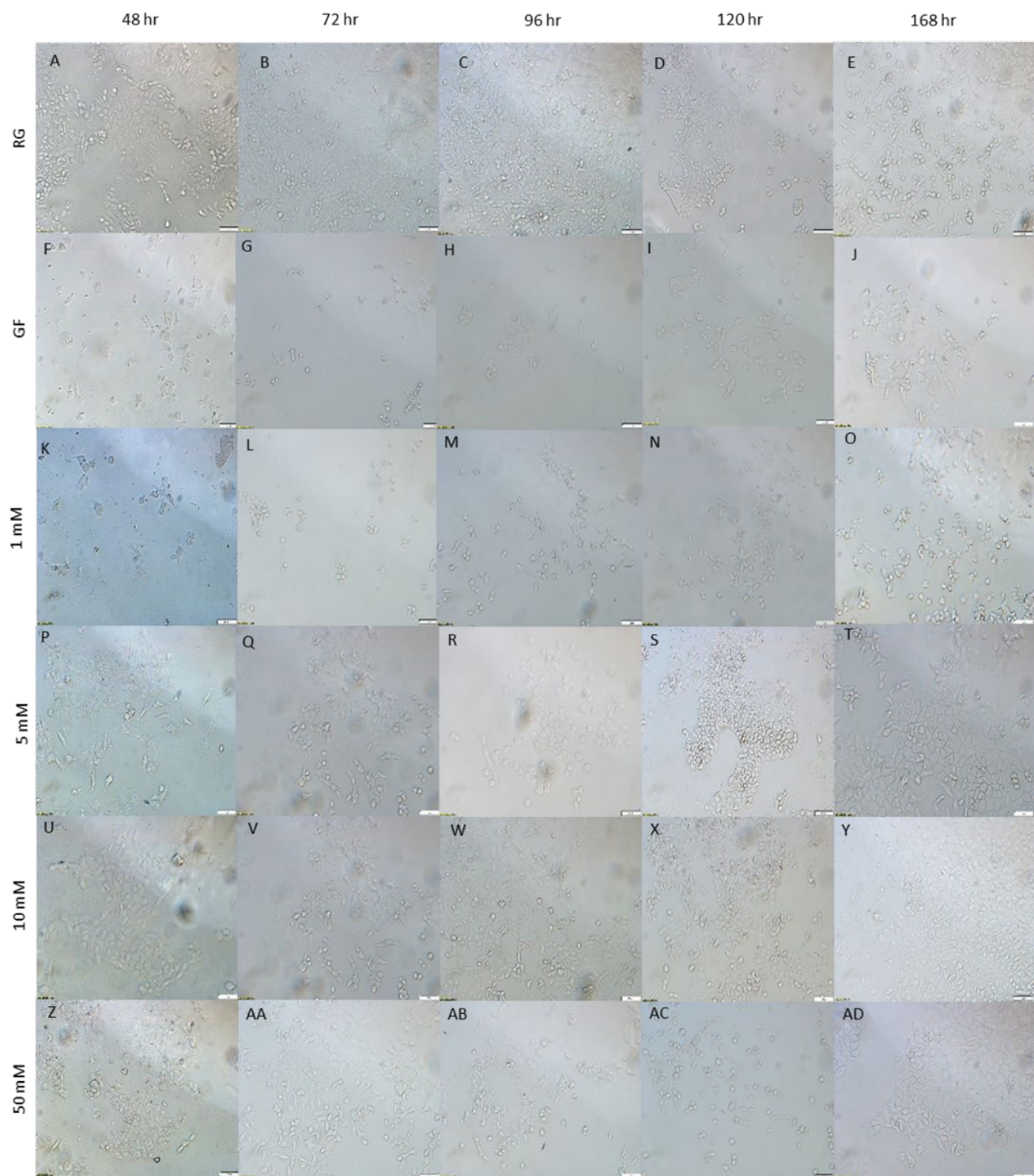


Figure 4.14 A –AD Brightfield representative images of NE-4C cells cultured in RG, GF, 1 mM β OHB, 5 mM β OHB, 10 mM β OHB and 50 mM β OHB at 48 hr, 72 hr, 96 hr, 120 hr and 168 hr. Scale bar at 50 μ m.

4.3.10 NE-4C Cell Density in the RG and GF Groups over 168 hr

An overall effect of time ($F=6.3$, $p=0.0019$) and growth medium ($F=92.6$, $p<0.0001$) was observed for NE-4C cell density. There was no significant interaction effect between time and growth medium. Post hoc testing within time revealed significant differences between 48 hr and 168 hr ($t=4.4$, $p=0.0029$), 96 hr and 168 hr ($t=4.2$, $p=0.0044$) and 120 hr and 168 hr ($t=3.5$, $p=0.0236$). Post hoc testing media conditions comparing time revealed cell density was significantly less in GF conditions when comparing 48 hr ($t=3.6$, $p=0.016$), 72 hr ($t=3.7$, $p=0.0135$), 96 hr ($t=3.9$, $p=0.0081$) and 120 hr ($t=3.6$, $p=0.016$) to GF conditions at 168 hr. Post hoc testing comparing different media conditions at specific time points revealed NE-4C cell was significantly less comparing GF to RG conditions at 48 hr ($t=3.6$, $p=0.008$), 72 hr ($t=5.9$, $p<0.0001$), 96 hr ($t=4.5$, $p=0.0011$) and 120 hr ($t=4.9$, $p=0.0004$) (Fig 4.15).

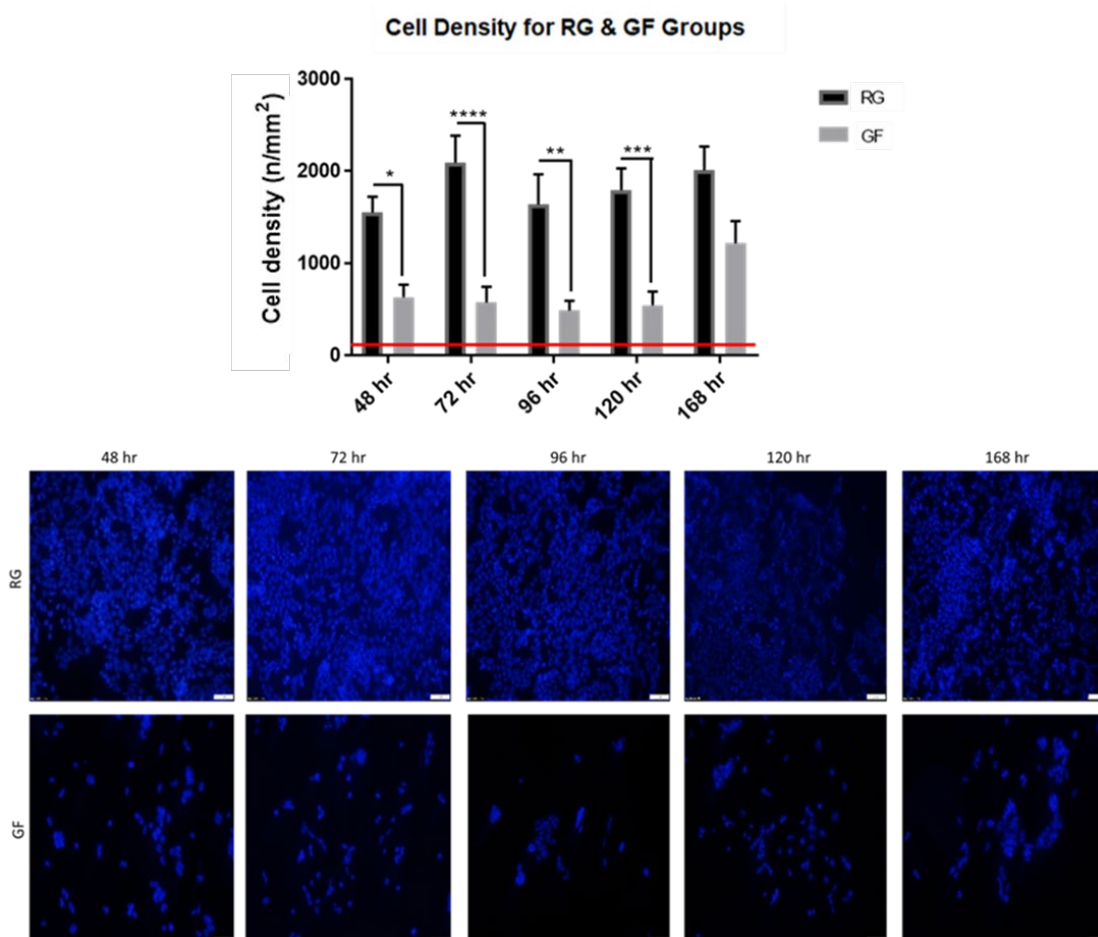


Figure 4.15 Cell density at 48, 72, 96, 120 and 168 hr in RG and GF conditions. The red bar indicates cell density per mm^2 ($115.21 \text{ cell}/\text{mm}^2$). DAPI labelled images of NE-4C cells in RG and GF at 48, 72, 96, 120 and 168 hr. Scale bar at $50 \mu\text{m}$. Two – way anova with Bonferroni Multiple Comparisons test, Mean \pm SEM; * $P < 0.05$, ** $P < 0.01$, *** $P < 0.001$, **** $P < 0.0001$; $N = 3$

4.3.11 NE-4C Cell Density for All Treatment Groups across 168 hr

An overall effect of time ($F=10.2$, $p<0.0001$) and growth medium ($F=4.5$, $p=0.0036$) was observed for NE-4C cell density across 168 hr. There was no significant interaction effect between time and growth medium. Post-hoc testing within time revealed significant differences in growth media comparing 48 hr and 168 hr ($t=4.3$, $p=0.0007$), 72 hr and 168 hr ($t=5.3$, $p<0.0001$), 96 hr and 168 hr ($t=5.5$, $p<0.0001$) and 120 hr and 168 hr ($t=4.6$, $p=0.0003$). Post hoc testing within media comparing time revealed cell density was significantly less in GF conditions when comparing 96 hr ($t=3.4$, $p=0.0124$) and 120 hr ($t=3.4$, $p=0.0133$) to GF conditions at 168 hr. Cell density was significantly less in 5 mM β OHB conditions when comparing 72 hr to 120 hr ($t=3.2$, $p=0.0257$) and 72 hr to 168 hr ($t=2.9$, $p=0.0486$) and when comparing 96 hr to 120 hr ($t=3.1$, $p=0.0354$). Post hoc testing within time comparing media, revealed cell density was significantly less comparing GF ($t=3.2$, $p=0.0257$) and 1 mM β OHB ($t=3.0$, $p=0.0378$) to 5 mM β OHB at 120 hr (Fig. 4.16).

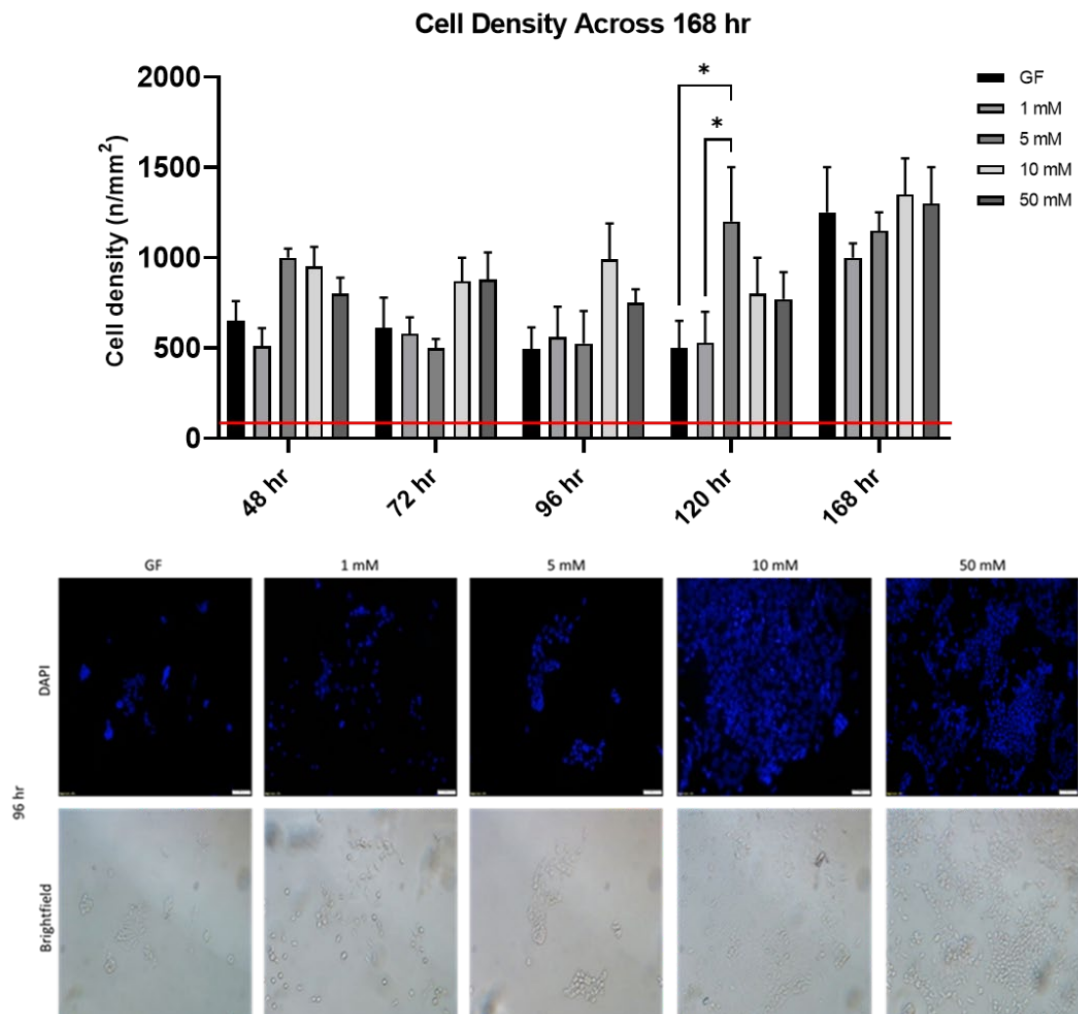


Figure 4.16 Cell density at 48, 72, 96, 120 and 168 hr in GF, 1 mM, 5 mM, 10 mM, and 50 mM β OHB. The red bar indicates cell density per mm^2 ($115.21 \text{ cell}/\text{mm}^2$). DAPI labelled images and brightfield images of NE-4C cells in GF, 1 mM, 5 mM, 10 mM, and 50 mM β OHB at 96 hr. Scale bar at 50 μm .

4.4 Discussion

Under normal circumstances in the adult mammalian brain, glucose is the preferred substrate which is metabolised for ATP production (Mergenthaler et al., 2013). However, the brain can utilize alternative substrates as an energy source when deprived of glucose, such as ketones, lactate (Dienel and Hertz, 2001) and pyruvate (Gonzalez et al., 2005). Neuronal subtypes such as astrocytes, microglia and oligodendrocytes can breakdown ketone bodies, yet preference for ketone body use as an energy or lipid source varies. The present study focused on the impact of β OHB on immature SH-SY5Y and NE-4C cell growth further investigated the impact of β OHB on mature SH-SY5Y cell density, proliferation, and differentiation.

The initial findings of this study showed that over 120 hrs, SH-SY5Y NB cell density is significantly reduced in certain concentrations of β OHB, suggesting in a glucose deprived environment β OHB does not rescue cell growth. Over 120 hrs, the percentage of proliferating cells, measured by BrdU expression, was not significantly different to GF or RG indicating that cell proliferation is unaffected by β OHB concentrations. SH-SY5Y cytotoxicity was significantly reduced in certain concentrations of β OHB. However, a second experiment investigating cell viability using the MTT assay showed there is no significant difference in cell viability between β OHB and GF, suggesting β OHB does not rescue cell viability in a glucose-deprived environment. SH-SY5Y cell density decreased over 120 hrs in RG post RA differentiation suggesting cell death but remained at similar levels at 120 to 168 hrs, suggesting cell recovery following the addition of fresh medium. Following RA differentiation, the percentage of BrdU levels decreased in all groups and the percentage of NeuN (a marker of neuronal of differentiation) was decreased in RG but increased in GF and 10 mM β OHB over 168 hr. In the NE-4C line, β OHB supplementation partially rescued the effects of glucose-deprivation on cell proliferation however this restoration was only to the levels of the cells cultured in the presence of glucose.

4.4.1 β OHB Supplementation Does Not Rescue Cell Growth in a Glucose Deprived Environment

The RG group provided baseline data on the survival and growth of SH-SY5Y cells in the presence of glucose. As observed in the cell densities between 48 hr and 120 hr there is a significant increase in cell density in the RG group, demonstrating a glucose environment is best for cell growth. Furthermore, comparisons of cell density between RG, GF and β OHB concentrations showed RG had the highest cell density. The significant decrease in cell densities in 1 mM β OHB, 5 mM β OHB and 50 mM β OHB when compared to RG and with no significant differences observed when compared to GF indicates ketone supplementation does not rescue cell growth in a glucose deprived environment. Furthermore, analysis of the proliferation data amongst the different groups of media showed that β OHB allows cells to proliferate at the same rate as RG and GF, showing proliferation rates are unaffected.

The results of this experiment are consistent with previous *in vitro* studies, which demonstrated ketone body utilization in primary cell cultures and in embryonic *in vivo* studies (Chechik et al., 1987, Lopes-Cardozo et al., 1986). No statistical difference in cell proliferation was observed between 48 hr and 120 hr in the RG, GF, 1 mM β OHB, 5 mM β OHB, 10 mM β OHB and 50 mM β OHB groups. The observable increase in cell number is potentially due to the addition of pyruvate in the GF media, which is oxidised to acetyl – coA, a major substrate for the citric acid cycle (Gray et al., 2014). The presence of pyruvate in the media may have impacted the results of the BrdU analysis of cell proliferation, which showed no significance across the groups.

Furthermore, glutamine is a known reagent in glucose free DMEM, this may have potentially impacted cell growth also as glutamine driven OXPHOS has been shown to be a major means of ATP production in mouse epithelial cancer cells (Fan et al., 2013). Glutamine is utilized through the glutaminolysis pathway and cancer cells were found to rely on this pathway for durable supply of carbon and nitrogen (DeBerardinis and Cheng, 2010). Yet, many CNS cell types can use ketone bodies as a replacement for glucose. β OHB may be synthesized by astrocytes, the only neural cell type capable of oxidizing fatty acids (Edmond et al., 1987) and then released to other brain cell types for energy. For example, *in vitro* studies have demonstrated that prolonged β OHB exposure rescued primary astrocytes, hippocampal neurons, and C6 (rat glioblastoma) cells from glucose deprivation (Eloqayli et al., 2011a, Maurer et al., 2011a) and oligodendrocytes *in vitro* can use ketone bodies for cellular respiration (Edmond et al., 1987).

When SH-SY5Y NB cells were grown in glucose deficient conditions, treatment with 10 mM β OHB rescued cells from death, likely by decreasing ROS and ERK phosphorylation (Lamichhane et al., 2017b). This may be potentially why 10 mM β OHB was the only group of the β OHB treatment groups to have a higher cell density.

4.4.2 β OHB Impacts SH –SY5Y Toxicity and Viability

To determine if the utilization of β OHB as an energy source affects cell viability, a cytotoxicity assay and MTT assay was performed which determined mitochondrial and metabolic viability. The results of the cytotoxicity and MTT assays indicate that differing levels of β OHB alter mitochondrial function and cell viability. The cytotoxicity assay shows that out of all the groups, the GF group impacts mitochondrial health the most, with the highest percentage of dead cells; this is followed by the 50 mM β OHB group which out of the β OHB treatment groups has the highest percentage of dead cells. The RG group had the lowest percentage of dead cells at both timepoints, out of the β OHB groups, 5 mM β OHB followed by 10 mM β OHB had the lowest percentage of dead cells out of the β OHB groups. This would suggest that these levels of β OHB are tolerable for SH-SY5Y cell growth. When GF was compared to the β OHB concentrations; there was a significant decrease in the percentage of dead cells in the 5 mM β OHB and 10 mM β OHB groups and the significant increase in the percentage of dead cells would suggest again that 50 mM β OHB is toxic to SH-SY5Y cells.

BACE1 activity-dependent deficit in glucose oxidation was alleviated by the presence of 10 mM β OHB (Findlay et al., 2015b). This could be a potential avenue to further investigate to see if this is the reason 5 mM β OHB and 10 mM β OHB have a lower percentage of dead cells. However, the MTT assay has shown that compared to RG and LG, there is a significant decrease in cell viability in all β OHB groups, which shows that even though cells exposed to ketone supplementation may be growing and dividing at a similar rate to the RG and GF groups, they are less healthy than cells grown in a glucose environment.

A study by (Lamichhane et al., 2017b) showed 10 mM β OHB attenuating glucose deficiency induced cytotoxicity in SH-SY5Y cells using an MTT assay following 4 hr of glucose deficiency. SH-SY5Y cells were then treated with 10 mM β OHB over a 24-hr period and cell viability increased. However, the timeframe investigated in that experiment was shorter than the 96 hr timepoint performed in this experiment.

4.4.3 Cell Density Decreases Following RA Differentiation

After differentiation, there is a significant decrease in cell number at 72 hr post differentiation in the GF and 10 mM β OHB. SH-SY5Y cells underwent differentiation into a mature neuronal phenotype after being 120 hr in culture. When looking at Fig. 4.2, cell density levels are higher in GF and 10 mM β OHB at 120 hrs when compared to GF and 10 mM β OHB 72 hr post differentiation (Fig. 4.10). This decrease is likely a result of RA differentiation. When cells become post-mitotic, they can no longer proliferate.

However, cell number per mm² in the GF and 10 mM β OHB at 168 hr remained at a similar level to the 120-hr level, this is likely because of fresh media being added to each treatment group at 120 hr. The significant decrease in cell density in the RG group from 72 hr to 168 hr may be a result of cell death. Media concentrations which fuel multiple pathways at the same time can allow cells to grow and divide rapidly to the point where cells begin to die as a result of a lack of space to grow (Amoyel and Bach, 2014).

4.4.4 Proliferation Rates are Slowed by β OHB Following RA Differentiation

To examine the rate of proliferation in each treatment group, the percentage of cells expressing BrdU was calculated at 72 hr and 168 hr post RA differentiation. BrdU is a marker of cell proliferation as it integrates into the cell nucleus during the S-phase of mitosis (Konishi et al., 2011). BrdU expression decreases in all groups from 72 hr to 168 hr. The significant decrease in the GF group at 72 hr, may suggest that as cells begin to differentiate the lack of glucose may further hinder proliferation. As cells differentiate, they stop proliferating so it's understandable that they would not express BrdU, but this may be decreased further if glucose is not the main energy source. Additionally, the significant difference in BrdU expression between the RG and 10 mM β OHB groups at 168 hr may suggest that the SH-SY5Y proliferation rate may be affected by β OHB when treated with RA.

4.4.5 Differentiation is not Affected by β OHB Following RA Treatment

The study set out to assess the rate of differentiation of ketotic cells into neurons compared to controls by measuring NeuN expression, a marker of post-mitotic neurons. As cells differentiate, it is expected that percentage of NeuN expression would increase (Kovalevich and Langford, 2013, Lopes et al., 2010, Shipley et al., 2016). In this investigation, NeuN expression decreased between from 72 to 168 hr post RA differentiation in the RG group.

There may be less of neuronal lineage in RG due to cell death. SH-SY5Y cells at 168 hr post RA differentiation have been in culture 12 days in total at that stage, and there may be too much competition for space and nutrients, so cells begin to die and de-adhere from the well. Yet NeuN expression increased in the GF and 10 mM β OHB group between time-points. This increase is likely a result of the decrease in BrdU expression as cells begin to take on a mature neuronal phenotype but also because of more space being available to them.

4.4.6 NE-4C Cells Show Enhance Growth and Survival in Glucose Media Compared to Glucose-Free Media

The RG group provided baseline data on the survival and growth of the cells in the presence of glucose. As can be seen in the cell densities of the RG groups across 168 hr, there is a general upward trend over time indicating the cells can utilize glucose and survive and proliferate *in vitro*. The cells in RG grow in monolayers with an epithelial morphology which was clear from inspection of the brightfield images. This is the same pattern of growth and morphology as described in the literature of NE-4C cells growing in the presence of glucose (Varga et al., 2008). The GF group provided baseline data for the survival and growth of the NE-4C cells in the absence of both glucose and ketone bodies. There are significant differences between the cell densities of the RG and GF groups from 48 hr to 120 hr. This is an expected result as the cells should show an increased survival and rate of proliferation in the presence of glucose compared to glucose free conditions. At 168 hr, there is a notable difference in cell density between the RG and GF groups. It is possible that this unexpected increase in cell density at 168 hr in the GF groups could be caused by the presence of pyruvate in the GF media, for pyruvate can be oxidised to acetyl-CoA which feeds into the TCA cycle resulting in ATP production (Gray et al., 2014). This may explain the increased cell density seen in the GF group at 168 hr. Additionally, cells in the GF groups at all timepoints increase in cell density compared to the initial seeding density which may be the action of the NE-4C cells depleting their intracellular glycogen stores and producing glucose via glycogenolysis.

4.4.7 NE-4C Cells Can Both Survive and Proliferate in Varying Concentrations Of β OHB Over 168 Hr

To determine the effect of β OHB supplementation on the proliferation and survival of the NE-4C cells, the cell density of the β OHB treatment groups was compared to the GF group. There are no significant differences in the mean cell density of the GF and 1 mM β OHB conditions between 48 hr and 120 hr. This is expected as the 1 mM β OHB group is at the

lowest concentration of the four β OHB media groups and even though this concentration of β OHB is similar to physiological concentration of β OHB during the foetal stage (Nehlig, 2004), *in vivo* NSCs would also be in the presence of acetoacetate, lactate and glucose each at similar concentrations (Dahlquist and Persson, 1976). For NE-4C cells in the 1 mM β OHB concentration medium, β OHB is present in isolation at 1 mM and this concentration appears insufficient to allow cells to proliferate excessively due to ketone metabolism.

The increased mean cell density in the 5 mM, 10 mM and 50 mM β OHB indicates that NE-4C cells can utilize β OHB as an alternative energy source allowing the cells to survive and proliferate however at a diminished rate compared to the cells in the RG control groups. This validates part of the hypothesis of this experiment, which predicted that NE-4C cells could both survive and divide in all β OHB treatment groups across 168 hr, which was expected considering that ketone oxidation is reportedly responsible for 70% of energy production in the developing CNS of foetal rats (Hawkins et al., 1971a). Furthermore, β OHB not only contributes directly to energy production in conditions of glucose deprivation but is also involved in glucose homeostasis. During fasting, β OHB acts as an epigenetic regulator by increasing the expression of the glucose transporter GLUT1 by inhibiting the action of histone deacetylase in mice (Tanegashima et al., 2017). This highlights the complex role of β OHB in the CNS, both as a metabolic substrate and epigenetic regulator of metabolic genes. This epigenetic action of β OHB is a potential separate pathway by which β OHB alters the development of the embryonic nervous system.

4.5 Conclusion

The data presented here shows using SH-SY5Y cells, β OHB can allow cells to grow and proliferate in a glucose-deprived environment, albeit not to the same extent as RG. β OHB alters mitochondrial membrane potential and cell viability to varying degrees, leading to SH-SY5Y cytotoxicity at certain concentrations. NE-4C cells can utilize β OHB as a substrate for energy production in glucose-free conditions with a general trend of increasing cell density with increasing concentrations of β OHB. However, cell density across 168 hr for cells cultured in the β OHB treatment media was reduced compared to cell cultured in the glucose-containing RG. Further experiments on cell growth without different media components is necessary to see if any of the results observed are valid or are they a result from other media components such as glucose, pyruvate, or glutamine.

Chapter 5

The Impact of Nutrient Deprivation and
Ketone Supplementation on the
Differentiation and Metabolic Health of
Neural Stem and Neuronal Precursor
Cells

5.1 Introduction

Cellular metabolism involves interconnected pathways that allow cells to grow, reproduce and respond to their environment. Depending on their energy requirements, different cell types including developing and adult brain cells, utilize varying metabolic processes. This metabolic plasticity confers the selective prioritization of metabolic pathways that can adapt to the anabolic and catabolic demands of cell types across their lifecycles or during self-renewal (Folmes et al., 2012). Rapidly dividing cells in the developing brain employ glycolysis for ATP production instead of OXPHOS, even in the presence of oxygen. This metabolic process adapts to OXPHOS as brain cells mature. As such, a greater understanding of how metabolic phenotypes may be manipulated based on anaplerotic and glycolytic inputs as cells divide and then differentiate will give insights into how their fuel sources may be targeted to understand cellular viability in circumstances of starvation, fasting, exercise and dieting.

To investigate the effect of nutrient deprivation and ketone supplementation on NE-4C NSC and SH-SY5Y neural precursor cell growth, glucose, pyruvate, and glutamine were removed from the culturing media and supplemented with 10 mM β OHB over 5, 10 and 15 DIV. These proliferative cell lines are glycolytic and have high requirements for NADPH, ATP, carbon, nitrogen, and hydrogen to support biosynthesis (Folmes et al., 2012). As cells mature, OXPHOS provides most of the ATP responsible for setting and maintaining metabolic homeostasis. A common feature of neoplastic cells such as NE-4C and SH-SY5Y cells is their reliance on anaerobic glycolysis, in the phenomenon known as the “Warburg effect”, which occurs when rapidly dividing cells require additional resources to drive proliferation (Vander Heiden et al., 2009, Miyazawa and Aulehla, 2018, DeBerardinis et al., 2008a, Warburg, 1925b). The persistent activation of aerobic glycolysis in cancer cells such as SH-SY5Y cells is linked to oncogene activation or a deletion of tumour suppressors (Jang et al., 2013). Most cancer cells use glycolysis for energy production regardless of whether they are under normoxic or hypoxic condition.(Koppenol et al., 2011). NSCs initially exist in a state of hypoxia due to the absence of a developed vascular system to deliver oxygen to their local environment (Jády et al., 2016). NSCs generate ATP anaerobically and subsequently use glycolysis followed by lactic acid fermentation. Additionally, NSCs utilize glycolysis even in normoxia (Jády et al., 2016). This process appears paradoxical, as metabolism should shift to OXPHOS in the presence of oxygen.

To further understand the roles of glucose, pyruvate, and glutamine during this metabolic transition on cell development, we investigated the health and phenotypes of differentiating neural stem and neuronal precursor cells in various conditions of substrate deprivation and β OHB supplementation over time. These data may contribute to the impact of fasting, starvation and dieting on foetal brain cell maturation and function in utero and in postnatal stages of nervous system development.

5.2 Experimental aims

In the present study, we assessed the impact of glucose, pyruvate and glutamine deprivation and ketone supplementation on the maturation of the NE-4C and SH-SY5Y cell lines by measuring **cell density, morphology, lineage, and metabolic viability** as indicators of cell health and function.

5.2.1 Aims

5.2.1.1 To investigate the impact of low glucose and glucose deprived conditions on differentiating NE-4C and SH-SY5Y cells over 5, 10 and 15 DIV.

5.2.1.2 To investigate the growth of NE-4C and SH-SY5Y cell differentiation in the absence of pyruvate and L-glutamine in glucose deprived conditions over 5, 10 and 15 DIV.

5.2.1.3 To investigate whether ketone supplementation can rescue the effects of glucose, pyruvate, and L-glutamine deprivation on differentiating NE-4C and SH-SY5Y cells over 5, 10 and 15 DIV.

5.2.2 Hypothesis

5.2.2.1 As growing and differentiating brain cells have different biosynthetic and metabolic needs, the shift from glycolysis to OXPHOS as cells mature may be impacted by the deprivation of fuel inputs which may have consequences for cellular development and function. Ketone bodies are metabolised using OXPHOS and it is hypothesised that β OHB may rescue the effects of glucose deprivation in differentiating neural stem and neural precursor cells.

5.3 Methods

5.3.1 Cell Lines and General Culture Conditions

The NE-4C mouse neuroectodermal and the SH-SY5Y human NB cell lines were recovered and subcultured as described in the general methods section of Chapter 2. SH-SY5Y cells were cultured at density of 5×10^3 and NE-4C cells were cultured at a density of 2×10^3 per well. Cells were seeded in freshly prepared RG medium and were cultured for four days in this medium in coated 96-well plates. A 100 mM RA stock solution was made up and diluted using DMSO to 0.01 mM. Medium was removed, and RA differentiation media were freshly prepared (RG, LG, GF, GF-Pyr, GF-Lglut, GF-Pyr-Lglut and with 10 mM β OHB supplemented conditions) and carefully added to each well. Thereafter, the differentiation media was changed every two days (100 μ l removed and 100 μ l added in). All procedures were carried out aseptically with minimal exposure to light.

5.3.2 Experimental Design

To assess the impact of glucose deprivation on differentiating NE-4C and SH-SY5Y cells, both cell lines were grown for four days in an individual T75 flask before being seeded in a 96 well plate. Cells were then grown in RG, LG, and GF conditions. To investigate the effects pyruvate and L-glutamine deprivation and β OHB supplementation had on the health and the differentiation of NE-4C cells and SH-SY5Y cells, cells were grown in GF, GF-Pyr, GF-Lglut, and GF-Pyr-Lglut conditions. These conditions were simultaneously cultured with 10 mM β OHB for 5, 10 and 15 DIV (Table 5.1).

| Experiment 1 | Experiment 2 | |
|--------------|---------------|---------------|
| | $-\beta$ OHB | $+\beta$ OHB |
| RG | GF | GF |
| LG | GF-Pyr | GF-Pyr |
| GF | GF-Lglut | GF-Lglut |
| | GF-Pyr/-Lglut | GF-Pyr/-Lglut |

Table 5.1 A summary of the media groups in each experiment.

5.3.3 Experiments Undertaken

5.3.3.1 Cell Viability

MTT assays were performed to assess cell viability at 5, 10 and 15 DIV. MTT was added to cells at a concentration of 0.5 mg/ml to the culture medium and incubated for 3 hrs and 30 min. The culture medium was removed, and the cells were lysed in DMSO. The plate was placed on a plate rocker for 5 min to ensure the precipitated formazan crystals were completely solubilized. Colorimetric absorbance was measured at a wavelength of 562 nm using a microplate spectrophotometer.

5.3.3.2 Immunocytochemistry

Cultures were fixed in 4% PFA in PBS for 15 min at RT. A blocking solution was applied for 1 hr, which consisted of 5% NGS in 0.05% PBS-T. To assess cells undergoing differentiation, cells were stained with an anti- β -III tubulin (1:500) primary antibody overnight at 4°C in 0.05% PBS-T. To assess cell density, and cell size, cells were permeabilized and stained with DAPI (1:5000) and actin (2 drops per ml) along with the FITC secondary for 2 hr in 0.05% PBS-T the following day. After this incubation, cells underwent 3 x 5-min 1X PBS washes. A summary of the fluorescent imaging-based parameters and their method of quantification in this study is shown in Table 5.2 below.

| Image-Based Assay | Method |
|-------------------|--|
| Cell density | 3 random fields were taken of DAPI stained nuclei. Density was measured as the number of nuclei per mm ² . |
| Cell Size | Average cell size was calculated by measuring the total area of actin fluorescence using the analyse particles function in ImageJ. This was divided by the number of cells in an image to obtain the average size. |
| Differentiation | The total area of β -III tubulin fluorescence was measured using the analyse particles function in ImageJ and this was divided by the percentage area of DAPI expressing cells. |
| Neurite Number | Neurites were counted per image and measured in micrometres. |

Table 5.2 A list of the image-based assays

5.3.3.3 Imaging and Analysis

Cells were imaged using an Olympus IX81 motorized epifluorescent microscope using Cellsens Dimension software (version 2.8). ImageJ Fiji was subsequently used for processing and analysis. Data is presented as the mean \pm the SEM. The assumption of normality was verified using QQ plots of the residual errors. Statistical analysis and graphs were generated using Graphpad prism version 9.5. Statistical differences in the data were analysed using one-way or two-way ANOVA as appropriate with a post hoc Bonferroni

Multiple Comparisons test to reveal the differences between the groups. P-values of ≤ 0.05 were considered statistically significant.

5.4 Results

5.4.1 The Effects of Glucose Deprivation on Differentiating NE-4C Density, Phenotype, Morphology and Metabolic Viability

An overall effect of time ($F=4.2$, $p=0.0404$) and growth medium ($F=32.9$, $p<0.0001$) was observed for NE-4C cell density. There was no significant interaction effect between time and growth medium. Post-hoc testing revealed no significant time effects within any of the individual media groups. Within time, NE4C cell density was significantly less comparing LG ($t=3.2$, $p=0.0049$) and GF ($t=6.9$, $p<0.0001$) media to the RG medium at 5 DIV. In addition, GF was significantly lower when compared to LG conditions at 5 DIV ($t=3.6$, $p=0.0013$). At 15 DIV, there was no longer a significant difference between RG and LG conditions. However, there was still a significantly lower cell density in GF conditions when compared to RF conditions ($t=4.6$ and $p<0.0001$) and in GF when compared to the LG condition ($t=2.9$, $p=0.0144$) (Fig. 5.1A, G).

An overall effect of time ($F=38.3$, $p<0.0001$), growth medium ($F=57.3$, $p<0.0001$) and an interaction between growth medium and time ($F=11.6$, $p<0.0001$) was observed for β -III tubulin expression in NE-4C cells. Post hoc testing revealed significant time effect differences for the media conditions between 5DIV and 10DIV ($t=4.5$, $p<0.0001$), 5DIV and 15DIV ($t=9.1$, $p<0.0001$) and 10DIV and 15DIV ($t=2.9$, $p=0.0145$). Post hoc testing within media conditions comparing time revealed that β -III tubulin levels were significantly higher at 10DIV ($t=4.2$, $p=0.0009$) and 15 DIV ($t=12.5$, $p<0.0001$) when compared to RG conditions at 5DIV. In addition, β -III tubulin levels were significantly higher comparing 10DIV ($t=3.6$, $p=0.0041$) and 15DIV ($t=7.0$, $p<0.0001$) to LG conditions at 5DIV. β -III tubulin levels were significantly lower comparing 10DIV ($t=4.1$, $p=0.001$) to 5DIV in GF conditions and were significantly higher comparing 15DIV ($t=2.8$, $p=0.0301$) to 10DIV in GF conditions. Post hoc testing within time comparing media conditions revealed β -III tubulin levels were significantly less comparing GF ($t=3.5$, $p=0.0045$) to RG conditions at 5DIV. At 10DIV, β -III tubulin levels were significantly less comparing LG ($t=2.5$, $p<0.0485$) and GF ($t=5.3$, $p<0.0001$) to RG conditions. Additionally, β -III tubulin levels were significantly less comparing GF ($t=5.9$, $p<0.0001$) to LG conditions at 10DIV. At 15DIV, β -III tubulin levels were significantly less comparing LG ($t=5.5$, $p<0.0001$) and

GF ($t=12.8$, $p<0.0001$) to RG conditions, as were GF ($t=6.6$, $p<0.0001$) when compared to LG (Fig. 5.1B, G).

An overall effect of time ($F=10.6$, $p<0.0001$), growth medium ($F=63.4$, $p<0.0001$) and interaction between time and growth medium ($F=157.5$, $p<0.0001$) for the number of neurites was observed. Post hoc testing revealed significant time effect differences within the media groups between 5DIV and 10DIV ($t=5.8$, $p<0.0001$), 5DIV and 15DIV ($t=11.3$, $p<0.0001$) and 10DIV and 15DIV ($t=5.6$, $p<0.0001$). Post-hoc testing within media conditions comparing time revealed the number of neurites were significantly higher comparing 10DIV ($t=3.5$, $p=0.0017$) and 15DIV ($t=8.9$, $p<0.0001$) to RG at 5DIV and comparing 15DIV ($t=5.4$, $p<0.0001$) to RG conditions at 10DIV. In addition, the number of neurites were significantly higher comparing 10DIV ($t=7.1$, $p<0.0001$) and 15DIV ($t=8.8$, $p<0.0001$) to LG conditions at 5DIV. Post hoc testing within time comparing media conditions revealed the number of neurites was significantly less comparing GF conditions to RG ($t=5.9$, $p<0.0001$) and LG ($t=3.6$, $p=0.0013$) at 5DIV. At 10DIV, the number of neurites was significantly less comparing GF conditions to RG ($t=9.9$, $p<0.0001$) and LG ($t=11.2$, $p<0.0001$) conditions. At 15DIV, the number of neurites was significantly less comparing GF conditions to RG ($t=12.32$, $p<0.0001$) and LG ($t=10.5$, $p<0.0001$) conditions (Fig. 5.1C, G).

An overall effect of time ($F=5.9$, $p=0.0107$) and growth medium ($F=10.85$, $p=0.0008$) was observed for NE-4C cell volume over 15DIV. There was no significant interaction effect between time and growth medium. Post hoc testing revealed significant time effect differences within media groups between 5DIV and 15DIV ($t=2.8$, $p=0.0365$) and between 10DIV and 15DIV ($t=3.1$, $p=0.0173$). Post hoc testing within media conditions comparing time revealed the cell volume was significantly less comparing 15DIV to 10DIV ($t=2.6$, $p=0.0499$) and 5DIV ($t=3.6$, $p=0.006$) in RG conditions. Post hoc testing within time comparing media conditions revealed cell volume was significantly less comparing LG ($t=3.5$, $p=0.0068$) and GF ($t=4.2$, $p=0.0015$) to RG conditions at 5DIV. No significant differences in cell volume were found between groups at 10DIV and 15DIV (Fig. 5.1D, G).

An overall effect of time ($F=4.6$, $p=0.0237$) and growth media ($F=30.80$, $p<0.0001$) was observed for NE-4C cell viability over 15DIV. There was no significant interaction effect between time and growth media. Post hoc testing revealed significant time effect differences within media groups between 5DIV and 10DIV ($t=2.8$, $p=0.0338$). Post hoc testing within

media conditions comparing time revealed cell viability was significantly higher comparing 10DIV ($t=2.7$, $p=0.0456$) to 5DIV in LG conditions. Post hoc testing within time comparing media conditions revealed cell viability was significantly less comparing GF ($t=3.2$, $p=0.0146$) to RG conditions at 5DIV. At 10DIV, cell viability was significantly less comparing GF to LG ($t=3.7$, $p=0.0051$) and RG ($t=5.5$, $p=0.0001$) conditions. At 15DIV, cell viability was significantly less comparing GF to LG ($t=3.4$, $p=0.0105$) and RG ($t=4.8$, $p=0.0004$) conditions (Fig. 5.1E, G).

An overall effect of time ($F=11.4$, $p=0.0001$) and growth media ($F=32.85$, $p<0.0001$) was observed for NE-4C cell viability with the addition of β OHB. There was no significant interaction effect between time and growth media. Post-hoc testing revealed significant time effects between 5DIV and 10DIV ($t=4.0$, $p=0.0009$) and between 5DIV and 15DIV ($t=4.2$, $p=0.0004$). Cell viability was significantly higher in RG + β OHB conditions comparing 10DIV ($t=2.7$, $p=0.0325$) and 15DIV ($t=3.0$, $p=0.0148$) to 5DIV RG + β OHB conditions. Cell viability was significantly increased in LG conditions comparing 10DIV ($t=2.8$, $p=0.0268$) to LG conditions at 5DIV. Cell viability was significantly increased in LG + β OHB conditions comparing 15DIV ($t=2.7$, $p=0.0305$) to LG + β OHB conditions at 5DIV. When comparing the control media conditions to the β OHB supplemented, no significant differences were observed (Fig. 5.1F, G).

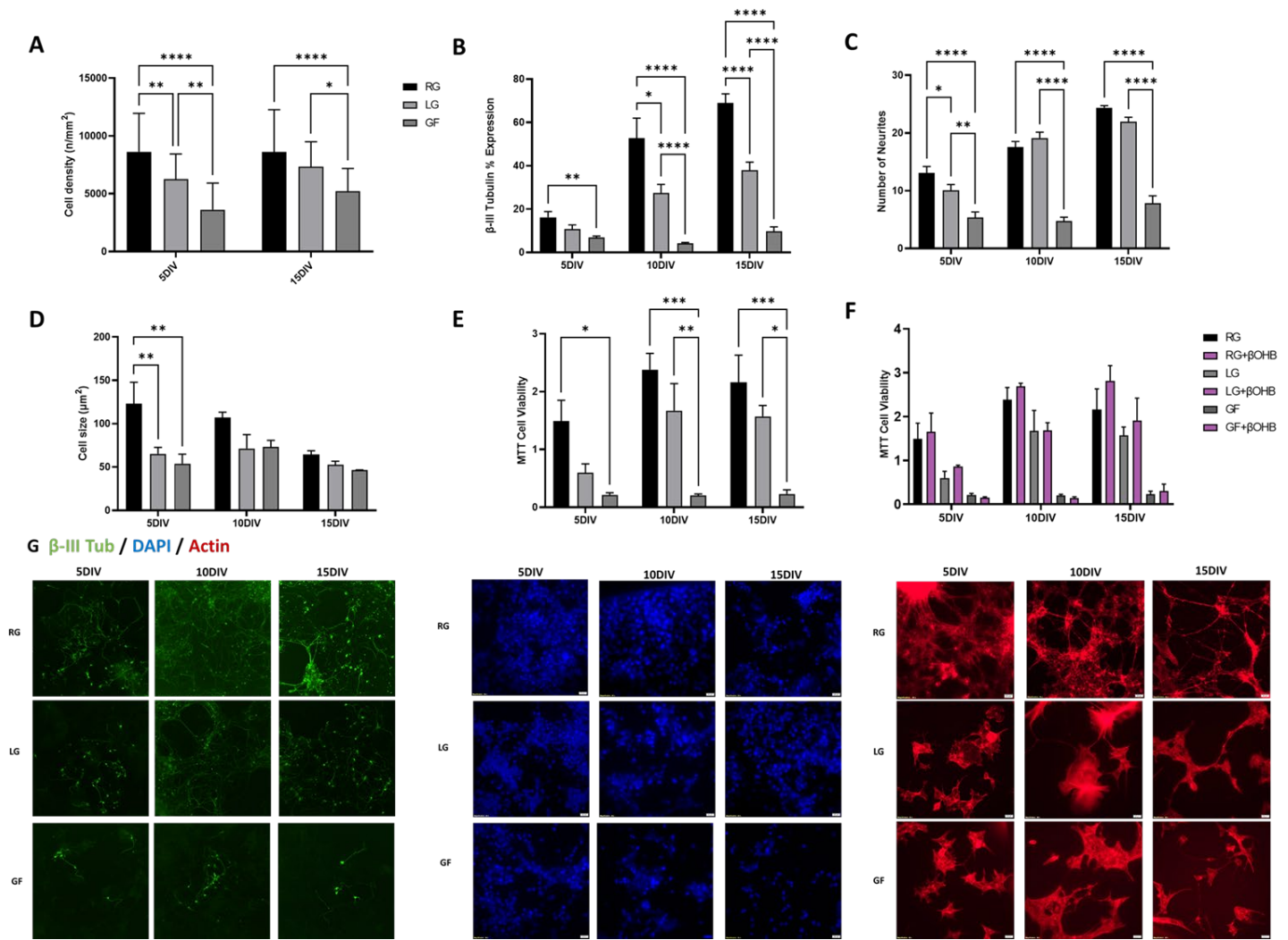


Figure 5.1 Growth and viability of NE-4C cells in RG, LG, and GF condition at 5, 10 and 15 DIV. **A)** Cell density. **B)** β -III tubulin expression. **C)** Neurite number. **D)** Cell volume. **E)** Metabolic viability **F)** Metabolic viability after β OHB supplementation. **G) Left panel:** β -III tubulin expression in RG, LG, and GF conditions. **Middle panel:** DAPI labelled nuclei showing cell density in RG, LG, and GF conditions. **Right panel:** Actin labelled cytoskeleton of cells in RG, LG, and GF conditions. N = 3 independently for each assay. Two-way ANOVA with a post hoc Bonferroni Multiple Comparisons test comparing glucose containing and GF conditions over 5, 10 and 15 DIV. Scale bar = 20 μ m in G

5.4.2 The Impact of Substrate Deprivation and β OHB Supplementation on Differentiated NE-4C Viability, Density, and Morphology at 5 DIV

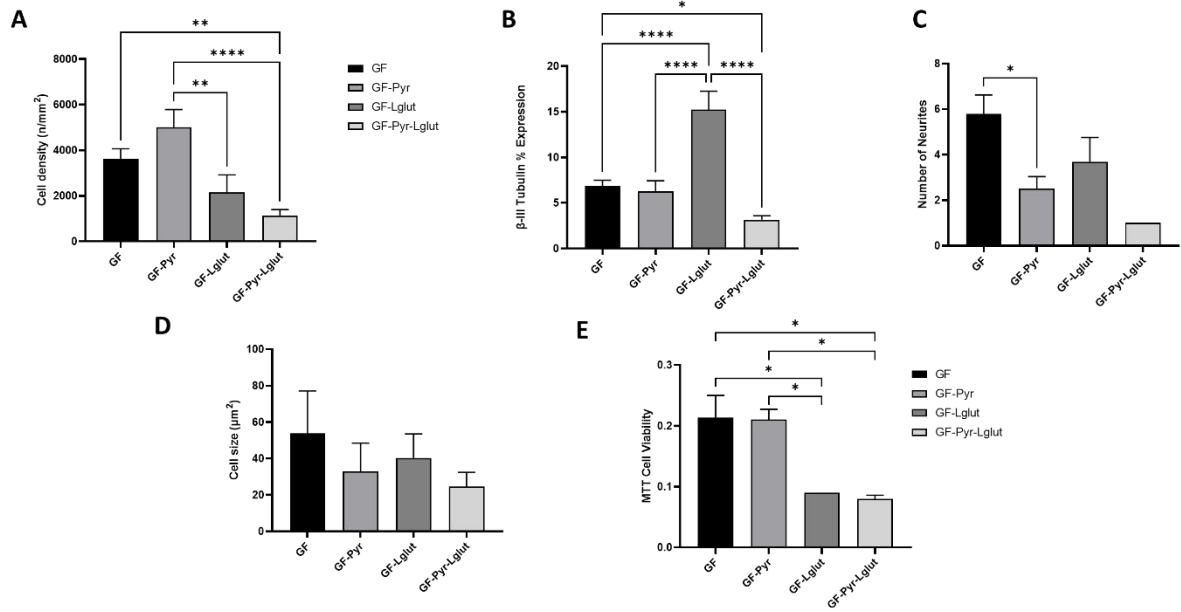
An overall effect of substrate deprivation on cell density was observed at 5DIV ($F=9.9$, $p<0.0001$). Post-hoc testing revealed cell density was significantly less comparing GF-Pyr-Lglut ($t=3.7$, $p=0.0022$) to GF conditions. Additionally, cell density was significantly less comparing GF-Lglut ($t=3.3$, $p=0.0088$) and GF-Pyr-Lglut ($t=5.1$, $p<0.0001$) to GF-Pyr conditions at 5DIV. A significantly lower cell density was revealed comparing GF-Pyr-Lglut ($t=5.1$, $p<0.0001$) and GF-Lglut ($t=3.3$, $p=0.0088$) to GF-Pyr conditions (Fig. 5.2A, F).

An overall effect of substrate deprivation on β -III tubulin expression was observed at 5DIV ($F=23.0$, $p<0.0001$). Post-hoc testing revealed β -III tubulin expression was significantly less comparing GF-Pyr-Lglut ($t=3.0$, $p=0.0196$) to GF conditions. β -III tubulin expression was significantly less comparing GF-Pyr-Lglut ($t=8.3$, $p<0.0001$), GF-Pyr ($t=5.6$, $p<0.0001$) and GF ($t=5.8$, $p<0.0001$) to GF-Lglut conditions (Fig. 5.2B, F).

An overall effect of substrate deprivation on neurite number was observed at 5DIV ($F=3.0$, $p=0.0387$). Post-hoc testing revealed neurite number was significantly less in GF-Pyr conditions when compared to GF ($p = 0.0462$) (Fig. 5.2C, F).

No overall significant effect of substrate deprivation on cell volume was observed at 5DIV. Thus post hoc testing was not performed (Fig. 5.2D, F)

An overall effect of substrate deprivation on cell viability was observed at 5DIV ($F=12.79$, $p=0.0020$). Post hoc testing revealed cell viability was significantly less comparing GF-Lglut ($t=4.3$, $p=0.0166$) and GF-Pyr-Lglut ($t=4.6$, $p=0.0105$) to GF conditions. Additionally, cell viability was significantly less comparing GF-Lglut ($t=4.1$, $p=0.0194$) and GF-Pyr-Lglut ($t=4.5$, $p=0.0122$) to GF-Pyr conditions (Fig. 5.2E, F).



F DAPI / β -III Tub / Actin

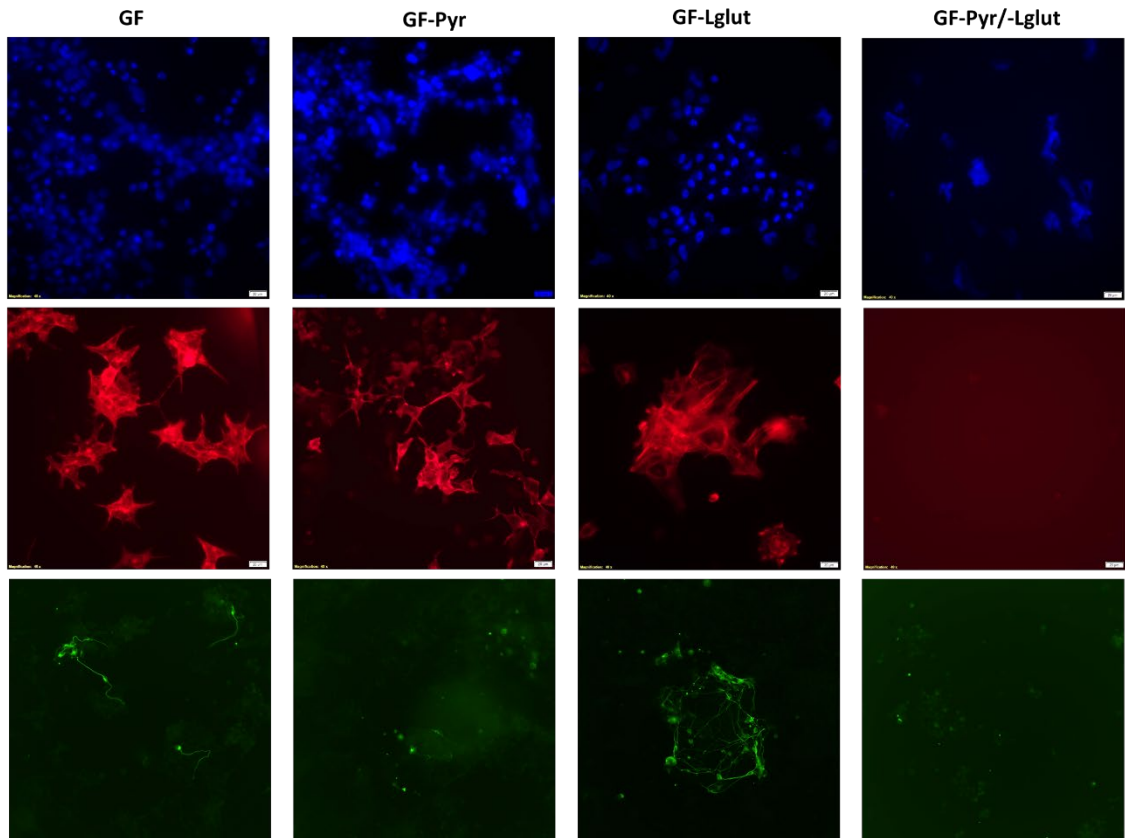


Figure 5.2 Growth and viability of NE-4C cells in GF, GF-Pyr, GF-Lglut, GF-Pyr-Lglut at 5 DIV. **A)** Cell density. **B)** β -III tubulin expression. **C)** Neurite number. **D)** Cell volume. **E)** MTT viability assay. **F) Top panel:** DAPI labelled nuclei showing cell density. **Middle panel:** Actin labelled cytoskeleton of cells. **Bottom panel:** β -III tubulin labelled neurons. (N = 3 independently for each assay). One-way ANOVA with a post hoc Bonferroni Multiple Comparisons test at 5 DIV. Scale bar = 20 μ m in F respectively. **P<0.01, ***P<0.0001

To determine if these morphological and cellular reductions in cell health can be rescued by ketone supplementation, β OHB was added to each condition. An overall effect of the growth media ($F=9.5$, $p<0.0001$) and the addition β OHB ($F=12.2$, $p=0.0006$) was observed. No significant interaction effect was observed for NE-4C cell density. Post hoc testing media conditions revealed significant effects comparing GF and GF-Pyr-Lglut ($t=3.5$, $p=0.0033$), GF-Pyr and GF-Lglut ($t=3.7$, $p=0.0018$) and GF-Pyr and GF-Pyr-Lglut ($t=4.7$, $p=<0.0001$) conditions. Post hoc testing the control media conditions revealed NE-4C cell density was significantly less comparing GF-Pyr-Lglut to GF ($t=2.8$, $p=0.0302$) and GF-Pyr conditions ($t=3.9$, $p=0.001$). Post hoc testing the media conditions supplemented with 10 mM β OHB revealed cell density was significantly less comparing GF-Lglut + 10 mM β OHB ($t=2.8$, $p=0.0333$) and GF-Pyr-Lglut + 10 mM β OHB ($t=2.7$, $p=0.0426$) to GF-Pyr + 10 mM β OHB conditions. Post hoc testing comparing the control media conditions to the β OHB supplemented media conditions revealed cell density was significantly higher in GF-Pyr-Lglut + 10 mM β OHB ($t=2.8$, $p=0.0212$) when compared to GF-Pyr-Lglut conditions (Fig. 5.3A, F).

An overall effect of the growth media ($F=15.8$, $p=<0.0001$) and the addition of β OHB ($F=4.5$, $p=0.0357$) was observed for NE-4C β -III tubulin expression levels. No significant interaction effect was observed. Post hoc testing media conditions revealed significant effects comparing GF and GF-Lglut ($t=4.9$, $p=<0.0001$), GF-Pyr and GF-Lglut ($t=5.0$, $p=<0.0001$) and GF-Lglut and GF-Pyr-Lglut ($t=6.6$, $p=<0.0001$) conditions. Post-hoc testing the control media conditions revealed β -III tubulin expression levels were significantly less comparing GF ($t=3.5$, $p=0.0042$), GF-Pyr ($t=3.3$, $p=0.0067$) and GF-Pyr-Lglut ($t=4.9$, $p=<0.0001$). Post hoc testing the media conditions supplemented with 10 mM β OHB revealed cell density was significantly less comparing GF + 10 mM β OHB ($t=3.5$, $p=0.0034$), GF-Pyr + 10 mM β OHB ($t=4.0$, $p=0.0006$) and GF-Pyr-Lglut + 10 mM β OHB ($t=4.5$, $p=<0.0001$) when compared to GF-Lglut + 10 mM β OHB conditions. No significant differences were observed between the control media groups and their β OHB supplemented counterparts (Fig. 5.3B, F). No overall effect of the growth media and the addition of β OHB was observed for the number of neurites or cell volume, thus post-hoc testing was not performed (Fig. 5.3C, D, F).

An overall effect of the growth media ($F=11.1$, $p=0.0004$) was observed for NE-4C cell viability. No effect following the addition of β OHB, or interaction effect was observed. Post hoc testing the control media conditions revealed significant effects comparing GF-Pyr and

GF-Lglut ($t=4.7$, $p=0.0014$) and GF-Pyr and GF-Pyr-Lglut ($t=5.1$, $p=0.0006$). Post hoc testing the media conditions supplemented with 10 mM β OHB revealed that cell viability was significantly less comparing GF + 10 mM β OHB ($t=3.8$, $p=0.0099$), GF-Lglut + 10 mM β OHB ($t=4.5$, $p=0.002$) and GF-Pyr-Lglut + 10 mM β OHB ($t=5.0$, $p=0.0009$) to GF-Pyr + 10 mM β OHB. No significant differences were observed between the control media groups and their β OHB supplemented counterparts (Fig. 5.3E, F).

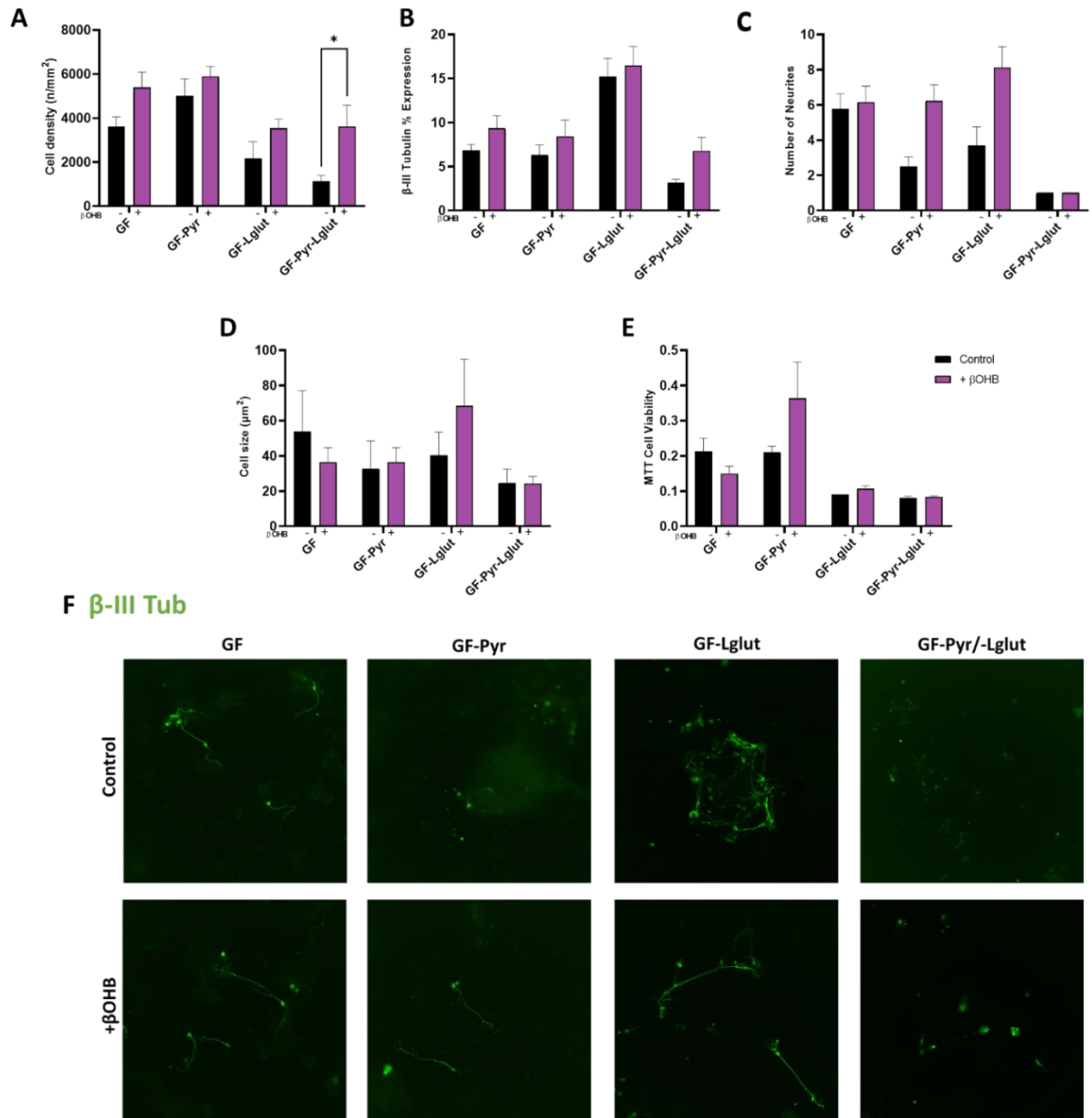


Figure 5.3 Growth and viability of NE-4C cells in GF, GF-Pyr, GF-Lglut, GF-Pyr-Lglut conditions at 5 DIV compared to 10 mM β OHB supplemented conditions. **A)** Cell density. **B)** β -III tubulin expression. **C)** Neurite number. **D)** Cell volume. **E)** Metabolic viability. **F) Top panel:** DAPI labelled nuclei showing cell density. **Middle panel:** Actin labelled cytoskeleton of cells. **Bottom panel:** β -III tubulin labelled neurons. (N = 3 independently for each assay). Two-way ANOVA with a post hoc Bonferroni Multiple Comparisons test comparing GF conditions to β OHB supplemented conditions at 5 DIV. Scale bar = 20 μ m in F respectively. * $P < 0.05$

5.4.3 The Impact of Substrate Deprivation and β OHB Supplementation on Differentiated NE-4C Viability, Density, and Morphology at 10 DIV

An overall effect of substrate deprivation on cell density was observed at 10DIV ($F=26.3$, $p<0.0001$). Post-hoc testing revealed cell density was significantly less comparing GF-Pyr ($t=3.8$, $p=0.0019$), GF-Lglut ($t=7.1$, $p<0.0001$) and GF-Pyr-Lglut ($t=7.9$, $p<0.0001$) were compared to GF conditions at 10DIV. Additionally, cell density was significantly less in GF-Lglut ($t=3.4$, $p=0.0067$) and GF-Pyr-Lglut ($t=4.0$, $p=0.0007$) when compared to GF-Pyr conditions at 10DIV (Fig. 5.4A, F).

No overall significant effect of substrate deprivation on β -III tubulin expression was observed at 10DIV. Post hoc testing was not performed (Fig. 5.4B, F).

An overall effect of substrate deprivation on neurite number was observed at 10DIV ($F=4.4$, $p=0.0184$). Post-hoc testing revealed that the number of neurites is significantly higher comparing GF-Lglut ($t=2.8$, $p=0.0227$) to GF-Pyr conditions at 10 DIV (Fig. 5.4C, F).

No overall significant effect of substrate deprivation on cell volume was observed at 10DIV. Post hoc testing was not performed (Fig. 5.4D, F).

An overall effect of substrate deprivation on cell viability was observed at 10DIV ($F=13.0$, $p=0.0019$). Post-hoc testing revealed that cell viability was significantly less comparing GF-Lglut ($t=3.9$, $p=0.0272$) and GF-Pyr-Lglut ($t=4.6$, $p=0.0106$) to GF conditions at 10DIV. Additionally, cell viability was significantly less comparing GF-Lglut ($t=4.2$, $p=0.0185$) and GF-Pyr-Lglut ($t=4.9$, $p=0.0074$) to GF-Pyr conditions (Fig. 5.4E, F).

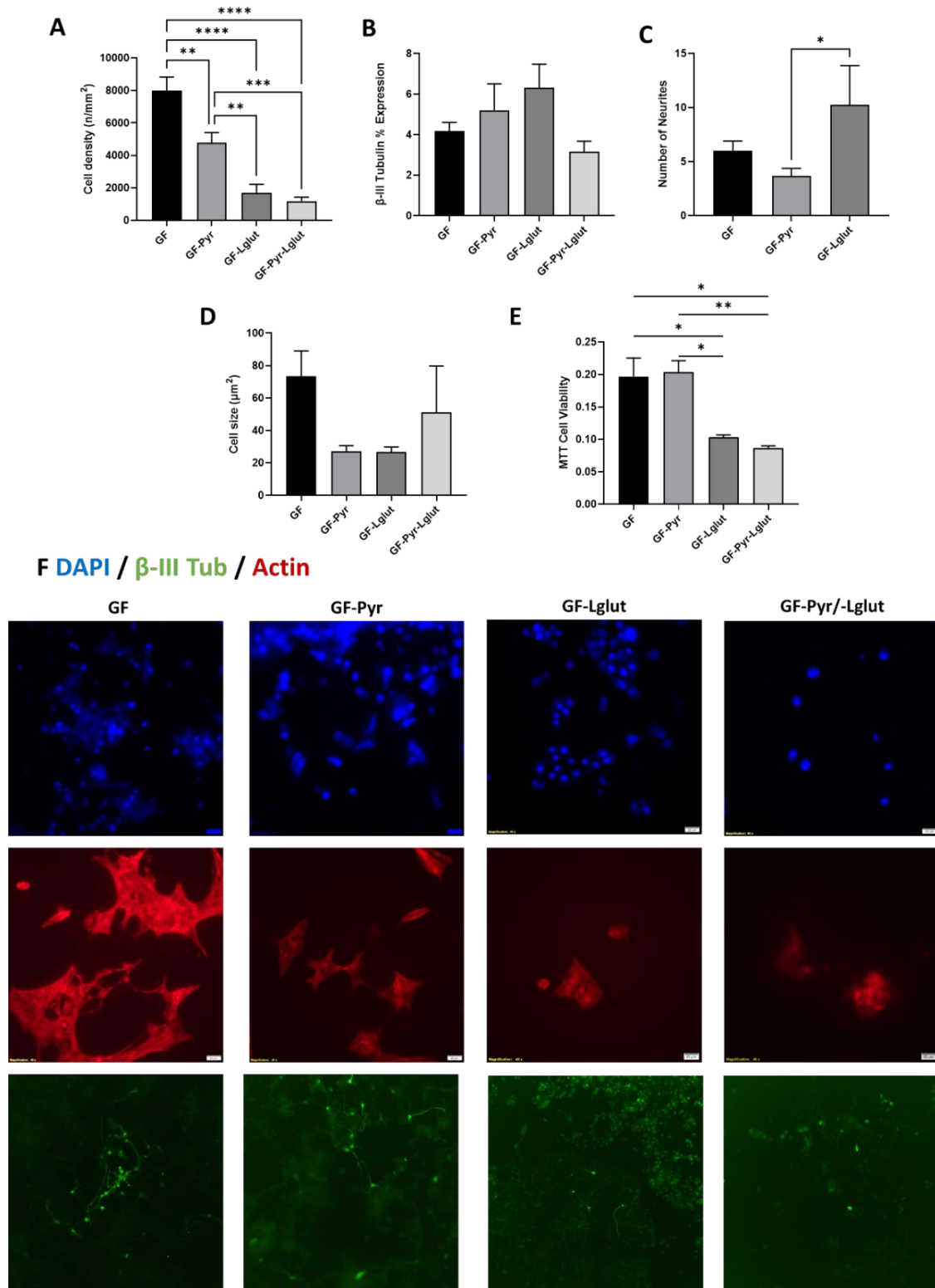


Figure 5.4 Growth and viability of NE-4C cells in GF, GF-Pyr, GF-Lglut, GF-Pyr-Lglut at 10 DIV. **A)** Cell density. **B)** β -III tubulin expression. **C)** Neurite number. **D)** Cell volume. **E)** Metabolic viability. **F) Top panel:** DAPI labelled nuclei showing cell density. **Middle panel:** Actin labelled cytoskeleton of cells. **Bottom panel:** β -III tubulin labelled neurons. (N = 3 independently for each assay). One-way ANOVA with a post hoc Bonferroni Multiple Comparisons test comparing GF conditions at 10 DIV. Scale bar = 20 μ m in F respectively. *P<0.05, **P<0.01, ***P<0.001, ****P<0.0001.

An overall effect of the growth medium ($F=11.0$, $t<0.0001$) and an interaction between the growth medium and the addition of β OHB ($F=20.0$, $p<0.0001$) for NE-4C cell density was observed at 10DIV. Post hoc testing media conditions revealed significant effects comparing GF and GF-Pyr-Lglut ($t=5.0$, $p<0.0001$), GF-Pyr and GF-Pyr-Lglut ($t=4.6$, $p<0.0001$) and GF-Lglut and GF-Pyr-Lglut ($t=2.8$, $p=0.0308$). Post hoc testing the control media conditions revealed cell density was significantly less comparing GF-Pyr ($t=3.5$, $p=0.0030$), GF-Lglut ($t=6.7$, $p<0.0001$) and GF-Pyr-Lglut ($t=6.2$, $p<0.0001$) to GF conditions. Additionally, cell density was significantly less comparing GF-Lglut ($t=3.2$, $p=0.0103$) to GF-Pyr conditions. Post hoc testing the media conditions supplemented with β OHB revealed cell density was significantly less comparing GF + 10 mM β OHB to GF-Pyr + 10 mM β OHB ($t=3.2$, $p=0.0182$) and GF-Lglut + 10 mM β OHB conditions ($t=4.1$, $p=0.0003$). Additionally, cell density was significantly less comparing GF-Pyr-Lglut + 10 mM β OHB to GF-Pyr + 10 mM β OHB ($t=4.1$, $p=0.0004$) and to GF-Lglut + 10 mM β OHB ($t=5.0$, $p<0.0001$) conditions. Post hoc testing comparing the control media conditions to the β OHB supplemented conditions revealed cell density was significantly lower in GF + 10 mM β OHB ($t=6.5$, $p<0.0001$) when compared to GF and cell density was significantly higher in GF-Lglut + 10 mM β OHB ($t=4.5$, $p<0.0001$) when compared to GF-Lglut conditions (Fig. 5.5A, F).

An overall effect of the growth medium ($F=9.8$, $p<0.0001$), the addition of β OHB ($F=11.6$, $p=0.008$) and an interaction ($F=4.5$, $p=0.0047$) effect between them was observed for the expression levels of β -III tubulin for NE-4C cells at 10DIV. Post hoc testing media conditions revealed significant effects comparing GF and GF-Lglut ($t=4.9$, $p<0.0001$), GF-Pyr and GF-Lglut ($t=3.2$, $p=0.0109$) and GF-Lglut and GF-Pyr-Lglut ($t=4.7$, $p<0.0001$) conditions. Post hoc testing the control media conditions revealed no significant differences between the media groups. Post hoc testing the media conditions supplemented with 10 mM β OHB revealed that β -III tubulin expression was significantly less comparing GF + 10 mM β OHB ($t=6.2$, $p<0.0001$), GF-Pyr + 10 mM β OHB ($t=4.5$, $p<0.0001$) and GF-Pyr-Lglut + 10 mM β OHB ($t=5.5$, $p<0.0001$) to GF-Lglut + 10 mM β OHB conditions at 10DIV. Post hoc testing comparing the control media conditions to the β OHB supplemented conditions revealed β -III tubulin levels were significantly higher in GF-Lglut + 10 mM β OHB ($t=4.4$, $p<0.0001$) when compared to GF-Lglut at 10DIV (Fig. 5.5B, F).

An overall effect of the growth medium ($F=8.7$, $p=0.0003$) was observed for the number of neurites in the NE-4C Cells at 10DIV. No significant effect was observed following the addition of β OHB treat and no significant interaction was observed. Post hoc testing media conditions revealed significant effects comparing GF and GF-Lglut ($t=4.0$, $p=0.0004$) and GF-Pyr and GF-Lglut ($t=3.8$, $p=0.0007$). Post hoc testing the control media conditions revealed no significant differences between media conditions. Post hoc testing the media conditions supplemented with 10 mM β OHB revealed the number of neurites were significantly less comparing GF + 10 mM β OHB ($t=5.2$, $p<0.0001$) and GF-Pyr + 10 mM β OHB ($t=4.3$, $p=0.0001$) to GF-Lglut + 10 mM β OHB conditions. No significant differences were observed between the control media groups and their β OHB supplemented counterparts (Fig. 5.5C, F).

No overall significant effect of the growth media or the addition of β OHB was observed on cell volume thus post hoc testing was not undertaken (Fig 5.5D, F).

An overall effect of the growth media ($F=10.9$, $p=0.0004$) and an interaction effect ($F=3.3$, $p=0.0483$) was observed in NE-4C cell viability at 10DIV following the addition of 10 mM β OHB. Post-hoc testing media conditions revealed significant effects comparing GF-Pyr and GF-Lglut ($t=3.4$, $p=0.0206$) and GF-Pyr and GF-Pyr-Lglut ($t=5.7$, $p=0.0002$). Post hoc testing the control media conditions revealed no significant differences between media conditions. Post hoc testing the media conditions supplemented with 10 mM β OHB revealed that cell viability was significantly less in GF + 10 mM β OHB ($F=3.8$, $p=0.0102$) and GF-Pyr-Lglut + 10 mM β OHB when compared to GF-Pyr + 10 mM β OHB at 10DIV. No significant differences were observed between the control medias and their β OHB supplemented counterparts (Fig. 5.5E, F).

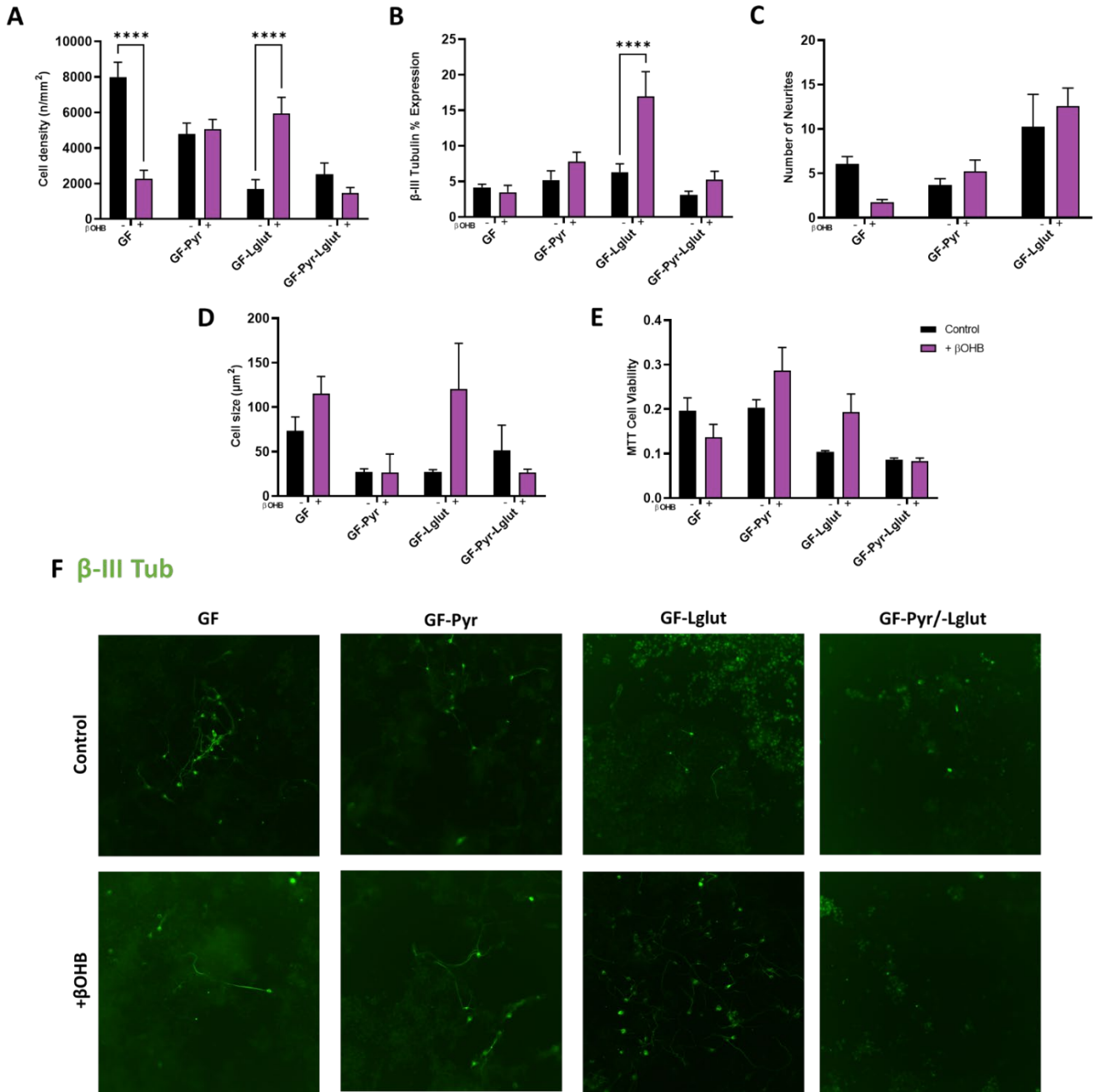


Figure 5.5 Growth and viability of NE-4C cells in GF, GF-Pyr, GF-Lglut, GF-Pyr-Lglut conditions at 10 DIV compared to 10 mM β OHB supplemented conditions. **A)** Cell density. **B)** β -III tubulin expression. **C)** Neurite number. **D)** Cell volume. **E)** Metabolic viability. **F) Top panel:** DAPI labelled nuclei showing cell density. **Middle panel:** Actin labelled cytoskeleton of cells. **Bottom panel:** β -III tubulin labelled neurons. (N = 3 independently for each assay). Two-way ANOVA with a post hoc Bonferroni Multiple Comparisons test comparing GF conditions to β OHB supplemented conditions at 10 DIV. Scale bar = 20 μ m in F respectively. ****P<0.0001.

5.4.4 The Impact of Substrate Deprivation and β OHB Supplementation on Differentiated NE-4C Viability, Density, and Morphology at 15 DIV

An overall effect of substrate deprivation on cell density was observed at 15DIV ($F=58.0$, $p<0.0001$). Post-hoc testing revealed cell density was significantly less comparing in GF-Pyr ($t=5.1$, $p<0.0001$), GF-Lglut ($t=11.0$, $p<0.0001$) and GF-Pyr-Lglut ($t=11.12$, $p<0.0001$) to GF conditions. Additionally, cell density was significantly less comparing GF-Lglut ($t=5.7$, $p<0.0001$) and GF-Pyr-Lglut ($t=6.1$, $p<0.0001$) to GF-Pyr conditions (Fig. 5.6A, F).

An overall effect of substrate deprivation on β -III tubulin expression was observed at 15DIV ($F=5.4$, $p=0.0017$). Post-hoc testing revealed that β -III tubulin expression was significantly less comparing GF-Lglut ($t=3.0$, $p=0.0183$) and GF-Pyr-Lglut ($t=3.4$, $p=0.0069$) to GF conditions (Fig. 5.6B, F).

No overall significant effect of substrate deprivation on the number of neurites was observed at 15DIV. Post hoc testing was not performed (Fig. 5.6C, F)

An overall effect of substrate deprivation on cell volume was observed at 15DIV ($F=5.1$, $p=0.0288$). Post-hoc testing revealed cell density was significantly less comparing GF-Lglut ($t=3.6$, $p=0.043$) to GF conditions (Fig. 5.6D, F)

No overall significant effect of substrate deprivation on cell viability was observed at 15DIV. Thus post hoc testing was not performed (Fig 5.6E, F).

An overall effect of the growth media ($F=28.6$, $p<0.0001$) and the addition of β OHB ($F=5.0$, $p=0.0258$) and an interaction effect ($F=16.10$, $p<0.0001$) was observed for NE-4C cell density at 15DIV. Post hoc testing media conditions revealed significant differences comparing GF and GF-Lglut ($t=5.2$, $p<0.0001$), GF and GF-Pyr-Lglut ($t=8.9$, $p<0.0001$), GF-Pyr and GF-Pyr-Lglut ($t=6.6$, $p<0.0001$) and GF-Lglut and GF-Pyr-Lglut ($t=4.4$, $p=0.0001$). Post-hoc testing the control media conditions revealed cell density was significantly less comparing GF-Pyr ($t=5.0$, $p<0.0001$), GF-Lglut ($t=8.5$, $p<0.0001$) and GF-Pyr-Lglut ($t=7.4$, $p<0.0001$) to GF conditions at 15DIV. Additionally cell density was significantly less comparing GF-Lglut ($t=3.2$, $p=0.0084$) and GF-Pyr-Lglut ($t=3.3$, $p=0.0084$) to GF-Pyr conditions at 15DIV. Post hoc testing the media conditions supplemented with 10 mM β OHB revealed cell density was significantly less comparing GF-Pyr-Lglut + 10 mM β OHB to GF + 10 mM β OHB ($t=5.0$, $p<0.0001$), GF-Pyr + 10 mM

β OHB ($t=6.7$, $p<0.0001$) and GF-Lglut + 10 mM β OHB ($t=6.3$, $p<0.0001$) conditions. Post hoc testing comparing the control media conditions and the β OHB supplemented media conditions revealed that cell density was significantly less comparing GF + 10 mM β OHB to GF ($t=3.9$, $p=0.0007$) and was significantly higher comparing GF-Pyr + 10 mM β OHB to GF-Pyr ($t=2.7$, $p=0.0301$) and when comparing GF-Lglut + 10 mM β OHB to GF-Lglut ($t=5.7$, $p<0.0001$) (Fig. 5.7A, F).

An overall effect of the growth media ($F=11.8$, $p<0.0001$), and the addition of β OHB ($F=7.3$, $p=0.0001$) and an interaction effect ($F=4.9$, $p=0.0279$) was observed for the expression levels of β -III tubulin in NE-4C cells at 15DIV. Post hoc testing media conditions revealed significant differences comparing GF-Pyr and GF-Pyr-Lglut ($t=3.8$, $p=0.0013$) and GF-Lglut and GF-Pyr-Lglut ($t=4.1$, $p=0.0003$). Post hoc testing the control media conditions revealed β -III tubulin expression was significantly less in GF-Pyr-Lglut ($t=2.9$, $p=0.0275$) when compared to GF conditions at 15DIV. Post hoc testing the media conditions supplemented with 10 mM β OHB revealed β -III tubulin expression was significantly less comparing GF + 10 mM β OHB to GF-Pyr + 10 mM β OHB ($t=3.9$, $p=0.0052$) and to GF-Lglut + 10 mM β OHB ($t=5.6$, $p<0.0001$) conditions. Additionally, β -III tubulin expression was significantly less comparing GF-Pyr-Lglut + 10 mM β OHB to GF-Pyr + 10 mM β OHB ($t=3.2$, $p=0.0102$) and to GF-Lglut + 10 mM β OHB ($t=5.4$, $p<0.0001$) conditions. Post hoc testing between the control medium and the media conditions supplemented with 10 mM β OHB treated media revealed β -III tubulin expression was significantly less in GF + 10 mM β OHB ($t=2.7$, $p=0.0268$) compared to GF conditions and was significantly higher in GF-Lglut + 10 mM β OHB ($t=5.6$, $p<0.0001$) compared to GF-Lglut (Fig. 5.7B, F).

An overall effect of the addition of β OHB ($F=8.5$, $p=0.0050$) was observed for the overall number of neurites at 15DIV. No significant media effect or interaction effect was observed. Post hoc testing between the control medium and the media conditions supplemented with 10 mM β OHB revealed that neurite number was significantly higher in the GF-Pyr + 10 mM β OHB ($t=3.0$, $p=0.0080$) compared to GF-Pyr (Fig. 5.7C, F). An overall effect of the addition of β OHB ($F=4.8$, $p=0.0437$) was observed for NE-4C cell volume at 15DIV. No significant media effect or interaction effect was observed. Post hoc testing between the control medium and the β OHB treated media revealed no significant differences between the media groups (Fig. 5.7D, F). No overall media effect or β OHB and the interaction of

β OHB with the control medium was observed, thus post hoc tests were not performed (Fig. 5.7E, F).

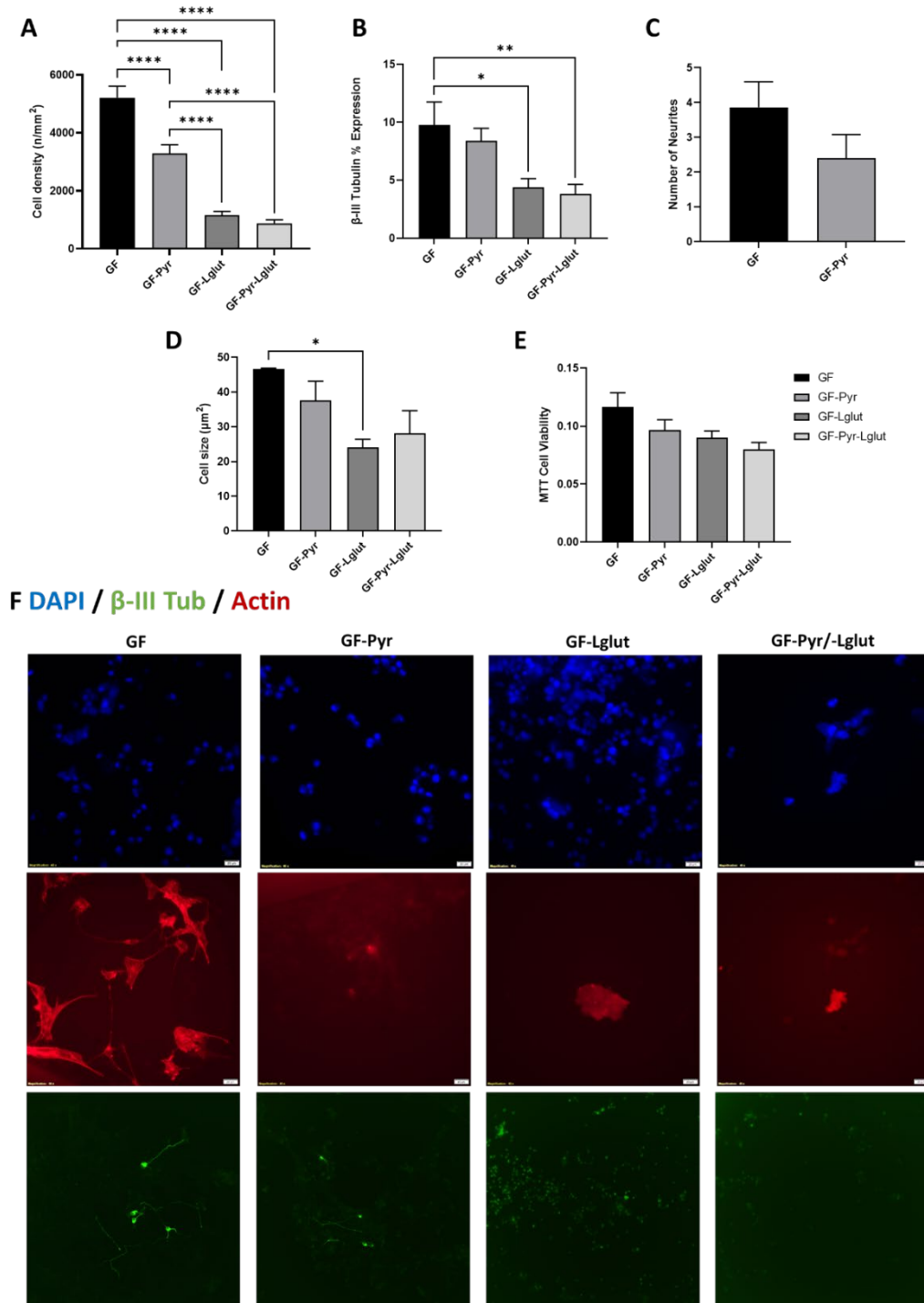
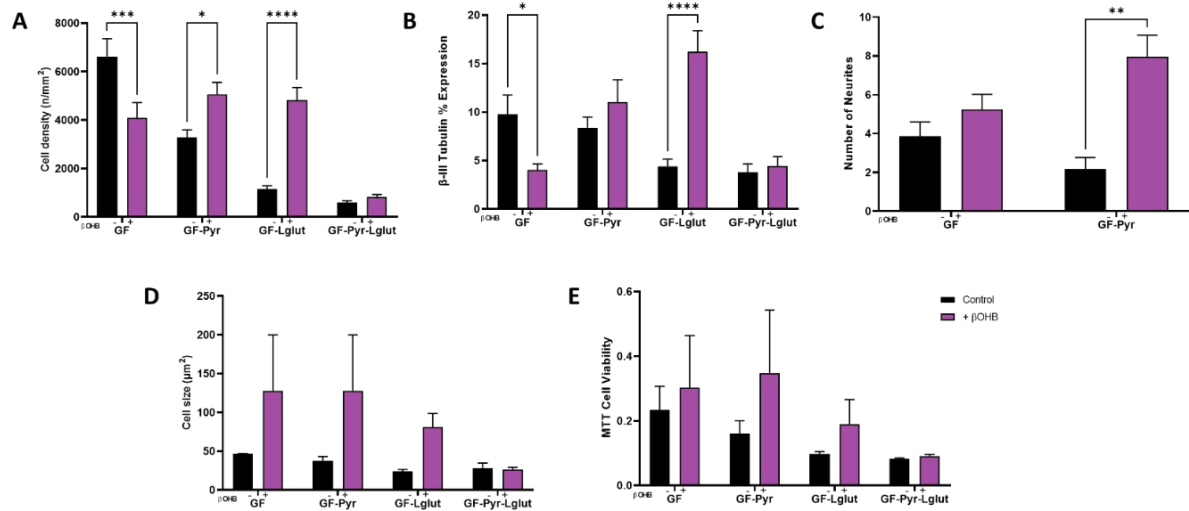


Figure 5.6 Growth and viability of NE-4C cells in GF, GF-Pyr, GF-Lglut, GF-Pyr-Lglut at 15 DIV. **A)** Cell density. **B)** β -III tubulin expression. **C)** Neurite number. **D)** Cell volume. **E)** Metabolic viability. **F) Top panel:** DAPI labelled nuclei showing cell density. **Middle panel:** Actin labelled cytoskeleton of cells. **Bottom panel:** β -III tubulin labelled neurons. (N = 3 independently for each assay). One-way ANOVA with a post hoc Bonferroni Multiple Comparisons test comparing GF conditions at 15 DIV. Scale bar = 20 μ m in F respectively. *P<0.05, **P<0.01, ****P<0.0001.



F β-III Tub

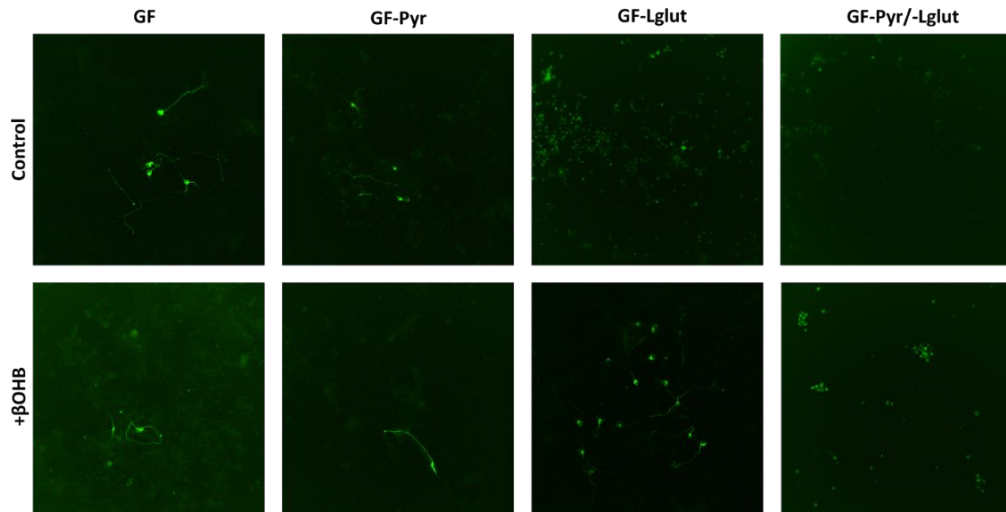


Figure 5.7 Growth and viability of NE-4C cells in GF, GF-Pyr, GF-Lglut, GF-Pyr-Lglut conditions at 15 DIV compared to 10 mM βOHB supplemented conditions. **A)** Cell density. **B)** β-III tubulin expression. **C)** Neurite number. **D)** Cell volume. **E)** Metabolic viability. **F) Top panel:** DAPI labelled nuclei showing cell density. **Middle panel:** Actin labelled cytoskeleton of cells. **Bottom panel:** β-III tubulin labelled neurons. (N = 3 independently for each assay). One-way ANOVA with post hoc Sidák's test comparing GF conditions to βOHB supplemented conditions at 15 DIV. Two-way ANOVA with post hoc Bonferroni Multiple Comparisons test at 15 DIV. Scale bar = 20 μm in F respectively. *P<0.05, ***P<0.001, ****P<0.0001.

5.4.5 The Effects of Glucose Deprivation on Differentiating SH-SY5Y Density, Phenotype, Morphology and Metabolic Viability

An overall effect of time ($F=12.5$, $p=0.0007$) for SH-SY5Y cell density was observed. No significant growth media effect or interaction effect was observed. Post hoc testing of the growth media over time revealed that cell density was significantly higher comparing LG ($t=3.4$, $p=0.002$) from 5DIV to 15DIV (Fig. 5.8A, G).

An overall effect of growth media ($F=34.12$, $p<0.0001$) and interaction effect of time and growth media ($F=4.5$, $p=0.0020$) on β -III tubulin expression levels was observed. No significant time effect was observed. Post hoc testing within media conditions comparing time revealed that β -III tubulin expression was significantly higher comparing 15DIV ($t=2.7$, $p=0.037$) to 5DIV in RG conditions. Additionally, β -III tubulin expression was significantly less comparing 15DIV ($t=3.0$, $p=0.0169$) to 5DIV in GF conditions. Post hoc testing within time comparing growth media revealed that β -III tubulin expression was significantly less comparing GF to RG ($t=5.6$, $p<0.0001$) and to LG ($t=4.8$, $p<0.0001$) conditions at 10DIV. Additionally, at 15 DIV, β -III tubulin expression was significantly less comparing GF to RG ($t=49.7$, $p<0.0001$) and LG ($t=41.0$, $p<0.0001$) conditions (Fig. 5.8B, G).

An overall effect of growth media ($F=43.8$, $p<0.0001$), time ($F=10.6$, $p=0.0005$) and an interaction effect between growth media and time ($F=4.7$, $p=0.0014$) for the number of neurites was observed. Post-hoc testing comparing time revealed significant differences between 5DIV and 15DIV ($t=2.5$, $p=0.0379$) and 10DIV and 15DIV ($t=4.5$, $p<0.0001$). Post-hoc testing within media conditions comparing time revealed that the number of neurites were significantly higher comparing 10DIV ($t=2.8$, $p=0.0326$) to 5DIV in RG conditions. Additionally, the number of neurites were significantly higher comparing 10DIV ($t=3.8$, $p=0.0024$) to 5DIV and was significantly less comparing 15DIV ($t=4.4$, $p=0.0005$) to 10DIV in LG conditions. The number of neurites were significantly less comparing 15DIV ($t=2.7$, $p=0.0378$) to 5DIV in GF conditions. Post-hoc testing within time comparing media conditions revealed that the number of neurites were significantly less comparing GF to RG ($t=9.5$, $p<0.0001$) and LG ($t=7.6$, $p<0.0001$) conditions at 10DIV. Additionally, the number of neurites were significantly less comparing LG ($t=3.0$, $p=0.0129$) to RG conditions at 15DIV. The number of neurites were significantly less comparing GF to RG ($t=6.4$, $p<0.0001$) and LG ($t=3.2$, $p=0.0078$) conditions (Fig. 5.8C, G).

An overall time effect ($F=5.3$, $p=0.0154$) was observed for SH-SY5Y cell volume over 15DIV. No growth media effect or interaction effect was observed. Post-hoc testing

comparing time revealed that significant effects were observed between 5DIV and 15DIV ($t=3.0$, $p=0.0224$). Post hoc testing with media conditions comparing revealed that cell volume was significantly larger comparing 10DIV ($t=3.0$, $p=0.0206$) to 5DIV in LG conditions (Fig. 5.8D, G).

An overall media effect ($F=38.0$, $p<0.0001$) was observed for SH-SY5Y cell viability over 15DIV. No time effect or interaction effect was observed. Post-hoc testing within time comparing media conditions revealed that cell viability was significantly less comparing GF to RG ($t=4.6$, $p=0.0006$) and LG ($t=4.5$, $p=0.0008$) conditions at 5DIV. At 10DIV, cell viability was significantly less comparing GF to RG ($t=4.5$, $p=0.0007$) and LG ($t=4.4$, $p=0.0011$) conditions. At 15DIV, cell viability was significantly less comparing GF to RG ($t=4.6$, $p=0.0004$) and LG ($t=4.4$, $p=0.0257$) conditions (Fig 5.8E, G).

An overall media effect ($F=16.5$, $p<0.0001$) was observed for SH-SY5Y cell viability following the addition of 10 mM β OHB. No significant time effect or interaction effect was observed. Post-hoc testing within time comparing media conditions revealed no significant differences between media groups (Fig. 5.8F, G).

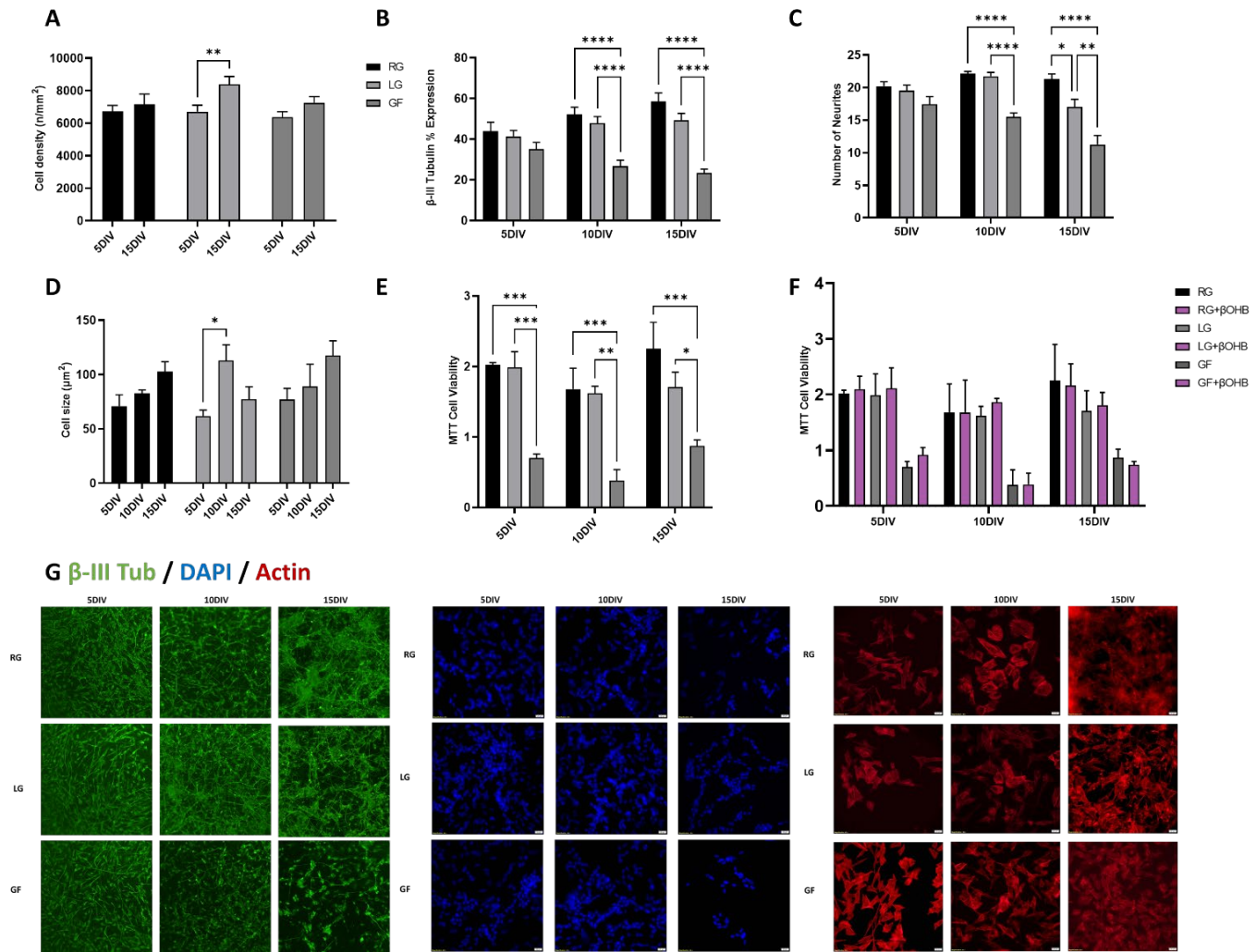


Figure 5.8 Growth and viability of SH-SY5Y cells in RG, LF and GF condition at 5, 10 and 15 DIV. **A)** Cell density. **B)** β -III tubulin expression. **C)** Neurite number. **D)** Cell volume. **E)** MTT viability assay. **F)** MTT viability assay for β OHB groups. **G) Left panel:** β -III labelled neurons in RG, LG, and GF conditions. **Middle panel:** DAPI labelled nuclei showing cell density in RG, LG, and GF conditions. **Right panel:** Actin labelled cytoskeleton of cells in RG, LG, and GF conditions. (N = 3 independently for each assay). Two-way ANOVA with a post hoc Bonferroni Multiple Comparisons test comparing GF conditions over 5, 10 and 15 DIV. Scale bar = 20 μ m in F. ** $P < 0.01$, **** $P < 0.0001$.

5.4.6 The Impact of Substrate Deprivation and β OHB Supplementation on Differentiated SH-SY5Y Viability and Density and Morphology at 5 DIV

An overall effect of substrate deprivation on cell density was observed at 5DIV ($F=18.6$, $p < 0.0001$). Post-hoc testing revealed cell density was significantly less comparing GF-Pyr-Lglut to GF ($t=6.6$, $p < 0.0001$), GF-Pyr ($t=6.2$, $p < 0.0001$) and GF-Lglut ($t=5.0$, $p < 0.0001$) conditions (Fig. 5.9A, F).

An overall effect of substrate deprivation on β -III tubulin expression was observed at 5DIV ($F=4.5$, $p=0.0050$). Post-hoc testing revealed β -III tubulin expression was significantly less comparing GF-Pyr-Lglut ($t=3.4$, $p=0.0056$) to GF-Pyr conditions (Fig. 5.9B, F).

An overall effect of substrate deprivation on neurite number was observed at 5DIV ($F=12.5$, $p<0.0001$). Post-hoc testing revealed neurite number was significantly less comparing GF-Pyr-Lglut conditions to GF ($t=5.7$, $p<0.0001$), GF-Pyr ($t=4.8$, $p<0.0001$) and GF-Lglut ($t=3.7$, $p=0.0018$) conditions (Fig. 5.9C, F).

No overall significant effect of substrate deprivation on cell volume and cell viability was observed at 5DIV. Post hoc testing was not performed (Fig. 5.9D, E, F)

An overall effect of growth media ($F=10.3$, $p<0.0001$) and the addition of β OHB ($F=8.9$, $p=0.0032$) was observed for SH-SY5Y cell density at 5DIV. No interaction effect was observed. Post hoc testing within media conditions revealed significant differences comparing GF and GF-Pyr-Lglut ($t=4.9$, $p<0.0001$), GF-Pyr and GF-Pyr-Lglut ($t=4.7$, $p<0.0001$) and GF-Lglut and GF-Pyr-Lglut ($t=3.1$, $p=0.0121$). Post-hoc testing within the control media conditions revealed cell density was significantly less comparing GF-Pyr-Lglut to GF ($t=4.0$, $p=0.0005$), GF-Pyr ($t=2.9$, $p=0.0013$) and GF-Lglut ($t=2.8$, $p=0.0352$). Post hoc testing within the β OHB supplemented conditions revealed that cell density was significantly less comparing GF-Pyr-Lglut + 10 mM β OHB to GF + 10 mM β OHB ($t=2.9$, $p=0.0249$) and GF-Pyr + 10 mM β OHB ($t=2.9$, $p=0.0216$). No significant differences were observed when the control media conditions were compared to the β OHB supplemented conditions (Fig. 5.10A, F).

An overall effect of the addition of β OHB ($F=8.3$, $p=0.0044$) was observed for the expression levels of β -III tubulin at 5DIV. No overall media effect or interaction effect was observed. Post hoc testing comparing the control media conditions to the β OHB supplemented conditions revealed that β -III tubulin expression levels were significantly higher comparing GF-Lglut + 10 mM β OHB to GF-Lglut ($t=2.5$, $p=0.0465$) (Fig. 5.10B, F).

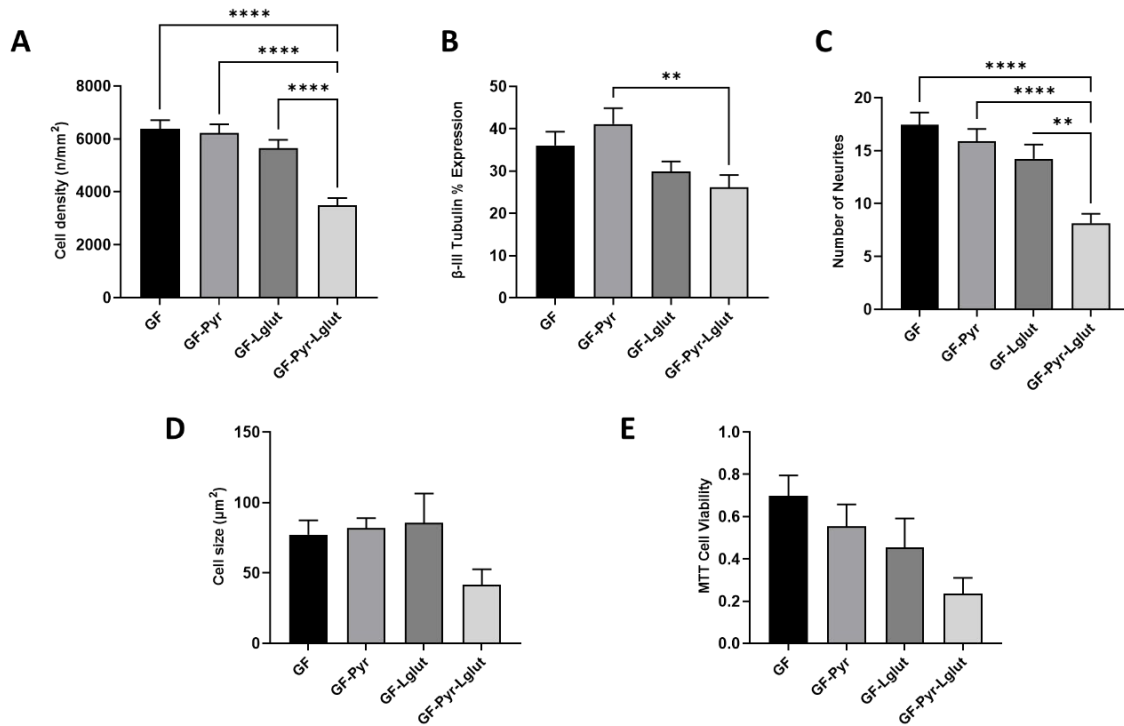
An overall effect of the growth media ($F=23.8$, $p<0.0001$) and the addition of β OHB was observed ($F=23.4$, $p<0.0001$) for the number of neurites at 5DIV. No interaction effect was observed. Post hoc testing within media conditions revealed significant differences comparing GF and GF-Lglut ($t=3.7$, $p=0.0055$), GF and GF-Pyr-Lglut ($t=8.1$, $p<0.0001$), GF-Pyr and GF-Pyr-Lglut ($t=6.1$, $p<0.0001$) and GF-Lglut and GF-Pyr-Lglut ($t=4.8$, $p<0.0001$). Post hoc testing within the control media conditions revealed that the number

of neurites were significantly less comparing GF-Pyr-Lglut to GF ($t=6.2$, $p<0.0001$), GF-Pyr ($t=5.1$, $p<0.0001$) and GF-Lglut ($t=4.0$, $p=0.0005$). Post hoc testing within the β OHB supplemented conditions revealed that the number of neurites were significantly less comparing GF-Pyr-Lglut + 10 mM β OHB to GF + 10 mM β OHB ($t=5.3$, $p<0.0001$), GF-Pyr + 10 mM β OHB ($t=3.4$, $p=0.0045$) and GF-Lglut + 10 mM β OHB ($t=2.7$, $p=0.0438$). Post hoc testing comparing the control media conditions to the β OHB supplemented conditions revealed that the number of neurites were significantly greater comparing GF + 10 mM β OHB ($t=2.5$, $p=0.0476$) to GF and when comparing GF-Pyr-Lglut + 10 mM β OHB ($t=3.4$, $p=0.0032$) to GF-Pyr-Lglut (Fig. 5.10C, F).

No overall effect of the growth media, the addition of β OHB or an interaction effect was observed for cell volume, thus post hoc testing was not performed (Fig. 5.10D, E).

An overall effect of the growth media ($F=33.5$, $p<0.0001$) and the addition of β OHB ($F=33.4$, $p<0.0001$) was observed for cell viability at 5DIV. No interaction effect was observed. Post hoc testing within media conditions revealed significant differences comparing GF-Pyr ($t=3.1$, $p=0.013$), GF-Lglut ($t=4.4$, $p<0.0001$) and GF-Pyr-Lglut ($t=9.8$, $p<0.0001$). Significant differences were also observed comparing GF-Pyr-Lglut to GF-Pyr ($t=6.7$, $p<0.0001$) and GF-Lglut ($t=5.4$, $p<0.0001$). Post hoc testing within the control media conditions revealed that cell viability was significantly less comparing GF-Lglut ($t=3.4$, $p=0.0058$) and GF-Pyr-Lglut ($t=6.4$, $p<0.0001$) to GF conditions. Additionally, cell viability was significantly less comparing GF-Pyr-Lglut to GF-Pyr ($t=4.4$, $p=0.0001$) and GF-Lglut ($t=3.0$, $p=0.0169$). Post hoc testing within the β OHB supplemented conditions revealed that cell viability was significantly less comparing GF-Lglut + 10 mM β OHB ($t=2.8$, $p=0.0341$) and GF-Pyr-Lglut + 10 mM β OHB ($t=7.5$, $p<0.0001$) to GF + 10 mM β OHB conditions. Cell viability was significantly less comparing GF-Pyr-Lglut + 10 mM β OHB to GF-Pyr + 10 mM β OHB ($t=5.0$, $p<0.0001$) and to GF-Lglut + 10 mM β OHB ($t=4.6$, $p<0.0001$) conditions. Post hoc testing between the control media conditions and the β OHB supplemented conditions revealed that cell viability was significantly higher comparing GF + 10 mM β OHB ($t=3.1$, $p=0.0093$), GF-Pyr + 10 mM β OHB ($t=2.7$,

p=0.0308) and GF-Lglut + 10 mM β OHB (t=3.6, p=0.0014) to their respective control media groups (Fig. 5.10E, F).



F DAPI / Actin / β -III Tub

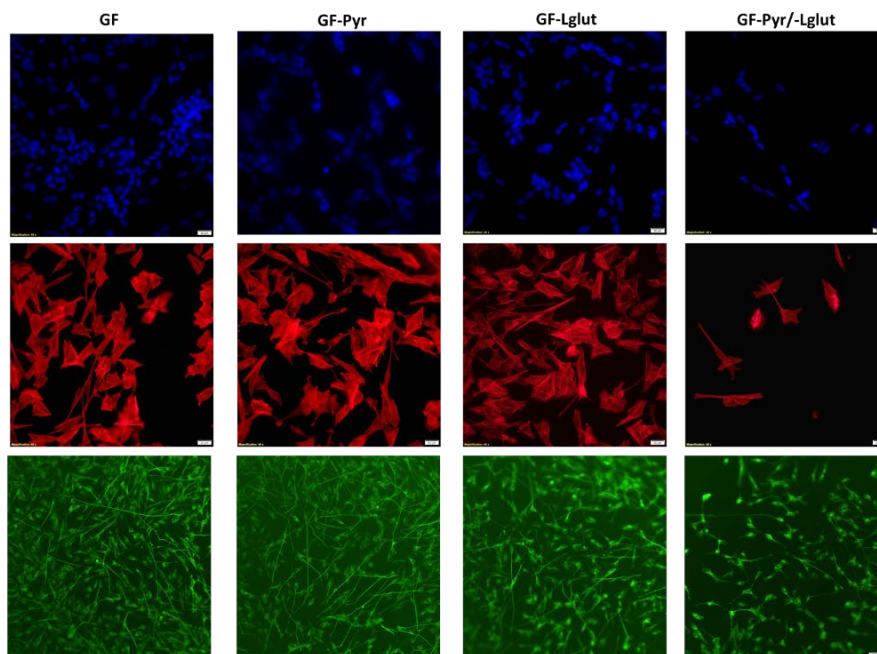


Figure 5.9 Growth and viability of SH-SY5Y cells in GF, GF-Pyr, GF-Lglut, GF-Pyr-Lglut at 5 DIV. **A)** Cell density. **B)** β -III tubulin expression. **C)** Neurite number. **D)** Cell volume. **E)** MTT viability assay. **F) Top panel:** DAPI labelled nuclei showing cell density. **Middle panel:** Actin labelled cytoskeleton of cells. **Bottom panel:** β -III tubulin labelled neurons. (N = 3 independently for each assay). One-way ANOVA with a post hoc Bonferroni Multiple Comparisons test at 5 DIV. Scale bar = 20 μ m in F respectively. **P<0.01, ****P<0.0001

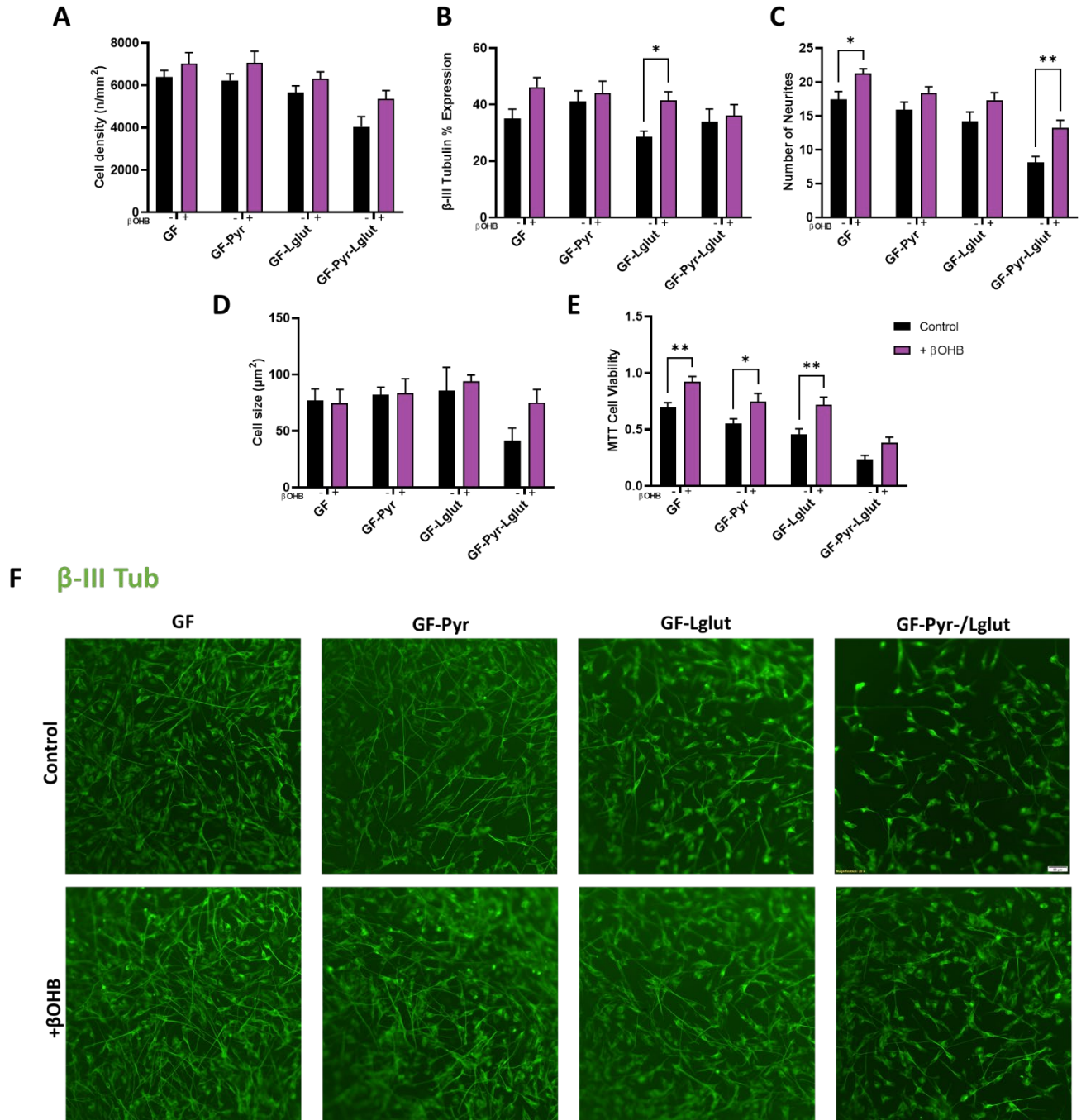


Figure 5.10 Growth and viability of SH-SY5Y cells in GF, GF-Pyr, GF-Lglut, GF-Pyr-Lglut supplemented with 10 mM β OHB at 5 DIV. **A)** Cell density. **B)** β -III tubulin expression. **C)** Neurite number. **D)** Cell volume. **E)** MTT viability assay. **F) Top panel:** β -III tubulin labelled neurons in GF, GF-Pyr, GF-Lglut, GF-Pyr-Lglut, **Bottom panel:** β -III tubulin labelled neurons in GF, GF-Pyr, GF-Lglut, GF-Pyr-Lglut conditions supplemented with 10 mM β OHB. (N = 3 independently for each assay). Two-way ANOVA with a post hoc Bonferroni Multiple Comparisons test at 5 DIV. Scale bar= 20 μ m in F respectively. *P<0.05, **P<0.01.

5.4.7 The Impact of Substrate Deprivation and β OHB Supplementation on Differentiated SH-SY5Y Viability and Density and Morphology at 10 DIV

An overall effect of substrate deprivation on cell density was observed at 10DIV ($F=46.3$, $p<0.0001$). Post-hoc testing revealed cell density was significantly less comparing GF-Lglut ($t=4.1$, $p=0.0005$) and GF-Pyr-Lglut ($t=10.5$, $p<0.0001$) to GF conditions. Additionally, cell density was significantly less comparing GF-Lglut ($t=3.4$, $p=0.0051$) and GF-Pyr-Lglut ($t=9.8$, $p<0.0001$) to GF-Pyr conditions. Cell density was significantly less comparing GF-Pyr-Lglut ($t=6.4$, $p<0.0001$) to GF-Lglut (Fig. 5.11A, F).

No overall effect of substrate deprivation on β -III tubulin expression was observed at 10DIV. Post hoc testing was not performed (Fig. 5.11B, F).

An overall effect of substrate deprivation on neurite number was observed at 10DIV ($F=21.5$, $p<0.0001$). Post-hoc testing revealed neurite number was significantly less comparing GF-Pyr ($t=6.3$, $p<0.0001$), GF-Lglut ($t=6.8$, $p<0.0001$) and GF-Pyr-Lglut ($t=6.5$, $p<0.0001$) conditions (Fig. 5.11C, F).

No overall significant effect of substrate deprivation on cell volume and cell viability was observed at 10DIV. Thus post hoc testing was not performed (Fig. 5.11D, E, F).

An overall effect of the growth media ($F=50.9$, $p<0.0001$) and the addition of β OHB ($F=10.8$, $p=0.0012$) was observed for cell density at 10DIV. An overall interaction effect was observed ($F=5.0$, $p=0.0023$). Post hoc testing within media conditions revealed significant differences comparing GF and GF-Pyr-Lglut ($t=10.5$, $p<0.0001$), GF-Pyr and GF-Pyr-Lglut ($t=10.6$, $p<0.0001$) and GF-Lglut and GF-Pyr-Lglut ($t=8.8$, $p<0.0001$). Post-hoc testing within the control media conditions revealed cell density was significantly less comparing GF-Lglut ($t=3.7$, $p=0.0019$) and GF-Pyr-Lglut ($t=9.3$, $p<0.0001$) to GF conditions. Additionally, cell density was significant cell comparing GF-Lglut ($t=3.0$, $p=0.0155$) and GF-Pyr-Lglut ($t=8.7$, $p<0.0001$) to GF-Pyr conditions. Cell density was significantly less comparing GF-Pyr-Lglut ($t=5.7$, $p<0.0001$) to GF-Lglut conditions. Post hoc testing within the β OHB supplemented conditions revealed that cell density was significantly less comparing GF-Pyr-Lglut + 10 mM β OHB to GF 10 mM + β OHB ($t=5.5$, $p<0.0001$), GF-Pyr + 10 mM β OHB ($t=6.2$, $p<0.0001$) and GF-Lglut + 10 mM β OHB ($t=6.7$, $p<0.0001$) conditions. Post hoc testing comparing the control media conditions to the β OHB supplemented conditions revealed that cell density was significantly higher

comparing GF-Lglut + 10 mM β OHB ($t=4.0$, $p=0.0003$) and when comparing GF-Pyr-Lglut + 10 mM β OHB to GF-Pyr-Lglut ($t=3.0$, $p=0.0132$) (Fig. 5.12A, F).

An overall effect of the addition of β OHB on the expression levels of β -III tubulin was observed ($F=17.6$, $p<0.0001$). No overall growth media effect or interaction effect was observed. Post hoc testing comparing the control media conditions to the β OHB supplemented conditions revealed that β -III tubulin expression was significantly higher comparing GF-Pyr-Lglut + 10 mM β OHB ($t=3.6$, $p=0.0018$) to GF-Pyr-Lglut (Fig. 5.12B, F)

An overall effect of the growth media ($F=20.9$, $p<0.0001$) and the addition of β OHB ($F=40.2$, $p<0.0001$) was observed for the number of neurites. No significant interaction effect was observed. Post hoc testing within media conditions revealed significant differences comparing GF and GF-Pyr ($t=6.2$, $p<0.0001$), GF and GF-Lglut ($t=7.2$, $p<0.0001$) and GF and GF-Pyr-Lglut ($t=5.8$, $p<0.0001$). Post-hoc testing within the control media conditions revealed that neurite number was significantly less comparing GF-Pyr ($t=4.6$, $p<0.0001$), GF-Lglut ($t=5.0$, $p<0.0001$) and GF-Pyr-Lglut ($t=4.8$, $p<0.0001$) to GF conditions. Post hoc testing with the β OHB supplemented conditions revealed that the neurite number was significantly less comparing GF-Pyr + 10 mM β OHB ($t=4.1$, $p=0.0004$), GF-Lglut + 10 mM β OHB ($t=5.1$, $p<0.0001$) and GF-Pyr-Lglut + 10 mM β OHB ($t=3.3$, $p=0.0062$) to GF + 10 mM β OHB. Post hoc testing comparing the control media conditions to the β OHB supplemented conditions revealed that neurite number was significantly higher comparing GF + 10 mM β OHB ($t=2.7$, $p=0.0328$) to GF, GF-Pyr + 10 mM β OHB ($t=3.3$, $p=0.0058$) to GF-Pyr, GF-Lglut + 10 mM β OHB ($t=2.6$, $p=0.0379$) to GF-Lglut and GF-Pyr-Lglut + 10 mM β OHB ($t=4.2$, $p=0.0002$) to GF-Pyr-Lglut conditions (Fig. 5.12C, F).

No overall growth media effect or interaction effect or effect following the addition of β OHB was observed for cell volume and cell viability at 10DIV, post hoc testing was not performed (Fig. 5.12D, E, F).

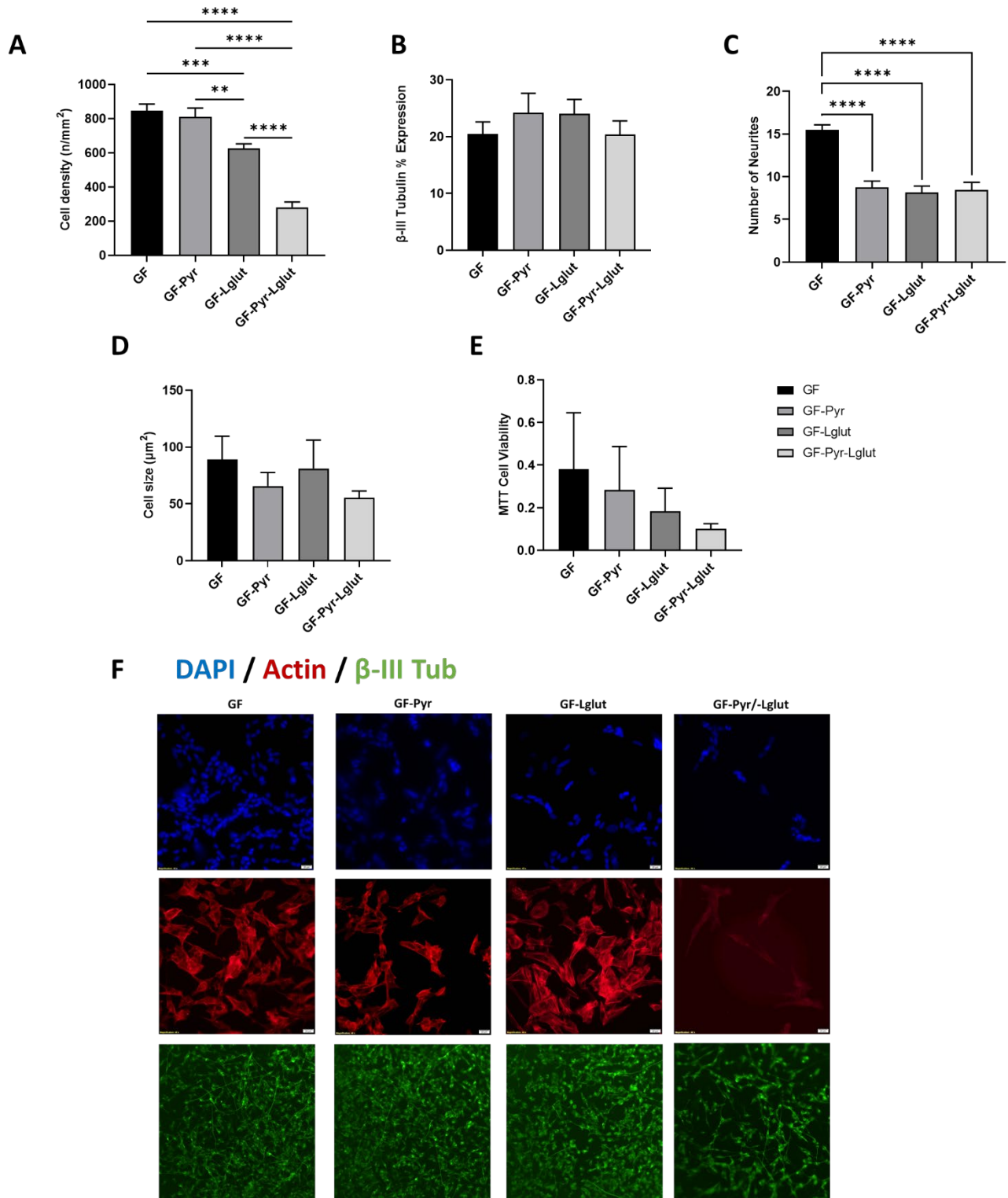


Figure 5.11 Growth and viability of SH-SY5Y cells in GF, GF-Pyr, GF-Lglut, GF-Pyr-Lglut at 10 DIV. **A)** Cell density. **B)** β -III tubulin expression. **C)** Neurite number. **D)** Cell volume. **E)** MTT viability assay. **F) Top panel:** DAPI labelled nuclei showing cell density. **Middle panel:** Actin labelled cytoskeleton of cells. **Bottom panel:** β -III tubulin labelled neurons. (N = 3 independently for each assay). One-way ANOVA with a post hoc Bonferroni Multiple Comparisons test at 10 DIV. Scale bar = 20 μ m in F respectively. *P<0.05, **P<0.01, ****P<0.0001.

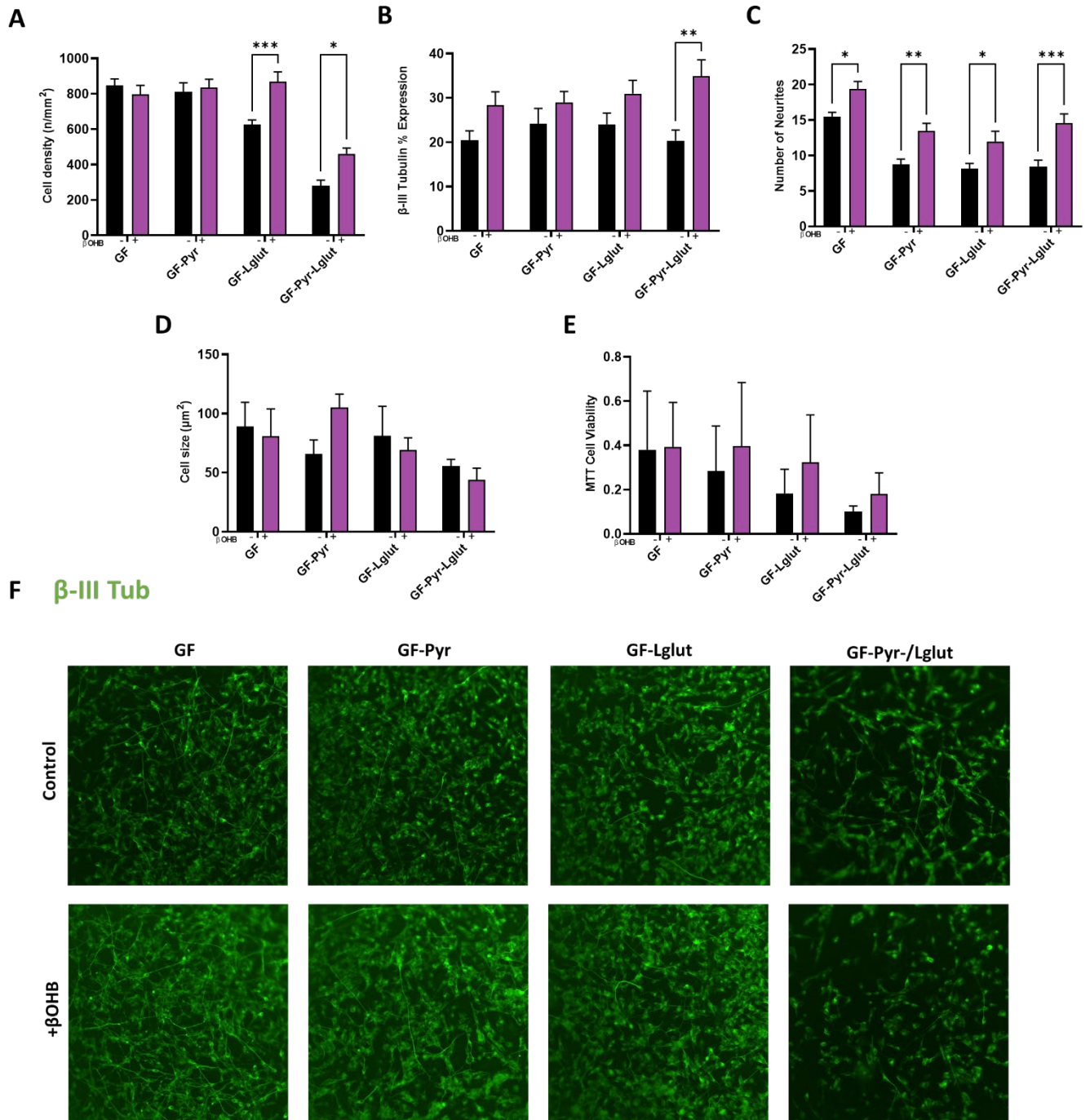


Figure 5.12 Growth and viability of SH-SY5Y cells in GF, GF-Pyr, GF-Lglut, GF-Pyr-Lglut supplemented with 10 mM β OHB at 10 DIV. **A)** Cell density. **B)** β -III tubulin expression. **C)** Neurite number. **D)** Cell volume. **E)** MTT viability assay. **F) Top panel:** β -III tubulin labelled neurons in GF, GF-Pyr, GF-Lglut, GF-Pyr-Lglut, **Bottom panel:** β -III tubulin labelled neurons in GF, GF-Pyr, GF-Lglut, GF-Pyr-Lglut conditions supplemented with 10 mM β OHB. (N = 3 independently for each assay). Two-way ANOVA with a post hoc Bonferroni Multiple Comparisons test at 10 DIV. Scale bar = 20 μ m in F respectively. *P<0.05, **P<0.01, ***P<0.001.

5.4.8 The Impact of Substrates Deprivation on Differentiated SH-SY5Y Viability and Density and Morphology at 15 DIV

An overall effect of substrate deprivation on cell density was observed at 15DIV ($F=81.9$, $p<0.0001$). Post-hoc testing revealed cell density was significantly less comparing GF-Lglut ($t=4.4$, $p=0.0002$) and GF-Pyr-Lglut ($t=13.9$, $p<0.0001$) to GF conditions. Additionally, cell density was significantly less comparing GF-Lglut ($t=3.7$, $p=0.0019$) and GF-Pyr-Lglut ($t=13.23$, $p<0.0001$) to GF-Pyr conditions. Cell density was significantly less comparing GF-Pyr-Lglut ($t=9.5$, $p<0.0001$) to GF-Lglut (Fig. 5.13A, F).

No overall effect of substrate deprivation on β -III tubulin expression or neurite number was observed at 15DIV. Thus post hoc testing was not performed (Fig. 5.13B, C, F).

An overall effect of substrate deprivation on cell volume was observed at 15DIV ($F=7.5$, $p=0.0103$). Post-hoc testing revealed cell volume was significantly less comparing GF-Lglut ($t=3.7$ $p=0.0387$) and GF-Pyr-Lglut ($t=4.2$, $p=0.0181$) to GF conditions (Fig. 5.13D, F).

An overall effect of substrate deprivation on cell viability was observed at 15DIV ($F=9.9$, $p=0.0045$). Post-hoc testing revealed cell viability was significantly less comparing GF-Pyr-Lglut to GF ($t=5.3$, $p=0.0046$) and GF-Pyr ($t=3.8$, $p=0.0291$) conditions (Fig. 5.13E, F).

An overall effect of the growth media ($F=123.0$, $p<0.0001$) and an interaction effect ($F=9.0$, $p<0.0001$) was observed for NE-4C cell density at 15DIV. Post hoc testing media conditions revealed significant differences comparing GF and GF-Lglut ($t=3.3$, $t=0.0062$), GF and GF-Pyr-Lglut ($t=16.0$, $p<0.0001$), GF-Pyr and GF-Pyr-Lglut ($t=4.5$, $p<0.0001$), GF-Pyr and GF-Pyr-Lglut ($t=17.1$, $p<0.0001$) and GF-Lglut and GF-Pyr-Lglut ($t=12.6$, $p<0.0001$). Post-hoc testing the control media conditions revealed cell density was significantly less comparing GF-Lglut ($t=4.7$, $p<0.0001$) and GF-Pyr-Lglut ($t=14.9$, $p<0.0001$) to GF conditions. Additionally, cell density was significantly less comparing GF-Lglut ($t=4.0$, $p=0.0006$) and GF-Pyr-Lglut ($t=14.2$, $p<0.0001$) to GF-Pyr conditions. Cell density was significantly less comparing GF-Pyr-Lglut ($t=10.2$, $p<0.0001$) to GF-Lglut conditions. Post hoc testing the media conditions supplemented with + 10 mM β OHB revealed that cell density was significantly less comparing GF-Pyr-Lglut + 10 mM β OHB to GF + 10 mM β OHB ($t=7.7$, $p<0.0001$), GF-Pyr + 10 mM β OHB ($t=10.0$, $p<0.0001$) and GF-Lglut + 10 mM β OHB ($t=7.7$, $p<0.0001$) conditions. Post hoc testing comparing the control media conditions to the β OHB supplemented media conditions revealed that cell density was significantly less comparing GF + 10 mM β OHB ($t=3.8$, $p=0.0007$) to GF and

was significantly higher comparing GF-Pyr-Lglut + 10 mM β OHB ($t=3.3$, $p=0.0042$) to GF-Pyr-Lglut conditions (Fig. 5.14A, F).

An overall effect of the addition of β OHB was observed ($F=48.6$, $p<0.0001$) for β -III tubulin expression levels. No overall growth media effect or interaction effect was observed. Post hoc testing comparing the control media conditions to the β OHB supplemented conditions revealed that β -III tubulin expression was significantly higher comparing GF + 10 mM β OHB ($t=3.9$, $p=0.0005$) to GF, GF-Pyr + 10 mM β OHB ($t=3.3$, $p=0.0047$) to GF-Pyr, GF-Lglut + 10 mM β OHB ($t=3.6$, $p=0.0016$) to GF-Lglut and GF-Pyr-Lglut + 10 mM β OHB ($t=3.1$, $p=0.0081$) to GF-Pyr-Lglut conditions (Fig. 5.14B, F).

An overall effect of the addition of β OHB was observed ($F=7.5$, $p=0.0068$) for the neurite number. No overall growth media effect or interaction was observed. Post hoc testing comparing the control media conditions to the β OHB supplemented conditions revealed no significant differences between the media conditions (Fig. 5.14C, F).

An overall effect of the growth media ($F=4.6$, $p=0.0167$) and an interaction effect ($F=4.8$, $p=0.0147$) was observed for cell volume at 15DIV. No effect was observed following the addition of β OHB to the medium. Post hoc testing media conditions revealed significant differences between GF and GF-Lglut ($t=3.2$, $p=0.0309$). Post-hoc testing the control media conditions revealed that cell volume was significantly less comparing GF-Lglut ($t=3.8$, $p=0.0083$) and GF-Pyr-Lglut ($t=4.4$, $p=0.0025$) to GF. Post hoc testing comparing control media conditions to the β OHB supplemented media conditions revealed that cell volume was significantly less comparing GF + 10 mM β OHB ($t=3.1$, $p=0.0277$) to GF (Fig. 5.14D, F).

An overall effect of the growth media ($F=24.0$, $p<0.0001$) and the addition of β OHB ($F=5.2$, $p<0.0368$) was observed for cell viability. No interaction effect was observed. Post hoc testing media conditions revealed significant differences comparing GF-Pyr-Lglut and GF ($t=7.3$, $p<0.0001$), GF-Pyr-Lglut and GF-Pyr ($t=7.4$, $p<0.0001$) and GF-Pyr-Lglut and GF-Lglut ($t=4.7$, $p=0.0014$). Post-hoc testing the control media conditions revealed that cell viability was significantly less comparing GF-Lglut ($t=3.0$, $p=0.048$) and GF-Pyr-Lglut ($t=6.5$, $p<0.0001$) to GF. Cell viability was significantly less comparing GF-Pyr-Lglut to GF-Pyr ($t=4.8$, $p=0.0013$) and GF-Lglut ($t=3.5$, $p=0.019$). Post hoc testing the β OHB supplemented media conditions revealed that cell viability was significantly less comparing GF-Pyr-Lglut + 10 mM β OHB to GF + 10 mM β OHB ($t=3.8$, $p=0.0096$), to GF-Pyr + 10

mM β OHB ($t=5.7$, $p=0.0013$) and to GF-Lglut + 10 mM β OHB ($t=3.2$, $p=0.00332$) conditions. No significant differences were observed comparing the control media conditions to the β OHB supplemented conditions (Fig. 5.14E, F).

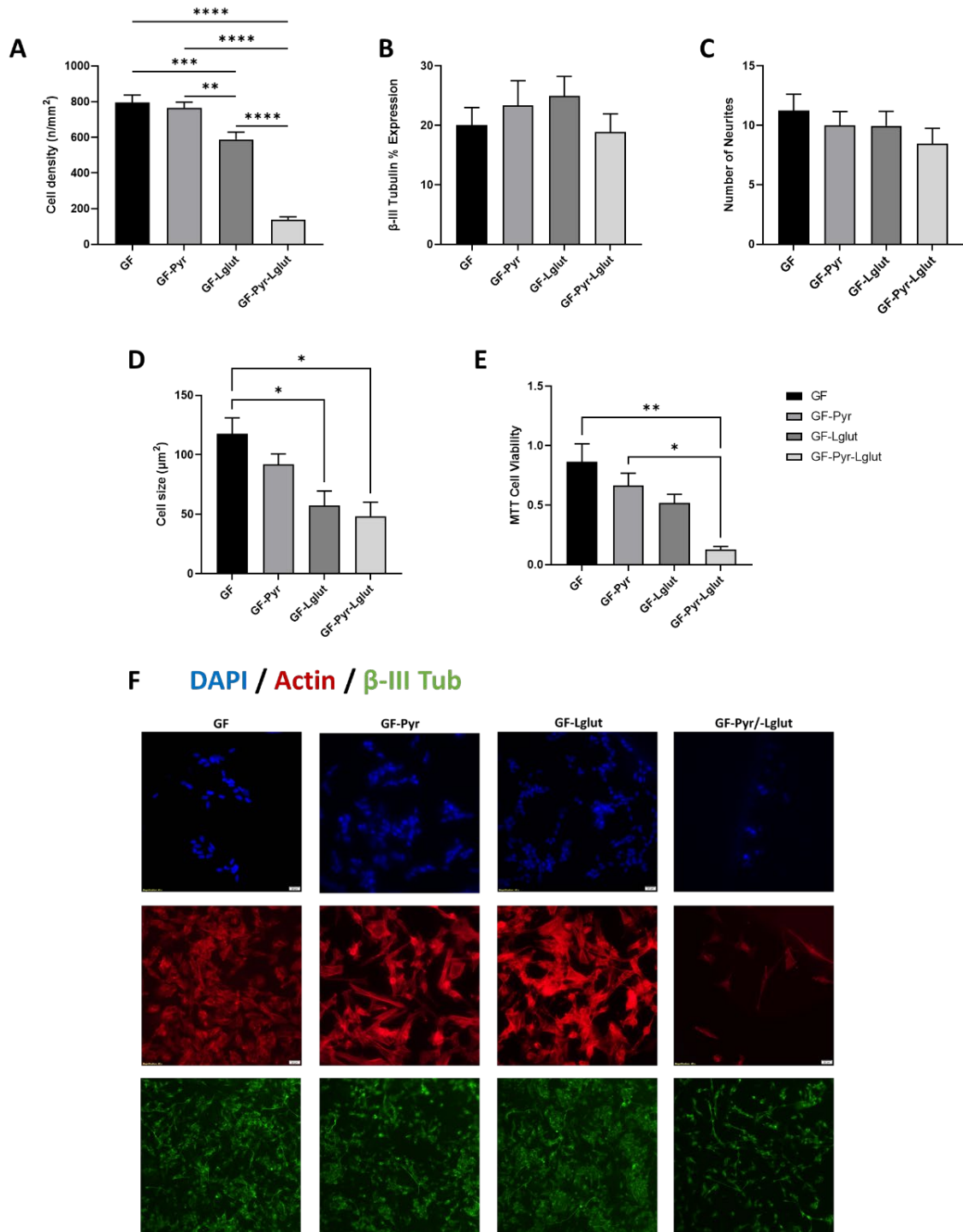


Figure 5.13 Growth and viability of SH-SY5Y cells in GF, GF-Pyr, GF-Lglut, GF-Pyr-Lglut at 15 DIV. **A)** Cell density. **B)** β -III tubulin expression. **C)** Neurite number. **D)** Cell volume. **E)** MTT viability assay. **F) Top panel:** DAPI labelled nuclei showing cell density. **Middle panel:** Actin labelled cytoskeleton of cells. **Bottom panel:** β -III tubulin labelled neurons. (N = 3 independently for each assay). One-way ANOVA with a post hoc Bonferroni Multiple Comparisons test at 15 DIV. Scale bar = 20 μ m in F respectively. * $P < 0.05$ ** $P < 0.01$, *** $P < 0.001$ **** $P < 0.0001$.

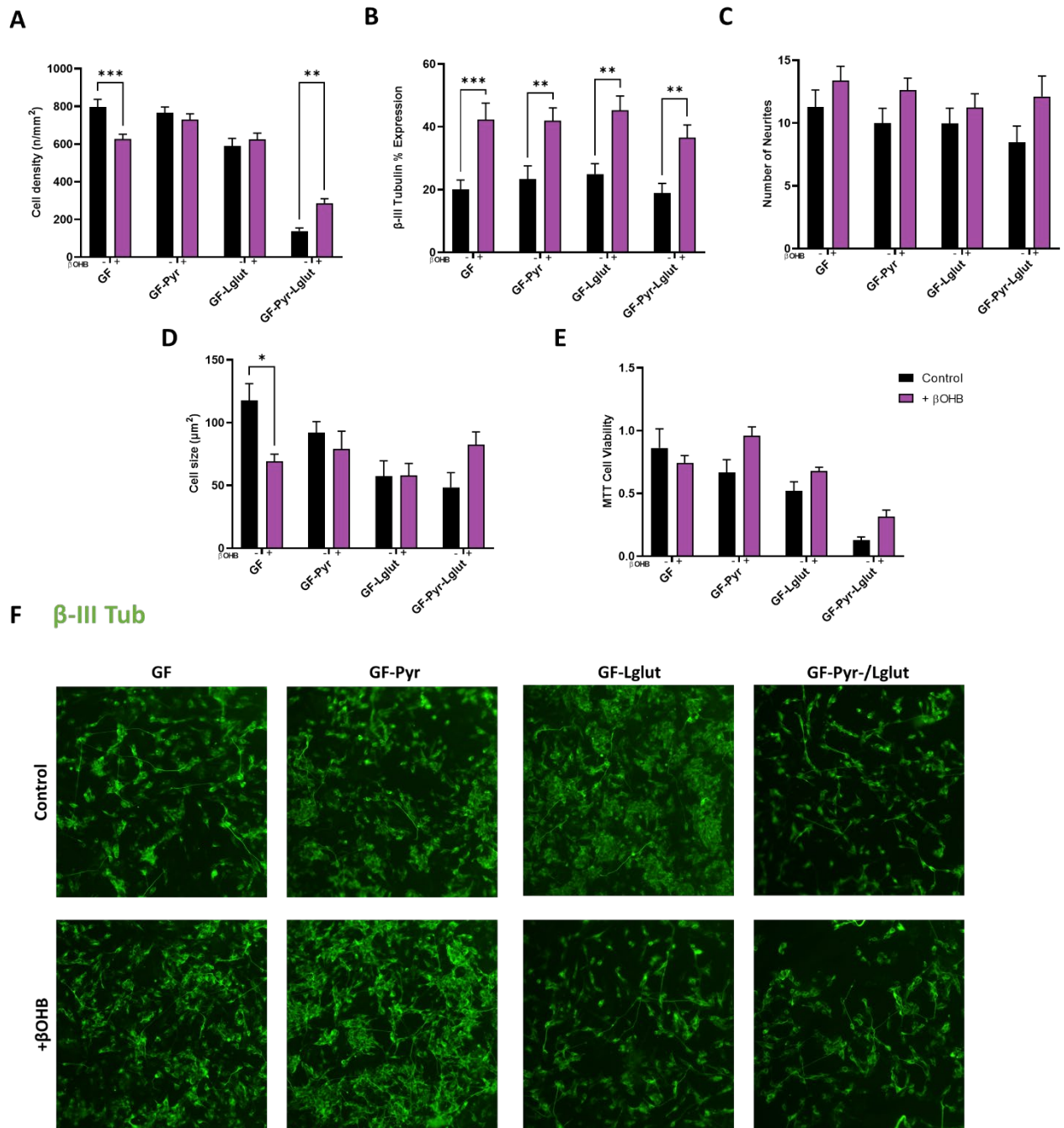


Figure 5.14 Growth and viability of SH-SY5Y cells in GF, GF-Pyr, GF-Lglut, GF-Pyr-Lglut supplemented with 10 mM β OHB at 15 DIV. **A)** Cell density. **B)** β -III tubulin expression. **C)** Neurite number. **D)** Cell volume. **E)** MTT viability assay. **F) Top panel:** β -III tubulin labelled neurons in GF, GF-Pyr, GF-Lglut, GF-Pyr-Lglut, **Bottom panel:** β -III tubulin labelled neurons in GF, GF-Pyr, GF-Lglut, GF-Pyr-Lglut conditions supplemented with 10 mM β OHB. (N = 3 independently for each assay). Two-way ANOVA with a post hoc Bonferroni Multiple Comparisons test at 15 DIV. Scale bar = 20 μ m in F respectively. *P<0.05, **P<0.01, ***P<0.001.

5.5 Discussion

During development NE-4C NSCs and SH-SY5Y cells use aerobic glycolysis as their primary means of energy production (Zheng et al., 2016). A metabolic switch to OXPHOS occurs when cells differentiate to a mature neuronal phenotype.

We firstly characterized the impact of glucose and glucose deprivation on NSC and NB growth over 5, 10 and 15DIV. Our results demonstrate that NE-4C and SH-SY5Y cells do not differentiate or survive in glucose-free conditions.

Reductions in cell morphology, neuronal phenotype and metabolic health were also evident in low glucose conditions when compared to regular glucose containing culture conditions. Further reductions in cell health were observed when the remaining culture metabolic substrates were removed. Ketone supplementation was unsuccessful in remediating the effects of substrate deprivation at 5 and 10DIV; however, metabolic health, phenotype and morphologies could be preserved at 15DIV presumably as cells began to shift available metabolic substrates using OXPHOS.

5.5.1 Glucose and Nutrient Deprivation is Detrimental to Cell Differentiation

Glucose is the primary energy source for neurons and is oxidized through glycolysis and OXPHOS (Nehlig and Coles, 2007). NE-4C cells fully differentiate over a period of 14 DIV (Hádinger et al., 2009), whereas SH-SY5Y cells fully differentiate over 18 DIV (Shipley et al., 2016). NE-4C and SH-SY5Y cells were differentiated using RA over 5, 10 and 15 DIV in glucose containing and glucose free conditions. The removal of glucose or the decrease in its concentration prevents cells from undergoing differentiation and reduces neurite number and metabolic viability. The withdrawal of glucose has been shown to be detrimental to cellular differentiation, morphology and metabolic viability and causes phosphor-tyrosine signalling and ROS mediated cell death (Graham et al., 2012). Likewise, we observed a significant decrease in β -III tubulin, a neuronal phenotype marker, and a decrease in neurite number and metabolic viability in both the NE-4C and SH-SY5Y cell lines. As expected, cell size decreased in NE-4C cells in LG and GF environments at 5DIV and remains constant in all groups at 10 and 15DIV. When cells are metabolically unhealthy decrease in size (Chen et al., 2020),

During *in vitro* differentiation of cortical neurons, glycolytic activity and glucose metabolism increased exponentially over 2, 5 and 7DIV which was linked to an increased

expression of GLUT3, and other enzymes associated with the glycolytic pathway and an increase in glucose uptake (Agostini et al., 2016).

In a separate study that investigated the metabolism of differentiating SH-SY5Y cells and human NSCs, the authors outline that glycolysis (including basal glycolysis and glycolytic capacity) and OXPHOS of both cell lines is significantly increased after neurons have fully differentiated (Li et al., 2020a). Our data is further reinforced with findings from another study that outlines the importance of glycolysis in maintaining an aerobic profile capable in facilitating an upregulation of the genes needed for OXPHOS, allowing NSC and neural progenitor differentiation to occur (Maffezzini et al., 2020). Once NSCs and neural progenitor cells begin differentiation, a series of developmental events occur that include dendrite morphogenesis and axonal elongation (de la Torre-Ubieta and Bonni, 2011, Kristiansen and Ham, 2014). Hence, when the glucose concentration is reduced to below its physiological concentration or completely removed, a decrease in the expression of β -III tubulin, neurite number and metabolic viability in both cell lines is evident.

To investigate the potential impact of the other culture substrates on cell growth and differentiation, we also investigated the effects of removing glutamine and pyruvate from the glucose deprived medium and supplemented the medium with 10 mM β OHB at 5, 10 and 15DIV.

In the NE-4C and SH-SY5Y cell lines, a significant reduction in cell density and metabolic health over 5, 10 and 15DIV was evident in the GF-Pyr, GF-Lglut and GF-Pyr-Lglut conditions. Pyruvate is critical molecule for numerous aspects of metabolism, it's a product of glycolysis and produces ATP via OXPHOS in the mitochondria and through additional metabolic pathways intersecting the citric acid cycle (Gray et al., 2014). Glutamine is crucial for metabolism and bioenergetic requirements supplying both carbon and nitrogen to fuel biosynthesis (Gwangwa et al., 2019, Yoo et al., 2020). In cells dependent on glucose and its by-product of pyruvate for survival, glucose and pyruvate deprivation induce oxidative stress driven by NOX and mitochondria.

This oxidative stress generates superoxide anions and amplifies ROS generation which results in ROS mediated cell death (Graham et al., 2012). Glutamine deprivation results in decreased cell proliferation, aberrant mitochondrial membrane potential, generates ROS, and disrupts cell cycle progression (Gwangwa et al., 2019). Thus, further removing pyruvate and glutamine along with glucose in both cell lines decreases cell densities and metabolic

viability when compared to conditions where only glucose was removed and demonstrates that differentiating NE-4C and SH-SY5Y cells cannot survive and in environments where these metabolic inputs are completely removed and undergoes apoptosis.

In the NE-4C and SH-SY5Y lines, a decrease in cell morphology was evident in glucose, pyruvate, and glutamine deprived conditions over 5, 10 and 15DIV. Glucose metabolism is necessary for activity dependent neurite outgrowth, knockdown of GLUT3, the main glucose transporter in neurons, abolishes activity mediated growth (Segarra-Mondejar et al., 2018). When glutamine enters the mitochondria of the cell it's converted to glutamate. Glutamate regulates neurite outgrowth and promotes branching by affecting cytoskeletal dynamics in the growth cone and neurite shaft (Mattson, 2008). As these metabolic substrates were absent, this prevented neurites from branching out from the dying and metabolically unhealthy cells and decreased the overall number of neurites. As previously mentioned, when cells are metabolically unhealthy their cell size decreases (Chen et al., 2020), this was evident in the GF-Pyr and GF-Lglut conditions for both cell lines at 15 DIV. Taken together, our data implicates the major fuel substrates in culture conditions as necessary metabolic components which maintain and promote growth during differentiation as NE-4Cs and SH-SY5Y cells undergo differentiation and switch their metabolism from glycolysis to OXPHOS. Without these substrates, especially glucose, differentiation could not occur.

5.5.2 Ketone Supplementation May Rescue the Effects of Nutrient Deprivation When Cells are Undergoing OXPHOS

Supplementing the LG and GF conditions with 10 mM β OHB over 5, 10 and 15DIV indicates that β OHB cannot rescue the differentiation capability and metabolic viability imposed by lowering the glucose concentration or removing it completely in NE-4C and SH-SY5Y cells. This is in agreement with previous research utilizing the SH-SY5Y line which showed that ketone supplementation was ineffective in restoring cell viability reduced by glucose deprivation, albeit comparing β OHB in glucose free medium to a glucose supplemented control (Skinner et al., 2009). Previous studies have demonstrated that glucose metabolism is decreased in the presence of β OHB, but these studies did not outline whether it was due to inhibition of glycolysis or OXPHOS (Lund et al., 2011, Lund et al., 2009, McKenna et al., 1994). However, in a study investigating the metabolic impact of β OHB on neurotransmission, β OHB was found to reduce growth in glutamatergic neurons by attenuating glycolysis (Lund et al., 2015).

In the NE-4C line, β OHB increases cell density in GF-Pyr-Lglut and neurite number in GF-Pyr and GF-Lglut conditions at 5DIV. At 10DIV, β OHB prevented cell growth in GF conditions and promoted growth in GF-Lglut conditions. In the SH-SY5Y line, β OHB increased neurite number in GF and GF-Pyr-Lglut conditions at 5DIV. At 10DIV, β OHB increases cell density in GF-Lglut and GF-Pyr-Lglut conditions and increases neurite number in GF, GF-Pyr, GF-Lglut and GF-Pyr-Lglut at 10 DIV.

MCTs are bi-directional transporters that shuttle β OHB across neuronal membranes (Halestrap and Wilson, 2012) and also transports other substrates such as pyruvate and lactate (Pérez-Escuredo et al., 2016b). The beneficial effects of β OHB on cell density in the NE-4C and SH-SY5Y cells in the GF-Lglut and GF-Pyr-Lglut at 5 and 10DIV and the negative effects in cell density in GF conditions in NE-4C cells at 10DIV, suggest competition with MCT substrates may limit the entry of β OHB into the cell (Tildon et al., 1994, McKenna, 2012). In rat hippocampal brain slices when β OHB and glucose are present in the same culture environment, glucose is preferred for the generation of acetyl-CoA (Valente-Silva et al., 2015), this would support the data describing the reduced cell density in the GF conditions when supplemented with β OHB.

Yet, at both timepoints for both cell lines, viability is not improved through β OHB supplementation indicating that though cell growth and neurite number is increased, the cells are still metabolically unhealthy. This suggests that β OHB does not consistently maintain cell density, β -III tubulin expression, neurite number, cell size or metabolic viability over 5 and 10DIV. This would further support the theory that the cells are still differentiating as it takes 14DIV and 18DIV for NE-4C and SH-SY5Y cells to fully differentiate and are still metabolising glucose and have not yet switched to OXPHOS, hence why we see these inconsistent results at 5 and 10DIV. (Shipley et al., 2016, Hádinger et al., 2009).

However, at 15DIV, we begin to see a partial restoration of effects in the β OHB supplemented groups as the NE-4C and SH-SY5Y cells begin to mature to a neuronal phenotype.

In the NE-4C line, β OHB increases cell density in the GF-Pyr and GF-Lglut conditions and decreases cell density in GF conditions. In the SH-SY5Y line, β OHB decreases cell density in GF conditions and increases density in GF-Pyr-Lglut conditions. These beneficial and negative effects may suggest competition for substrates and a preference for glucose over

β OHB as was observed in 5 and 10DIV and may limit β OHBs entry into the cell (McKenna et al., 1994, Tildon et al., 1994, Valente-Silva et al., 2015).

β -III tubulin expression is decreased in GF conditions and increased in GF-Pyr conditions following β OHB supplementation in the NE-4C line. β -III tubulin expression is increased in all conditions following supplementation in the SH-SY5Y line. Ketone bodies are the main source of energy during periods of glucose starvation, however only when cells are fully differentiated and using OXPHOS metabolism can they begin to utilize ketones during this period (García-Rodríguez and Giménez-Cassina, 2021).

As NE-4C cells and SH-SY5Y cells take 14 and 18DIV to differentiate, we therefore observe a greater increase in the expression of the neuronal marker β -III tubulin in SH-SY5Y cells at 15DIV as opposed to 5 and 10DIV (Hádinger et al., 2009, Shipley et al., 2016). There is a gap in the literature investigating the impact of ketones on neurite growth, however as cellular processes such as remodelling of the cytoskeleton and neurite growth and branching require ATP. β OHB may provide this necessary energy to increase the number of neurites in the GF-Pyr condition in the NE-4C line at 15DIV as it can now metabolize ketones as its fully differentiated and using OXPHOS (Jensen et al., 2020).

The metabolic viability of the NE-4C line was increased by β OHB supplementation at 15DIV. Metabolic viability is not restored to the same levels as glucose containing conditions but is restored to the same level as glucose free conditions. As cells have now fully differentiated and as they're deprived of the critical metabolic inputs of glucose, pyruvate, and glutamine, they can now begin to metabolise β OHB. Whereas at 5 and 10DIV, cells were still undergoing differentiation and were not fully matured.

Taken together, our data implicates that ketone supplementation cannot remediate the impact of substrate deprivation at 5 and 10DIV. However, metabolic health, phenotype and morphologies could be preserved to the same levels as GF conditions at 15DIV as cells shift from glycolysis to OXPHOS.

5.6 Conclusion

These data demonstrate that differentiating NE-4C and SH-SY5Y cells cannot survive in environments where glucose has been removed completely. Removal of glucose, pyruvate and glutamine and supplementation with β OHB maintains metabolic health and cell density but does not rescue the effects of glucose deprivation in the early stages of NE-4C and SH-SY5Y differentiation. The removal of pyruvate and glutamine further reduces NE-4C cell health and viability as they differentiate. β OHB can mildly rescue the effects of glucose deprivation as NE-4Cs and SH-SY5Ys mature to a neuronal phenotype and switch their metabolism from glycolysis to OXPHOS.

Together, the data indicates that culture conditions and media reagents may influence the effect of ketone supplementation in cell culture conditions and must be considered when designing experimental paradigms. Ketone metabolism appears to be dependent on the metabolic status of NSCs during development and differentiation *in vitro* (Jády et al., 2016, Shyh-Chang et al., 2013). Further research will be undertaken to investigate the use of a standard control, depending on time and media when researching the effect of ketone bodies on the differentiation of cortical NSCs. These data contribute to research underlying the role of ketone body metabolism on NSC and neural progenitor growth *in vitro* and may have implications for our understanding of the roles of ketone metabolism on brain growth and function. Future investigations will investigate the capability of differentiated NE-4C and SH-SY5Y cells to metabolize β OHB past 15DIV.

Chapter 6

General Discussion & Future Directions

6.1 General Discussion

6.1.1 Study Overview

Ketone bodies are endogenously synthesized metabolites which become crucial sources of energy in mammals during physiological periods such as long-term starvation, short-term fasting, the neonatal period, or pregnancy. Recently, ketone body metabolism has garnered significant interest as a spotlight has been placed on the high fat, low carbohydrate KDs and the application of ketone bodies in clinical studies with the aim of improving health and fighting disease (Caffa et al., 2020, de Cabo and Mattson, 2019, Hopkins et al., 2018). Attention to the roles of ketone bodies in rapidly dividing cells such as the NE-4C NSC line and in cancerous cells such as the SH-SY5Y NB cell line has also recently intensified. For tumours to expand, cancer cells such as SH-SY5Y cells metabolize glucose through the glycolytic pathway, otherwise known as the Warburg effect, and metabolize phosphate through the PPP and metabolize fats through the lipogenesis pathway to provide energy whilst OXPHOS is downregulated (Kang et al., 2015, Shukla et al., 2014).

β OHB, the bodies most abundant ketone body has been under intense investigation as of late for its potential therapeutic roles for malignancies outside of the digestive system. It has been reported that β OHB can enable (Huang et al., 2017, Kang et al., 2015, Rodrigues et al., 2017, Xia et al., 2017) or inhibit (Cui et al., 2019) cell growth and tumour expansion. β OHB may facilitate cell growth and expansion through signalling mechanisms or meeting specific energy demands (Huang et al., 2017, Kang et al., 2015, Rodrigues et al., 2017, Xia et al., 2017). The metabolism of β OHB may influence their effect on cancer cells. A β OHB paradox exists where cells oxidize ketones at a lower capacity but are then more response to HDAC inhibition (Rodrigues et al., 2017).

The work carried out here was an investigation into the impact of ketone bodies, specifically β OHB on neural progenitor and NSC growth with the overall aim of elucidating its effects on cell growth. The answer as to whether ketone bodies positively or negatively impact cell growth is still ambiguous with studies reporting ketone bodies both positively and negatively influencing cell growth (Cui et al., 2019, Huang et al., 2017, Kang et al., 2015, Rodrigues et al., 2017, Xia et al., 2017).

With the current study, we focused mainly on the impact of β OHB on NSC and NB cell growth in the context of whether it benefited or negatively impacted cell growth. At the same time, we wished to investigate the impact and involvement of other media substrates that could potentially hamper the effect of the ketone body. We initially focused on reviewing the existing literature where ketone bodies were specifically used in *in vitro* studies. We wished to get a consensus on the effect ketone bodies had on cell lines. After reviewing the literature, we planned a series of experiments investigating the impact of varying concentrations of β OHB and substrate deprivation on cell growth through experiments that investigated cell density, cell size, differentiation and metabolic health and viability, and proliferation. An outline of the main findings from each chapter can be seen in Fig. 6.1.

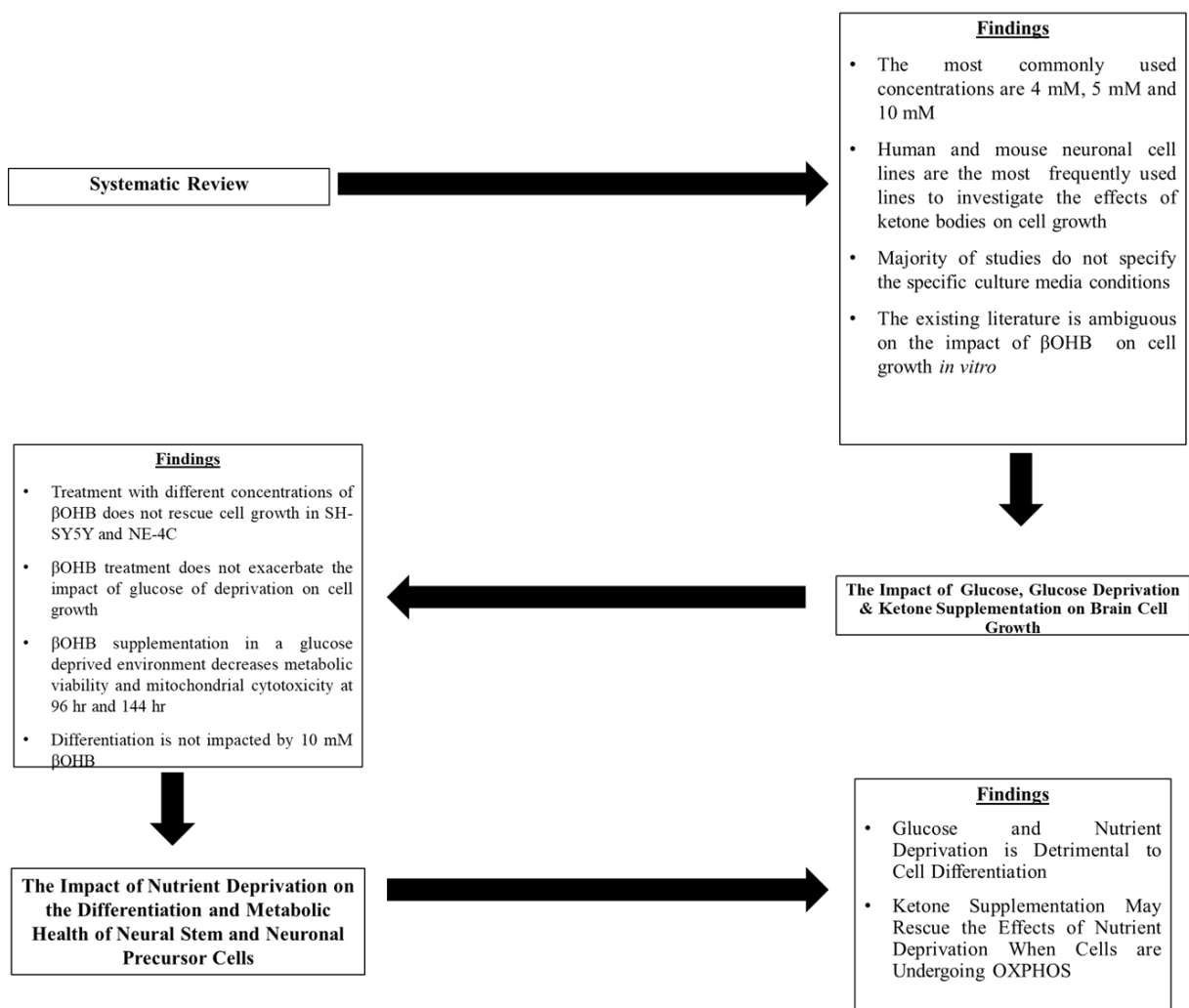


Figure 6.1 An overview of the findings from each chapter

6.1.2 A Systematic Review of the Effects of Ketone Body Supplementation on Cells *In Vitro*

To get a thorough understanding of the existing literature surrounding the effect of ketones on cell growth we undertook a systematic review and looked at specific parameters which included which type of ketone was used and its concentration and its overall impact. One of the aims of this systematic review was to find cell lines we could use to experiment and to test the ketones effect on cell growth and to find a specific concentration range to culture the cells in. Our systematic review (Chapter 3) showed that the existing literature is ambiguous in detailing the impact of ketones on cell growth where 51% of the studies outlined a beneficial effect of ketones on cell growth and 35% of studies outlined a negative effect of cell growth. We also observed that neuronal cell lines, especially the SH-SY5Y cell line was the most common cell line used where positive effects were observed (Imamura et al., 2006, Kabiraj et al., 2012, Lamichhane et al., 2017b, Li et al., 2020b, Zhang et al., 2018a). The most frequently used ketone was β OHB and the concentrations where positive effects were observed in cell lines were 4 mM and 10 mM β OHB. Paradoxically, neuronal cell lines were the most frequently used cell lines where negative effects were observed and the concentrations where negative effects were observed was 5 mM and 10 mM also (Skinner et al., 2009, Vallejo et al., 2020). Lastly, a large proportion of studies did not specify whether growth substrates such as glucose, pyruvate and glutamine were included in their growth media. It was concluded that the existing literature was ambiguous in detail the specific culturing conditions that β OHB was added to.

Using the data we gathered from the systematic review, it was decided that the SH-SY5Y NB and the NE-4C NSC cell lines would be used to investigate the impact of glucose deprivation and β OHB supplementation on cell growth. The concentrations used would be 1 mM, 5 mM, 10 mM, and 50 mM β OHB, as both 5 mM and 10 mM as they were both found to the most frequently used concentrations that produced a negative and positive effect on cell growth (Supplementary Tables 7.13 and 7.14).

6.1.3 The Impact of Glucose, Glucose Deprivation and Ketone Body Supplementation on Cell Growth

Much like the data obtained from the systematic review, the results from the experiments in Chapter 4 were ambiguous in providing an answer to whether ketone bodies can positively impact cell growth. The overall decrease in cell density in both cell lines shows that glucose is fundamental to cell growth. This is in line with previous studies investigating glucose deprivation on rapidly dividing cells which demonstrate a reduction in cell density upon the removal of glucose (Chiodi et al., 2019). Supplementing glucose free conditions with 1 mM, 5 mM, 10 mM, and 50 mM β OHB over 48, 72, 96 and 120 hr did not impact proliferation rates.

This data is supported by previous research suggesting that β OHB can promote cell proliferation in fibroblasts. (Martinez-Outschoorn et al., 2012b). However, contradicting to our data described from this chapter, β OHB was found to reduce growth in SH-SY5Y cells (Skinner et al., 2009).

Both mitochondrial cytotoxicity and viability were decreased in glucose free conditions when supplemented with β OHB over 96 hrs and 144 hrs. Previous research has described ketone bodies decreasing mitochondrial biogenesis (Xu et al., 2021) and findings from our systematic review further support this evidence, where β OHB has promoted apoptosis and caused mitochondrial damage through ROS generation and oxidative stress in glioma stem like cells (Kadochi et al., 2017, Ji et al., 2020). However conflicting research exists that describes how β OHB inhibits mitochondrial mediated apoptosis and decreases intracellular ROS levels (Cheng et al., 2010). Cell proliferation and differentiation, confirmed by BrdU and NeuN staining decreased over time. Cells decreasing their level of proliferation is in line with previous studies describing that when cells are terminally differentiated, they no longer undergo mitosis in glucose free and β OHB supplemented conditions (Aranda-Anzaldo, 2012). Taken together, our data is line with the systematic review we conducted, in that our results are ambiguous. It was concluded from the ambiguous data that the media conditions the cells were cultured in should be investigated and scrutinized further to outline their potential role in influencing cell growth.

The data from the experiments undertaken in Chapter 4 is in line with existing literature describing the effect of ketone supplementation on NB cells which have been equivocal due to largely inconsistent *in vitro* experimental designs and the potential involvement of culture supplementations such as glucose, pyruvate, and glutamine. In particular, the “ β OHB paradox” describes contradicting observations of the effect of ketone bodies on cell growth and development (Rodrigues et al., 2017). Several studies utilising SH-SY5Y and other cancer cell lines have shown an inhibitory, anti-proliferative effect (Martuscello et al., 2016a, Poff et al., 2014, Shukla et al., 2014, Skinner et al., 2009), while others have demonstrated that ketone bodies promote the growth and survival of cancer cells (Abdelwahab et al., 2012, Bonuccelli et al., 2010, Martinez-Outschoorn et al., 2011c, Whitaker-Menezes et al., 2011) or had no impact on growth (Bartmann et al., 2018). Considering the roles of SH-SY5Y culture conditions and media conditions in influencing experimental outcomes (Cantor et al., 2017), the differential effects of ketones may be due to changes in the availability of other metabolic substrates such as glucose, pyruvate, and glutamine.

6.1.4 Ketone Supplementation May Rescue the Impact of Nutrient Deprivation When Cells are Undergoing OXPHOS

To further understand the roles of glucose, pyruvate, and glutamine during the metabolic transition in cell development, we investigated the health and phenotypes of differentiating neural stem and neuronal precursor cells in various conditions of substrate deprivation and β OHB supplementation over 5, 10 and 15DIV. These specific timepoints of investigation were chosen as NE-4C cells fully differentiate over 14DIV (Hádinger et al., 2009), whereas SH-SY5Y cells fully differentiate over 18DIV (Shipley et al., 2016).

We observed over 5, 10 and 15DIV that removing glucose is detrimental to cell health and growth in both cell lines as they are undergoing differentiation and switching their phenotype from glycolysis to OXPHOS. As previously discussed, glucose deprivation is detrimental to cell growth, morphology and viability and causes ROS mediated cell death (Graham et al., 2012). We observed a decrease in the expression of the neuronal phenotype marker β -III tubulin in glucose free conditions and in the number of neurites, confirming that the cells capacity to differentiate in these conditions is reduced. Previous studies that investigated the metabolism of SH-SY5Y and NSC's undergoing differentiation have outlined that basal glycolysis, glycolytic capacity and OXPHOS is significantly increased after they have fully differentiated (Li et al., 2020a). Since glucose has been removed from

our culturing media, the cells glycolytic capacity and OXPHOS is completely reduced and prevents the cells from generating energy to allow the differentiation process and morphological transformation steps that come with the process to take place. Unsurprisingly, further removing pyruvate and glutamine from an already glucose deprived environment decreased cell density and metabolic health over 5, 10 and 15DIV in both the NE-4C NSC and the SH-SY5Y NB cell lines.

Both pyruvate and glutamine are critical sources of energy for multiple aspects of metabolism, where pyruvate generates energy via OXPHOS and glutamine supplies carbon and nitrogen to fuel biosynthetic pathways (Gwangwa et al., 2019, Gray et al., 2014). Pyruvate and glutamine deprivation induces oxidative stress and increases the levels of ROS which causes cell death and disrupts cell cycle progression (Graham et al., 2012, Gwangwa et al., 2019).

Supplementing low glucose and glucose free conditions with β OHB failed to rescue the metabolic viability and the growth of NE-4C and SH-SY5Y cells undergoing differentiation. Previous studies have shown that β OHB reduces growth in neurons in by attenuating glycolysis (Lund et al., 2011). Over 5 and 10DIV, the morphological results are ambiguous in detailing if β OHB supplementation fails to either rescue or further exacerbate the effects of glucose, pyruvate, and glutamine withdrawal, yet in the metabolic viability assays, β OHB fails to increase viability. This suggests that the cells are still undergoing their switch from glycolysis to OXPHOS and cannot yet use ketone body in the culturing media.

The metabolic viability of the NE-4C NSC line was non-significantly increased by β OHB supplementation at 15DIV, metabolic viability is not restored to the same levels as the glucose containing conditions, but the importance of this insignificance is that it does not further exacerbate the effect of glucose deprivation on metabolic viability. As cells have now fully differentiated, they can now metabolize ketone bodies in their period of prolonged starvation as they have switched their metabolism from glycolysis to OXPHOS.

6.2 Future Directions

The area of ketone metabolism and its potentials for therapeutic application is growing in popularity and scientific relevance. Investigating the impact of β OHB on cell growth and expansion past 15DIV would allow us to further understand its metabolism and functionality as cells become fully differentiated.

Translating this research and replicating it in primary cell cultures with neurons taken from a developing embryonic mouse cortex would better allow us to understand the actions of nutrient deprivation and ketone body supplementation on the growth and phenotype of a developing neuron.

For *in vivo* studies, a set of experiments could be devised where the pregnant mouse/dam is fed a specific ketogenic pellet diet that's deprived of glucose, glutamine and pyruvate and any other potential metabolic input that could produce energy. Then at specific brain development timepoints such as E13.5, the female and her pups could be sacrificed, and embryonic brains could be sectioned and stained using immunohistochemistry to investigate how ketone body metabolism in utero impacts the growth and development of the CNS.

Chapter 7

Appendices

Cell Lines

| Cell lines | Manufacturer | Catalogue Number |
|-------------------|--|-------------------------|
| NE-4C Cells | ATCC | CRL-2925 |
| SH-SY5Y Cells | European Collection of Authenticated Cell Cultures | 9403004 |

Table 7.1 Cell lines used

Cell Culture Reagents

| Material | Manufacture | Catalogue Number |
|--|----------------------|-------------------------|
| DMEM | Gibco | 11966-025 |
| Falcon Tubes | Coming Life Sciences | C35196 |
| Foetal Bovine Serum | Sigma-Aldrich | F2442 |
| Haemocytometer | Bürker-Turk | BRND719505 |
| Hank's Balanced Salt Solution (HBSS) | Sigma-Aldrich | H6648 |
| Glucose Solution | Gibco | A2494001 |
| Glucose Free DMEM | Gibco | 11966-025 |
| L-Glutamine | Sigma-Aldrich | G3126 |
| Metformin Hydrochloride | MP Biomedicals | 151691 |
| Penicillin/Streptomycin | Sigma-Aldrich | P4333 |
| Poly-L-lysine coated 96 well plates | Coming Life Sciences | 354516 |
| Sodium Pyruvate | Sigma-Aldrich | S8636 |
| Trypan-blue | Sigma-Aldrich | T8154 |
| T25 flask | Greiner Bio-One | 690160 |
| T50 flask | Greiner Bio-One | 690170 |
| T75 flask | Greiner Bio-One | 658975 |
| β -hydroxybutyric acid sodium salt | Sigma-Aldrich | 298360 |

Table 7.2 Cell Culture Reagents

Cell Assays

| Material | Manufacturer | Catalogue Number |
|---------------------------|---------------|------------------|
| MTT Assay | Abcam | ab211091 |
| Dimethyl Sulfoxide (DMSO) | Sigma-Aldrich | ab211091 |

Table 7.3 Cell Assays

General Laboratory Chemicals

| Material | Manufacture | Catalogue Number |
|---|------------------------|------------------|
| Acrylamide | Sigma-Aldrich | A9099 |
| Calcium Chloride (CaCl ₂) | VWR International Ltd. | 22322.295 |
| Dimethyl Sulfoxide (DMSO) | Sigma-Aldrich | D2650 |
| EDTA | Sigma-Aldrich | E9884 |
| Ethanol | Sigma-Aldrich | E7023 |
| Hydrochloric acid (HCl) | Sigma-Aldrich | 320331 |
| Magnesium sulphate (MgSO ₄) | Sigma-Aldrich | 1374361 |
| Methanol | Sigma-Aldrich | 34860 |
| Potassium bicarbonate (KHCO ₃) | Sigma-Aldrich | 237205 |
| Potassium Chloride (KCl) | Sigma-Aldrich | P3911 |
| Potassium phosphate, dibasic (KH ₂ PO ₄) | Sigma-Aldrich | P3786 |
| Sodium Chloride (NaCl) | Sigma-Aldrich | S9888 |
| Sodium dodecylsulphate (SDS) | Sigma-Aldrich | L3771 |
| Triton X-100 | Sigma-Aldrich | T8787 |
| Tween | Sigma-Aldrich | P1629 |

Table 7.4 General Laboratory Chemicals

General Laboratory Products

| Material | Manufacture | Catalogue Number |
|---|------------------------------|--|
| Eppendorf's – 0.5ml, 1.5ml, 2ml | Sarstedt, Numbrecht, Germany | 72.735.100 |
| Fisherbrand Multichannel Pipette | Thermofisher Scientific Inc. | 11835772 |
| Microscope slides | Thermofisher Scientific Inc. | 12383118 |
| Lens cleaning wipes | VWR International Ltd | 111-5000 |
| Parafilm | Thermofisher Scientific Inc. | 11762644 |
| Pipette tips – 0.5µl, 1µl, 5µl, 10µl, 20µl, 200µl, 1000µl | Greiner Bio | 776353/ 773353/ 771353/ 773353/ 775353/ 778353 |
| 6 well plates | Greiner Bio | 657160 |
| 96 well plates | Greiner Bio | 655074 |
| | | |

Table 7.5 General Laboratory Products

Immunocytochemistry

| Reagent | Manufacturer | Catalogue Number |
|---|----------------------------|------------------|
| ActinRed Probe | Invitrogen | R37112 |
| Anti-BrdU primary antibody | Sigma-Aldrich | B2531 |
| Anti-Mouse IgG FITC secondary antibody | Sigma-Aldrich | F0257 |
| Apoptosis and Necrosis Quantification Kit | Biotium | 30017 |
| BrdU | BioLegend | 423401 |
| DAPI | Sigma-Aldrich | D9542 |
| Normal Goat Serum | Cell Signalling Technology | 5425 |
| Paraformaldehyde | Sigma-Aldrich | BCBK8016V |
| PBS | Sigma-Aldrich | SLBV2666 |
| Triton X100 | Sigma-Aldrich | X100 |

Table 7.6 Immunocytochemistry Reagents

| Cell Culture Media Reagent | Purpose |
|---|--|
| Dulbecco's Modified Eagle's Medium/Nutrient Mixture F-12 Ham (DMEM), containing glucose, without L-glutamine, liquid, (Sigma Aldrich) | Useful in a wide range of cell culture applications, (especially when supplemented with fetal bovine serum (FBS)) and is protein free containing. It has an increased level of amino acids and vitamins to support cell growth. |
| DMEM, no glucose | DMEM without glucose but contains L – glutamine. |
| Fetal Bovine Serum (FBS) (Sigma Aldrich) | FBS contains biomolecules, such as growth factors, proteins, vitamins, trace elements, hormone that help with the growth and maintenance of cells. FBS was heat inactivated before being used to create the specific media concentrations. Once FBS was heated to 56°C, it was left for 30 mins before being aliquoted to its appropriate amounts. |
| L – glutamine (200 mM) (Bioxtra) | Essential amino acid that is a crucial component of culture media and serves as a major energy source |
| Penicillin-Streptomycin (5,000 U/mL) (5000 units/ mL of penicillin and 5000 µg/mL of streptomycin) | Reduces the risk of infection from human error in cell culture. |
| Sodium pyruvate (100 mM) (Sigma) | Used in the glucose free and βOHB media as a carbohydrate source. Involved in amino acid metabolism and initiates the Krebs cycle. |

Table 7.7 Cell culture media reagents

Supplementary file 1

Search Strategy: PubMed, Web of Science, Embase (Last search: 16 June 2020)

(Beta-hydroxybutyrate OR β -hydroxybutyrate OR Ketone bodies) AND (proliferation OR survival OR growth OR viability OR health OR metabolism OR effect OR response OR metastasis OR apoptosis OR necrosis OR death) AND (Cells OR In vitro OR cell line OR cancer OR tumour) NOT (polyhydroxybutyrate OR PHB OR poly-beta-hydroxybutyrate OR bacteria OR microbe)

Inclusion Criteria

- In vitro experiment
- Exogenous BHB supplementation
- Comparison with control
- Quantitative outcome

Exclusion Criteria

- Reviews/letters, case reports, personal opinions, conference abstracts, book chapters, clinical studies
- Exclusively in vivo studies

Extracted study parameters

- **Reference** (Author&Year)
- **Tissue type** (Neuronal/Intestinal/Breast etc.)
- **Cell type** (Primary, stem, cancer, animal cell)
- **Cell line/s** (E.g., SH-SY5Y)
- **Medium** (E.g., DMEM/RPMI)
- **Serum** (none/FBS/FCS, %concentration)
- **Antibiotics** (yes/no)
- **L-glutamine** (yes/no, concentration),
- **Pyruvate** (yes/no, concentration),
- **Glucose** (yes/no, concentration),
- **Other media components**
- **β OHB concentration**
- **Duration of β OHB administration** (hr),
- **Additional ketone bodies tested** (Acetoacetate etc)
- **Combination therapy** (added with other drugs?)
- **Assays used** (e.g., MTT, OCR, proliferation)
- **Findings** (positive/negative/unchanged for each tested parameter),
- **Proposed mechanism of action**

| Study ID | Investigated effects | Summary of findings | Proposed mechanism for ketone effect |
|--------------|---|---|--|
| Maurer 2011 | KB metabolising enzyme expression levels/ Protective effects of ketones on glucose withdrawal induced Apoptosis | KBs metabolising enzymes are expressed in the five glioma cell lines and primary rat lines both at the mRNA and the protein level. KBs don't alter growth or proliferation of glioma cell lines in presence of sufficient glucose and varying O ₂ concentrations. p53 inhibition did not appear to induce ketone metabolism, Exposure to βOHB does not modulate glioma cell motility and invasiveness. Treatment with βOHB does not modify the expression of hypoxia-inducible factor-1a (HIF-1a) and of its target genes. βOHB does not influence glioma cell sensitivity towards different triggers of cell death. | Intracellular: OXCT1 is a mitochondrial matrix enzyme that plays a central role in extrahepatic ketone body catabolism by catalysing the reversible transfer of coenzyme A (CoA) from succinyl-CoA to acetoacetate. |
| Cheng 2013 | Apoptosis /Glutathione (GSH) content /Intracellular ROS level /Mitochondrial Membrane Potential /Viability | βOHB inhibited the decrease of cell viability induced by H ₂ O ₂ in PC12 cells. It inhibited the apoptosis induced by H ₂ O ₂ in PC12. βOHB inhibited the increase of intracellular ROS induced by H ₂ O ₂ . βOHB inhibited the decrease of GSH levels induced by H ₂ O ₂ . βOHB inhibited the decrease of MMP induced by H ₂ O ₂ . βOHB inhibited the increase of caspase-3 activity induced by H ₂ O ₂ . | Intracellular: ROS over production |
| Xie 2015 | Apoptosis /Intracellular Ca ²⁺ /Intracellular ROS /Protein Concentration /mRNA concentration /Viability | βOHB relieves the oxidative stress in Aβ-induced PC12 cells. The apoptotic pathway is also inhibited by βOHB in these cells also. | Intracellular: ROS regulation and Ca ²⁺ mobilization and p53 activation |
| Cheng 2010 | Apoptosis /GSH total /Intracellular ROS /Mitochondrial Membrane Potential (MMP) /Malondialdehyde (MDA) formation /Viability | βOHB inhibited MPP ⁺ -induced apoptosis. The measurement of MDA formation showed that βOHB alleviated lipid peroxidation induced by MPP ⁺ . The loss of mitochondrial membrane potential (MMP) induced by MPP ⁺ was preventative by βOHB. The changes of intracellular ROS and total glutathione induced by MPP ⁺ were reversed by βOHB. βOHB protected PC12 cells against MPP ⁺ induced death and apoptosis. | Intracellular: Inhibition of mitochondrial mediated apoptosis and oxidative stress. It decreases intracellular ROS and MDA formation, protected from MPP ⁺ induced apoptosis via mitochondrial mediated signal pathway |
| Durigon 2018 | Cell Density /Mitochondrial DNA re-organization in response to nutrient changes | WHS-derived fibroblasts survive on KBs, which can be attributed to their reduced dependence on glucose oxidation. | Intracellular: When LETM1 is scarce, there's a switch to a consumption and use of ketone bodies |
| Cheng 2005 | Cell cycle changes /Intracellular Ca ²⁺ /Proliferation | βOHB promoted cell proliferation for each cell line. Cell cycle analysis indicated that βOHB had a stimulatory effect on DNA synthesis. | Intracellular/Genetic: βOHB had a stimulatory effect on cell cycle progression that is mediated by a signalling pathway dependent upon increases in intracellular calcium ([Ca ²⁺] _i) |
| Jiang 2011 | ATP levels/ Viability | AcAc and βOHB supported the growth of TSc2 ^{-/-} cells. | None provided |
| Tagawa 2019 | mRNA expression/ Protein expression /SIRT1 activity /Viability | βOHB treatment suppressed the protein expression of ER stress responsive genes and increased cell viability, while reducing the protein expression of apoptosis inducible genes. | Intracellular: suppresses hepatic ER stress via both AMPK-dependent and independent pathways |
| Wang 2019 | mRNA expression /Proliferation /Protein Expression /Viability (MTT and Trypan Blue) /Wound-Healing Migration Assay | KB treatment reduced the proliferation and migration promoting effects of HMGCS2 knockdown in cells. | Intracellular: Ketone bodies inhibited growth and induced apoptosis in pancreatic cancer cell lines. Ketone bodies appears to be involved in 3-hydroxy-3-methylglutaryl-CoA synthase 2 (HMGCS2 -promoted HCC progression. |
| Mikami 2020 | Apoptosis /HDAC expression /Proliferation /Survivin expression | βOHB increased cisplatin-induced apoptosis and cleavage of caspase-3 and caspase-8. βOHB diminished the expression of HDAC 3, 5 and 6 and survivin. | Genetic: decreased HDAC 3 and 6 expressions, leading to a downregulation of survivin and then increased cisplatin-induced cleaved caspase 3 and caspase 8 in HepG2 cells |

| | | | |
|-----------------|--|---|--|
| VilÅ -Brau 2011 | FGF21 and its relation to SirT1 during Fed-to-Fast Transition/ FGF21 mRNA Expression /HMGCS2 Expression on Fatty Acid Oxidation and Ketogenesis/ HMGCS2 Expression for PPAR mediated Induction of Fatty Acid Oxidation/HMGCS2 Regulation of FGF21 Expression | AcAc induced FGF21 expression in a dose-dependent manner, while β OHB did so to a lesser extent. This was dependant on SirT1 expression. This suggests that the products of ketogenesis can stimulate gene expression through the SirT1 activity and therefore that HMGCS2 could control metabolic processes other than ketogenesis in this cell line. | Genetic: through AcAc (but not β OHB) generation could modulate the cytosolic [NAD]/[NADH] ratio and therefore SirT1 activity. |
| Wang 2016 | ROS Production and Lipid Peroxidation /p38 MAPK and JNK pathway activation /Viability | β OHB did not have any significant effect on HT22 cell viability up to 10mM compared to controls. β OHB protected HT22 cells against glutamate-induced toxicity. Cells pre-treated with β OHB maintained their normal neurite morphology. β OHB significantly suppressed ROS generation. β OHB treated cells also showed significantly reduced levels of MDA (marker of lipid peroxidation) following glutamate treatment compared to glutamate alone. β OHB activated the p38 MAPK and JNK pathway. Significantly less phosphorylation of both was seen in β OHB treated cells compared to glutamate alone. Phosphorylation of these can promote cell death. | Intracellular: Reduced ROS production, reduced p38, and JNK |
| Patel 1981 | Activities of Ketone Body-Metabolizing Enzymes in Glioma and Neuroblastoma Cells /Lipid Synthesis / Regulation of CoA-Transferase Activity by KBs | The incorporation of glucose carbon into lipids is significantly reduced in cells of both lines in the presence of KBs. Addition of AcAc but not β OHB to the culture medium resulted in a significant increase in the activity of 3-keto acid CoA-transferase and in the rate of AcAc oxidation in neuroblastoma cells but not glioma cells. | Intracellular: AcAc and not β OHB accelerates the increase in the specific activity of CoA-transferase in neuroblastoma cells but not in glioma cells. The mechanisms by which AcAc does this is unclear. |
| Lamichhane 2017 | Apoptosis/ ATP levels /Cytotoxicity /ROS generation/ Viability | β OHB attenuates glucose deficiency induced cytotoxicity and ROS production in SH-SY5Y cells. β OHB also reverses glucose deficiency-induced reduction in the phosphorylation of ERK and GSK3b in SH-SY5Y Cells. Metformin and β OHB affect low glucose-induced cell death in primary neuronal cells. | Intracellular: β OHB induced protective effect in glucose deficiency was mediated by ERK activation, but not by GSK3inhibition. |
| Xu 2011 | Cytokine concentrations /Intracellular ROS /Nitrite Measurement /Viability | β OHB improved the viability, decreased the intracellular levels of ROS and NO, and prevented the release IL-1B, IL-6 and TNF-alpha of LPS treated BV2 cells | Intracellular: β OHB protects neurons against MPTP induced toxicity, inhibiting microglial reactive oxygen species and nitrogen monoxide |
| Kweon 2004 | Rotenone induced toxicity | Supplementation with β OHB decreased rotenone induced toxicity in the differentiated MN9D cells | Intracellular: β OHB markedly reduced toxicity following by enhancing cellular energy state |
| Li 2020 | mRNA & Protein expression / Viability | β OHB improved cell viability and prevented downregulation of TrkA expression induced by A β . β OHB inhibited the upregulation of HDAC1/2/3 expression and downregulation of histone acetylation (Ace-H3K9 and Ace-H4K12) levels in A β treated cells. | Genetic/Extracellular: β OHBs upregulation of TrkA is possibly controlled by lowering HDAC1 and HDAC3 |
| Cheng 2007 | Apoptosis (through acridine orange (AO) staining & TUNEL labelling) /Bcl-2 and Bax expression /Caspase - 3 activity / Viability | β OHB prevented the decrease of cell viability and the increase of caspase-3 activity induced by 6-OHDA in a dose-dependent manner in PC12 cells. The data showed that β OHB inhibited the apoptosis of PC12 cells induced by 6-OHDA in relation to up-regulating the ratio of Bcl-2/Bax mRNA. | Intracellular: Bcl-2/Bax to protect neural cells, |

| | | | |
|--------------|---|--|--|
| Imamura 2006 | Caspase activities /Cytotoxicity /Lactate Dehydrogenase levels /Mitochondrial Membrane Potential/ Oxidation Reduction | Pre-treatment of cells with 8 mM β OHB provided significant protection to SH-SY5Y cells against rotenone. Whereas rotenone caused the loss of mitochondrial membrane potential, released cytochrome c into the cytosol, and reduced cytochrome c content in mitochondria, addition of β OHB blocked this toxic effect. β OHB also attenuated the rotenone-induced activation of caspase-9 and caspase-3. Pre-treatment with 8 mM β OHB attenuated the decrease of AlamarBlue fluorescence. | Intracellular/Genetic: Addition of ketones reverse the inhibition of flavoprotein reduction at complex I and II by supplying cytosolic and mitochondrial free NADH. |
| Zhang 2018 | mRNA & Protein expression | LPL and microRNA-29a expression were separately increased and down-regulated in 2 μ M A β 25–35 exposed SH-SY5Y cells, but respectively decreased and up-regulated in 10 μ M A β 25–35-exposed cells, which were all reversed by β OHB. The increase of HDAC2/3 expression and the decrease of acetylated H3K9 and H4K12 levels were alleviated in 2 or 10 μ M A β 25–35-exposed cells by β OHB treatment. | Intracellular/Genetic: β OHB may mediate, at least partly, the effect of alternate date fasting (ADF) on the reduction of brain-derived LPL expression in AD. Inhibition of HDACs by β OHB plays a role in regulation of ADF on LPL expression. miR-29a was found to mediate the effect of β OHB on LPL expression, which HDAC2/3 may be implicated in the effect of β OHB on miR-29a expression. β OHB may also participate in protecting against AD via anti-oxidation pathway. |
| Zhang 2017 | mRNA & Protein expression | β OHB downregulated the expression of AQP4-M1 and HDAC3, reduced the AQP4-M1/M23 ratio, and increased AQP4-M23 and miR-130a expression in 2 μ M A β treated U251 cells. | Intracellular/Genetic: β OHB may at least partly mediate the effect of ADF on the reduction of AQP4-M1/M23 ratio in AD. miR-130a partly mediated the effect of β OHB on the AQP4-M1/M23 ratio, in which other ways may be involved. HDAC3 may be involved in the reduction of AQP4-M1/M23 ratio induced by β OHB, and in which miR-130a may be implicated |
| Findlay 2015 | Glucose oxidation | BACE1 activity-dependent deficit in glucose oxidation was alleviated by the presence of β OHB | Intracellular: By directly increasing the availability of acetyl CoA to the TCA cycle, thus circumventing PDH. |
| Shang 2018 | LPS & ATP Triggered Activation of NLRP3 Inflammasome and migration /Motility /NLRP3 Inflammasome and downstream effectors function/Protein function/PTX function /Viability | β OHB decreased C6 cells migration and NLRP3 inflammasome activation, decreased the levels of activated caspase1 and IL-1 β . The enhancement p-STAT3, degradation of degradation of nuclear factor of kappa light polypeptide gene enhancer in B-cells inhibitor alpha (κ B α) as well as the overexpression of FGF2 resulting from LPS/ATP treatment, and subsequent IL-1 β maturation could also be compensated by β OHB. | Intracellular: The inhibitory effect of β OHB on NLRP3 inflammasome contributed a lot to the suppression of C6 migration. Furthermore, the results suggest that β OHB might act as a signalling molecule to regulate certain G α i-coupled receptors to inhibit the activation of NLRP3 inflammasome. |
| Kabiraj 2012 | Apoptosis & Necrosis /Cytotoxicity /Nuclearpoly (ADP-ribose) polymerase (PARP) cleavage /Synphilin-1 levels | Overall treatment of cells with β OHB prior to rotenone was protective against rotenone induced apoptosis and synphilin-1 aggregation. | Intracellular: By reducing nitrosative stress related apoptotic cell death through acting on an element within the cascade. |
| Liu 2018 | Hypothalamic Fe ²⁺ levels/ Luciferase activities of mutated Fto promoters /Protein expression /Serum and hypothalamic β OHB levels /Transcription levels of Fto, Foxo3a, Mt2, Lcn2, and beta-actin genes | β OHB induces transiently elevated levels of FTO expression. β OHB increases the Fto promoter activity. Overexpression or knockdown of Fto alters the Fto promoter activity. | Intracellular/Genetic: β OHB induces transient upregulation of Fto expression. β OHB could induce the reporter gene expression through the Fto promoter fragment. β OHB upregulates the expression of a number of genes by increasing histone acetylation at their promoters |

| | | | |
|--------------------------|---|---|--|
| Hasan 2008 | Insulin release | Both Methyl succinate and β OHB form a strong stimulant of insulin release in INS-1 cells. | Intracellular: The anaplerotic input of pyruvate carboxylase generated oxaloacetate into mitochondrial pathways is necessary. Also, alpha-ketoglutarate catalysed by glutamate dehydrogenase for glutamate derived from glutamine in BCH plus glutamine-stimulated cells and at succinate in methyl succinate plus β OHB cells. |
| Macdonald 2008 | Fuel secretagogue metabolism /Insulin release /Metabolite measurements /Short chain acyl-CoA levels | In the INS-1 cell line, insulin release by BCH was decreased and adding β OHB or α -ketoisocaproate, which increases mitochondrial acetoacetate, normalized BCH-induced insulin release. | Intracellular: The normalization of BCH-induced insulin release by β OHB further solidifies the theory that acetoacetate is a carrier molecule of acyl groups from mitochondria to the cytosol where it is converted to short chain acyl-CoAs |
| MacDonald 2008 | Carbon incorporation from β OHB /Insulin release / Metabolite measurements /Short-chain acyl-CoAs measurements | AcAc and β OHB alone did not stimulate insulin release. AcAc and β OHB when combined with MMS, or either ketone body was combined with lactate, insulin release was stimulated 10-fold to 20-fold the controls (almost as much as with glucose). In rat pancreatic islets, β OHB potentiated MMS and glucose induced insulin release. In line with this, citrate was increased by β OHB plus MMS in INS-1 cells and β OHB plus succinate in mitochondria. | Intracellular: The results support the idea that anaplerosis is critical for the insulin release and suggests that short-chain acyl-CoAs may be some of the products of anaplerosis in the β cell |
| Wang 2017 | Autophagy | β OHB were capable of inducing autophagy in cancer cells post-radiation and promoting cancer cell recovery from radiation-induced damage in vitro | Intracellular: β OHB increased ROS levels which increased PP2A activity, repressing mTOR activation |
| McGee 1974 | Fatty acid synthesis | Glucose was found to be a much better substrate for fatty acid synthesis than AcAc, β OHB, or amino acids. | Intracellular: Defective regulation of fatty acid biosynthesis in tumours involves regulation of enzyme production but not short-term modulation of enzyme activity. |
| Martinez-Outschoorn 2011 | Tamoxifen-resistance in MCF7 cells. | Single cell cultures of MCF7 cells were incubated with β OHB prior to treatment with tamoxifen. Tamoxifen treatment induces the apoptosis of MCF7 cells. However, treatment with L-lactate, β OHB, decreases tamoxifen-induced apoptosis 3.7-fold | Intracellular: Ketone bodies in epithelial cancer cells induces mitochondrial activity, in the same way as coculture with Cav-1 deficient fibroblasts. |
| Martinez-Outschoorn 2012 | Ketone enzyme expression /Ketone transmembrane transporter (MCT1) inhibition /Ketone production and re-utilisation enzyme localisation /Mitochondrial biogenesis /Mitochondrial anti stress response/Smad2&3 activation | Fibroblast/MCF 7 breast cancer co-culture induces an increased expression of HMGCL (ketone production enzyme) and decreased expression of ACAT1 (ketone re-utilisation enzyme). Serum starvation of fibroblasts resulted in increased expression of ketogenic enzymes β DH1 and HMGCS1 in fibroblasts. Ketone bodies can induce mitochondrial biogenesis in human breast cancer cells (MCF7). β OHB increased mitochondrial mass. The MCT1 inhibitor CHC inhibits mitochondrial biogenesis in MCF7 cells under co-culture conditions. Secretions of ketone bodies by fibroblasts are taken up by breast cancer cells via MCT1. Inhibiting this transporter prevents mitochondrial biogenesis in MCF7-fibroblasts co-culture. Ketone bodies induce Smad2/3 activation in MCF7 cells. Smad 2 and 3 are involved in propagation of the TGF β signal pathway in cell differentiation/proliferations. Cancer-associated fibroblasts and ketone bodies induce the mitochondrial anti-stress response in MCF7 cells. | Intracellular: This allows the cancer cells to use the ketones as mitochondrial fuel as the ketones are converted back to acetyl-CoA. Thus, ketone metabolising enzymes (such as ACAT1) are upregulated by the cancer cells. |

Table 7.8 Proposed mechanisms for positive ketone effect on cell lines

| Study ID | Investigated effects | Summary of findings | Proposed mechanism for ketone effect (Extra/Intracellular/Genetic) |
|----------------|--|---|---|
| Huang 2017 | Gene expression /Metabolite levels /Mitochondrial respiration /Tumour volume | β OHB is secreted by MGDAs and enhances cancer cells malignancy. Upon co-culturing with MGDAs or treatment with β OHB, breast cancer cells expressing MCT2 increase the global histone H3K9 acetylation and up regulate several tumour-promoting genes. | Genetic: Consistently, treatment of MCT2-expressing breast cancer cells with either β OHB or co-culture with MGDAs enhances tumorigenic properties and leads to increased acetylation of histones and transcriptional upregulation of tumour-promoting genes such as IL-1b and LCN2 in breast cancer cells expressing MCT2. |
| Rodrigues 2017 | β OHB uptake /Glucose uptake /Lactate output | Cells cultured in β OHB showed β OHB uptake equal to 54% of glycolytic ATP phosphorylation. | Intracellular: The cultured cancer cells would have substantially increased their ATP generation by oxidizing β OHB and that oxidation of β OHB seems to have substituted for oxidative metabolism of glucose |
| Zhang 2018 | Cell density /Protein expression | β OHB added to each cell culture significantly increased proliferation of HeLa cells. Downregulation of both β DH1 and OXCT1 rendered HeLa cells sensitive to the KD | Intracellular: very low expression levels of β DH1 and OXCT1 maybe sensitive to KD therapy. |
| Kaya 2018 | Viability | HFF cells showed a decrease in viability when cultured in glucose-free media. Addition of AcAc or β OHB also resulted in a small non-significant increase in viability. MCF-7 cells were subjected to glucose-free media, their viability decreased significantly compared to controls. This was not reversed by AcAc and β OHB. | Intracellular: MCF-7 lack the ability to use KBs as an energy source. This is thought to be due to their lower expression of Succinyl-coenzyme A transferase, which represents the rate limiting step in the metabolic processing of KBs for energy production. HFF have a high expression of this enzyme. |
| Shukla 2014 | Apoptosis /Central carbon metabolism /c-Myc expression and activity /Glycolytic enzyme expression /Glycolytic flux /Metabolic alterations /Tumour cell-induced muscle fibre and adipocyte degradation /Viability | KBs diminish pancreatic cancer cell growth, induce apoptosis in a dose-dependent manner, diminish the expression of glycolytic enzymes and c-Myc expression and activity. KBs inhibit tumour cell-induced muscle fibre and adipocyte degradation and alter carbon metabolism in pancreatic cancer cells. | Intracellular/Nuclear: The reversal of metabolic syndrome in cancer cells by KBs might be related to levels of c-Myc. This may be due to c-Myc's role in promoting glucose transporter and glycolytic enzymes which showed reduced expression with ketone treatment. |
| Shakery 2018 | Colony Formation Assay/Extracellular Acidification Rates/ Gene expression /Oxygen consumption /Scratch Assay /Viability | β OHB increased cell viability in cells. β OHB significantly decreased ECAR and increased OCR in both cell types following β OHB treatment reflecting the superiority of OXPHOS profile compared to glycolysis in both cell types. β OHB increased the expression of genes associated with stemness and mitochondrial biogenesis and decreased the expression of genes related to glycolysis and differentiation in 5FU treated cells. Self-renewal and migration potential of β OHB treated cells increased significantly. | Intracellular/Genetic: β OHB acts as a tumour growth booster both through fuelling via mitochondrial metabolism and through epigenetic mechanisms |
| Kadochi 2017 | ALP activity /Cell growth /GSSG quantity in cell lysates /Gene expression /Mitochondrial volume /Oxidative stress /Viability | β OHB and AcAc under glucose starvation had a synergistic effect on cell growth inhibition. In addition, AcAc and AcAc + β OHB promoted an imbalance in the expression of enzymes in the electron transport chain. β OHB and AcAc decreased lactate fermentation, particularly under glucose starvation. | Intracellular: β OHB and AcAc switch the energy production pathway from glycolysis and lactate fermentation to OXPHOS, increasing oxidative stress and ROS species, thus damaging mitochondria, and ultimately resulting in apoptosis. |
| Guh 2003 | Collagen production /Cell cycle distribution /Gene expression /Proliferation /Tubular trans differentiation | The effects of β OHB on cultured HK-2 cells includes a decrease in cellular proliferation, oxidative stress dependent activation of Smad 2/3, increased TGF- β 1 mRNA/transcriptional activity, increased TGF- β 1 bioactivity, and post transcriptional increases in p21WAF1 and p27kip1 protein expression. Moreover, β OHB induced growth inhibition was dependent on TGF- β band Smad3 while β OHB induced-collagen production and p21WAF1/p27kip1 protein expression were dependent on Smad3. | Intracellular/Nuclear: β OHB induced growth inhibition is likely dependent on TGF- β induced p21WAF1 and p27kip1 protein expression in HK-2 cells. β OHB induced p21WAF1 and p27kip1 protein expression by increasing p21WAF1 and p27kip1 protein stabilities in HK-2 cells. β OHB-inhibited Mito-genesis was dependent on TGF- β . β OHB time dependently increased nuclear Smad2/3 protein expression at 2 to 8 hr in HK-2 cells |

| | | | |
|------------|---|---|--|
| Liu 2019 | Cell growth /k β OHB p53 activity. | Doxorubicin induces p53 activation and these production of p21 and PUMA proteins. Both protein levels were much lower when doxorubicin was administered with β OHB. p53 cell growth arrest and apoptosis-inducing functions are attenuated in the β OHB-treated cells. Nutlin treatment stabilises p53 and thus causes cells to grow slowly. However, when administered with β OHB cells grew at the same rate as controls. | Intracellular/ Nuclear: The findings show that p53 K β OHB is induced by β OHB and that k β OHB attenuates p53 activity. Since p53 is an important tumour suppressor protein, attenuation of its activity in the presence of β OHB might partially explain the role of KBs in cancer. |
| Magee 1979 | β OHB concentration /Effect of glycolytic inhibitors and chemical analogues /Glucose utilization /Inhibition of cell proliferation / Proliferation/ / Total lactate production /Viability | Cell growth was inhibited, and this effect was reversible, non-toxic, and proportional to the concentration of β OHB up to 20mM. The total glucose utilization and the total lactate production were reduced in proportion to the inhibition of cell proliferation. β OHB was not metabolized by the cells. | Intracellular: Inhibiting the metabolism of glucose |
| Jain 2003 | IL-6 levels/ Intracellular ROS levels | Exogenous addition of AcAc, but not β OHB, increases IL-6 secretion and ROS generation in U937 cells. | Intracellular: The study shows that the IL-6 secretion inactivated monocytes were stimulated by both AcAc and high glucose, separately as well as when used together, whereas β OHB did not have any effect on IL-6 secretion. Similarly, AcAc can generate ROS, whereas β OHB does not, which suggests that ROS may be involved in the increased IL-6 secretion in AcAc-treated monocytes. |
| Jain 2002 | TNF-alpha secretion, reactive oxygen species (ROS) production, protein oxidation, cell growth and cellular cyclic AMP measurements | AcAc treatment increases TNF- α secretion, increases oxygen radicals' production, and lowers cAMP levels in U937 cells. However, β OHB did not have any effect on TNF-alpha secretion or oxygen radicals' production in U937 cells. | Intracellular: TNF- α secretion in activated monocytes was stimulated by both AcAc and HG, separately as well as together, whereas β OHB did not have any effect on TNF- α secretion. AcAc can generate ROS, whereas β OHB does not. This suggests that ROS may be involved in the increased TNF- α secretion in AcAc-treated monocytes |
| Rains 2011 | Mitochondrial membrane potential /Viability | AcAc & β OHB treatment with different concentrations of AcAc caused a decrease in MMP in monocytes. The change in MMP in treated monocytes increased with increasing concentrations of AcAc. However, monocytes treated with β OHB did not show any change in MMP. | Intracellular: It is speculated that effects seen with AcAc may be due to the generation of oxygen radicals. While both can generate oxygen radicals which may ultimately lead to an oxidative environment, AcAc contains 2 keto groups compared to β OHB's one keto group. This may account for the different effects seen. |
| Jain 1999 | AcAc and β OHB determinations /Apoptosis (by TUNEL assay) /GSH, lipid peroxidation /Proliferation (through Alamar Blue Assay) | A dose-dependent growth inhibition and induction of apoptosis as a result of treatment with AcAc in U937 cells was observed. Furthermore, there was a significant decrease in GSH and increase in lipid peroxidation products in AcAc-treated U937 cells. | Intracellular and Extracellular: AcAc may cause phosphatidylserine (PS) externalization and monocyte activation resulting in the secretion of proinflammatory cytokines. This, in turn, might chemoattract monocytes and macrophages to the site of lesion, starting an immunological cascade of events leading to inflammation and microvascular lesions. |
| Luo 2017 | Extracellular β OHB impact on NPC cell proliferation and migration /Identification of differentially expressed ketogenesis genes in nasopharyngeal cancer tumours /Impact of HMGCL on intracellular levels β OHB and AcAc and generates ROS in NPC cells. | Two genes, HMGCL and β DH1, both involved in the ketogenesis pathway, were significantly downregulated in NPC tissue. The expression of HMGCL is downregulated in NPC. HMGCL increases intracellular level of β OHB and AcAc and generates ROS in NPC cells. β OHB generated by ectopic expression of HMGCL as well as extracellular β OHB treatment elevated ROS production in NPC cells. Exogenous expression of HMGCL suppresses NPC cell proliferation in vitro. Extracellular β OHB inhibits NPC cell proliferation and migration depends on increasing ROS levels. Both intracellular and extracellular β OHB could stimulate ROS generation in NPC cells. Growth and motility of HK1 cells were dose-dependently suppressed with β OHB | Intracellular: Thus, ROS is a major downstream mediator of the effects of intracellular ketone bodies, and the inhibition of proliferation caused by KBs depends on ROS in NPC. |

| | | | |
|-------------------|---|--|---|
| | | treatment. β OHB treatment attenuates the migration of 5-8F cells. The combined treatment of β OHB and NAC increased the migration of HK1 cells. | |
| Vallejo 2020 | Combined effect of 2-DG and AcAc on cell viability /Ketone enzyme expression and cell viability with ketone treatment /Neurospheres formation of GSCs with AcAc treatment | β DH1, OXCT1 and ACAT1 (enzymes necessary for ketone metabolism) are downregulated in adult and paediatric GBM. GSC mitochondrial ultrastructure suggested defects in OXPHOS. Treatment of both GBM and GSC cell lines resulted in dose-dependent decreases in viability in response to glycolytic inhibitor 2-deoxy-Dglucose (2-DG), and AcAc but not β OHB. AcAc induced apoptosis. AcAc reduced neurosphere formation at concentrations as low as 1 mM. Combined treatment of low dose 2-DG (50 μ M) with AcAc resulted in more cell death than either treatment alone. The effect was greater than additive at low concentrations of AcAc, reducing viability approximately 50% at 1 mM AcAc. AcAc upregulated mitochondrial uncoupling protein 2 (UCP2), which may explain this potential drug synergism via multi-faceted inhibition of the glycolytic pathway | Intracellular: AcAc but not β OHB may be increasing ROS while decreasing ATP levels and triggering apoptosis. This may be due AcAc's ability to impact UCP2 (over expressed in tumour cells and important in ATP production). This upregulation may explain the potential synergy observed due to increased decoupling of the mitochondrial membrane by UCP2, thereby allowing TCA cycle intermediates to accumulate and leak into the cytosol negatively affecting enzymes at the beginning of the glycolytic pathway. Hence this may explain the further decreased cell viability in AcAc/2-DG combo treatment with 2-DG inhibiting glycolysis and AcAc causing initiating enzymes of glycolysis to be negatively inhibited from increased TCA intermediates in the cytosol. |
| Ji 2020 | Apoptosis /Gene expression / Glucose transport /Mitochondrial function and morphology /Proliferation /ROS production / Viability | β OHB inhibits the proliferation of GSCs but not normal NSCs in vitro, promote GSC apoptosis, as well as attenuating stemness of GSCs. β OHB treatment appears to inhibit glycolysis, cause mitochondrial damage, and increase ROS production in GSCs, however, ROS scavenging reverses the effect of β OHB on GSCs. | Intracellular: KBs combined with low glucose levels derange the metabolic balance in GSCs, resulting in an energy crisis and thus, oxidative stress, which in turn reduces cell proliferation and stemness and induces apoptosis. |
| Poff 2014 | Proliferation /Viability | KB supplementation decreased VM-M3 cell proliferation and viability in vitro. | Intracellular: Lack of necessary enzymes e.g., SCOT |
| D'Alessandro 2011 | β OHB as an alternative to glutamine on glutamate and GSH (Glutathione) levels /Glutamate-Cysteine Ligase Modifier (GCLM) and GCL activity in the effects of glutamine and β OHB on GSH / β OHB as an alternative to glutamine on Malate Dehydrogenase (MDH) activity, Pyruvate Dehydrogenase Kinase 1 (PDK1) protein level and lactate release | β OHB reversed the decreases of cytosolic malate dehydrogenase activity and glutamate and glutathione. However, in the G93ASOD1 cell line, in all culture conditions, the expression of pyruvate dehydrogenase kinase 1 protein, which down-regulates pyruvate dehydrogenase activity, was induced, together with an increase in lactate release in the medium. | Intracellular: β OHB affected GSH homeostasis differently in the G93A-tTA cell line since they differently counteracted the effects of mitochondrial dysfunction associated with the increase of lactate release and induction of PDK1. This evidence suggests a down-regulation of the activity of the pyruvate dehydrogenase complex, and this is expected to reduce the flux of glucose-derived pyruvate towards the TCA cycle. |
| Skinner 2009 | Apoptosis /SCOT (Succinyl-CoA:3-ketoacid-coenzyme A transferase) levels /Viability | Fibroblast viability decreased slightly in glucose free media and the addition of β OHB/AcAc showed a non-statistically significant small increase. The neuroblastoma cells showed a significant decrease in viability without glucose that was not rescued with the addition of β OHB/AcAc. Levels of apoptosis were unaffected between glucose, glucose free, and glucose free + β OHB/AcAc in the fibroblast populations. Neuroblastoma cells showed an | Intracellular: As SCOT is a rate limiting step in ketone metabolism this may explain the neuroblastoma cells' reduced ability to utilise ketones for energy. The increase in apoptosis seen with increased concentrations of β OHB/AcAc. This may be due to increased ROS production from ketone metabolism and neuroblastoma cells' inability to detoxify ROS. |

| | | | |
|-------------|---|--|---|
| | | increase in apoptosis in glucose free media which was increased further with the addition of ketones. Higher concentrations saw higher levels of apoptosis. | |
| Meroni 2018 | Activation of the Nrf2 Pathway/ Gene and Protein Expression of Nrf2 /Genotoxicity of KBs /HO-1 Gene Expression /Viability | Concentrations up to 4 mM β OHB and 1 mM AcAc showed no significant effects on cell viability up to 48 hr. Higher concentrations were harmful at 48 hr, and lower concentrations were damaging at 72 hr. Ketones induced moderate stress to cells at every incubation time point; in particular, it was found that DNA damage, expressed as the percentage of DNA in the tail, was about to 21% in KB-treated cells vs. 2% in control cells. The ketones conferred some protection to cells from H ₂ O ₂ oxidative injury compared to control cells. Notably the reduction in DNA damage increased with exposure time to the ketones. A significant increase in mRNA expression of Nrf2 in ketone treated cells at 2 hr vs controls was observed. Nrf2 protein levels also increased at 2hrs compared to controls. This difference was greatest in the nuclear (as opposed to cytosol) extracts, where Nrf2 is primarily active. | Intracellular/ Nuclear: Primary impact of β OHB/AcAc to endothelial cells as studied here appears to result from the oxidative stress they induce which causes oxidative damage to DNA. According to the authors the literature is conflicting on ketones, with some showing reduced ROS production and others increased across various cell types. However, there is consensus that ketones cause oxidative stress in endothelial cells with the up regulation of NADPH oxidase 4/lipid peroxidation/etc. The decrease DNA damage following exposure to the oxidative insult of H ₂ O ₂ seen in cells treated with ketones for 48 hrs was notable. Previous studies have found ketones to be protective against ROS. May be due to ketones activating an antioxidant defence system ahead of the oxidative insult. Nrf2 gene expression was initially increased when cells were treated with ketones, but the levels below control at later time points. The may due to increased nuclear translocation of Nrf2 (where it exerts its main effects) and thus increased activity. The authors speculate ketone induce mild but sufficient ROS production to activate this transcription factor. HO-1 is a key target gene of Nrf2, and its gene expression was increased at all time points in ketone treated cells. This confirms the activation of Nrf2 pathway. In conclusion, the metabolic response caused by ketone exposure makes endothelial cells more resistant to a secondary insult (in this case H ₂ O ₂) leading to a reduction in DNA oxidative damage. |
| Dardis 2016 | Cell growth Table 7.9 Proposed mechanisms for negative ketone effect on cell lines | The inhibitory effects of β OHB on the growth of neoplastic cells were observed in the cell line B16. Impairment of growth was noted. Impaired motility was also noted. | Intracellular/ Genetic: Growth impairment has been suggested to occur due to polyacetylation of histones. KBs also impair glycolysis. This likely negatively impacts the neoplastic cells, which are highly dependent on this process for energy. This occurs in part through inhibition of the activity of phosphofructokinase and hexokinase. |

| Study ID | Investigated effects | Summary of findings | Proposed mechanism for ketone effect (Extra/Intracellular/Genetic) |
|-----------------|--|--|--|
| Mehdikhani 2019 | Cytotoxicity /Histone modifications | β OHB enrichment nor glucose restriction failed to elicit a significant impact on the butyrylation or acetylation level of histone H3 upon long term treatment | No mechanism provided |
| Otto 2014 | Metabolism of β OHB & Glucose & Lactate at 21% and 1% oxygen. | Cell cultures of the 6 tumour cell lines were able to metabolise KBs as well as lactate at 21% oxygen, but not at 1%. Glucose, by contrast, was metabolised at both oxygen concentrations by all 6 tumour cell lines. | Intracellular: The data presented support the concept that metabolism in solid tumours is significantly influenced by the local oxygenation. Oxygen concentrations of 1%, usually found in solid tumours (tumour hypoxia), are insufficient for the in vitro metabolism of KBs and lactate in tumour cell lines, in contrast to glucose that is metabolised under these conditions. |
| Bennett 2011 | The regulation of human G6PC3 promoter activity | β OHB did not increase G6PC3 promoter activity when added to the 3 different concentrations of glucose | No mechanism elucidated to |
| DuYan 2000 | ABAD Metabolism of β OHB /C-NMR spectroscopy /Energy Charge /Viability | ABAD can catalyse the oxidation of β OHB. When placed in medium with β OHB as the principal energy substrate, COS cells stably transfected to overexpress wild-type ABAD (COS/wtABAD) were better maintained 3-(4,5-dimethylthiazol2yl)-2,5-diphenyl tetrazolium bromide reduction, cellular energy charge, and morphologic phenotype compared with COS/vector cells. | Intracellular: The NMR data indicates that KBs, such as β OHB can provide both a substrate for maintenance for cellular energy charge, as well as a source for increased production of neurotransmitters. |
| Cui 2019 | Migration /Proliferation | The proliferation of 768-0 cells was significantly suppressed by β OHB treatment in a dose-dependent manner and the migrative capacity of 768-0 cells was slightly inhibited by β OHB when the ACAT1, β DH2 and HMGCL were over expressed | No mechanism provided |
| Briscoe 1994 | CO2 production /Oxygen Consumption /Utilization of AcAc | AcAc appears to be readily utilized by the AS-30D cells yet β OHB appears to be poorly utilized by AS-30D cells and is not readily oxidized by hepatoma mitochondria. | No mechanism elucidated to |
| Tisdale 1984 | Enzyme assays /Lipid Synthesis | All three major KB metabolizing enzymes are present both in neuroblastoma and glioma cell lines. The activities of β DH and acetoacetyl-CoA thiolase are higher in glioma cells than in neuroblastoma and 3-ketoacid CoA-transferase is 2-fold higher in neuroblastoma cells than in glioma cells. The specific activity of 3-ketoacid CoA transferase in both cell lines increased as the cultures achieved confluence, then decreased. The incorporation of glucose carbon into lipids is significantly reduced in cells of both lines in the presence of KBs. Addition of AcAc but not β OHB to the culture medium resulted in a significant increase in the activity of 3-ketoacid CoA-transferase and also in the rate of AcAc oxidation in neuroblastoma cells but not glioma cells. | Intracellular: The presence of KBs in the medium caused a reduction in the incorporation of glucose carbon into lipid fractions in both cell lines. The data suggest that the increase in lipid synthesis is due to an increased flux through the mitochondrial pathway of ketone body oxidation. |
| Eloqayli 2011 | The function of astrocytes and neurons in the presence of KBs | Using [2,4- 13 C] β OHB and [1- 13 C] glucose it could be shown that C6 cells had efficient mitochondrial activity, evidenced by 13 C labelling of glutamate, glutamine and aspartate. However, in the presence of glucose, astrocytes were able to produce and release glutamine, whereas this was not accomplished by the C6 cells, suggesting lack of anaplerosis in the latter. | Intracellular: It appears that β OHB increases mitochondrial metabolism of glucose in both cell types |
| Denton 1987 | Mitochondrial respiration | Mitochondria from the treated cells respired normally in the presence of added succinate but not β OHB, a finding that indicates MPP+ inhibits the oxidation of some substrates selectively. | Intracellular: MPP+ inhibits the oxidation of NAD- linked substrates by isolated mitochondria prepared from rodent liver or brain |

Table 7.10 Proposed mechanisms for no ketone effect on cell lines.

| Study ID | Medium type | Serum (FBS/FCS) | Antibiotics | Glucose | Glucose concentration (mM) | Pyruvate | Pyruvate concentration (mM) | Glutamine | Glutamine concentration (mM) | Other media components? | Ketone Effect |
|-----------------|--|-----------------|-------------|---------------|---|---------------|--------------------------------------|---------------|------------------------------|---|---------------|
| Maurer 2011 | DMEM | Yes | Yes | Yes | Glucose in concentrations of 0, 1, 2.5, 5, 10 and 25 mM was added "for some experiments" to "serum and glucose-free medium" | No | No | Yes | 2mM | Rotenone and 3-bromo-pyruvate were used in one experiment to investigate influence of ketones on cell sensitivity to cell death triggers. | Positive |
| Cheng 2013 | DMEM | Yes | Yes | Not specified | Not specified | Not specified | Not specified | Not specified | Not specified | Culture media supplemented with horse serum then cells were treated with different concentrations of H2O2 | Positive |
| Xie 2015 | RPMI 1640 medium | Yes | Yes | Not specified | Not specified | Not specified | Not specified | Not specified | Not specified | Not specified | Positive |
| Cheng 2010 | DMEM | Yes | Yes | Not specified | Not specified | Not specified | Not specified | Not specified | Not specified | Heat inactivated horse serum | Positive |
| Durigon 2018 | DMEM | Yes | Yes | Yes | 5 mM | Yes | 1 mM | Yes | Specified but not given | Not specified | Positive |
| Cheng 2005 | DMEM | Yes | Yes | Not specified | Not specified | Not specified | Pyruvate concentration not specified | Not specified | Not specified | Not specified | Positive |
| Jiang 2011 | DMEM/F12 medium | Yes | Yes | Yes | 2 mM | Not specified | Not specified | Not specified | Not specified | Not specified | Positive |
| Tagawa 2019 | Hepa1c1c7 - Minimum essential medium alpha (MEM α) HepG2 cells - RPMI 1640 medium | Yes | Yes | Not specified | Not specified | Not specified | Not specified | Not specified | Not specified | Not specified | Positive |
| Wang 2019 | DMEM | Yes | Yes | Not specified | Not specified | Not specified | Not specified | Yes | 2 mM | Non-essential amino acids (0.1 mM) | Positive |
| Mikami 2020 | DMEM | Yes | Yes | Not specified | Not specified | Not specified | Not specified | Not specified | Not specified | Not specified | Positive |
| Vilã -Brau 2011 | DMEM | Yes | Yes | Not specified | Not specified | Not specified | Not specified | Not specified | Not specified | Not specified | Positive |

| | | | | | | | | | | | |
|-----------------|---|-----|---------------|---------------|--|---------------|---------------|---------------|---------------|--|----------|
| Wang 2016 | DMEM | Yes | Yes | Not specified | Not specified | Not specified | Not specified | Not specified | Not specified | Not specified | Positive |
| Patel 1981 | DMEM | Yes | Yes | Yes | 5mM | Not specified | Not specified | Yes | 2mM | Cells routinely subcultured with 0.5% trypsin (Difco, 1:250) in phosphate-buffered saline containing 0.5mM ethylene glycol bis(3-aminoethylether)-N, N, N', N'-tetraacetic acid (EGTA) | Positive |
| Lamichhane 2017 | DMEM | Yes | Yes | Yes | 1mM, 5mM, 25nM | Not specified | Not specified | Not specified | Not specified | Not specified | Positive |
| Xu 2011 | DMEM | Yes | Yes | Not specified | Not specified | Not specified | Not specified | Not specified | Not specified | LPS | Positive |
| Kweon 2004 | DMEM | Yes | Not specified | No | No | Not specified | Not specified | Not specified | Not specified | 1 mM NaBu was used to differentiate the cells | Positive |
| Li 2020 | A 1:1 vol/vol mixture of DMEM and DMEM/F12 medium | Yes | No | Not specified | Not specified | Not specified | Not specified | Not specified | Not specified | Trans Retinoic acid was used to differentiate the cells | Positive |
| Cheng 2007 | DMEM | Yes | Yes | Not specified | Not specified | Not specified | Not specified | Not specified | Not specified | 7% horse serum | Positive |
| Imamura 2006 | DMEM/F12 medium | Yes | Yes | Not specified | Not specified | Not specified | Not specified | Not specified | Not specified | Not specified | Positive |
| Zhang 2018 | DMEM/F12 medium | Yes | Yes | Not specified | Not specified | Not specified | Not specified | Not specified | Not specified | Not specified | Positive |
| Zhang 2017 | DMEM | Yes | Yes | Yes | Not specified | Not specified | Not specified | Not specified | Not specified | Not specified | Positive |
| Findlay 2015 | DMEM/F12 medium | Yes | Yes | Yes | 2.5 mM | Not specified | Not specified | Yes | 4 mM | Not specified | Positive |
| Shang 2018 | DMEM | Yes | Yes | Yes | "High glucose" is all that's described | Not specified | Not specified | Not specified | Not specified | Not specified | Positive |
| Kabiraj 2012 | 1:1 mixture of DMEM and Ham's F12 medium | Yes | Yes | Not specified | Not specified | Not specified | Not specified | Not specified | Not specified | Not specified | Positive |
| Liu 2018 | DMEM | Yes | Yes | No | No | Not specified | Not specified | Not specified | Not specified | Not specified | Positive |
| Hasan 2008 | RPMI 1640 medium | Yes | Yes | Yes | 11 mM | Yes | 1 mM | Yes | 10 mM | 50 uM B-mercaptoethanol, 10 mM Sodium Hepes buffer | Positive |

| | | | | | | | | | | | |
|--------------------------|---|-----|---------------|---------------|---|---------------|---------------|---------------|----------------|--|----------|
| Macdonald 2008 | RPMI 1640 tissue culture medium / Krebs ringer bicarbonate buffer | Yes | Yes | Yes | Cells maintained in a glucose concentration of 11.1 but 22 hrs before the insulin release experiment the concentration was reduced in 5 mM and 2 hrs before the experiment the concentration was reduced again to 3 mM | Yes | 1 mM | Yes | 2 mM and 10 mM | The Krebs Ringer Bicarbonate buffer contained 15 mM sodium HEPES and 15 mM NaHCO ₃ | Positive |
| MacDonald 2008 | RPMI 1640 medium, two hr before the experiments began, the medium was replaced with Krebs-Ringer bicarbonate buffer | Yes | Yes | Yes | 11.1 mM, one day before the experiment was to begin the glucose concentration was reduced to 5 mM, the concentration was further decreased when the Krebs Ringer solution was added in 2 hr before the experiment to 3 mM | Yes | 1 mM and 5 mM | Not specified | Not specified | 50 uM B-mercaptoethanol, 10 mM sodium HEPES - Given with the INS-1 medium 15 mM HEPES and 15 mM NaHCO ₃ - Given in the Krebs-Ringer solution | Positive |
| Wang 2017 | DMEM | Yes | Not specified | Yes | Glucose Deprived DMEM was used (5.5mM) | Not specified | Not specified | Not specified | Not specified | The cells were cultured in either CAF or fibroblast conditioned media and also non-conditioned media for controls in experiment 1 | Positive |
| McGee 1974 | Bicarbonate Buffer | Yes | Not specified | Yes | 11mM | Not specified | Not specified | Not specified | Not specified | The Bovine Serum Albumin was added after it had been "defatted" and fatty acids were subsequently added. Bicarbonate buffer was also used. | Positive |
| Martinez-Outschoorn 2011 | DMEM | Yes | Yes | Not specified | Not specified | Not specified | Not specified | Not specified | Not specified | No | Positive |
| Martinez-Outschoorn 2012 | DMEM | Yes | Yes | Not specified | Not specified | Not specified | Not specified | Not specified | Not specified | Not specified | Positive |
| Huang 2017 | DMEM/F12 medium | Yes | Yes | Not specified | Not specified | Yes | 1 mM | Yes | 2 mM | 1 mM non-essential amino acids | Negative |
| Rodrigues 2017 | DMEM | Yes | Yes | Not specified | Not specified | Not specified | Not specified | Not specified | Not specified | Not specified | Negative |

| | | | | | | | | | | | |
|--------------|--|-----|---------------|---------------|---|---------------|--|---------------|--|--|----------|
| Zhang 2018 | DMEM or RPMI-1640 medium | Yes | Yes | Yes | For the cell number experiments, the concentration was 3 mM (Low glucose) | Not specified | Not specified | Not specified | Not specified | Not specified | Negative |
| Kaya 2018 | DMEM | Yes | Yes | | Controls: 4.5g/L, 1.125g/L, 0g/L Ketone Treated: 0g/L | Not specified | Not specified | Not specified | Not specified | Not specified | Negative |
| Shukla 2014 | DMEM | Yes | Yes | No | No | Not specified | Not specified | Not specified | | C2C12 and 3T3L cells were also differentiated using extra media components. C2C12: 2% horse serum and 10µg/mL insulin containing DMEM. 3T3L: DMEM containing 10% FBS, 1µM dexamethasone, 0.5 mM methylisobutylxanthine (IBMX), and 1 µg/mL insulin. They were then switched back to standard DMEM after 72 and 48 hr respectively. | Negative |
| Shakery 2018 | DMEM | Yes | Yes | Not specified | Not specified | Not specified | Not specified | Yes | 1% L-glutamine | Not specified | Negative |
| Kadochi 2017 | DMEM | Yes | Not specified | Yes | 450mg/dl, 100mg/dl, 0mg/dl | Not specified | Not specified | Not specified | Not specified | Not specified | Negative |
| Guh 2003 | DMEM/F12 medium | Yes | Yes | Yes | 11 mM | No | Not specified | Yes | L-glutamine, 5ug/mL | insulin, 5ug/mL, transferrin, 5 ng/mL, sodium selenite, 5 pg/mL, T3, 5 ng/mL hydrocortisone, 5 pg/mL prostaglandin E1 (PGE1), and 10 ng/mL epidermal growth factor. | Negative |
| Liu 2019 | DMEM: H1299, 293T and U2OS MCOY: HCT116 | Yes | Not specified | Not specified | Not specified | Yes | Not specified but used as control for βOHB | Yes | Not specified but used as control for βOHB | Not specified | Negative |
| Magee 1979 | RPMI 1640 medium | Yes | Yes | Not specified | Not specified | Not specified | Not specified | Yes | 2 - 7 mM | 20 mM Hepes | Negative |
| Jain 2003 | RPMI 1640 medium | Yes | Yes | Yes | Normal glucose (7 mM) and high glucose (30 mM) | Not specified | Not specified | Yes | 2 mM | 12 mmol/l sodium bicarbonate, 12 mmol/l HEPES | Negative |
| Jain 2002 | RPMI 1640 medium | Yes | Yes | Yes | Normal glucose (5 mM) and High glucose (30 mM) | Not specified | Not specified | Yes | 2 mM | 12 mmol/l sodium carbonate, 12 mmol/l HEPES, | Negative |

| | | | | | | | | | | | |
|-------------------|---|---------------|---------------|---------------|---------------|---------------|---------------|---------------|--|--|----------|
| Rains 2011 | RPMI 1640 medium | Yes | Yes | Yes | 7 mM | Not specified | Not specified | Yes | 2 mM | 12 mM sodium carbonate 12 mM HEPES (buffer) | Negative |
| Jain 1999 | RPMI 1640 medium | Yes | Yes | Not specified | Not specified | Not specified | Not specified | Yes | 2 mM | Not specified | Negative |
| Luo 2017 | DMEM & Defined keratinocyte serum-free medium | Yes | Not specified | Not specified | Not specified | Not specified | | Not specified | Not specified | Not specified | Negative |
| Vallejo 2020 | RPMI 1640 medium (U82 and SJGBM2) DMEM/F12 medium (all glioblastoma cultures) | Yes | Yes | Not specified | Not specified | Not specified | Not specified | Not specified | Not specified | Glioblastoma cultures only: 20 ng/ml each of human epidermal growth factor and human fibroblast growth factor, and 2% Gem21 NeuroPlex Serum-Free Supplement | Negative |
| Ji 2020 | DMEM/F12 medium | Not specified | Not specified | Yes | 2.5mM | Not specified | Not specified | Not specified | Not specified | epidermal growth factor (20ng/ml), basic fibroblast growth factor (20ng/ml) | Negative |
| Poff 2014 | Eagles' minimum essential medium | Yes | Yes | Yes | 3 mM or 25 mM | Yes | 2mM | Not specified | Not specified | Not specified | Negative |
| D'Alessandro 2011 | DMEM | Yes | Yes | Not specified | Not specified | Yes | 1 mM | Not specified | No glutamine added when β OHB was in media | WT-tTA and G93A-tTA cell lines were kept in selection by further addition of hygromycin B (0.2 mg/mL) and cultured without doxycycline, thus permitting full expression of the transgenic SOD1. 0.02 mM cystine was added to the β OHB media also. | Negative |
| Skinner 2009 | DMEM | Yes | Yes | Yes | Not specified | Not specified | Not specified | Not specified | Not specified | Not specified | Negative |
| Meroni 2018 | MCDB131 medium | Yes | Yes | Not specified | Not specified | Not specified | Not specified | Yes | 2 mM | 10 ng/mL epidermal growth factor | Negative |

| | | | | | | | | | | | |
|-----------------|------------------------------------|---------------|---------------|---------------|--|---------------|---------------|---------------|---------------|--|-----------|
| | | | | | | | | | | 1g/mL hydrocortisone 20 mM HEPES buffer. | |
| Dardis 2016 | Not specified | Not specified | Not specified | Not specified | Not specified | Not specified | Not specified | Not specified | Not specified | Not specified | No Effect |
| DuYan 2000 | DMEM | Yes | Not specified | Not specified | Not specified | Not specified | Not specified | Not specified | Not specified | None | No Effect |
| Tisdale 1984 | Eagles' minimal essential medium | Yes | Yes | Yes | 5 mM | Not specified | Not specified | Yes | 2 mM | None | No Effect |
| Cui 2019 | RPMI 1640 medium | Yes | Not specified | Not specified | Not specified | Not specified | Not specified | Not specified | Not specified | None | No Effect |
| Mehdikhani 2019 | DMEM | Yes | Not specified | Yes | DMEM medium with 1 g/L glucose or DMEM with restricted glucose with 250 mg/L | Not specified | Not specified | Not specified | Not specified | Not specified | No Effect |
| Otto 2014 | RPMI 1640 medium | Yes | Yes | Yes | 2 or 5 mM | Not specified | Not specified | Yes | 2 mM | No | No Effect |
| Eloqayli 2011 | DMEM | Yes | Yes | Yes | 3 mM | Not specified | Not specified | Not specified | Not specified | Not specified | No Effect |
| Bennett 2011 | DMEM | Yes | Yes | Yes | 1 - 5.5 mM | Yes | 3.5 mM | Yes | 2 mM | Phenol red | No Effect |
| Briscoe 1994 | Krebs Henseleit bicarbonate buffer | Not specified | Not specified | Yes | 6 mM | Yes | 0.2 mM | Yes | 0.75 mM | 125 mM KCl, 2 mM K ₂ HPO ₄ , 1 mM MgCl ₂ , 0.4 mM ADP, 20 mM HEPES, 0.1 mM Malate | No Effect |
| Denton 1987 | DMEM | Yes | Not specified | Yes | 5.6 mM | Yes | 7 mM | Not specified | Not specified | None | No Effect |

Table 7.11 Relationship with the medium

| Study ID | Ketone used | Ketone concentration | Duration of β OHB administration (hr) | Ketone Effect |
|-----------------|----------------------|---|---|---------------|
| Maurer 2011 | AcAc and β OHB | 5 mM for both | 24 hrs, 48 hrs, 84 hrs, 144 hrs | Positive |
| Cheng 2013 | β OHB | 4 mM | 2 hrs | Positive |
| Xie 2015 | β OHB | 0 mM, 0.5 mM, 1 mM, 2 mM, 4 mM | 24 hrs | Positive |
| Cheng 2010 | β OHB | 4 mM | 4 hrs | Positive |
| Durigon 2018 | β OHB | 0.3 mM | 48 hrs / 96 hrs / 144 hrs / 188 hrs / 504 hrs (media changed every 48 hrs) | Positive |
| Cheng 2005 | β OHB | 0.1 mM - 2.17 mM (originally 0.005-0.10 g/L) | 72 hrs (L929 cells), 96 hrs (HUVECs), 120 hrs (Rabbit chondrocytes) | Positive |
| Jiang 2011 | AcAc and β OHB | AcAc is 21.74 mM (originally 1 mg/ml), β OHB is 54.35 mM (originally 2.5 mg/ml) | Viability Assay - 24 hrs, ATP level measurement - 6 hrs after having been in culture medium for 24 hrs | Positive |
| Tagawa 2019 | β OHB | 10 mM | 3 hrs or 6 hrs (mRNA and Protein Expression and SIRT1 activity) or 24 hrs (Cell Viability Assay) | Positive |
| Wang 2019 | β OHB | 5 mM, 10 mM, and 20 mM | Trypan Blue Cell Viability Assay (Cell Number) - 144 hrs, MTT Cell Viability Assay - 3 hrs Proliferation - 48 hrs, Wound Healing Migration Assay - 24 hrs | Positive |
| Mikami 2020 | β OHB | 10 mM | 24 hrs, 48 hrs, 72 hrs | Positive |
| Vil  -Brau 2011 | AcAc and β OHB | AcAc: 1mM and 10mM; β OHB: 2mM and 20mM | 5 hrs | Positive |
| Wang 2016 | β OHB | 2, 4, 8, 10 mM for impact of β OHB on cell viability alone. 4 mM and 8 mM for subsequent experiments. | 12 hrs | Positive |
| Patel 1981 | AcAc and β OHB | AcAc: 0.5mM β OHB: 2.5mM | 96 hrs or 144 hrs for both cell lines | Positive |
| Lamichhane 2017 | β OHB | 8mM, 10mM | 24 hrs | Positive |
| Xu 2011 | β OHB | 4 mM | BV2 cells pre-treated with β OHB for 2 hrs before it was added to (LPS for another 24 hrs | Positive |
| Kweon 2004 | β OHB | 0, 4 and 8 mM | Preincubated with each concentration for 24 hrs and then incubated for a further 72 hrs | Positive |
| Li 2020 | β OHB | 0, 5, 10, 20, 40 or 80 mM | 24 hrs (Cells were seeded with antibiotic free normal growth medium for 24 hrs beforehand) | Positive |
| Cheng 2007 | β OHB | 4 mM | 24 hrs | Positive |
| Imamura 2006 | β OHB | 8 mM | 1 hr | Positive |
| Zhang 2018 | β OHB | 2 mM | 3 hrs | Positive |
| Zhang 2017 | β OHB | 1 mM | 3 hrs | Positive |
| Findlay 2015 | β OHB | 0.0005 mM, 0.001 mM, 0.01 mM | 48 hrs | Positive |
| Shang 2018 | β OHB | 0, 1, 10 and 25 mM | Cell viability & Cell Migration assays & NLRP3 inflammasome function & LPS and ATP-promoted cell migration of C6 - 24 hrs Wound Closure by ECIS - 15 hrs LPS & ATP-induced activation of Caspase-1 and maturation of IL-1β & LPS & ATP-induced degradation of IκBα, activation of STAT3 and the expression of FGF2 and PTX function - 2 hrs | Positive |
| Kabiraj 2012 | β OHB | 0.1 mM | 144 hrs | Positive |
| Liu 2018 | β OHB | 0.0005 mM, 0.001 mM, 0.005 mM, 0.01 mM | 120 hrs | Positive |
| Hasan 2008 | β OHB | 5 mM | 1 hr | Positive |
| Macdonald 2008 | β OHB | 5 mM | 1 hr | Positive |

| | | | | |
|--------------------------|----------------------|---|--|----------|
| MacDonald 2008 | AcAc and β OHB | AcAc (10 mM), β OHB (5 mM) for insulin release studies. β OHB was then used at concentrations of 2 mM, 4 mM, 6 mM, 8 mM, and 10 mM in combination with different concentrations of MMS. Inhibiting the MCT for insulin release studies, the concentration of AcAc and β OHB were 5 mM. In the insulin release studies from pancreatic islets, β OHB is 5 mM. When measuring carbon incorporation from β OHB, β OHB is 5 mM. | 1 hr | Positive |
| Wang 2017 | β OHB | 0.0000011 mM | 24 hrs | Positive |
| McGee 1974 | β OHB | 86.96 mM | 0.5 hrs | Positive |
| Martinez-Outschoorn 2011 | β OHB | 10 mM | 48 hrs | Positive |
| Martinez-Outschoorn 2012 | β OHB | 10 mM | 48 hrs | Positive |
| Huang 2017 | β OHB | 20 mM | 1 hr | Negative |
| Rodrigues 2017 | β OHB | 0.5 mM, 5 mM, and 10 mM | 0 hrs and 24 hrs | Negative |
| Zhang 2018 | β OHB | 5 mM, 10 mM | 0 hrs, 12 hrs, 24 hrs, 48 hrs, 72 hrs and 96 hrs | Negative |
| Kaya 2018 | AcAc and β OHB | 10 mM and 20 mM | 24 hrs | Negative |
| Shukla 2014 | AcAc and β OHB | 1 mM, 5 mM, 10 mM, 20 mM | 24 hrs to 72 hrs | Negative |
| Shakery 2018 | β OHB | Viability Assay - 0.1 mM, 0.25 mM, 0.5 mM, 1 mM, 2.5 mM, 5 mM: Oxygen Consumption/ Extracellular Acidification Rates/ Colony formation assay/ Scratch Assay - 0.25 mM | Viability Assay (72 hrs) /Oxygen Consumption (2 hrs) / Extracellular Acidification Rates (2 hrs) / Colony formation assay (14 days) / Scratch Assay (36 hr and 72 hr) | Negative |
| Kadochi 2017 | β OHB | 1 mM | 24 hrs | Negative |
| Guh 2003 | β OHB | 0.1 - 10 mM | 24 hrs and 48 hrs | Negative |
| Liu 2019 | β OHB | 10 mM | Mostly 24 hr but EdU staining (U2OS), and apoptosis (HCT116) saw 16 hr | Negative |
| Magee 1979 | β OHB | 0 mM, 10 mM, 20 mM, 40 mM | Proliferation/ βOHB concentration/Glucose utilization/ Total lactate production / Inhibition of cell proliferation - 0 hrs, 24 hrs, 48 hrs, 72 hrs - Comparative cell study - 0 hrs, 72 hrs and 144 hrs | Negative |
| Jain 2003 | AcAc and β OHB | 0 - 3 mM | 24 hrs | Negative |
| Jain 2002 | AcAc and β OHB | 0 - 3 mM | 24 hrs | Negative |
| Rains 2011 | AcAc and β OHB | 0 - 10 mM | 24 hrs | Negative |
| Jain 1999 | AcAc and β OHB | Both AcAc and β OHB were used at concentrations of 0 mM 0.005 mM, 0.01 mM, and 0.02 mM | AlamarBlue cell proliferation assay - 4 hr, Apoptosis TUNEL assays 0 - 72 hrs | Negative |
| Luo 2017 | AcAc and β OHB | 0 mM, 2.5 mM, 5 mM, 10 mM | 24 hrs | Negative |
| Vallejo 2020 | AcAc and β OHB | 0 mM, 1 mM, 5 mM, 10 mM, 20mM | Cell Viability: 72 hrs: Neurosphere formation: 336 hrs (14 days) Apoptosis: 24 hrs | Negative |
| Ji 2020 | β OHB | 0 mM, 1 mM, 5 mM, or 10 mM | 120 hrs, 144 hrs and 168 hrs | Negative |
| Poff 2014 | β OHB | 5 mM | Proliferation: 24, 48, 72, 96, 120 and 144 hr Viability: 24 hrs | Negative |
| D'Alessandro 2011 | β OHB | 5 mM | 24 hrs | Negative |

| | | | | |
|-----------------|----------------------|---|--|-----------|
| Skinner 2009 | AcAc and β OHB | 54.35 mM or 97.83 mM for both β OHB and AcAc | 24 hrs | Negative |
| Meroni 2018 | AcAc and β OHB | Cell Viability: β OHB (2 to 20 mM) and AcAc (0.5 to 5 mM) All further experiments were performed using 4 mM β OHB and 1mM AcAc | Cell Viability: 24, 48, and 72 hrs. Genotoxicity: 2, 24 and 48 hrs. Nrf2 Expression & HO-1 Expression: 2, 6, 14, 24 hrs | Negative |
| Dardis 2016 | β OHB | 10 mM | 0 hrs, 24 hrs, 48 hrs, 72 hrs, 96 hrs - Cell growth; 20 hrs for migration assay | Negative |
| DuYan 2000 | β OHB | Viability Assay and Energy Charge - 0 mM, 5 mM, 10 mM, and 20 mM ABAD metabolism 0 mM, 10 mM, 20 mM, 30 mM, 40 mM - NMR Spectroscopy - 10 mM | Viability Assay and Energy Charge (24, 48, 72, 96 and 120 hrs - 10 mM concentration only), another viability assay used concentrations of 0, 5, 10 and 20 mM at for 120 hrs only (5 days only) ABAD metabolism of βOHB - 10 mM over 30 minutes (but only data from the first 10 minutes were used) NMR spectroscopy - 10 mM over 2, 4, 6, and 8 days | No Effect |
| Tisdale 1984 | AcAc and β OHB | 0.5 mM AcAc and 2.5 mM β OHB | 96 hrs | No Effect |
| Cui 2019 | β OHB | 0 mM, 2.5 mM, 5 mM, 10 mM | 24 hrs - 144 hrs (1 - 6 days) | No Effect |
| Mehdikhani 2019 | β OHB | 5 mM (long term study), 25 - 1000 mM (cytotoxicity), | 720 hrs (30 days) | No Effect |
| Otto 2014 | β OHB | 4 mM | 96 hrs (4 days) | No Effect |
| Eloqayli 2011 | β OHB | 1 mM | 4 hrs | No Effect |
| Bennett 2011 | β OHB | 3.5 mM | 18 - 24 hrs | No Effect |
| Briscoe 1994 | AcAc, β OHB | AcAc (0.5 mM, 1mM, 2 mM, 5 mM, 10 mM), β OHB (10 mM) | 1 hr | No Effect |
| Denton 1987 | β OHB | 20 mM | 2 mins | No Effect |

Table 7.12 Relationship with the ketone

| Positive Studies | | | | | |
|---|--|-----|--|-------------------|-----|
| β OHB Concentration | Number of studies using these concentrations | % | AcAc and β OHB Concentration | Number of studies | % |
| 0 mM, 0.5 mM, 1 mM, 2 mM, 4 mM | 1 | 4 | AcAc: 0.5mM β OHB: 2.5mM | 1 | 20 |
| 0, 1, 10 and 25 mM | 1 | 4 | AcAc: 1mM and 10mM β OHB: 2mM and 20mM | 1 | 20 |
| 0, 4 and 8 mM | 1 | 4 | 5 mM for both | 1 | 20 |
| 0, 5, 10, 20, 40 or 80 mM | 1 | 4 | AcAc (10 mM), β OHB (5 mM) for the insulin release studies. β OHB was then used at concentrations of 2 mM, 4 mM, 6 mM, 8 mM and 10 mM in combination with different concentrations of MMS which were (10 mM - paired with 2 mM β OHB, 8 mM - paired with 4 mM β OHB, 6 mM - paired with 6 mM β OHB, 4 mM - paired with 8 mM β OHB and 2 mM - paired with 10 mM β OHB). | 1 | 20 |
| 0.0000011 mM | 1 | 4 | AcAc is 21.74 mM, β OHB is 54.35 mM | 1 | 20 |
| 0.0005 mM, 0.001 mM, 0.01 mM | 1 | 4 | Total | 5 | 100 |
| 0.0005 mM, 0.001 mM, 0.005 mM, 0.01 mM | 1 | 4 | | | |
| 0.1 mM - 2.17 mM | 1 | 4 | | | |
| 0.1 mM | 1 | 4 | | | |
| 0.3 mM | 1 | 4 | | | |
| 1 mM | 1 | 4 | | | |
| 2 mM | 1 | 4 | | | |
| 2, 4, 8, 10 mM for impact of β OHB on cell viability alone. 4 mM and 8 mM for subsequent experiments. | 1 | 4 | | | |
| 4 mM | 4 | 15 | | | |
| 5 mM | 2 | 7 | | | |
| 5 mM, 10 mM and 20 mM | 1 | 4 | | | |
| 8 mM | 1 | 4 | | | |
| 8mM, 10mM | 1 | 4 | | | |
| 10 mM | 4 | 15 | | | |
| 86.96 mM | 1 | 4 | | | |
| Total | 27 | 100 | | | |

Table 7.13 Recorded ketone concentrations for the positive studies

| Negative Effect Studies | | | | | |
|---|---|----------|---|--------------------------|----------|
| βOHB Concentration | Number of studies using these concentrations | % | AcAc and βOHB Concentration | Number of studies | % |
| 0 mM, 1 mM, 5 mM, or 10 mM | 1 | 8 | Both AcAc and βOHB were used at concentrations of 0 mM 0.005 mM, 0.01 mM and 0.02 mM (originally 0 μM, 5 μM, 10 μM and 20 μM) | 1 | 10 |
| 0 mM, 10 mM, 20 mM, 40 mM | 1 | 8 | 0 mM, 1 mM, 5 mM, 10 mM, 20mM | 1 | 10 |
| 0.1 - 10 mM | 1 | 8 | 0 mM, 2.5 mM, 5 mM, 10 mM | 1 | 10 |
| 0.5 mM, 5 mM and 10 mM | 1 | 8 | 1 mM, 5 mM, 10 mM, 20 mM | 1 | 10 |
| Viability Assay - 0.1 mM, 0.25 mM, 0.5 mM, 1 mM, 2.5 mM, 5 mM Oxygen Consumption/ Extracellular Acidification Rates/ Colony formation assay/ Scratch Assay - 0.25 mM | 1 | 8 | Cell Viability: βOHB (2 to 20 mM) and AcAc (0.5 to 5 mM). All further experiments were performed using 4 mM βOHB and 1mM AcAc | 1 | 10 |
| 1 mM | 1 | 8 | 0 - 10 mM | 1 | 10 |
| 5 mM | 2 | 17 | 0 - 3 mM | 2 | 20 |
| 5 mM, 10 mM | 1 | 8 | 10 mM and 20 mM | 1 | 10 |
| 10 mM | 2 | 17 | 54.35 mM or 97.83 mM for both βOHB and AcAc | 1 | 10 |
| 20 mM | 1 | 8 | Total | 10 | 100 |
| Total | 12 | 100 | | | |

Table 7.14 Recorded ketone concentrations for the negative effect studies

| No Effect Studies | | | | | |
|---|---|----------|---|--------------------------|----------|
| βOHB Concentration | Number of studies using these concentrations | % | AcAc and βOHB Concentration | Number of studies | % |
| 0 mM, 2.5 mM, 5 mM, 10 mM | 1 | 14 | 0.5 mM AcAc and 2.5 mM βOHB | 1 | 50 |
| 0 mM, 5 mM, 10 mM and 20 mM - Viability Assay and Energy Charge 0 mM, 10 mM, 20 mM, 30 mM, 40 mM - ABAD metabolism 10 mM - NMR Spectroscopy | 1 | 14 | AcAc (0.5 mM, 1mM, 2 mM, 5 mM, 10 mM), βOHB (10 mM) | 1 | 50 |
| 1 mM | 1 | 14 | Total | 2 | 100 |
| 3.5 mM | 1 | 14 | | | |
| 4 mM | 1 | 14 | | | |
| 5 mM, 25 – 1000 mM | 1 | 14 | | | |
| 20 mM | 1 | 14 | | | |
| Total | 7 | 100 | | | |

Table 7.15 Recorded ketone concentrations for the no effect ketone studies

| Study ID | Ketone used | Combined therapy | Ketone Effect |
|---------------------------|----------------------|--|---------------|
| Maurer 2011 | AcAc and β OHB | No | Positive |
| Cheng 2013 | β OHB | No | Positive |
| Xie 2015 | β OHB | Given with or without Amyloid Beta | Positive |
| Cheng 2010 | β OHB | No | Positive |
| Durigon 2018 | β OHB | In one instance β OHB is given with DMEM with glutamine, without glucose and without pyruvate. In another instance it's given with DMEM, without glutamine but then with glucose and pyruvate | Positive |
| Cheng 2005 | β OHB | Yes, two sections of the study investigated the effect of Verapamil + β OHB on induced proliferation and another section investigated the effect of Diltiazem + β OHB on $[Ca^{2+}]_i$ in mouse fibroblasts | Positive |
| Jiang 2011 | AcAc and β OHB | 2 mM Glucose is supplemented with either AcAc (1 mg/ml) or β OHB (2.5 mg/ml) | Positive |
| Tagawa 2019 | β OHB | β OHB is either given with or without tunicamycin | Positive |
| Wang 2019 | β OHB | No | Positive |
| Mikami 2020 | β OHB | β OHB is combined with cisplatin (25 μ m) when investigating proliferation/apoptosis / HDAC expression and Survivin expression | Positive |
| Vil \ddot{A} -Brau 2011 | AcAc and β OHB | No | Positive |
| Wang 2016 | β OHB | 5mM glutamate for 24 hrs after 12 hrs of treatment with β OHB. | Positive |
| Patel 1981 | AcAc and β OHB | For Lipid Synthesis Experiment the Glucose, AcAc, and β OHB were radio labelled. | Positive |
| Lamichhane 2017 | β OHB | Metformin (0.6mM, 1.2mM, 2mM), ERK inhibitor PD98059, GSK3inhibitor FH535, or NAC, -ERK, ERK, p-GSK3, GSK3, PARP, Bax, Bcl-2, and GAPDH expression, | Positive |
| Xu 2011 | β OHB | β OHB Given with LPS | Positive |
| Kweon 2004 | β OHB | 10 nM rotenone | Positive |
| Li 2020 | β OHB | No | Positive |
| Cheng 2007 | β OHB | With different concentrations of 6-OHDA (4 mM β OHB + 50 μ M 6 - OHDA and 4 mM β OHB + 10 μ M 6 - OHDA) | Positive |
| Imamura 2006 | β OHB | No | Positive |
| Zhang 2018 | β OHB | The ketone is either given on its own or with A β | Positive |
| Zhang 2017 | β OHB | One group is treated with solely β OHB whilst the other is treated with β OHB and Amyloid Beta | Positive |
| Findlay 2015 | β OHB | No | Positive |
| Shang 2018 | β OHB | To examine β OHBs effect on LPS & ATP Triggered Activation of NLRP3 Inflammasome and migration cells were pre-treated with LPS for 4 hrs and then treated with β OHB (0, 1, 10 and 25 mM) for 2 hrs, followed by 5 mM ATP simulation for 30 mins. To examine β OHBs effect on PTXs (a toxin) function, cells were pre-treated with PTX and then treated with β OHB (0, 1, 10, 25 mM) | Positive |
| Kabiraj 2012 | β OHB | Rotenone 300nM for 12 hr following 6 hr treatment with 100 μ M NA- β OHB. Rotenone is a model ROS generator via the induced production of NOx. This instigates the release of cytochrome c from the mitochondria into the cytosol, where it triggers autocatalytic processing of procaspase 9. Cas-pase-3 gets activated along with other effector proteins by cas-pase-9, resulting in the proteolytic cleavage of substrate Nuclearpoly (ADP-ribose) polymerase (PARP). | Positive |
| Liu 2018 | β OHB | No | Positive |
| Hasan 2008 | β OHB | β OHB given with 10 mM methyl succinate | Positive |
| Macdonald 2008 | β OHB | β OHB is added either individually, or with Leucine, or with BCH | Positive |
| MacDonald 2008 | AcAc and β OHB | In the insulin release experiments, AcAc and β OHB are given individually. Also, AcAc is combined with β OHB and AcAc is combined with monomethyl succinate (MMS) and β OHB is combined with MMS also, the concentration of MMS was 10 mM. AcAc is combined with lactate and β OHB is combined with lactate also, where the concentration of lactate was 5 mM. These combinations are used when the MCT as inhibited also. Glucose is combined with β OHB and Lactate with β OHB (where β OHB is 5 mM, glucose is 5.6 mM and lactate are 5 mM) when investigating insulin release from pancreatic islets. In the measurements of carbon incorporation from β OHB, β OHB is combined MMS and Succinate (where succinate and β OHB were 5 mM and MMS was 10 mM). | Positive |

| | | | |
|--------------------------|---------------|--|-----------|
| Wang 2017 | βOHB | No | Positive |
| McGee 1974 | βOHB | No | Positive |
| Martinez-Outschoorn 2011 | βOHB | Tamoxifen or Arsenic Trioxide or Metformin depending on the experiment. | Positive |
| Martinez-Outschoorn 2012 | βOHB | No | Positive |
| Huang 2017 | βOHB | During supplement experiments, it would be given with pyruvate, lactate, human recombinant IL-1b/LCN2 (R&D) and aIL-1b antibody every 4 days | Negative |
| Rodrigues 2017 | βOHB | None | Negative |
| Zhang 2018 | βOHB | 5 mM or 10 mM given with or without LG (3 mM glucose) supplementation | Negative |
| Kaya 2018 | AcAc and βOHB | No | Negative |
| Shukla 2014 | AcAc and βOHB | No | Negative |
| Shakery 2018 | βOHB | No | Negative |
| Kadochi 2017 | βOHB | LLA(1.5mM) | Negative |
| Guh 2003 | βOHB | The 0.1 to 10 mM in 11 mM of glucose | Negative |
| Liu 2019 | βOHB | Yes, U2OS cells received 10uM Nutlin for 8hrs, or 10mM βOHB for 16hrs, or both for 8 and 16 hrs respectively. This was repeated but with doxorubicin instead Nutlin with the same concentrations/times. Then cells were EdU stained (50 uM EdU for 2hrs before fixing). HCT116 cells were treated identically with just Nutlin groups for apoptosis study. | Negative |
| Magee 1979 | βOHB | No | Negative |
| Jain 2003 | AcAc and βOHB | AcAc and βOHB given in the presence or absence of glucose | Negative |
| Jain 2002 | AcAc and βOHB | AcAc and βOHB is given in the presence and absence of glucose | Negative |
| Rains 2011 | AcAc and βOHB | Chromium niacinate (Chromium III) & Lipopolysaccharides (to activate cells(4ug/L)) | Negative |
| Jain 1999 | AcAc and βOHB | Given with fresh medium containing serum and other supplements | Negative |
| Luo 2017 | AcAc and βOHB | N-acetyl cysteine in final experiment. | Negative |
| Vallejo 2020 | AcAc and βOHB | 2-DG 0.05 mM (glycolysis inhibitor) but ketones alone also investigated | Negative |
| Ji 2020 | βOHB | N-acetylcysteine | Negative |
| Poff 2014 | βOHB | No | Negative |
| D'Alessandro 2011 | βOHB | No - however, the ketone was given with a medium without FBS and glutamine | Negative |
| Skinner 2009 | AcAc and βOHB | No | Negative |
| Meroni 2018 | AcAc and βOHB | No | Negative |
| Dardis 2016 | βOHB | No | Negative |
| DuYan 2000 | βOHB | βOHB is given with the enzyme Amyloid Beta-Peptide-binding Alcohol Dehydrogenase to investigate ABADs metabolism of βOHB | No Effect |
| Tisdale 1984 | AcAc and βOHB | Given with a radioactive label (either for AcAc or βOHB) on the 4th day to investigate lipid synthesis | No Effect |
| Cui 2019 | βOHB | None | No Effect |
| Mehdikhani 2019 | βOHB | Given with DMEM with restricted glucose (250 mg/L of glucose) | No Effect |
| Otto 2014 | βOHB | Lactate was given to cell cultures separately to βOHB | No Effect |
| Eloqayli 2011 | βOHB | The ketone is given with a [2,4-13C] isotope label | No Effect |
| Bennett 2011 | βOHB | The 3.5 mM concentration of βOHB was administered with either 1 - 5.5 mM glucose | No Effect |
| Briscoe 1994 | AcAc, βOHB | Radioactive isotopes | No Effect |
| Denton 1987 | βOHB | No | No Effect |

Table 7.16 Combination Therapy

Chapter 8

Bibliography

References

- ABDELWAHAB, M. G., FENTON, K. E., PREUL, M. C., RHO, J. M., LYNCH, A., STAFFORD, P. & SCHECK, A. C. 2012. The Ketogenic Diet Is an Effective Adjuvant to Radiation Therapy for the Treatment of Malignant Glioma. *PLOS ONE*, 7, e36197.
- ACKERMANN, T. & TARDITO, S. 2019. Cell Culture Medium Formulation and Its Implications in Cancer Metabolism. *Trends in cancer*, 5, 329-332.
- AGOSTINI, M., ROMEO, F., INOUE, S., NIKLISON-CHIROU, M. V., ELIA, A. J., DINSDALE, D., MORONE, N., KNIGHT, R. A., MAK, T. W. & MELINO, G. 2016. Metabolic reprogramming during neuronal differentiation. *Cell Death Differ*, 23, 1502-14.
- ALVES, R. W., DORETTO-SILVA, L., DA SILVA, E. M., FÜRSTENAU, C. R. & ANDRADE-OLIVEIRA, V. 2020. The Non-canonical Role of Metabolic Enzymes in Immune Cells and Its Impact on Diseases. *Current Tissue Microenvironment Reports*, 1, 221-237.
- AMINZADEH-GOHARI, S., FEICHTINGER, R. G., VIDALI, S., LOCKER, F., RUTHERFORD, T., O'DONNELL, M., STÖGER-KLEIBER, A., MAYR, J. A., SPERL, W. & KOFLER, B. 2017. A ketogenic diet supplemented with medium-chain triglycerides enhances the anti-tumor and anti-angiogenic efficacy of chemotherapy on neuroblastoma xenografts in a CD1-nu mouse model. *Oncotarget*, 8, 64728-64744.
- AMOYEL, M. & BACH, E. A. 2014. Cell competition: how to eliminate your neighbours. *Development (Cambridge, England)*, 141, 988-1000.
- ARANDA-ANZALDO, A. 2012. The post-mitotic state in neurons correlates with a stable nuclear higher-order structure. *Commun Integr Biol*, 5, 134-9.
- BABICH, H., LIEBLING, E. J., BURGER, R. F., ZUCKERBRAUN, H. L. & SCHUCK, A. G. 2009. Choice of DMEM, formulated with or without pyruvate, plays an important role in assessing the in vitro cytotoxicity of oxidants and prooxidant nutraceuticals. *In Vitro Cell Dev Biol Anim*, 45, 226-33.
- BARRY, D., ELLUL, S., WATTERS, L., LEE, D., HALUSKA, R. & WHITE, R. 2018a. The ketogenic diet in disease and development. *Int J Dev Neurosci*, 68, 53-58.

- BARRY, D., ELLUL, S., WATTERS, L., LEE, D., HALUSKA, R. & WHITE, R. 2018b. The ketogenic diet in disease and development. *International Journal of Developmental Neuroscience*, 68, 53-58.
- BARTMANN, C., JANAKI RAMAN, S. R., FLÖTER, J., SCHULZE, A., BAHLKE, K., WILLINGSTORFER, J., STRUNZ, M., WÖCKEL, A., KLEMENT, R. J., KAPP, M., DJUZENOVA, C. S., OTTO, C. & KÄMMERER, U. 2018. Beta-hydroxybutyrate (3-OHB) can influence the energetic phenotype of breast cancer cells, but does not impact their proliferation and the response to chemotherapy or radiation. *Cancer Metab*, 6, 8.
- BEGLEY, C. G. & ELLIS, L. M. 2012. Raise standards for preclinical cancer research. *Nature*, 483, 531-533.
- BENNETT, K. A., FORSYTH, L. & BURCHELL, A. 2011. Functional analysis of the 5' flanking region of the human G6PC3 gene: regulation of promoter activity by glucose, pyruvate, AMP kinase and the pentose phosphate pathway. *Mol Genet Metab*, 103, 254-61.
- BERGSTRÖM, J., FÜRST, P., NORÉE, L. O. & VINNARS, E. 1974. Intracellular free amino acid concentration in human muscle tissue. *J Appl Physiol*, 36, 693-7.
- BERTOLI, S., TRENTANI, C., FERRARIS, C., DE GIORGIS, V., VEGGIOTTI, P. & TAGLIABUE, A. 2014. Long-term effects of a ketogenic diet on body composition and bone mineralization in GLUT-1 deficiency syndrome: A case series. *Nutrition*, 30, 726-728.
- BIRKET, M. J., ORR, A. L., GERENCSEK, A. A., MADDEN, D. T., VITELLI, C., SWISTOWSKI, A., BRAND, M. D. & ZENG, X. 2011. A reduction in ATP demand and mitochondrial activity with neural differentiation of human embryonic stem cells. *J Cell Sci*, 124, 348-58.
- BONUCCELLI, G., TSIRIGOS, A., WHITAKER-MENEZES, D., PAVLIDES, S., PESTELL, R. G., CHIAVARINA, B., FRANK, P. G., FLOMENBERG, N., HOWELL, A., MARTINEZ-OUTSCHOORN, U. E., SOTGIA, F. & LISANTI, M. P. 2010. Ketones and lactate "fuel" tumor growth and metastasis: Evidence that epithelial cancer cells use oxidative mitochondrial metabolism. *Cell Cycle*, 9, 3506-14.
- BREKKE, E., MORKEN, T. S. & SONNEWALD, U. 2015. Glucose metabolism and astrocyte-neuron interactions in the neonatal brain. *Neurochem Int*, 82, 33-41.

- BRISCOE, D. A., FISKUM, G., HOLLERAN, A. L. & KELLEHER, J. K. 1994. Acetoacetate metabolism in AS-30D hepatoma cells. *Mol Cell Biochem*, 136, 131-7.
- BRODEUR, G. M. 2003. Neuroblastoma: biological insights into a clinical enigma. *Nature Reviews Cancer*, 3, 203-216.
- BRODEUR, G. M. & BAGATELL, R. 2014. Mechanisms of neuroblastoma regression. *Nature Reviews Clinical Oncology*, 11, 704-713.
- CAFFA, I., SPAGNOLO, V., VERNIERI, C., VALDEMARIN, F., BECHERINI, P., WEI, M., BRANDHORST, S., ZUCAL, C., DRIEHUIS, E., FERRANDO, L., PIACENTE, F., TAGLIAFICO, A., CILLI, M., MASTRACCI, L., VELLONE, V. G., PIAZZA, S., CREMONINI, A. L., GRADASCHI, R., MANTERO, C., PASSALACQUA, M., BALLESTRERO, A., ZOPPOLI, G., CEA, M., ARRIGHI, A., ODETTI, P., MONACELLI, F., SALVADORI, G., CORTELLINO, S., CLEVERS, H., DE BRAUD, F., SUKKAR, S. G., PROVENZANI, A., LONGO, V. D. & NENCIONI, A. 2020. Fasting-mimicking diet and hormone therapy induce breast cancer regression. *Nature*, 583, 620-624.
- CAHILL, G. F. & VEECH, R. L. 2003. Ketoacids? Good medicine? *Trans Am Clin Climatol Assoc*, 114, 149-61; discussion 162-3.
- CAMARERO, N., MASCARÓ, C., MAYORDOMO, C., VILARDELL, F., HARO, D. & MARRERO, P. F. 2006. Ketogenic HMGCS2 Is a c-Myc target gene expressed in differentiated cells of human colonic epithelium and down-regulated in colon cancer. *Mol Cancer Res*, 4, 645-53.
- CANTOR, J. R., ABU-REMAILEH, M., KANAREK, N., FREINKMAN, E., GAO, X., LOUISSAINT, A., JR., LEWIS, C. A. & SABATINI, D. M. 2017. Physiologic Medium Rewires Cellular Metabolism and Reveals Uric Acid as an Endogenous Inhibitor of UMP Synthase. *Cell*, 169, 258-272.e17.
- CARLSEN, N. L. 1990. How frequent is spontaneous remission of neuroblastomas? Implications for screening. *British journal of cancer*, 61, 441-446.
- CARNEIRO, L., GELLER, S., HÉBERT, A., REPOND, C., FIORAMONTI, X., LELOUP, C. & PELLERIN, L. 2016. Hypothalamic sensing of ketone bodies after prolonged cerebral exposure leads to metabolic control dysregulation. *Scientific Reports*, 6, 34909.
- CHECHIK, T., ROEDER, L. M., TILDON, J. T. & PODUSLO, S. E. 1987. Ketone body enzyme activities in purified neurons, astrocytes and oligodendroglia. *Neurochem Int*, 10, 95-9.

- CHEN, H., QIAN, W. & GOOD, M. C. 2020. Integrating cellular dimensions with cell differentiation during early development. *Current Opinion in Cell Biology*, 67, 109-117.
- CHEN, S. W., CHOU, C. T., CHANG, C. C., LI, Y. J., CHEN, S. T., LIN, I. C., KOK, S. H., CHENG, S. J., LEE, J. J., WU, T. S., KUO, M. L. & LIN, B. R. 2017. HMGCS2 enhances invasion and metastasis via direct interaction with PPAR α to activate Src signaling in colorectal cancer and oral cancer. *Oncotarget*, 8, 22460-22476.
- CHEN, X., SHEN, W. B., YANG, P., DONG, D., SUN, W. & YANG, P. 2018. High Glucose Inhibits Neural Stem Cell Differentiation Through Oxidative Stress and Endoplasmic Reticulum Stress. *Stem Cells Dev*, 27, 745-755.
- CHENG, B., LU, H., BAI, B. & CHEN, J. 2013. d- β -Hydroxybutyrate inhibited the apoptosis of PC12 cells induced by H₂O₂ via inhibiting oxidative stress. *Neurochem Int*, 62, 620-5.
- CHENG, B., YANG, X., CHEN, C., CHENG, D., XU, X. & ZHANG, X. 2010. D-beta-hydroxybutyrate prevents MPP⁺-induced neurotoxicity in PC12 cells. *Neurochem Res*, 35, 444-51.
- CHENG, B., YANG, X., HOU, Z., LIN, X., MENG, H., LI, Z. & LIU, S. 2007. D-beta-hydroxybutyrate inhibits the apoptosis of PC12 cells induced by 6-OHDA in relation to up-regulating the ratio of Bcl-2/Bax mRNA. *Auton Neurosci*, 134, 38-44.
- CHENG, S., WU, Q., YANG, F., XU, M., LESKI, M. & CHEN, G. Q. 2005. Influence of DL-beta-hydroxybutyric acid on cell proliferation and calcium influx. *Biomacromolecules*, 6, 593-7.
- CHIODI, I., PICCO, G., MARTINO, C. & MONDELLO, C. 2019. Cellular response to glutamine and/or glucose deprivation in in vitro transformed human fibroblasts. *Oncol Rep*, 41, 3555-3564.
- COMERFORD, S. A., HUANG, Z., DU, X., WANG, Y., CAI, L., WITKIEWICZ, A. K., WALTERS, H., TANTAWY, M. N., FU, A., MANNING, H. C., HORTON, J. D., HAMMER, R. E., MCKNIGHT, S. L. & TU, B. P. 2014. Acetate dependence of tumors. *Cell*, 159, 1591-602.
- COTTER, D. G., SCHUGAR, R. C. & CRAWFORD, P. A. 2013. Ketone body metabolism and cardiovascular disease. *Am J Physiol Heart Circ Physiol*, 304, H1060-76.
- CUI, W., LUO, W., ZHOU, X., LU, Y., XU, W., ZHONG, S., FENG, G., LIANG, Y., LIANG, L., MO, Y., XIAO, X., HUANG, G., MATSKOVA, L., ZHANG, Z., LI, P.

- & ZHOU, X. 2019. Dysregulation of Ketone Body Metabolism Is Associated With Poor Prognosis for Clear Cell Renal Cell Carcinoma Patients. *Front Oncol*, 9, 1422.
- D'ALESSANDRO, G., CALCAGNO, E., TARTARI, S., RIZZARDINI, M., INVERNIZZI, R. W. & CANTONI, L. 2011. Glutamate and glutathione interplay in a motor neuronal model of amyotrophic lateral sclerosis reveals altered energy metabolism. *Neurobiol Dis*, 43, 346-55.
- DAHLQUIST, G. & PERSSON, B. 1976. The rate of cerebral utilization of glucose, ketone bodies, and oxygen: a comparative in vivo study of infant and adult rats. *Pediatr Res*, 10, 910-7.
- DARDIS, C., WOOLF, E. & SCHECK, A. 2016. A tool for reproducible research: From data analysis (in R) to a typeset laboratory notebook (as .pdf) using the text editor Emacs with the 'mp' package [version 2; referees: 2 not approved]. 4.
- DAVIDOFF, A. M. 2012. Neuroblastoma. *Semin Pediatr Surg*, 21, 2-14.
- DE CABO, R. & MATTSON, M. P. 2019. Effects of Intermittent Fasting on Health, Aging, and Disease. *N Engl J Med*, 381, 2541-2551.
- DE FEYTER, H. M., BEHAR, K. L., RAO, J. U., MADDEN-HENNESSEY, K., IP, K. L., HYDER, F., DREWES, L. R., GESCHWIND, J. F., DE GRAAF, R. A. & ROTHMAN, D. L. 2016. A ketogenic diet increases transport and oxidation of ketone bodies in RG2 and 9L gliomas without affecting tumor growth. *Neuro Oncol*, 18, 1079-87.
- DE LA TORRE-UBIETA, L. & BONNI, A. 2011. Transcriptional regulation of neuronal polarity and morphogenesis in the mammalian brain. *Neuron*, 72, 22-40.
- DE VIVO, D. C., TRIFILETTI, R. R., JACOBSON, R. I., RONEN, G. M., BEHMAND, R. A. & HARIK, S. I. 1991. Defective glucose transport across the blood-brain barrier as a cause of persistent hypoglycorrhachia, seizures, and developmental delay. *N Engl J Med*, 325, 703-9.
- DEBERARDINIS, R. J. & CHENG, T. 2010. Q's next: the diverse functions of glutamine in metabolism, cell biology and cancer. *Oncogene*, 29, 313-24.
- DEBERARDINIS, R. J., LUM, J. J., HATZIVASSILIOU, G. & THOMPSON, C. B. 2008a. The Biology of Cancer: Metabolic Reprogramming Fuels Cell Growth and Proliferation. *Cell Metabolism*, 7, 11-20.
- DEBERARDINIS, R. J., LUM, J. J., HATZIVASSILIOU, G. & THOMPSON, C. B. 2008b. The biology of cancer: metabolic reprogramming fuels cell growth and proliferation. *Cell Metab*, 7, 11-20.

- DEBERARDINIS, R. J., MANCUSO, A., DAIKHIN, E., NISSIM, I., YUDKOFF, M., WEHRLI, S. & THOMPSON, C. B. 2007. Beyond aerobic glycolysis: Transformed cells can engage in glutamine metabolism that exceeds the requirement for protein and nucleotide synthesis. *Proceedings of the National Academy of Sciences*, 104, 19345-19350.
- DEMETER, K., HERBERTH, B., DUDA, E., DOMONKOS, A., JAFFREDO, T., HERMAN, J. P. & MADARÁSZ, E. 2004. Fate of cloned embryonic neuroectodermal cells implanted into the adult, newborn and embryonic forebrain. *Exp Neurol*, 188, 254-67.
- DENICOLA, G. M. & CANTLEY, L. C. 2015. Cancer's Fuel Choice: New Flavors for a Picky Eater. *Mol Cell*, 60, 514-23.
- DENTON, T. & HOWARD, B. D. 1987. A dopaminergic cell line variant resistant to the neurotoxin 1-methyl-4-phenyl-1,2,3,6-tetrahydropyridine. *J Neurochem*, 49, 622-30.
- DEVIC, S. 2016. Warburg Effect - a Consequence or the Cause of Carcinogenesis? *Journal of Cancer*, 7, 817-822.
- DIENEL, G. A. & HERTZ, L. 2001. Glucose and lactate metabolism during brain activation. *J Neurosci Res*, 66, 824-38.
- DU YAN, S., ZHU, Y., STERN, E. D., HWANG, Y. C., HORI, O., OGAWA, S., FROSCH, M. P., CONNOLLY, E. S., JR., MCTAGGERT, R., PINSKY, D. J., CLARKE, S., STERN, D. M. & RAMASAMY, R. 2000. Amyloid beta -peptide-binding alcohol dehydrogenase is a component of the cellular response to nutritional stress. *J Biol Chem*, 275, 27100-9.
- DURIGON, R., MITCHELL, A. L., JONES, A. W., MANOLE, A., MENNUNI, M., HIRST, E. M., HOULDEN, H., MARAGNI, G., LATTANTE, S., DORONZIO, P. N., DALLA ROSA, I., ZOLLINO, M., HOLT, I. J. & SPINAZZOLA, A. 2018. LETM1 couples mitochondrial DNA metabolism and nutrient preference. *EMBO Mol Med*, 10.
- EDMOND, J., ROBBINS, R. A., BERGSTROM, J. D., COLE, R. A. & DE VELLIS, J. 1987. Capacity for substrate utilization in oxidative metabolism by neurons, astrocytes, and oligodendrocytes from developing brain in primary culture. *J Neurosci Res*, 18, 551-61.
- ELOQAYLI, H., MELO, T. M., HAUKVIK, A. & SONNEWALD, U. 2011a. [2,4-(13)C]beta-hydroxybutyrate metabolism in astrocytes and C6 glioblastoma cells. *Neurochem Res*, 36, 1566-73.

- ELOQAYLI, H., MELØ, T. M., HAUKVIK, A. & SONNEWALD, U. 2011b. [2,4-(13)C]β-hydroxybutyrate metabolism in astrocytes and C6 glioblastoma cells. *Neurochem Res*, 36, 1566-73.
- ERECINSKA, M., CHERIAN, S. & SILVER, I. A. 2004. Energy metabolism in mammalian brain during development. *Prog Neurobiol*, 73, 397-445.
- FAN, J., KAMPHORST, J. J., MATHEW, R., CHUNG, M. K., WHITE, E., SHLOMI, T. & RABINOWITZ, J. D. 2013. Glutamine-driven oxidative phosphorylation is a major ATP source in transformed mammalian cells in both normoxia and hypoxia. *Molecular systems biology*, 9, 712-712.
- FAWAL, M. A. & DAVY, A. 2018. Impact of Metabolic Pathways and Epigenetics on Neural Stem Cells. *Epigenet Insights*, 11, 2516865718820946.
- FINDLAY, J. A., HAMILTON, D. L. & ASHFORD, M. L. 2015a. BACE1 activity impairs neuronal glucose oxidation: rescue by beta-hydroxybutyrate and lipoic acid. *Front Cell Neurosci*, 9, 382.
- FINDLAY, J. A., HAMILTON, D. L. & ASHFORD, M. L. J. 2015b. BACE1 activity impairs neuronal glucose oxidation: rescue by beta-hydroxybutyrate and lipoic acid. *Frontiers in cellular neuroscience*, 9, 382-382.
- FISHER, G. J. & VOORHEES, J. J. 1996. Molecular mechanisms of retinoid actions in skin. *Faseb j*, 10, 1002-13.
- FOLL, C. L. & LEVIN, B. E. 2016. Fatty acid-induced astrocyte ketone production and the control of food intake. *American Journal of Physiology-Regulatory, Integrative and Comparative Physiology*, 310, R1186-R1192.
- FOLMES, C. D., DZEJA, P. P., NELSON, T. J. & TERZIC, A. 2012. Metabolic plasticity in stem cell homeostasis and differentiation. *Cell Stem Cell*, 11, 596-606.
- FREEDLAND, S. J., MAVROPOULOS, J., WANG, A., DARSHAN, M., DEMARK-WAHNEFRIED, W., ARONSON, W. J., COHEN, P., HWANG, D., PETERSON, B., FIELDS, T., PIZZO, S. V. & ISAACS, W. B. 2008. Carbohydrate restriction, prostate cancer growth, and the insulin-like growth factor axis. *Prostate*, 68, 11-9.
- FREY, S., GEFFROY, G., DESQUIRET-DUMAS, V., GUEGUEN, N., BRIS, C., BELAL, S., AMATI-BONNEAU, P., CHEVROLLIER, A., BARTH, M., HENRION, D., LENAERS, G., BONNEAU, D., REYNIER, P. & PROCACCIO, V. 2017. The addition of ketone bodies alleviates mitochondrial dysfunction by restoring complex I assembly in a MELAS cellular model. *Biochim Biophys Acta Mol Basis Dis*, 1863, 284-291.

- GAO, P., TCHERNYSHYOV, I., CHANG, T.-C., LEE, Y.-S., KITA, K., OCHI, T., ZELLER, K. I., DE MARZO, A. M., VAN EYK, J. E., MENDELL, J. T. & DANG, C. V. 2009. c-Myc suppression of miR-23a/b enhances mitochondrial glutaminase expression and glutamine metabolism. *Nature*, 458, 762-765.
- GARCÍA-RODRÍGUEZ, D. & GIMÉNEZ-CASSINA, A. 2021. Ketone Bodies in the Brain Beyond Fuel Metabolism: From Excitability to Gene Expression and Cell Signaling. *Frontiers in Molecular Neuroscience*, 14.
- GONZALEZ, S. V., NGUYEN, N. H., RISE, F. & HASSEL, B. 2005. Brain metabolism of exogenous pyruvate. *J Neurochem*, 95, 284-93.
- GRABACKA, M. M., WILK, A., ANTONCZYK, A., BANKS, P., WALCZYK-TYTOKO, E., DEAN, M., PIERZCHALSKA, M. & REISS, K. 2016. Fenofibrate Induces Ketone Body Production in Melanoma and Glioblastoma Cells. *Front Endocrinol (Lausanne)*, 7, 5.
- GRAHAM, N. A., TAHMASIAN, M., KOHLI, B., KOMISOPOULOU, E., ZHU, M., VIVANCO, I., TEITELL, M. A., WU, H., RIBAS, A., LO, R. S., MELLINGHOFF, I. K., MISCHER, P. S. & GRAEBER, T. G. 2012. Glucose deprivation activates a metabolic and signaling amplification loop leading to cell death. *Mol Syst Biol*, 8, 589.
- GRAY, L. R., TOMPKINS, S. C. & TAYLOR, E. B. 2014. Regulation of pyruvate metabolism and human disease. *Cell Mol Life Sci*, 71, 2577-604.
- GROESBECK, D. K., BLUML, R. M. & KOSSOFF, E. H. 2006. Long-term use of the ketogenic diet in the treatment of epilepsy. *Dev Med Child Neurol*, 48, 978-81.
- GUH, J. Y., CHUANG, T. D., CHEN, H. C., HUNG, W. C., LAI, Y. H., SHIN, S. J. & CHUANG, L. Y. 2003. Beta-hydroxybutyrate-induced growth inhibition and collagen production in HK-2 cells are dependent on TGF-beta and Smad3. *Kidney Int*, 64, 2041-51.
- GUPPY, M., GREINER, E. & BRAND, K. 1993. The role of the Crabtree effect and an endogenous fuel in the energy metabolism of resting and proliferating thymocytes. *Eur J Biochem*, 212, 95-9.
- GWANGWA, M. V., JOUBERT, A. M. & VISAGIE, M. H. 2019. Effects of glutamine deprivation on oxidative stress and cell survival in breast cell lines. *Biological Research*, 52, 15.

- HÁDINGER, N., VARGA, B. V., BERZSENYI, S., KÖRNYEI, Z., MADARÁSZ, E. & HERBERTH, B. 2009. Astroglia genesis in vitro: distinct effects of retinoic acid in different phases of neural stem cell differentiation. *Int J Dev Neurosci*, 27, 365-75.
- HALESTRAP, A. P. & WILSON, M. C. 2012. The monocarboxylate transporter family--role and regulation. *IUBMB Life*, 64, 109-19.
- HALL, S. E., WASTNEY, M. E., BOLTON, T. M., BRAATEN, J. T. & BERMAN, M. 1984. Ketone body kinetics in humans: the effects of insulin-dependent diabetes, obesity, and starvation. *J Lipid Res*, 25, 1184-94.
- HASAN, N. M., LONGACRE, M. J., STOKER, S. W., BOONSAEN, T., JITRAPAKDEE, S., KENDRICK, M. A., WALLACE, J. C. & MACDONALD, M. J. 2008. Impaired anaplerosis and insulin secretion in insulinoma cells caused by small interfering RNA-mediated suppression of pyruvate carboxylase. *J Biol Chem*, 283, 28048-59.
- HASEGAWA, S., KUME, H., IINUMA, S., YAMASAKI, M., TAKAHASHI, N. & FUKUI, T. 2012a. Acetoacetyl-CoA synthetase is essential for normal neuronal development. *Biochem Biophys Res Commun*, 427, 398-403.
- HASEGAWA, S., NODA, K., MAEDA, A., MATSUOKA, M., YAMASAKI, M. & FUKUI, T. 2012b. Acetoacetyl-CoA synthetase, a ketone body-utilizing enzyme, is controlled by SREBP-2 and affects serum cholesterol levels. *Mol Genet Metab*, 107, 553-60.
- HAWKINS, R. A., ALBERTI, K. G., HOUGHTON, C. R., WILLIAMSON, D. H. & KREBS, H. A. 1971a. The effect of acetoacetate on plasma insulin concentration. *Biochem J*, 125, 541-4.
- HAWKINS, R. A., MANS, A. M. & DAVIS, D. W. 1986. Regional ketone body utilization by rat brain in starvation and diabetes. *Am J Physiol*, 250, E169-78.
- HAWKINS, R. A., WILLIAMSON, D. H. & KREBS, H. A. 1971b. Ketone-body utilization by adult and suckling rat brain in vivo. *Biochem J*, 122, 13-8.
- HENSLEY, C. T., WASTI, A. T. & DEBERARDINIS, R. J. 2013. Glutamine and cancer: cell biology, physiology, and clinical opportunities. *J Clin Invest*, 123, 3678-84.
- HERBERTH, B., PATAKI, A., JELITAI, M., SCHLETT, K., DEÁK, F., SPÄT, A. & MADARÁSZ, E. 2002. Changes of KCl sensitivity of proliferating neural progenitors during in vitro neurogenesis. *J Neurosci Res*, 67, 574-82.
- HERNANDEZ, A. R., HERNANDEZ, C. M., CAMPOS, K., TRUCKENBROD, L., FEDERICO, Q., MOON, B., MCQUAIL, J. A., MAURER, A. P., BIZON, J. L. & BURKE, S. N. 2018. A Ketogenic Diet Improves Cognition and Has Biochemical

- Effects in Prefrontal Cortex That Are Dissociable From Hippocampus. *Frontiers in Aging Neuroscience*, 10.
- HOPKINS, B. D., PAULI, C., DU, X., WANG, D. G., LI, X., WU, D., AMADIUME, S. C., GONCALVES, M. D., HODAKOSKI, C., LUNDQUIST, M. R., BAREJA, R., MA, Y., HARRIS, E. M., SBONER, A., BELTRAN, H., RUBIN, M. A., MUKHERJEE, S. & CANTLEY, L. C. 2018. Suppression of insulin feedback enhances the efficacy of PI3K inhibitors. *Nature*, 560, 499-503.
- HUANG, C.-K., CHANG, P.-H., KUO, W.-H., CHEN, C.-L., JENG, Y.-M., CHANG, K.-J., SHEW, J.-Y., HU, C.-M. & LEE, W.-H. 2017. Adipocytes promote malignant growth of breast tumours with monocarboxylate transporter 2 expression via β -hydroxybutyrate. *Nature Communications*, 8, 14706.
- HUANG, D., LI, T., WANG, L., ZHANG, L., YAN, R., LI, K., XING, S., WU, G., HU, L., JIA, W., LIN, S. C., DANG, C. V., SONG, L., GAO, P. & ZHANG, H. 2016. Hepatocellular carcinoma redirects to ketolysis for progression under nutrition deprivation stress. *Cell Res*, 26, 1112-1130.
- HUANG, Z., SHAO, W., GU, J., HU, X., SHI, Y., XU, W., HUANG, C. & LIN, D. 2015. Effects of culture media on metabolic profiling of the human gastric cancer cell line SGC7901. *Mol Biosyst*, 11, 1832-40.
- HUTCHINSON, L. & KIRK, R. 2011. High drug attrition rates—where are we going wrong? *Nature Reviews Clinical Oncology*, 8, 189-190.
- IMAMURA, K., TAKESHIMA, T., KASHIWAYA, Y., NAKASO, K. & NAKASHIMA, K. 2006. D-beta-hydroxybutyrate protects dopaminergic SH-SY5Y cells in a rotenone model of Parkinson's disease. *J Neurosci Res*, 84, 1376-84.
- JADVAR, H. 2016. Is There Use for FDG-PET in Prostate Cancer? *Semin Nucl Med*, 46, 502-506.
- JÁDY, A. G., NAGY, Á., KŐHIDI, T., FERENCZI, S., TRETTER, L. & MADARÁSZ, E. 2016. Differentiation-Dependent Energy Production and Metabolite Utilization: A Comparative Study on Neural Stem Cells, Neurons, and Astrocytes. *Stem Cells Dev*, 25, 995-1005.
- JAIN, S. K., KANNAN, K., LIM, G., MATTHEWS-GREER, J., MCVIE, R. & BOCCHINI, J. A., JR. 2003. Elevated blood interleukin-6 levels in hyperketonemic type 1 diabetic patients and secretion by acetoacetate-treated cultured U937 monocytes. *Diabetes Care*, 26, 2139-43.

- JAIN, S. K., KANNAN, K., LIM, G., MCVIE, R. & BOCCHINI, J. A., JR. 2002. Hyperketonemia increases tumor necrosis factor-alpha secretion in cultured U937 monocytes and Type 1 diabetic patients and is apparently mediated by oxidative stress and cAMP deficiency. *Diabetes*, 51, 2287-93.
- JAIN, S. K., KANNAN, K. & MCVIE, R. 1999. Effect of hyperketonemia on blood monocytes in type-I diabetic patients and apoptosis in cultured U937 monocytes. *Antioxid Redox Signal*, 1, 211-20.
- JANG, M., KIM, S. S. & LEE, J. 2013. Cancer cell metabolism: implications for therapeutic targets. *Experimental & Molecular Medicine*, 45, e45-e45.
- JAWORSKI, D. M., NAMBOODIRI, A. M. & MOFFETT, J. R. 2016. Acetate as a Metabolic and Epigenetic Modifier of Cancer Therapy. *J Cell Biochem*, 117, 574-88.
- JELITAI, M., ANDEROVÁ, M., MARKÓ, K., KÉKESI, K., KONCZ, P., SYKOVÁ, E. & MADARÁSZ, E. 2004. Role of gamma-aminobutyric acid in early neuronal development: studies with an embryonic neuroectodermal stem cell clone. *J Neurosci Res*, 76, 801-11.
- JELITAI, M., SCHLETT, K., VARJU, P., EISEL, U. & MADARÁSZ, E. 2002. Regulated appearance of NMDA receptor subunits and channel functions during in vitro neuronal differentiation. *J Neurobiol*, 51, 54-65.
- JENSEN, N. J., WODSCHOW, H. Z., NILSSON, M. & RUNGBY, J. 2020. Effects of Ketone Bodies on Brain Metabolism and Function in Neurodegenerative Diseases. *Int J Mol Sci*, 21.
- Jl, C. C., HU, Y. Y., CHENG, G., LIANG, L., GAO, B., REN, Y. P., LIU, J. T., CAO, X. L., ZHENG, M. H., LI, S. Z., WAN, F., HAN, H. & FEI, Z. 2020. A ketogenic diet attenuates proliferation and stemness of glioma stem-like cells by altering metabolism resulting in increased ROS production. *Int J Oncol*, 56, 606-617.
- JIANG, X., KENERSON, H. L. & YEUNG, R. S. 2011. Glucose deprivation in tuberous sclerosis complex-related tumors. *Cell Biosci*, 1, 34.
- JONES, C. T. & ROLPH, T. P. 1985. Metabolism during fetal life: a functional assessment of metabolic development. *Physiol Rev*, 65, 357-430.
- KABIRAJ, P., PAL, R., VARELA-RAMIREZ, A., MIRANDA, M. & NARAYAN, M. 2012. Nitrosative stress mediated misfolded protein aggregation mitigated by Na-d-β-hydroxybutyrate intervention. *Biochemical and Biophysical Research Communications*, 426, 438-444.

- KADOCHI, Y., MORI, S., FUJIWARA-TANI, R., LUO, Y., NISHIGUCHI, Y., KISHI, S., FUJII, K., OHMORI, H. & KUNIYASU, H. 2017. Remodeling of energy metabolism by a ketone body and medium-chain fatty acid suppressed the proliferation of CT26 mouse colon cancer cells. *Oncology letters*, 14, 673-680.
- KANG, H. B., FAN, J., LIN, R., ELF, S., JI, Q., ZHAO, L., JIN, L., SEO, J. H., SHAN, C., ARBISER, J. L., COHEN, C., BRAT, D., MIZIORKO, H. M., KIM, E., ABDELWAHAB, O., MERGHOUB, T., FRÖHLING, S., SCHOLL, C., TAMAYO, P., BARBIE, D. A., ZHOU, L., POLLACK, B. P., FISHER, K., KUDCHADKAR, R. R., LAWSON, D. H., SICA, G., ROSSI, M., LONIAL, S., KHOURY, H. J., KHURI, F. R., LEE, B. H., BOGGON, T. J., HE, C., KANG, S. & CHEN, J. 2015. Metabolic Rewiring by Oncogenic BRAF V600E Links Ketogenesis Pathway to BRAF-MEK1 Signaling. *Mol Cell*, 59, 345-358.
- KANSARA, M. & BERRIDGE, M. V. 2004. Oncogenes modulate cell sensitivity to apoptosis induced by glucose deprivation. *Anticancer Res*, 24, 2503-10.
- KAWADA, K., IEKUMO, T., SAITO, R., KANEKO, M., MIMORI, S., NOMURA, Y. & OKUMA, Y. 2014. Aberrant neuronal differentiation and inhibition of dendrite outgrowth resulting from endoplasmic reticulum stress. *J Neurosci Res*, 92, 1122-33.
- KAYA, Z. Z., YILMAZ, A. M. & YALÇIN, A. S. 2018. Effect of ketone bodies on viability of human breast cancer cells (MCF-7). *Marmara Medical Journal*, 31, 1-4.
- KLEPPER, J. 2008. Glucose transporter deficiency syndrome (GLUT1DS) and the ketogenic diet. *Epilepsia*, 49 Suppl 8, 46-9.
- KLEPPER, J. & VOIT, T. 2002. Facilitated glucose transporter protein type 1 (GLUT1) deficiency syndrome: impaired glucose transport into brain-- a review. *Eur J Pediatr*, 161, 295-304.
- KONISHI, T., TAKEYASU, A., NATSUME, T., FURUSAWA, Y. & HIEDA, K. 2011. Visualization of heavy ion tracks by labeling 3'-OH termini of induced DNA strand breaks. *J Radiat Res*, 52, 433-40.
- KOPPENOL, W. H., BOUNDS, P. L. & DANG, C. V. 2011. Otto Warburg's contributions to current concepts of cancer metabolism. *Nat Rev Cancer*, 11, 325-37.
- KOVALEVICH, J. & LANGFORD, D. 2013. Considerations for the use of SH-SY5Y neuroblastoma cells in neurobiology. *Methods Mol Biol*, 1078, 9-21.

- KRISTIANSEN, M. & HAM, J. 2014. Programmed cell death during neuronal development: the sympathetic neuron model. *Cell Death & Differentiation*, 21, 1025-1035.
- KWEON, G.-R., MARKS, J. D., KRENCIK, R., LEUNG, E. H., SCHUMACKER, P. T., HYLAND, K. & KANG, U. J. 2004. Distinct Mechanisms of Neurodegeneration Induced by Chronic Complex I Inhibition in Dopaminergic and Non-dopaminergic Cells*. *Journal of Biological Chemistry*, 279, 51783-51792.
- KWIATKOWSKI, J. L., RUTKOWSKI, J. L., YAMASHIRO, D. J., TENNEKOON, G. I. & BRODEUR, G. M. 1998. Schwann cell-conditioned medium promotes neuroblastoma survival and differentiation. *Cancer Res*, 58, 4602-6.
- LAFFEL, L. 1999. Ketone bodies: a review of physiology, pathophysiology and application of monitoring to diabetes. *Diabetes Metab Res Rev*, 15, 412-26.
- LAMICHHANE, S., BASTOLA, T., PARIYAR, R., LEE, E.-S., LEE, H.-S., LEE, D. H. & SEO, J. 2017a. ROS Production and ERK Activity Are Involved in the Effects of β -Hydroxybutyrate and Metformin in a Glucose Deficient Condition. *International journal of molecular sciences*, 18, 674.
- LAMICHHANE, S., BASTOLA, T., PARIYAR, R., LEE, E. S., LEE, H. S., LEE, D. H. & SEO, J. 2017b. ROS Production and ERK Activity Are Involved in the Effects of β -Hydroxybutyrate and Metformin in a Glucose Deficient Condition. *Int J Mol Sci*, 18.
- LEINO, R. L., GERHART, D. Z., DUELLI, R., ENERSON, B. E. & DREWES, L. R. 2001. Diet-induced ketosis increases monocarboxylate transporter (MCT1) levels in rat brain. *Neurochem Int*, 38, 519-27.
- LI, D., DING, Z., GUI, M., HOU, Y. & XIE, K. 2020a. Metabolic Enhancement of Glycolysis and Mitochondrial Respiration Are Essential for Neuronal Differentiation. *Cellular Reprogramming*, 22, 291-299.
- LI, X., ZHAN, Z., ZHANG, J., ZHOU, F. & AN, L. 2020b. β -Hydroxybutyrate Ameliorates A β -Induced Downregulation of TrkA Expression by Inhibiting HDAC1/3 in SH-SY5Y Cells. *Am J Alzheimers Dis Other Demen*, 35, 1533317519883496.
- LIBERTI, M. V. & LOCASALE, J. W. 2016. The Warburg Effect: How Does it Benefit Cancer Cells? *Trends Biochem Sci*, 41, 211-218.
- LIU, K., LI, F., SUN, Q., LIN, N., HAN, H., YOU, K., TIAN, F., MAO, Z., LI, T., TONG, T., GENG, M., ZHAO, Y., GU, W. & ZHAO, W. 2019a. p53 β -hydroxybutyrylation attenuates p53 activity. *Cell Death & Disease*, 10, 243.

- LIU, S. J., TANG, H. L., HE, Q., LU, P., FU, T., XU, X. L., SU, T., GAO, M. M., DUAN, S., LUO, Y. & LONG, Y. S. 2019b. FTO is a transcriptional repressor to auto-regulate its own gene and potentially associated with homeostasis of body weight. *J Mol Cell Biol*, 11, 118-132.
- LIVINGSTONE, L. R., WHITE, A., SPROUSE, J., LIVANOS, E., JACKS, T. & TLSTY, T. D. 1992. Altered cell cycle arrest and gene amplification potential accompany loss of wild-type p53. *Cell*, 70, 923-35.
- LOCASALE, J. W. & CANTLEY, L. C. 2011. Metabolic flux and the regulation of mammalian cell growth. *Cell Metab*, 14, 443-51.
- LONGO, V. D. & FONTANA, L. 2010. Calorie restriction and cancer prevention: metabolic and molecular mechanisms. *Trends Pharmacol Sci*, 31, 89-98.
- LOPES-CARDOZO, M., LARSSON, O. M. & SCHOUSBOE, A. 1986. Acetoacetate and glucose as lipid precursors and energy substrates in primary cultures of astrocytes and neurons from mouse cerebral cortex. *J Neurochem*, 46, 773-8.
- LOPES, F. M., SCHRODER, R., DA FROTA, M. L., JR., ZANOTTO-FILHO, A., MULLER, C. B., PIRES, A. S., MEURER, R. T., COLPO, G. D., GELAIN, D. P., KAPCZINSKI, F., MOREIRA, J. C., FERNANDES MDA, C. & KLAMT, F. 2010. Comparison between proliferative and neuron-like SH-SY5Y cells as an in vitro model for Parkinson disease studies. *Brain Res*, 1337, 85-94.
- LU, W., PELICANO, H. & HUANG, P. 2010. Cancer Metabolism: Is Glutamine Sweeter than Glucose? *Cancer Cell*, 18, 199-200.
- LUND, T. M., OBEL, L. F., RISA, Ø. & SONNEWALD, U. 2011. β -Hydroxybutyrate is the preferred substrate for GABA and glutamate synthesis while glucose is indispensable during depolarization in cultured GABAergic neurons. *Neurochem Int*, 59, 309-18.
- LUND, T. M., PLOUG, K. B., IVERSEN, A., JENSEN, A. A. & JANSEN-OLESEN, I. 2015. The metabolic impact of β -hydroxybutyrate on neurotransmission: Reduced glycolysis mediates changes in calcium responses and KATP channel receptor sensitivity. *Journal of Neurochemistry*, 132, 520-531.
- LUND, T. M., RISA, O., SONNEWALD, U., SCHOUSBOE, A. & WAAGEPETERSEN, H. S. 2009. Availability of neurotransmitter glutamate is diminished when beta-hydroxybutyrate replaces glucose in cultured neurons. *J Neurochem*, 110, 80-91.
- LUO, W., QIN, L., LI, B., LIAO, Z., LIANG, J., XIAO, X., XIAO, X., MO, Y., HUANG, G., ZHANG, Z., ZHOU, X. & LI, P. 2017. Inactivation of HMGCL promotes

- proliferation and metastasis of nasopharyngeal carcinoma by suppressing oxidative stress. *Scientific Reports*, 7, 11954.
- MACDONALD, M. J., HASAN, N. M. & LONGACRE, M. J. 2008a. Studies with leucine, beta-hydroxybutyrate and ATP citrate lyase-deficient beta cells support the acetoacetate pathway of insulin secretion. *Biochim Biophys Acta*, 1780, 966-72.
- MACDONALD, M. J., LONGACRE, M. J., STOKER, S. W., BROWN, L. J., HASAN, N. M. & KENDRICK, M. A. 2008b. Acetoacetate and beta-hydroxybutyrate in combination with other metabolites release insulin from INS-1 cells and provide clues about pathways in insulin secretion. *Am J Physiol Cell Physiol*, 294, C442-50.
- MAFFEZZINI, C., CALVO-GARRIDO, J., WREDENBERG, A. & FREYER, C. 2020. Metabolic regulation of neurodifferentiation in the adult brain. *Cell Mol Life Sci*, 77, 2483-2496.
- MAGEE, B. A., POTEZNY, N., ROFE, A. M. & CONYERS, R. A. 1979. The inhibition of malignant cell growth by ketone bodies. *Aust J Exp Biol Med Sci*, 57, 529-39.
- MARIE, S. K. N. & SHINJO, S. M. O. 2011. Metabolism and brain cancer. *Clinics (Sao Paulo, Brazil)*, 66 Suppl 1, 33-43.
- MARTINEZ-OUTSCHOORN, U. E., GOLDBERG, A., LIN, Z., KO, Y. H., FLOMENBERG, N., WANG, C., PAVLIDES, S., PESTELL, R. G., HOWELL, A., SOTGIA, F. & LISANTI, M. P. 2011a. Anti-estrogen resistance in breast cancer is induced by the tumor microenvironment and can be overcome by inhibiting mitochondrial function in epithelial cancer cells. *Cancer Biol Ther*, 12, 924-38.
- MARTINEZ-OUTSCHOORN, U. E., LIN, Z., WHITAKER-MENEZES, D., HOWELL, A., LISANTI, M. P. & SOTGIA, F. 2012a. Ketone bodies and two-compartment tumor metabolism: stromal ketone production fuels mitochondrial biogenesis in epithelial cancer cells. *Cell Cycle*, 11, 3956-63.
- MARTINEZ-OUTSCHOORN, U. E., LIN, Z., WHITAKER-MENEZES, D., HOWELL, A., SOTGIA, F. & LISANTI, M. P. 2012b. Ketone body utilization drives tumor growth and metastasis. *Cell Cycle*, 11, 3964-71.
- MARTINEZ-OUTSCHOORN, U. E., PRISCO, M., ERTEL, A., TSIRIGOS, A., LIN, Z., PAVLIDES, S., WANG, C., FLOMENBERG, N., KNUDSEN, E. S., HOWELL, A., PESTELL, R. G., SOTGIA, F. & LISANTI, M. P. 2011b. Ketones and lactate increase cancer cell "stemness," driving recurrence, metastasis and poor clinical outcome in breast cancer: achieving personalized medicine via Metabolo-Genomics. *Cell Cycle*, 10, 1271-86.

- MARTINEZ-OUTSCHOORN, U. E., PRISCO, M., ERTEL, A., TSIRIGOS, A., LIN, Z., PAVLIDES, S., WANG, C., FLOMENBERG, N., KNUDSEN, E. S., HOWELL, A., PESTELL, R. G., SOTGIA, F. & LISANTI, M. P. 2011c. Ketones and lactate increase cancer cell “stemness,” driving recurrence, metastasis and poor clinical outcome in breast cancer. *Cell Cycle*, 10, 1271-1286.
- MARTUSCELLO, R. T., VEDAM-MAI, V., MCCARTHY, D. J., SCHMOLL, M. E., JUNDI, M. A., LOUVIERE, C. D., GRIFFITH, B. G., SKINNER, C. L., SUSLOV, O., DELEYROLLE, L. P. & REYNOLDS, B. A. 2016a. A Supplemented High-Fat Low-Carbohydrate Diet for the Treatment of Glioblastoma. *Clinical Cancer Research*, 22, 2482-2495.
- MARTUSCELLO, R. T., VEDAM-MAI, V., MCCARTHY, D. J., SCHMOLL, M. E., JUNDI, M. A., LOUVIERE, C. D., GRIFFITH, B. G., SKINNER, C. L., SUSLOV, O., DELEYROLLE, L. P. & REYNOLDS, B. A. 2016b. A Supplemented High-Fat Low-Carbohydrate Diet for the Treatment of Glioblastoma. *Clin Cancer Res*, 22, 2482-95.
- MASHIMO, T., PICHUMANI, K., VEMIREDDY, V., HATANPAA, K. J., SINGH, D. K., SIRASANAGANDLA, S., NANNEPAGA, S., PICCIRILLO, S. G., KOVACS, Z., FOONG, C., HUANG, Z., BARNETT, S., MICKEY, B. E., DEBERARDINIS, R. J., TU, B. P., MAHER, E. A. & BACHOO, R. M. 2014. Acetate is a bioenergetic substrate for human glioblastoma and brain metastases. *Cell*, 159, 1603-14.
- MATÉS, J. M., PÉREZ-GÓMEZ, C., NÚÑEZ DE CASTRO, I., ASENJO, M. & MÁRQUEZ, J. 2002. Glutamine and its relationship with intracellular redox status, oxidative stress and cell proliferation/death. *Int J Biochem Cell Biol*, 34, 439-58.
- MATTHAY, K. K., MARIS, J. M., SCHLEIERMACHER, G., NAKAGAWARA, A., MACKALL, C. L., DILLER, L. & WEISS, W. A. 2016. Neuroblastoma. *Nature Reviews Disease Primers*, 2, 16078.
- MATTSON, M. P. 2008. Glutamate and neurotrophic factors in neuronal plasticity and disease. *Ann N Y Acad Sci*, 1144, 97-112.
- MATTSON, M. P., MOEHL, K., GHENA, N., SCHMAEDICK, M. & CHENG, A. 2018. Intermittent metabolic switching, neuroplasticity and brain health. *Nature Reviews Neuroscience*, 19, 81-94.
- MAURER, G. D., BRUCKER, D. P., BAHR, O., HARTER, P. N., HATTINGEN, E., WALENTA, S., MUELLER-KLIESER, W., STEINBACH, J. P. & RIEGER, J.

- 2011a. Differential utilization of ketone bodies by neurons and glioma cell lines: a rationale for ketogenic diet as experimental glioma therapy. *BMC Cancer*, 11, 315.
- MAURER, G. D., BRUCKER, D. P., BÄHR, O., HARTER, P. N., HATTINGEN, E., WALENTA, S., MUELLER-KLIESER, W., STEINBACH, J. P. & RIEGER, J. 2011b. Differential utilization of ketone bodies by neurons and glioma cell lines: a rationale for ketogenic diet as experimental glioma therapy. *BMC Cancer*, 11, 315.
- MAURER, M. H., GEOMOR, H. K., BÜRGERS, H. F., SCHELSHORN, D. W. & KUSCHINSKY, W. 2006. Adult neural stem cells express glucose transporters GLUT1 and GLUT3 and regulate GLUT3 expression. *FEBS Lett*, 580, 4430-4.
- MCGEE, R. & SPECTOR, A. A. 1974. Short-term effects of free fatty acids on the regulation of fatty acid biosynthesis in Ehrlich ascites tumor cells. *Cancer Res*, 34, 3355-62.
- MCKEE, T. J. & KOMAROVA, S. V. 2017. Is it time to reinvent basic cell culture medium? *Am J Physiol Cell Physiol*, 312, C624-c626.
- MCKENNA, M. C. 2012. Substrate competition studies demonstrate oxidative metabolism of glucose, glutamate, glutamine, lactate and 3-hydroxybutyrate in cortical astrocytes from rat brain. *Neurochem Res*, 37, 2613-26.
- MCKENNA, M. C., TILDON, J. T., STEVENSON, J. H. & HOPKINS, I. B. 1994. Energy metabolism in cortical synaptic terminals from weanling and mature rat brain: evidence for multiple compartments of tricarboxylic acid cycle activity. *Dev Neurosci*, 16, 291-300.
- MEHDIKHANI, F., GHAREMANI, H., NABATI, S., TAHMOURI, H., SIRATISABET, M. & SALAMI, S. 2019. Histone Butyrylation/ Acetylation Remains Unchanged in Triple Negative Breast Cancer Cells after a Long Term Metabolic Reprogramming. *Asian Pacific journal of cancer prevention : APJCP*, 20, 3597-3601.
- MELO, T. M., NEHLIG, A. & SONNEWALD, U. 2006. Neuronal-glia interactions in rats fed a ketogenic diet. *Neurochem Int*, 48, 498-507.
- MERGENTHALER, P., LINDAUER, U., DIENEL, G. A. & MEISEL, A. 2013. Sugar for the brain: the role of glucose in physiological and pathological brain function. *Trends in neurosciences*, 36, 587-597.
- MERONI, E., PAPINI, N., CRISCUOLI, F., CASIRAGHI, M. C., MASSACCESI, L., BASILICO, N. & ERBA, D. 2018. Metabolic Responses in Endothelial Cells Following Exposure to Ketone Bodies. *Nutrients*, 10.

- MIKAMI, D., KOBAYASHI, M., UWADA, J., YAZAWA, T., KAMIYAMA, K., NISHIMORI, K., NISHIKAWA, Y., NISHIKAWA, S., YOKOI, S., TANIGUCHI, T. & IWANO, M. 2020. β -Hydroxybutyrate enhances the cytotoxic effect of cisplatin via the inhibition of HDAC/survivin axis in human hepatocellular carcinoma cells. *J Pharmacol Sci*, 142, 1-8.
- MIYAZAWA, H. & AULEHLA, A. 2018. Revisiting the role of metabolism during development. *Development*, 145.
- MORSCHER, R. J., AMINZADEH-GOHARI, S., FEICHTINGER, R. G., MAYR, J. A., LANG, R., NEUREITER, D., SPERL, W. & KOFLER, B. 2015. Inhibition of Neuroblastoma Tumor Growth by Ketogenic Diet and/or Calorie Restriction in a CD1-Nu Mouse Model. *PLoS One*, 10, e0129802.
- MURPHY, P., LIKHODII, S., NYLEN, K. & BURNHAM, W. M. 2004. The antidepressant properties of the ketogenic diet. *Biol Psychiatry*, 56, 981-3.
- MURRAY, A. J., KNIGHT, N. S., COLE, M. A., COCHLIN, L. E., CARTER, E., TCHABANENKO, K., PICHULIK, T., GULSTON, M. K., ATHERTON, H. J., SCHROEDER, M. A., DEACON, R. M. J., KASHIWAYA, Y., KING, M. T., PAWLOSKEY, R., RAWLINS, J. N. P., TYLER, D. J., GRIFFIN, J. L., ROBERTSON, J., VEECH, R. L. & CLARKE, K. 2016. Novel ketone diet enhances physical and cognitive performance. *The FASEB Journal*, 30, 4021-4032.
- NAPOLI, J. L. 1996. Retinoic acid biosynthesis and metabolism. *Faseb j*, 10, 993-1001.
- NEHLIG, A. 2004. Brain uptake and metabolism of ketone bodies in animal models. *Prostaglandins Leukot Essent Fatty Acids*, 70, 265-75.
- NEHLIG, A. & COLES, J. A. 2007. Cellular pathways of energy metabolism in the brain: is glucose used by neurons or astrocytes? *Glia*, 55, 1238-1250.
- NEHLIG, A. & PEREIRA DE VASCONCELOS, A. 1993. Glucose and ketone body utilization by the brain of neonatal rats. *Prog Neurobiol*, 40, 163-221.
- NEI, M., NGO, L., SIRVEN, J. I. & SPERLING, M. R. 2014. Ketogenic diet in adolescents and adults with epilepsy. *Seizure*, 23, 439-42.
- NEWMAN, J. C. & VERDIN, E. 2014. Ketone bodies as signaling metabolites. *Trends Endocrinol Metab*, 25, 42-52.
- NICKLIN, P., BERGMAN, P., ZHANG, B., TRIANTAFELLOW, E., WANG, H., NYFELER, B., YANG, H., HILD, M., KUNG, C., WILSON, C., MYER, V. E., MACKEIGAN, J. P., PORTER, J. A., WANG, Y. K., CANTLEY, L. C., FINAN, P.

- M. & MURPHY, L. O. 2009. Bidirectional transport of amino acids regulates mTOR and autophagy. *Cell*, 136, 521-34.
- NOLFI-DONEGAN, D., BRAGANZA, A. & SHIVA, S. 2020. Mitochondrial electron transport chain: Oxidative phosphorylation, oxidant production, and methods of measurement. *Redox Biol*, 37, 101674.
- O'FLANAGAN, C. H., SMITH, L. A., MCDONELL, S. B. & HURSTING, S. D. 2017. When less may be more: calorie restriction and response to cancer therapy. *BMC Med*, 15, 106.
- OTTO, C., KAEMMERER, U., ILLERT, B., MUEHLING, B., PFETZER, N., WITTIG, R., VOELKER, H. U., THIEDE, A. & COY, J. F. 2008. Growth of human gastric cancer cells in nude mice is delayed by a ketogenic diet supplemented with omega-3 fatty acids and medium-chain triglycerides. *BMC Cancer*, 8, 122.
- OTTO, C., KLINGELHÖFFER, C., BIGGEMANN, L., MELKUS, G., MÖRCHEL, P., JÜRGENS, C., GAHN, S. & KÄMMERER, U. 2014. Analysis of the metabolism of ketone bodies and lactate by gastrointestinal tumour cells in vitro. *Aktuelle Ernährungsmedizin*, 39, 51-59.
- PAOLI, A., BOSCO, G., CAMPORESI, E. M. & MANGAR, D. 2015. Ketosis, ketogenic diet and food intake control: a complex relationship. *Frontiers in psychology*, 6, 27-27.
- PAOLI, A., RUBINI, A., VOLEK, J. S. & GRIMALDI, K. A. 2013. Beyond weight loss: a review of the therapeutic uses of very-low-carbohydrate (ketogenic) diets. *Eur J Clin Nutr*, 67, 789-96.
- PARK, S. J., SMITH, C. P., WILBUR, R. R., CAIN, C. P., KALLU, S. R., VALASAPALLI, S., SAHOO, A., GUDA, M. R., TSUNG, A. J. & VELPULA, K. K. 2018. An overview of MCT1 and MCT4 in GBM: small molecule transporters with large implications. *Am J Cancer Res*, 8, 1967-1976.
- PATEL, M. S., JOHNSON, C. A., RAJAN, R. & OWEN, O. E. 1975. The metabolism of ketone bodies in developing human brain: development of ketone-body-utilizing enzymes and ketone bodies as precursors for lipid synthesis. *J Neurochem*, 25, 905-8.
- PATEL, M. S., RUSSELL, J. J. & GERSHMAN, H. 1981. Ketone-body metabolism in glioma and neuroblastoma cells. *Proc Natl Acad Sci U S A*, 78, 7214-8.
- PAVLOVA, N. N. & THOMPSON, C. B. 2016. The Emerging Hallmarks of Cancer Metabolism. *Cell Metab*, 23, 27-47.

- PAYEN, V. L., MINA, E., VAN HÉE, V. F., PORPORATO, P. E. & SONVEAUX, P. 2020. Monocarboxylate transporters in cancer. *Mol Metab*, 33, 48-66.
- PÉREZ-ESCUREDO, J., VAN HÉE, V. F., SBOARINA, M., FALCES, J., PAYEN, V. L., PELLERIN, L. & SONVEAUX, P. 2016a. Monocarboxylate transporters in the brain and in cancer. *Biochim Biophys Acta*, 1863, 2481-97.
- PÉREZ-ESCUREDO, J., VAN HÉE, V. F., SBOARINA, M., FALCES, J., PAYEN, V. L., PELLERIN, L. & SONVEAUX, P. 2016b. Monocarboxylate transporters in the brain and in cancer. *Biochimica et Biophysica Acta (BBA) - Molecular Cell Research*, 1863, 2481-2497.
- PERSSON, B. & GENTZ, J. 1966. The pattern of blood lipids, glycerol and ketone bodies during the neonatal period, infancy and childhood. *Acta Paediatr Scand*, 55, 353-62.
- PIERRE, K., PELLERIN, L., DEBERNARDI, R., RIEDERER, B. M. & MAGISTRETTI, P. J. 2000. Cell-specific localization of monocarboxylate transporters, MCT1 and MCT2, in the adult mouse brain revealed by double immunohistochemical labeling and confocal microscopy. *Neuroscience*, 100, 617-27.
- POFF, A. M., ARI, C., ARNOLD, P., SEYFRIED, T. N. & D'AGOSTINO, D. P. 2014. Ketone supplementation decreases tumor cell viability and prolongs survival of mice with metastatic cancer. *Int J Cancer*, 135, 1711-20.
- PRINS, M. L. 2008. Cerebral metabolic adaptation and ketone metabolism after brain injury. *J Cereb Blood Flow Metab*, 28, 1-16.
- PRINS, M. L. & MATSUMOTO, J. H. 2014. The collective therapeutic potential of cerebral ketone metabolism in traumatic brain injury. *J Lipid Res*, 55, 2450-7.
- PUCHALSKA, P. & CRAWFORD, P. A. 2017. Multi-dimensional Roles of Ketone Bodies in Fuel Metabolism, Signaling, and Therapeutics. *Cell Metab*, 25, 262-284.
- QUANZ, M., BENDER, E., KOPITZ, C., GRÜNEWALD, S., SCHLICKER, A., SCHWEDE, W., EHEIM, A., TOSCHI, L., NEUHAUS, R., RICHTER, C., TOEDLING, J., MERZ, C., LESCHE, R., KAMBUROV, A., SIEBENEICHER, H., BAUSER, M. & HÄGEBARTH, A. 2018. Preclinical Efficacy of the Novel Monocarboxylate Transporter 1 Inhibitor BAY-8002 and Associated Markers of Resistance. *Mol Cancer Ther*, 17, 2285-2296.
- RAINS, J. L. & JAIN, S. K. 2011. Hyperketonemia decreases mitochondrial membrane potential and its normalization with chromium (III) supplementation in monocytes. *Mol Cell Biochem*, 349, 77-82.

- RIES LAG, S. M., GURNEY JG, LINET M, TAMRA T, YOUNG JL, BUNIN GR (EDS) 1999. Cancer Incidence and Survival among Children and Adolescents: United States SEER Program 1975-1995, National Cancer Institute, SEER Program. *NIH Pub. No. 99-4649*.
- RODRIGUES, L. M., URIBE-LEWIS, S., MADHU, B., HONESS, D. J., STUBBS, M. & GRIFFITHS, J. R. 2017. The action of β -hydroxybutyrate on the growth, metabolism and global histone H3 acetylation of spontaneous mouse mammary tumours: evidence of a β -hydroxybutyrate paradox. *Cancer Metab*, 5, 4.
- ROJAS-MORALES, P., TAPIA, E. & PEDRAZA-CHAVERRI, J. 2016. β -Hydroxybutyrate: A signaling metabolite in starvation response? *Cell Signal*, 28, 917-23.
- ROUBERGUE, A., PHILIBERT, B., GAUTIER, A., KUSTER, A., MARKOWICZ, K., BILLETTE DE VILLEMEUR, T., VUILLAUMIER-BARROT, S., NICOLE, S., ROZE, E. & DOUMMAR, D. 2015. Excellent response to a ketogenic diet in a patient with alternating hemiplegia of childhood. *JIMD Rep*, 15, 7-12.
- RUDOLF, M. C. & SHERWIN, R. S. 1983. Maternal ketosis and its effects on the fetus. *Clin Endocrinol Metab*, 12, 413-28.
- SAUNDERS, N. R., LIDDELOW, S. A. & DZIEGIELEWSKA, K. M. 2012. Barrier mechanisms in the developing brain. *Frontiers in pharmacology*, 3, 46-46.
- SCHLETT, K., HERBERTH, B. & MADARASZ, E. 1997. In vitro pattern formation during neurogenesis in neuroectodermal progenitor cells immortalized by p53-deficiency. *Int J Dev Neurosci*, 15, 795-804.
- SCHLETT, K. & MADARASZ, E. 1997. Retinoic acid induced neural differentiation in a neuroectodermal cell line immortalized by p53 deficiency. *J Neurosci Res*, 47, 405-15.
- SCHÖNFELD, P. & REISER, G. 2013. Why does brain metabolism not favor burning of fatty acids to provide energy? Reflections on disadvantages of the use of free fatty acids as fuel for brain. *J Cereb Blood Flow Metab*, 33, 1493-9.
- SEGARRA-MONDEJAR, M., CASELLAS-DÍAZ, S., RAMIRO-PARETA, M., MÜLLER-SÁNCHEZ, C., MARTORELL-RIERA, A., HERMELO, I., REINA, M., ARAGONÉS, J., MARTÍNEZ-ESTRADA, O. M. & SORIANO, F. X. 2018. Synaptic activity-induced glycolysis facilitates membrane lipid provision and neurite outgrowth. *Embo j*, 37.

- SEYFRIED, T. 2015. Cancer as a mitochondrial metabolic disease. *Frontiers in Cell and Developmental Biology*, 3.
- SHAKERY, A., POURVALI, K., GHORBANI, A., FERREIDANI, S. S. & ZAND, H. 2018. Beta-Hydroxybutyrate Promotes Proliferation, Migration and Stemness in a Subpopulation of 5FU Treated SW480 Cells: Evidence for Metabolic Plasticity in Colon Cancer. *Asian Pacific journal of cancer prevention : APJCP*, 19, 3287-3294.
- SHANG, S., WANG, L., ZHANG, Y., LU, H. & LU, X. 2018. The Beta-Hydroxybutyrate Suppresses the Migration of Glioma Cells by Inhibition of NLRP3 Inflammasome. *Cell Mol Neurobiol*, 38, 1479-1489.
- SHIPLEY, M. M., MANGOLD, C. A. & SZPARA, M. L. 2016. Differentiation of the SH-SY5Y Human Neuroblastoma Cell Line. *J Vis Exp*, 53193.
- SHUKLA, S. K., GEBREGIWORGIS, T., PUROHIT, V., CHAIKA, N. V., GUNDA, V., RADHAKRISHNAN, P., MEHLA, K., PIPINOS, II, POWERS, R., YU, F. & SINGH, P. K. 2014. Metabolic reprogramming induced by ketone bodies diminishes pancreatic cancer cachexia. *Cancer Metab*, 2, 18.
- SHYH-CHANG, N., DALEY, G. Q. & CANTLEY, L. C. 2013. Stem cell metabolism in tissue development and aging. *Development*, 140, 2535-47.
- SKINNER, R., TRUJILLO, A., MA, X. & BEIERLE, E. A. 2009. Ketone bodies inhibit the viability of human neuroblastoma cells. *J Pediatr Surg*, 44, 212-6; discussion 216.
- SLEIMAN, S. F., HENRY, J., AL-HADDAD, R., EL HAYEK, L., ABOU HAIDAR, E., STRINGER, T., ULJA, D., KARUPPAGOUNDER, S. S., HOLSON, E. B., RATAN, R. R., NINAN, I. & CHAO, M. V. 2016. Exercise promotes the expression of brain derived neurotrophic factor (BDNF) through the action of the ketone body beta-hydroxybutyrate. *Elife*, 5.
- SMITH, S. L., HEAL, D. J. & MARTIN, K. F. 2005. KTX 0101: a potential metabolic approach to cytoprotection in major surgery and neurological disorders. *CNS Drug Rev*, 11, 113-40.
- SON, J., LYSSIOTIS, C. A., YING, H., WANG, X., HUA, S., LIGORIO, M., PERERA, R. M., FERRONE, C. R., MULLARKY, E., SHYH-CHANG, N., KANG, Y. A., FLEMING, J. B., BARDEESY, N., ASARA, J. M., HAIGIS, M. C., DEPINHO, R. A., CANTLEY, L. C. & KIMMELMAN, A. C. 2013. Glutamine supports pancreatic cancer growth through a KRAS-regulated metabolic pathway. *Nature*, 496, 101-105.
- STAFSTROM, C. E. & RHO, J. M. 2012. The ketogenic diet as a treatment paradigm for diverse neurological disorders. *Front Pharmacol*, 3, 59.

- STILES, J. & JERNIGAN, T. L. 2010. The basics of brain development. *Neuropsychol Rev*, 20, 327-48.
- STOJANOVIC, V. & IHLE, S. 2011. Role of beta-hydroxybutyric acid in diabetic ketoacidosis: a review. *Can Vet J*, 52, 426-30.
- SULLIVAN, L. B., GUI, D. Y., HOSIOS, A. M., BUSH, L. N., FREINKMAN, E. & VANDER HEIDEN, M. G. 2015. Supporting Aspartate Biosynthesis Is an Essential Function of Respiration in Proliferating Cells. *Cell*, 162, 552-63.
- SUSSMAN, D., ELLEGOOD, J. & HENKELMAN, M. 2013a. A gestational ketogenic diet alters maternal metabolic status as well as offspring physiological growth and brain structure in the neonatal mouse. *BMC Pregnancy Childbirth*, 13, 198.
- SUSSMAN, D., VAN EEDE, M., WONG, M. D., ADAMSON, S. L. & HENKELMAN, M. 2013b. Effects of a ketogenic diet during pregnancy on embryonic growth in the mouse. *BMC Pregnancy Childbirth*, 13, 109.
- TAGAWA, R., KAWANO, Y., MINAMI, A., NISHIUMI, S., YANO, Y., YOSHIDA, M. & KODAMA, Y. 2019. β -hydroxybutyrate protects hepatocytes against endoplasmic reticulum stress in a sirtuin 1-independent manner. *Arch Biochem Biophys*, 663, 220-227.
- TANEGASHIMA, K., SATO-MIYATA, Y., FUNAKOSHI, M., NISHITO, Y., AIGAKI, T. & HARA, T. 2017. Epigenetic regulation of the glucose transporter gene *Slc2a1* by beta-hydroxybutyrate underlies preferential glucose supply to the brain of fasted mice. *Genes Cells*, 22, 71-83.
- TATAPUDY, S., ALOISIO, F., BARBER, D. & NYSTUL, T. 2017. Cell fate decisions: emerging roles for metabolic signals and cell morphology. *EMBO reports*, 18, 2105-2118.
- TIEU, K., PERIER, C., CASPERSEN, C., TEISMANN, P., WU, D. C., YAN, S. D., NAINI, A., VILA, M., JACKSON-LEWIS, V., RAMASAMY, R. & PRZEDBORSKI, S. 2003. D-beta-hydroxybutyrate rescues mitochondrial respiration and mitigates features of Parkinson disease. *J Clin Invest*, 112, 892-901.
- TILDON, J. T., MCKENNA, M. C. & STEVENSON, J. H., JR. 1994. Transport of 3-hydroxybutyrate by cultured rat brain astrocytes. *Neurochem Res*, 19, 1237-42.
- TISDALE, M. J. 1984. Role of acetoacetyl-CoA synthetase in acetoacetate utilization by tumor cells. *Cancer Biochem Biophys*, 7, 101-7.
- ULATE-CAMPOS, A., FONS, C., ARTUCH, R., CASTEJON, E., MARTORELL, L., OZELIUS, L., PASCUAL, J. & CAMPISTOL, J. 2014. Alternating hemiplegia of

- childhood with a de novo mutation in ATP1A3 and changes in SLC2A1 responsive to a ketogenic diet. *Pediatr Neurol*, 50, 377-9.
- VALENTE-SILVA, P., LEMOS, C., KÖFALVI, A., CUNHA, R. A. & JONES, J. G. 2015. Ketone bodies effectively compete with glucose for neuronal acetyl-CoA generation in rat hippocampal slices. *NMR Biomed*, 28, 1111-6.
- VALLEJO, F. A., SHAH, S. S., DE CORDOBA, N., WALTERS, W. M., PRINCE, J., KHATIB, Z., KOMOTAR, R. J., VANNI, S. & GRAHAM, R. M. 2020. The contribution of ketone bodies to glycolytic inhibition for the treatment of adult and pediatric glioblastoma. *J Neurooncol*, 147, 317-326.
- VAN DER LOUW, E. J., WILLIAMS, T. J., HENRY-BARRON, B. J., OLIEMAN, J. F., DUVEKOT, J. J., VERMEULEN, M. J., BANNINK, N., WILLIAMS, M., NEUTEBOOM, R. F., KOSSOFF, E. H., CATSMAN-BERREVOETS, C. E. & CERVENKA, M. C. 2017. Ketogenic diet therapy for epilepsy during pregnancy: A case series. *Seizure*, 45, 198-201.
- VANDER HEIDEN, M. G., CANTLEY, L. C. & THOMPSON, C. B. 2009. Understanding the Warburg effect: the metabolic requirements of cell proliferation. *Science*, 324, 1029-33.
- VANNUCCI, S. J. & SIMPSON, I. A. 2003. Developmental switch in brain nutrient transporter expression in the rat. *Am J Physiol Endocrinol Metab*, 285, E1127-34.
- VARGA, B. V., HADINGER, N., GOCZA, E., DULBERG, V., DEMETER, K., MADARASZ, E. & HERBERTH, B. 2008. Generation of diverse neuronal subtypes in cloned populations of stem-like cells. *Bmc Developmental Biology*, 8, 18.
- VILÀ-BRAU, A., DE SOUSA-COELHO, A. L., MAYORDOMO, C., HARO, D. & MARRERO, P. F. 2011. Human HMGCS2 regulates mitochondrial fatty acid oxidation and FGF21 expression in HepG2 cell line. *J Biol Chem*, 286, 20423-30.
- VOLPE, J. J. 2000. Overview: normal and abnormal human brain development. *Ment Retard Dev Disabil Res Rev*, 6, 1-5.
- WANG, Y., GAN, G., WANG, B., WU, J., CAO, Y., ZHU, D., XU, Y., WANG, X., HAN, H., LI, X., YE, M., ZHAO, J. & MI, J. 2017. Cancer-associated Fibroblasts Promote Irradiated Cancer Cell Recovery Through Autophagy. *EBioMedicine*, 17, 45-56.
- WANG, Y., LIU, N., ZHU, W., ZHANG, K., SI, J., BI, M., LV, X. & WANG, J. 2016. Protective effect of β -hydroxybutyrate on glutamate induced cell death in HT22 cells. *International Journal of Clinical and Experimental Medicine*, 9, 23433-23439.

- WANG, Y. H., LIU, C. L., CHIU, W. C., TWU, Y. C. & LIAO, Y. J. 2019. HMGCS2 Mediates Ketone Production and Regulates the Proliferation and Metastasis of Hepatocellular Carcinoma. *Cancers (Basel)*, 11.
- WARBURG, O. 1925a. The Metabolism of Carcinoma Cells. *The Journal of Cancer Research*, 9, 148-163.
- WARBURG, O. 1925b. The Metabolism of Carcinoma Cells¹. *The Journal of Cancer Research*, 9, 148-163.
- WEBER, D. D., AMINAZDEH-GOHARI, S. & KOFLER, B. 2018. Ketogenic diet in cancer therapy. *Aging*, 10, 164-165.
- WHITAKER-MENEZES, D., MARTINEZ-OUTSCHOORN, U. E., FLOMENBERG, N., BIRBE, R. C., WITKIEWICZ, A. K., HOWELL, A., PAVLIDES, S., TSIRIGOS, A., ERTEL, A., PESTELL, R. G., BRODA, P., MINETTI, C., LISANTI, M. P. & SOTGIA, F. 2011. Hyperactivation of oxidative mitochondrial metabolism in epithelial cancer cells in situ: visualizing the therapeutic effects of metformin in tumor tissue. *Cell cycle (Georgetown, Tex.)*, 10, 4047-4064.
- WILDENHOFF, K. E., JOHANSEN, J. P., KARSTOFT, H., YDE, H. & SORENSEN, N. S. 1974. Diurnal variations in the concentrations of blood acetoacetate and 3-hydroxybutyrate. The ketone body peak around midnight and its relationship to free fatty acids, glycerol, insulin, growth hormone and glucose in serum and plasma. *Acta Med Scand*, 195, 25-8.
- WILDER, R. M. 1921. The effects of ketonemia on the course of epilepsy. *Mayo Clin Proc*, 2, 307-308.
- WRIGHT, C. & SIMONE, N. L. 2016. Obesity and tumor growth: inflammation, immunity, and the role of a ketogenic diet. *Curr Opin Clin Nutr Metab Care*, 19, 294-9.
- WU, X., LIN, M., LI, Y., ZHAO, X. & YAN, F. 2009. Effects of DMEM and RPMI 1640 on the biological behavior of dog periosteum-derived cells. *Cytotechnology*, 59, 103-11.
- XIA, S., LIN, R., JIN, L., ZHAO, L., KANG, H. B., PAN, Y., LIU, S., QIAN, G., QIAN, Z., KONSTANTAKOU, E., ZHANG, B., DONG, J. T., CHUNG, Y. R., ABDELWAHAB, O., MERGHOUB, T., ZHOU, L., KUDCHADKAR, R. R., LAWSON, D. H., KHOURY, H. J., KHURI, F. R., BOISE, L. H., LONIAL, S., LEE, B. H., POLLACK, B. P., ARBISER, J. L., FAN, J., LEI, Q. Y. & CHEN, J. 2017. Prevention of Dietary-Fat-Fueled Ketogenesis Attenuates BRAF V600E Tumor Growth. *Cell Metab*, 25, 358-373.

- XICOY, H., WIERINGA, B. & MARTENS, G. J. M. 2017. The SH-SY5Y cell line in Parkinson's disease research: a systematic review. *Molecular Neurodegeneration*, 12, 10.
- XIE, G., TIAN, W., WEI, T. & LIU, F. 2015. The neuroprotective effects of β -hydroxybutyrate on A β -injected rat hippocampus in vivo and in A β -treated PC-12 cells in vitro. *Free Radic Res*, 49, 139-50.
- XU, S., TAO, H., CAO, W., CAO, L., LIN, Y., ZHAO, S.-M., XU, W., CAO, J. & ZHAO, J.-Y. 2021. Ketogenic diets inhibit mitochondrial biogenesis and induce cardiac fibrosis. *Signal Transduction and Targeted Therapy*, 6, 54.
- XU, X., ZHANG, Q., TU, J. & REN, Z. 2011. D- β -hydroxybutyrate inhibits microglial activation in a cell activation model in vitro. *Journal of Medical Colleges of PLA*, 26, 117-127.
- YANCY, W. S., JR., FOY, M., CHALECKI, A. M., VERNON, M. C. & WESTMAN, E. C. 2005. A low-carbohydrate, ketogenic diet to treat type 2 diabetes. *Nutr Metab (Lond)*, 2, 34.
- YANCY, W. S., JR., OLSEN, M. K., GUYTON, J. R., BAKST, R. P. & WESTMAN, E. C. 2004. A low-carbohydrate, ketogenic diet versus a low-fat diet to treat obesity and hyperlipidemia: a randomized, controlled trial. *Ann Intern Med*, 140, 769-77.
- YANG, C., KO, B., HENSLEY, C. T., JIANG, L., WASTI, A. T., KIM, J., SUDDERTH, J., CALVARUSO, M. A., LUMATA, L., MITSCHKE, M., RUTTER, J., MERRITT, M. E. & DEBERARDINIS, R. J. 2014. Glutamine oxidation maintains the TCA cycle and cell survival during impaired mitochondrial pyruvate transport. *Mol Cell*, 56, 414-424.
- YANG, P., SHEN, W. B., REECE, E. A., CHEN, X. & YANG, P. 2016. High glucose suppresses embryonic stem cell differentiation into neural lineage cells. *Biochem Biophys Res Commun*, 472, 306-12.
- YAO, T. & ASAYAMA, Y. 2017. Animal-cell culture media: History, characteristics, and current issues. *Reproductive medicine and biology*, 16, 99-117.
- YEO, H., LYSSIOTIS, C. A., ZHANG, Y., YING, H., ASARA, J. M., CANTLEY, L. C. & PAIK, J.-H. 2013. FoxO3 coordinates metabolic pathways to maintain redox balance in neural stem cells. *The EMBO journal*, 32, 2589-2602.
- YOO, H. C., YU, Y. C., SUNG, Y. & HAN, J. M. 2020. Glutamine reliance in cell metabolism. *Experimental & Molecular Medicine*, 52, 1496-1516.

- YOSHII, Y., FURUKAWA, T., SAGA, T. & FUJIBAYASHI, Y. 2015. Acetate/acetyl-CoA metabolism associated with cancer fatty acid synthesis: overview and application. *Cancer Lett*, 356, 211-6.
- YOUM, Y. H., NGUYEN, K. Y., GRANT, R. W., GOLDBERG, E. L., BODOGAI, M., KIM, D., D'AGOSTINO, D., PLANAVSKY, N., LUPFER, C., KANNEGANTI, T. D., KANG, S., HORVATH, T. L., FAHMY, T. M., CRAWFORD, P. A., BIRAGYN, A., ALNEMRI, E. & DIXIT, V. D. 2015. The ketone metabolite beta-hydroxybutyrate blocks NLRP3 inflammasome-mediated inflammatory disease. *Nat Med*, 21, 263-9.
- YOUNG, J. L., JR., RIES, L. G., SILVERBERG, E., HORM, J. W. & MILLER, R. W. 1986. Cancer incidence, survival, and mortality for children younger than age 15 years. *Cancer*, 58, 598-602.
- ZAMBRANO, M. C., PAWLAK, J. J., DAYSTAR, J., ANKENY, M., CHENG, J. J. & VENDITTI, R. A. 2019. Microfibers generated from the laundering of cotton, rayon and polyester based fabrics and their aquatic biodegradation. *Marine Pollution Bulletin*, 142, 394-407.
- ZHANG, J., JIA, P. P., LIU, Q. L., CONG, M. H., GAO, Y., SHI, H. P., YU, W. N. & MIAO, M. Y. 2018a. Low ketolytic enzyme levels in tumors predict ketogenic diet responses in cancer cell lines in vitro and in vivo. *J Lipid Res*, 59, 625-634.
- ZHANG, J., LI, X., REN, Y., ZHAO, Y., XING, A., JIANG, C., CHEN, Y. & AN, L. 2018b. Intermittent Fasting Alleviates the Increase of Lipoprotein Lipase Expression in Brain of a Mouse Model of Alzheimer's Disease: Possibly Mediated by β -hydroxybutyrate. *Front Cell Neurosci*, 12, 1.
- ZHANG, J., ZHAN, Z., LI, X., XING, A., JIANG, C., CHEN, Y., SHI, W. & AN, L. 2017. Intermittent Fasting Protects against Alzheimer's Disease Possible through Restoring Aquaporin-4 Polarity. *Front Mol Neurosci*, 10, 395.
- ZHANG, S. & XIE, C. 2017. The role of OXCT1 in the pathogenesis of cancer as a rate-limiting enzyme of ketone body metabolism. *Life Sci*, 183, 110-115.
- ZHANG, W. W., CHURCHILL, S., LINDAHL, R. & CHURCHILL, P. 1989. Regulation of D-beta-hydroxybutyrate dehydrogenase in rat hepatoma cell lines. *Cancer Res*, 49, 2433-7.
- ZHENG, X., BOYER, L., JIN, M., MERTENS, J., KIM, Y., MA, L., MA, L., HAMM, M., GAGE, F. H. & HUNTER, T. 2016. Metabolic reprogramming during neuronal

differentiation from aerobic glycolysis to neuronal oxidative phosphorylation. *eLife*, 5, e13374.

ZHOU, W., MUKHERJEE, P., KIEBISH, M. A., MARKIS, W. T., MANTIS, J. G. & SEYFRIED, T. N. 2007. The calorically restricted ketogenic diet, an effective alternative therapy for malignant brain cancer. *Nutrition & metabolism*, 4, 5-5.

ZHUANG, Y., CHAN, D. K., HAUGRUD, A. B. & MISKIMINS, W. K. 2014. Mechanisms by which low glucose enhances the cytotoxicity of metformin to cancer cells both in vitro and in vivo. *PLoS One*, 9, e108444.

